Numerical modeling of geomechanical effects of steam injection in SAGD heavy oil recovery

Setayesh Zandi

ParisTech
INSTITUT DES SCIENCES ET TECHNOLOGIES
PARIS INSTITUTE OF TECHNOLOGY

MINES ParisTech

École doctorale n°398 : Géosciences et Ressources Naturelles

Doctorat ParisTech

T H È S E

pour obtenir le grade de docteur délivré par

l'École nationale supérieure des mines de Paris

Spécialité "Technique et Economie de l'Exploitation du Sous-sol"

présentée et soutenue publiquement par

Setayesh ZANDI

5 septembre 2011

Numerical modeling of geomechanical effects of steam injection in SAGD heavy oil recovery

Modélisation des effets géomécaniques de l'injection de vapeur dans les réservoirs de bruts lourds

Directeur de thèse : **Michel TIJANI**
Co-encadrement de la thèse : **Jean-François NAUROY**

Jury

M. Pierre BEREST, Directeur de Recherche, Ecole Polytechnique	Rapporteur
M. Alain MILLARD, Professeur, Ecole Centrale	Rapporteur
M. Jean-François THIMUS, Professeur, Université Catholique de Louvain	Président
M. Atef ONAISI, Docteur Ingénieur, Directeur de « Geomecanics Services », TOTAL	Examinateur
M. Darius SEYEDI, Docteur Ingénieur, BRGM	Examinateur
M. Jean-François NAUROY, Docteur Ingénieur, IFPEN	Examinateur
M. Michel TIJANI, Directeur de Recherche, Ecole MinesParisTech	Examinateur

T H È S E

MINES ParisTech
Centre de Géosciences
35 rue Saint-Honoré 77305 Fontainebleau

I gratefully dedicate this thesis to my parents,
whose love and support I will forever be thankful.

And to my husband, Reza,
for his love, support, encouragement and for
giving me a happy and complete life.

ACKNOWLEDGEMENT

Science is the knowledge of consequences, and dependence of one fact upon another.
(*Thomas Hobbes (1588-1679) English philosopher, author*)

Life is a science: knowledge of consequences of our actions, and dependence of our existence on the others!

Although working on a PhD is a solitary and self-determined activity, you need many people to collaborate with, whose knowledge and experience allow the project's direction to be adjusted or reoriented. Here, I would like to express my gratitude to all those who gave me the possibility to start this thesis and mostly to the people who supported me to complete my PhD.

First and foremost I want to thank my supervisor, Professor Michel Tijani, who gave me the opportunity of being a PhD student at prestigious Mines Paris Tech. His special approach of guidance and support from the initial to the final level of this thesis enabled me to develop a successful research methodology.

I wish to express my deep and sincere gratitude to my advisor; Dr. Jean-François Nauroy, who taught me how to think about and analyse the geomechanical problems. I sincerely appreciate his knowledge, leadership, patience, continuos support and insightful comments during this project. His availability for discussions and his encouragements for trying new solutions when the project got blocked was one of the main sources of motivation for me.

I am deeply grateful to my co-advisor; Dr. Gerard Renard, who was my reference in reservoir engineering and directed me in reservoir simulation studies. I am thankful for his detailed and constructive comments, for his important support and encouragements especially during the difficult periods of research and writing my manuscript. I appreciate all his contributions of time and ideas to make my PhD a productive and stimulating experience.

I would like to thank Dr. Nicolas Guy, whose help, stimulating suggestions, kind support and guidance have been of great value in this study.

I wish to thank also Dr. Guillaume Servant; now at EDF, who defined this thesis project and initiated this work.

Furthermore, I would like to thank the members of my reading committee; Professor Pierre Berest; from Ecole Polytechnique, and Professor Alain Millard; from Ecole Centrale, for their time, detailed review, constructive criticism and excellent advice during the final phase of this thesis. I also convey my regards to the other members of my oral dissertation defence committee; Dr. Atef Onaisi; from TOTAL, Dr. Jean-François Thimus; from Université Catholique de Louvain, and Dr. Darius Seyedi; from BRGM, for their time and insightful questions.

During this work I have collaborated with many colleagues for whom I have great regard, and I wish to extend my warmest thanks to all those who have helped me with my work in the “Reservoir Engineering Division” and “Applied Mechanics Division” of IFP Energies Nouvells and the "TEES Group" of Mines Paris Tech. I offer my regards to Dr. Olga Vizika, Dr. Frederic Roggero and Dr. Patrick Lemonier and Dr. Eric Heinzé. My sincere thanks go to Dr. Laurent Cangemi, Dr. Axel Baroni, Gilles Férér, Dr. Florence Adjemian, Dr. Sandrine Vidal-Gilbert, Dr. Elisabeth Bemer, Dr. Habiba Boulhart, Sylvie Hoguet, Dominique Vasiliadis and Dovy Tristani.

I am grateful for the time spent with my former colleagues at IFP Energies Nouvelles especially Leila Heidari, Eleonor Roguet, Daniel Quesada, Ekaterina Sergienko, Zyed Bouzarkouna, Jeremy Rosak, Sandra Buret and Jeremy Dautriat.

Leila thank you, it was great to have the coffee breaks together, to share our happy moments of new discoveries, and to help each other in dealing with frustrations and disappointments.

I express my gratitude to Dr. Samir Ben Chaaban, Head of Mechanics Department at Ecole Supérieure d’Ingénieur Léonard de Vinci, who gave me the opportunity of working as a teaching assistant during the last year of my thesis. I owe my deepest gratitude to Dr. Yosra Guetari, my former finite element teacher at UVSQ and actual colleague at ESILV with whom I share an office, for her valuable advice and friendly help.

We would be lost without teachers. In my case, this is particularly true. I am indebted to many of my teachers and here I would like to express my gratitude to them. My special thanks to Dr. Gilles Perrin, Dr. Paolo Vannucci, Dr. Laurant Champany, Dr. Hélène Dumontet and Dr. Françoise Léné who taught me mechanics and Dr. Arezoo Modaressi from Central Paris.

Most importantly, none of this would have been possible without the love and patience of my family which has been a constant source of motivation, support and strength all these years. I would like to express my heartfelt gratitude to my parents; Parisima and Habib, my brothers; Soroosh and Sarshar, my parents in-law and my sisters in-law; Maryam and Marjan.

I owe my especial loving thanks to my dearest husband; Réza, for his help, patience and support. Without his encouragement and accompanying it would have been impossible for me to finish this work. Thank you Réza, you are my strength and you make each day worthwhile for me.

Setayesh ZANDI

Paris, 2011

CONTENTS

Chapitre 1

Introduction

Au cours des trois dernières décennies, le déclin des réserves de brut conventionnel a conduit au développement de plusieurs méthodes de production adaptées aux bruts lourds.

Le procédé SAGD (Steam Assisted Gravity Drainage) combiné avec la technologie des puits horizontaux est certainement un des concepts le plus important développé en ingénierie de réservoir pour exploiter les huiles lourdes des gisements canadiens. Deux puits horizontaux parallèles sont forés dans la partie basse du réservoir. La vapeur est injectée par le puits supérieur et l'huile est produite par le puits inférieur. La vapeur injectée accroît la température dans le matériau immédiatement en contact, fluidisant et mettant en mouvement le bitume. La différence de densité entre la vapeur et l'huile lourde permet à cette dernière de s'écouler par gravité vers le puits inférieur. La vapeur chaude remplace l'huile déplacée et vient de nouveau en contact avec la formation froide. La chambre de vapeur croit ainsi au cours de l'exploitation, verticalement et horizontalement

Les profils de production, donc de rentabilité du SAGD, peuvent être estimés à partir de simulations prenant en compte les écoulements polyphasiques de fluides à l'échelle du réservoir. Dans ce type d'approche, le couplage entre les effets mécaniques induits par les variations de température et de pression et les propriétés d'écoulement du milieu est rarement pris en compte, alors que l'on sait que ces effets mécaniques sont particulièrement importants pour ce type de réservoir et avec ce mode de production.

L'analyse du procédé SAGD peut être effectuée en utilisant soit des modèles de réservoirs conventionnel soit des modèles couplés géomécanique-réservoir. Le modèle géomécanique offre un cadre rigoureux pour l'analyse mécanique, mais ne permet pas une description complète des fluides. Le modèle de réservoir donne une bonne description des phases fluides, mais la description des phénomènes géomécaniques est alors simplifiée. Pour satisfaire

l'ensemble des équations, équilibre mécanique et équations de diffusivité, deux simulateurs peuvent être utilisés ensemble de façon séquentielle. Chacun des simulateurs résout son propre système de façon indépendante, et l'information passe entre les simulateurs dans les deux sens. Cette technique est généralement appelée le régime partiellement couplé.

Au cours de cette thèse, la modélisation couplée thermo-hydro-mécanique du procédé SAGD a été effectuée à l'aide du simulateur de réservoir PumaFlow, et du simulateur géomécanique Abaqus. La méthodologie proposée pour simuler le procédé SAGD a été appliquée sur un cas synthétique mais réaliste, appelé Senlac, situé au Canada. De plus, certaines études sur l'impact de la stratégie de couplage et de la géométrie sur les résultats de la modélisation couplée ont été réalisées.

Cette thèse commence par l'énoncé du problème et des solutions possibles pour résoudre une simulation couplée réservoir géomécanique.

Le chapitre 2 présente un examen des défis que pose la production des huiles lourdes et du bitume. Il fait l'inventaire des méthodes de récupération utilisées ou en projets et montre leurs avantages et inconvénients ainsi que leur impact sur l'environnement

Le chapitre 3 contient d'abord une présentation de la technique SAGD. qui est basée sur le développement de la chambre de vapeur selon le modèle de Butler. Les mécanismes de transfert de fluides et de chaleur sont présentés, ainsi que l'impact de l'injection de vapeur sur les équilibres géomécaniques et leurs conséquences en terme de déformation des couches d'une part et en terme de modification de la perméabilité d'autre part. . Par la suite, ce chapitre aborde les simulations numériques possibles de la technique SAGD. Enfin, deux exemples réels sont donnés qui illustrent l'importance de la géomécanique dans le processus SAGD.

Le but du chapitre 4 est d'expliquer un modèle thermo-hydro-mécanique et de son application dans le cas de la récupération du pétrole SAGD thermiques lourdes. Ce chapitre commence par une description générale du problème de THM couplé avec une interaction des phases fluides et un milieu poreux, déformant. Ensuite, il présente deux simulateurs utilisés lors de ce travail, PumaFlow simulateur de réservoir et Abaqus le simulateur géomécaniques. Dans l'étape suivante, les hypothèses appliquées simplifiant et les équations de réservoir-géomécanique couplé sont décrits. Dans la dernière section de ce chapitre, le simulateur

externe couplé, nommé PUMA2ABA, développé dans ce travail est présenté, dans lequel les approches de couplage appliquée et le module de couplage sont détaillées.

Dans le chapitre 5, la méthodologie proposée pour simuler le procédé SAGD est présenté. Dans la première section de ce chapitre une étude de cas synthétique nommé «Senlac» est présentée. Ce cas de test est construit sur la base du réservoir «Senlac 'huile lourde qui est classé comme un réservoir profond. Dans la deuxième section du sens unique et des méthodes de couplage explicite sont appliquées sur Senlac cas de test. L'influence du nombre de périodes de couplage en approche de couplage explicite est étudiée. Puis une comparaison entre les résultats obtenus par la simple et explicite des méthodes de couplage est fait. Dans la troisième section, afin de réduire le temps de calcul une méthode de couplage améliorée en utilisant deux grilles système est présentée. Cette approche de couplage qui est basé sur la méthode d'approximation diffuse est appliquée sur deux différentes études de cas synthétique. D'abord, il est testé sur des cas de test Senlac maillage différent (maillage) dans le réservoir et le modèle géomécanique. La deuxième étude de cas est construite sur la base de réservoir d'huile lourde 'Hangingstone' qui est un réservoir peu profond comparant à Senlac. Une méthode itérative couplage avec deux systèmes de grilles est appliquée sur les cas de test Hangingstone. Les résultats et les temps d'exécution de calcul sont présentés et comparés.

Enfin le chapitre 6 examine les conclusions et les perspectives pour les travaux futurs sur ce sujet.

Chapter 1

Introduction

1.1. Problem Statement

Over the past three decades, the decline in reserves of conventional crude oil has led to the development of several methods in order to enhance oil recovery for heavy oil deposits.
Globally, heavy oil accounts for approximately 50 % of hydrocarbon volume in place (Ehlig-Economides et al., 2000). Oil sand is a mixture of bitumen, sand, water and clay, which contains heavy oil. There exist sixteen major oil sands deposits all over the world. As a matter of fact, the two largest are the Athabasca oil sands in Northern Alberta and the Orionco-River deposit in Venezuela. By comparison, the Athabasca oil sands alone cover an area of more than 42000 km^2, in which oil storage is more than all the known reserves in Saudi Arabia.
It is found that only one sixth of over 1.7 trillion barrels of heavy oil are recoverable with current technologies. These technologies include mining, thermal recovery, cold production and etc. which are discussed in chapter 2. Mining only makes economic and engineering sense when the depth of overburden is less than about 75 metres. Hence, only about 10 – 20 % of the oil sands can be mined. As a result, recovery of the remaining 80 – 90 % of the oil sands depends on the so-called thermal-recovery process which basically depends on using energy to produce energy. In order to begin to separate the heavy oil from the sand, oil sands deposits have to be heated to lower the viscosity of the heavy oil. One of these thermal-recovery methods is the Steam Assisted Gravity Drainage (SAGD) process which appears tremendously successful, especially for bitumen. SAGD process involves drilling two horizontal wells one above the other. The top well is used to introduce hot steam into the oil sands. As the heavy oil thins and separates, gravity causes it to collect in the second parallel well where it can be pumped to the surface for further processing. Even though the injector well and producer can be very close, the mechanism of SAGD causes a growing steam-

saturated zone, known as the steam chamber, to expand gradually and eventually allow drainage from a very large volume.

The success of steam assisted gravity drainage has been demonstrated by both field and numerical simulation studies.

The prediction of SAGD performance by numerical simulation is an integral component in the design and management of a SAGD project. Conventional reservoir modelling approach computes multiphase flow in porous media but generally does not take the geomechanical effects into account. Unfortunately, this assumption is not valid for oil sand material, because of their high sensitivity on pore pressure and temperature variations.

Traditionally, more emphasis has been given to solve the flow problem alone by assuming a constant state of stress (total stress) in the system and by incorporating a time-invariant rock compressibility term into account for the complete mechanical response of the system. Conventional simulators neglect the interaction of a reservoir with its overburden and sideburden and implicitly assume equivalence of reservoir conditions with laboratory conditions under which the rock compressibility was measured. This results in an oversimplification of the physics governing fluid flow and geomechanics interactions [21].

In the SAGD process, continuous steam injection changes reservoir pore pressure and temperature, which can increase or decrease the effective stress in the reservoir. Indeed, oil sand material (skeleton and pores) strains induce changes in the fluid flow-related reservoir parameters. This is obviously a coupled problem. Therefore, coupled reservoir geomechanical simulations are required.

In SAGD process, reservoir geomechanics analysis is concerned with the simultaneous study of fluid flow and the mechanical response of the reservoir. Quantification of the state of deformation and stress in the reservoir is essential for the correct prediction of a number of processes, such as recovery from compaction drive, water flooding, surface subsidence, seal integrity, hydro fracturing, sand production and well failure. This is particularly important for the correct prediction of oil recovery and for the correct interpretation of 4D seismic to quantify the steam chamber growth since the seismic wave velocity depends on temperature, fluid pressure and saturations, but also on the strain and stress state of the reservoir and overburden.

The classical treatment of deformation of the reservoir through the rock compressibility is far from adequate, and the mechanical problem needs to be incorporated rigorously in the reservoir model.

Theoretical and practical difficulties have prevented coupled geomechanical models from being used routinely in oil and gas reservoir simulation studies. Some of these challenges are the complex mechanical behaviour of geomaterials, the strong coupling between the mechanical and fluid flow problems, and the fact that the reservoir models become very computationally intensive. As a result, the modelling of coupled flow and geomechanics is relatively new to the oil industry.

Analysis of SAGD process can be performed using either conventional reservoir models or coupled geomechanics-reservoir models. The geomechanical model offers a rigorous mechanical framework, but doesn't permit a complete description of the fluids. The reservoir model gives a good description of the fluid phases, but the description of the geomechanical phenomenon is then simplified. To satisfy the set of equations, as mechanical equilibrium and diffusivity equations, two simulators can be used together sequentially. Each of the simulators solves its own system independently, and information passes between simulators in both directions. This technique is usually referred to the partially coupled scheme.

In this study, SAGD numerical modeling is conducted using PumaFlow reservoir simulator, and Abaqus as the geomechanical simulator. The reservoir and geomechanical simulations show that the classical treatment of deformation of the reservoir through the rock compressibility is far from adequate, and the conventional reservoir theory is not a rigorous framework to represent the evolution of high porous rock strains during the SAGD process; so the mechanical problem needs to be incorporated rigorously in the reservoir model. Therefore we introduce a geomechanics-reservoir partially coupled approach, which permits to perform a better simulation of SAGD process.

The objective of this study was to show the importance of taking into account the role of geomechanics, in SAGD numerical modelling; and to provide a better description of the rock contribution to fluid flows in SAGD process numerical simulation.

During this PhD thesis, the SAGD coupled thermo-hydro-mechanical modelling is conducted using PumaFlow reservoir simulator, and Abaqus. Then the proposed methodology to simulate the SAGD process is applied on a synthetic but realistic case study, called Senlac, located in Canada. Also, some sensitivity studies on the impact of coupling strategy and geometry on the results of coupled modelling have been done.

Next step of this project at IFPEN is to apply the coupled methodology on a real heterogeneous case. Irrespective of the time coupling method being used, and considering the size and heterogeneity of this case study, application of developed coupled methodology on a real case is a very time-consuming job. So, the problem related to large computer memory

requirement and longue CPU running time should be taken into account. This is because a geomechanics simulator normally solves a much larger number of unknowns per gridblock than a reservoir simulator does. If the same (coincident) grid is used for both simulators, a full-field coupled problem requires significantly more CPU time and memory than the run without coupled geomechanics calculations, which makes the coupled runs unattractive. In order to overcome this challenge, the idea of using a reservoir/geomechanics separate-grid system to reduce the coupled simulation run time, was proposed by M. Tijani. With this approach, geomechanics grid or reservoir grid can be refined or coarsened in different regions independently according to the scale of various physical processes of interest. Using this technique in SAGD coupled simulation, the number of geomechanics gridblocks can be much smaller than the number of reservoir gridblocks, resulting in a much reduced CPU time and memory requirement for a coupled run.

1.2. Organisation of the report

This dissertation starts with the problem statement and the motivational statements on the significance of development and solving a SAGD coupled reservoir geomechanical simulation.

Chapter 2 presents a review of the challenges of heavy oil production from reservoir and fluid characterization to mobilisation into the wellbore. It summarizes the "Enhanced Oil Recovery" methods and their suitable application case. Then it explains the advantage of using SAGD method. It reviews the most important heavy oil projects in the world, the mining projects and in situ production projects.

Chapter 3 contains mostly a review on SAGD, the SAGD process issues, the elements of success, mechanics of SAGD like steam chamber rise mechanism, steam fingering theory, co-current and counter-current displacement, emulsification, residual oil saturation in steam chamber, heat transfer and distribution through steam chamber and the analytical model of Butler. Then it reviews the effects of reservoir properties on SAGD performance, like porosity, thickness, gas saturation, permeability, viscosity, wettability and heterogeneity. Then it contains a review on SAGD operation, the start-up procedure, length, spacing and placement of horizontal wells, steam tarp control, high pressure and low pressure SAGD and

steam chamber monitoring. In the next part of this chapter the SAGD numerical simulation; the different scheme of coupling and the recent work in reservoir-geomechanical coupled simulations are presented.

The purpose of chapter 4 is to explain a thermo-hydro-mechanical model and its application in the case of SAGD thermal heavy oil recovery. This chapter starts with a general description of coupled THM problem with interaction of fluid phases and a deforming porous medium. Then it presents two simulators used during this work, PumaFlow the reservoir simulator and Abaqus the geomechanical simulator. In the next step, the applied simplifying assumptions and the reservoir-geomechanics coupled equations are described. In the last section of this chapter, the external coupled simulator, named PUMA2ABA, developed in this work is presented, in which the applied coupling approaches and the coupling module are detailed.

In chapter 5, the proposed methodology to simulate the SAGD process is presented. In first section of this chapter a synthetic case study named ‘Senlac’ is presented. This test case is constructed based on ‘Senlac’ heavy oil reservoir which is classified as a deep reservoir. In second section the one-way and explicit coupling methods are applied on Senlac test case. The influence of the number of coupling periods in explicit coupling approach is studied. Then a comparison between the results obtained by one-way and explicit coupling methods is done. In third section in order to reduce the computation time an enhanced coupling method using two-grid system is presented. This coupling approach which is based on diffuse approximation method is applied on two different synthetic case studies. First it is tested on Senlac test case with different gridding (mesh size) in reservoir and geomechanical model.
The second case study is constructed based on ‘Hangingstone’ heavy oil reservoir which is a shallow reservoir comparing to Senlac. An iterative coupling method with two-grid system is applied on Hangingstone test case. The results and the computation run time are presented and compared.

Finally chapter 6 discusses the conclusions and the perspectives for future work on this subject.

Chapitre 2

Les défis des huiles lourdes

Les huiles lourdes, extra lourdes et le bitume sont des pétroles non conventionnels caractérisés par leur densité élevée et leur forte viscosité. La densité du brut est caractérisée par sa densité dite API (American Petroleum Institute) mesurée en degrés et calculée en utilisant la formule Densité API = (141,5/S.G.) - 131,5. Le brut léger a une densité API supérieure à 31.1°, le brut moyen a une densité comprise entre 22.3° et 31.1° et le pétrole lourd a une densité inférieure à 22.3°. Le pétrole lourd classique de la région de Lloydminster, en Alberta, a une densité API qui varie entre 9° et 18°.

Le bitume est un pétrole qui ne coule pas et qui ne peut pas être pompé sans être chauffé ou dilué, il a généralement une densité API inférieure à 10°. Le bitume recueilli à partir des dépôts de sables bitumineux de la région d'Athabasca au Canada a une densité API d'environ 8.

Géographiquement, on trouve du pétrole lourd partout dans le monde, mais c'est au Canada, au Venezuela (Ceinture de l'Orénoque) et dans l'ancienne Union Soviétique qu'on trouve la plus grande quantité des réserves. On évalue à 6.10^{12} le nombre de barils de pétrole que représentent les réserves de bruts lourds. Toutefois, il se peut que les réserves soient beaucoup plus abondantes en réalité, car les champs ne sont généralement pas bien documentés à moins qu'ils se révèlent économiquement viables dans la conjoncture actuelle.

Les bruts non conventionnels du Canada sont principalement des bitumes, tandis qu'au Vénézuéla ce sont essentiellement des huiles lourdes ou des huiles extra-lourdes. Les gisements bitumineux d'Alberta sont les plus importants du monde, Les dépôts bitumineux sont presque entièrement situés dans trois régions principales de la province d'Alberta: Athabasca, Cold Lake et Peace Rive, situés à la frontière de l'Alberta et du Saskatchewan, aux environs de la ville de Lloydminster. Les dépôts se situent à des profondeurs croissantes

vers le Sud-ouest: 300 m dans la région d'Athabasca, 400 m dans celle de Cold Lake et enfin 500 m dans celle de Peace River.

La vaste majorité des réserves bitumineuses d'Athabasca est contenue dans des sables peu consolidés du Crétacé Inférieur mais aussi dans des carbonates paléozoïques Dévoniens. Pour l'instant, seuls les réservoirs de sables bitumineux sont en cours d'exploitation. Le bitume hébergé au sein des réservoirs carbonatés n'est pas encore exploité. Au total, les champs s'étendent sur près de 141 000 kilomètres carrés. Le Nord oeuest de l'Alberta contient d'importantes réserves de bitume enfouies très profondément et leur exploitation ne serait pas économiquement viable à l'heure actuelle. Selon le Alberta Energy and Utilities Board, les réserves établies de bitume brut représentaient environ 174,5 milliards de barils au 31 décembre 2003, dont 10,8 milliards se trouvent dans des régions en exploitation.

Comment produit-on les sables bitumineux et les brut lourds?

Méthodes conventionnelles

Le brut lourd peut parfois être produit à l'aide de méthodes conventionnelles telles que forages verticaux, pompage et maintien de pression. Toutefois, comparativement aux autres méthodes plus sophistiquées, celles-ci se révèlent plutôt inefficaces.

Les forages horizontaux sont plus efficaces car ils augmentent la longueur de la partie du trou de sonde en contact avec le gisement. Le forage coil tubing permet d'accroître la rentabilité du puits, mais la densité et la viscosité du pétrole sont toujours des facteurs contraignants.

Production froide du pétrole lourd avec production de sable

La production simultanée d'huile lourde et de sable augmente la productivité de façon significative. Les puits qui ne produisaient auparavant que 20 barils par jour (trois mètres cubes par jour) produisent avec cette technique plus de 200 barils par jour (30 mètres cubes par jour) grâce au sable qui est soutiré en même temps que l'huile grâce à des pompes à cavité progressive. Le sable est ensuite séparé de l'huile par gravité en chauffant le mélange dans des grandes cuves

Cette technologie, mise au point au Canada semble convenir particulièrement aux gisements de pétrole où de grandes quantités de gaz sont dissoutes, mais les mécanismes de production ne sont pas encore pleinement compris. A l'heure actuelle, environ 22 pour cent de la production quotidienne de pétrole au Canada est issue de cette méthode.

Exploitation minière

Lorsque le sable bitumineux n'est pas très profond (<50 m) on peut procéder à son exploitation à partir de la surface. II faut d'abord raser la forêt pour enlever la terre de surface et la stocker pour éventuellement la réutiliser lors de la remise en état du terrain. Par la suite, on creuse et enlève le mort terrain, jusqu'à atteindre les sables bitumineux qu'on extrait de mines à ciel ouvert. Tout ce procédé est effectué à l'aide de camions et de grues colossales. Des excavateurs à godets et des convoyeurs à courroie permettent de transporter le sable bitumineux brut vers les installations de traitement se trouvant sur le site. La récupération atteint un pourcentage de 88 à 95%. On estime que près de 38% de la production d'huile du Canada viendra de l'exploitation minière des sables bitumineux en 2015.

Récupération thermique in situ

Pour les sables bitumineux comme pour le pétrole lourd, on utilise souvent de la vapeur pour faciliter la production. La vapeur permet de liquéfier le bitume et de le rendre plus mobile. On peut également utiliser la vapeur pour créer - ou élargir - des chenaux et des fissures où le pétrole liquéfié peut s'écouler.

La technologie in situ actuelle recourt à des chaudières alimentées au gaz naturel pour générer de la vapeur. Ce procédé utilise beaucoup d'eau (jusqu'à trois mètres cubes pour chaque mètre cube de bitume produit) mais plus de 80 pour cent de cette eau est recyclée.

Les techniques de production actuelles permettent de récupérer de 25 à 60 pour cent (et même plus) du bitume se trouvant dans le gisement. Il s'agit d'un taux de récupération sensiblement plus élevé que la plupart des puits de pétrole brut léger classique.

Les deux meilleures méthodes de récupération sont la stimulation cyclique par vapeur et le drainage par gravité au moyen de la vapeur (SAGD).

- ***Stimulation cyclique par vapeur** : le procédé consiste d'abord à injecter de la vapeur pendant une à trois semaines dans la formation. On laisse ensuite « inbiber » le gisement plusieurs jours, pour ensuite faire place à la production, au cours de laquelle le pétrole est produit par les mêmes puits où la vapeur a été injectée. Lorsque le taux de production diminue, un autre cycle d'injection de vapeur est commencé. La vapeur à haute pression a non seulement pour effet de liquéfier le bitume, mais elle crée des chenaux et des fissures dans lesquels le bitume peut s'écouler jusqu'au puits.*

- *Le **drainage par gravité (SAGD)** consiste en l'aménagement de deux puits horizontaux parallèles l'un au-dessus l'autre situés dans la partie basse du réservoir. De la vapeur est injectée sans arrêt dans le puits supérieur, amollissant le bitume qui est drainé dans le puits inférieur. Le bitume est ensuite pompé vers la surface.*

Méthodes expérimentales

Extraction à la vapeur (VAPEX)

Les sociétés évaluent actuellement une variante du procédé SAGD appelée extraction à la vapeur (VAPEX) qui utilise du gaz naturel tels que l'éthane, le propane ou le butane au lieu de la vapeur. Des méthodes hybrides vapeur-solvant sont également en cours de développement. Tout comme la technique de SAGD , ces méthodes peuvent être employées en ayant recours à des forages horizontaux, ou une combinaison de forages verticaux et horizontaux.

Combustion in situ

La combustion in situ est une méthode de récupération expérimentale qui consiste à injecter de l'oxygène dans la formation productrice. Cet oxygène est brûlé avec une partie du bitume pour augmenter la température du pétrole et lui permettre de s'écouler plus facilement vers un puits de production.

Le procédé THAI (Toe-to Heel Air injection) utilise des puits de production horizontaux à la base du réservoir jumelés avec des puits verticaux d'injection d'air forés à la pointe des puits horizontaux. De la vapeur est injectée à travers les puits verticaux et horizontaux pendant

deux à trois mois pour chauffer le réservoir près des puits. Lorsque le pétrole / bitume lourd atteint la température et la mobilité requise, de l'air est injecté dans la formation par les puits verticaux. Comme l'air atteint une roche chauffée, il amorce une réaction de combustion.

Lorsque l'air est injecté dans la formation, un front de combustion vertical se déplace le long du puits horizontal (de l'extrémité au coude de production) balayant ainsi le réservoir.

Les hautes températures (450°C-650°C) produites par le front de combustion in situ vont provoquer, d'une part, la valorisation des bitumes par craquage thermique, et d'autre part, un effet de flux forcé, qui couplé à la gravité, va provoquer le drainage des hydrocarbures jusqu'au puits de production horizontaux.

Chapter 2

Heavy Oil Challenges

Today, heavy crude oils appear to be major players in the outlook for the future of world energy. As far as resources are concerned, their volume represents as much as all resources of conventional oils. However, due to detrimental properties (mainly viscosity), their exploitation, including production, transport and upgrading, requires adaptation of the current means of the petroleum industry and, more importantly, active development of innovative technologies.

This chapter reviews the definition of heavy oil, extra heavy oil and bitumen. Then it summarizes the characteristics and the formation of these unconventional resources. In next step, the different recovery methods and the challenges faced by the heavy crude oil industry are presented. The diagram in Figure 2.1 illustrates the major factors that will influence the pace of heavy oil recovery development. This chapter also explains the unconventional worldwide resources and the recovery methods applied in each region. Finally the environmental issues related to heavy oil recovery are presented. Among these issues, the problem relative to the gas emissions, climate change and input energy, which are potentially higher than for conventional oils, must be addressed.

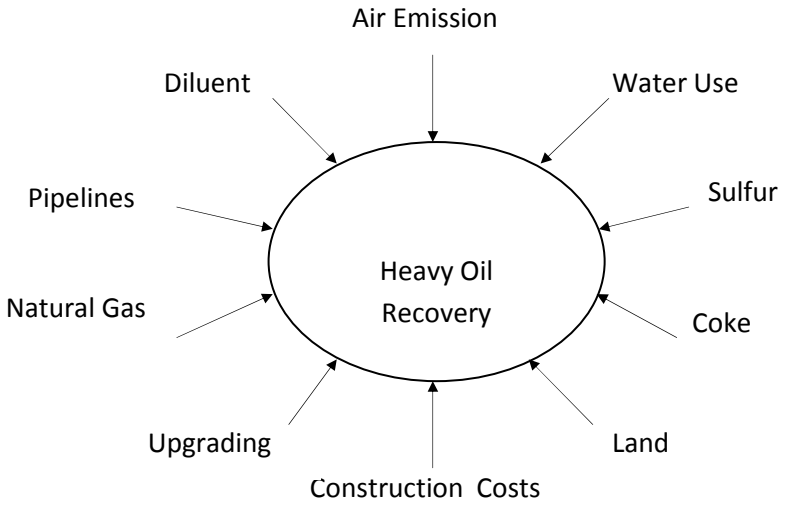

Fig. 2.1: Challenges of Heavy Oil Recovery

2.1. Definitions

Heavy oil, extra-heavy oil, and bitumen are unconventional, naturally-occurring petroleum substances and their definition is based on two important physical properties; their high specific gravity and high viscosity.

In the petroleum industry, for the purposes of providing a commercial value for crude oils, specific gravity is expressed as a scale defined by the American Petroleum Institute: the "API gravity" or "API degree". The API gravity is a direct calculation from the specific gravity:

API gravity = (141.5/Specific gravity) – 131.5

Specific gravity and API gravity evolve in opposite directions; thus, the smaller the API gravity, the heavier the fluid is. This equation is equal to 10 when the oil exhibits the specific gravity of pure water, which is given as 1.

According to the American Petroleum Institute, different types of oil are defined:

- Light crude oil, which has an API gravity greater than 31.1° API, i.e. specific gravity less than 0.87. For example, North Sea Brent is a light crude oil with 38° API gravity.
- Medium crude oil, defined as having an API gravity between 22.3° and 31.1° API, i.e. specific gravity between 0.87 and 0.92.
- Heavy crude oil, displays an API gravity less than 22.3° API, i.e. specific gravity greater than 0.92.

The distinction between bitumen and extra-heavy oil is not a matter of gravity or chemical composition, but of viscosity: bitumen is more viscous than extra-heavy oil at reservoir pressure and temperature. Note that there are various definitions of heavy crude, depending on the source used. According to the Canadian Centre of Energy, heavy crude oil is itself classified into different categories based on specific gravity and viscosity at reservoir conditions:

- Heavy oil, the API gravity is greater than 10; its viscosity is less than 10000 cp (mPa.s) and it flows at reservoir pressure and temperature.
- Extra-heavy oil, the API gravity is less than 10 and the in situ level of viscosity is less than 10000 cp (mPa.s), which means that it has some mobility at reservoir pressure and temperature.
- Natural bitumen, often associated with sands, and also referred to as tar sands (which is not scientifically correct) or oil sands, in which the API gravity is less than 10 and

the in situ viscosity is greater than 10000 cp (mPa.s), and it is virtually immobile at reservoir pressure and temperature.

According to the definition of the World Petroleum Congress (1980) and the United Nations through UNITAR (1982), Conventional oils are characterized by an API gravity higher than 20°; Heavy oils are defined as oils having an API gravity in the range of 10° - 20°; Extra heavy oils and natural bitumen display an API gravity lower than 10°.

Heavy oil promises to play a major role in the future of the oil industry, and many countries are moving now to increase their production, revise reserves estimates, test new technologies and invest in infrastructure to ensure that their heavy oil resources are not left behind.

This chapter describes how heavy hydrocarbon deposits are formed and how they are being produced.

2.2. Oil Sands and Bitumen Characteristics

The oil sands deposits are composed primarily of quartz sand, silt and clay, water and bitumen, along with minor amounts of other minerals, including titanium, zirconium, tourmaline and pyrite. Although there can be considerable variation, a typical composition would be:

- 75 to 80 percent inorganic material, with this inorganic portion comprised of 90 percent quartz sand;
- 3 to 5 percent water; and,
- 10 to 12 percent bitumen, with bitumen saturation varying between zero and 18 percent by weight.

The oil sands are generally unconsolidated and thus quite friable and crumble easily in the hand.

The bitumen contained in the oil sands is characterized by high densities, very high viscosities, high metal concentrations and a high ratio of carbon-to-hydrogen molecules in comparison with conventional crude oils. With a density range of 970 to 1015 kg/m3 (8 to 14°API), and a viscosity at room temperature typically greater than 50000 cp, bitumen is a thick, black, tar-like substance that pours extremely slowly.

Bitumen is deficient in hydrogen, when compared with typical crude oils, which contain approximately 14 percent hydrogen. Therefore, to make it an acceptable feedstock for conventional refineries, it must be upgraded through the addition of hydrogen or the rejection

of carbon. In order to transport bitumen to refineries equipped to process it, bitumen must be blended with diluents, traditionally condensate, to meet pipeline specifications for density and viscosity.

2.3. Formation of Vast Resources

Of the world 6 to 9 trillion barrels of heavy and extra heavy oil and bitumen, the largest accumulations occur in similar geological settings. These are supergiant, shallow deposits trapped on the flanks of foreland basins. Foreland basins are huge depressions formed by downwarping of the Earth's crust during mountain building. Marine sediments in the basin become source rock for hydrocarbons that migrate updip into sediments eroded from the newly built mountains. The new sediments often lack sealing caprocks. In these shallow, cool sediments, the hydrocarbon is biodegraded.

Biodegradation is the main cause of the formation of heavy oil. Over geological time scales, microorganisms degrade light and medium hydrocarbons, producing methane and enriched heavy hydrocarbons. The effect of biodegradation is to cause oxidation of oil, decreasing gas/oil ratio (GOR) and increasing density, acidity, viscosity and sulphur and other metal content. Through biodegradation, oils also lose a significant fraction of their original mass. Other mechanisms, such as water washing and phase fractionation, contribute to the formation of heavy oil, separating light ends from heavy oil by physical rather than biological means. Optimal conditions for microbial degradation of hydrocarbons occur in petroleum reservoirs at temperature less than 80°C; the process is therefore restricted to the shallow reservoirs, down to about 4 km.

The largest known individual petroleum accumulation is the Orinoco heavy oil belt in Venezuela with 1.2 trillion barrels of extra heavy oil with 6° to 12 ° API gravity. The combined extra heavy oil accumulations in the western Canada basin in Alberta total 1.7 trillion barrels. The sources of these oils are not completely understood, but it is agreed in both cases that they derive from severely biodegraded marine oils. The 5.3 trillion barrels in all the deposits of western Canada and eastern Venezuela represent the degraded remains of what was probably once 18 trillion barrels of light oils.

In any depositional environment, the right combination of water, temperature and microbes can cause degradation and formation of heavy oil. Tar mats occur in many reservoirs near the oil/water contacts, where conditions are conductive to microbial activity. The depositional

environment, the original oil composition, the degree to which it has been degraded, the influx of , or charging with, lighter oils and the final pressure and temperature conditions make every heavy oil reservoir unique, and all of them require different methods of recovery.

2.4. Heavy Oil Worldwide Resources

Heavy crude oil is difficult to exploit, but its volume is so significant that this fact alone justifies its interest. Due to its geographical location and the size of its resources, heavy crude oil development constitutes a major economic and energy challenge. In the current environment where the spectre of peak oil is omnipresent, heavy crude exploitation will help to offset the decline in worldwide production of conventional oil. Its development on a large scale requires that several technical challenges be met.

There are huge, well-known resources of heavy oil, extra-heavy oil, and bitumen in Canada, Venezuela, Russia, the USA and many other countries. The International Energy Agency (IEA) estimates that there are 6 trillion ($6.\ 10^{12}$) barrels in place worldwide; with 2.5 in Western Canada, 1.5 inVenezuela, 1 inRussia, and 0.100 to 0.18 in the United States. Heavy oil and bitumen resources in Western Canada and the United States could provide stable and secure sources of oil for the United States. Most of these resources are currently untapped.

Canada

Canada is the largest supplier of crude oil and refined products to the United States, supplying about 20% of total U.S. imports. In 2006, bitumen production averaged 1.25 million barrels per day through 81 oil sands projects, representing 47% of total Canadian petroleum production. This proportion is expected to increase in coming decades as bitumen production grows while conventional oil production declines [Gvt. of Alberta,2008].

Most of the oil sands of Canada are located in three major deposits in northern Alberta. These are the Athabasca-Wabiskaw oil sands of north - north eastern Alberta, the ColdLake deposits of east north eastern Alberta, and the Peace River deposits of north western Alberta (Figure 2.2). Together they cover over 140,000 square kilometres, an area larger than England, and hold proven reserves of 1.75 trillion barrels of bitumen in place. About 10% of this, or 173 billion barrels, is estimated by the government of Alberta to be recoverable at current prices using current technology, which amounts to 97% of Canadian oil reserves and 75% of total North American petroleum reserves [Gvt. of Alberta,2008]. The ColdLake deposits

extend across the Alberta's eastern border into Saskatchewan. In addition to the Alberta oil sands, there are major oil sands deposits on Melville Island in the Canadian Arctic islands which are unlikely to see commercial production in the future.

The Alberta oil sand deposits contain at least 85% of the world's reserves of natural bitumen (representing 40% of the combined crude bitumen and extra-heavy crude oil reserves in the world), but are the only bitumen deposits concentrated enough to be economically recoverable for conversion to synthetic crude oil at current prices. The largest bitumen deposit, containing about 80% of the Alberta total, and the only one suitable for surface mining, is the Athabasca Oil Sands along the AthabascaRiver. The mineable area (as defined by the Alberta government) includes 37 townships covering about 3,400 square kilometres near Fort McMurray. The smaller ColdLake deposits are important because some of the oil is fluid enough to be extracted by conventional methods. All three Alberta areas are suitable for production using in-situ methods such as cyclic steam stimulation (CSS) and steam assisted gravity drainage (SAGD).

Venezuela

Located in eastern Venezuela, north of the OrinocoRiver, the Orinoco oil Belt vies with the Canadian oil sand for largest known accumulation of bitumen in the world. Venezuela prefers to call its oil sands "extra heavy oil", and although the distinction is somewhat academic, the extra heavy crude oil deposit of the Orinoco Belt represent nearly 90% of the known global reserves of extra heavy crude oil, and nearly 45% of the combined crude bitumen and extra-heavy crude oil reserves in the world.

Bitumen and extra-heavy oil are closely related types of petroleum, differing only in the degree by which they have been degraded from the original crude oil by bacteria and erosion. The Venezuelan deposits are less degraded than the Canadian deposits and are at a higher temperature (over 50 degrees Celsius versus freezing for northern Canada), making them easier to extract by conventional techniques.

Fig. 2.2: AlbertaOil Sand deposits - Canada
(Source: Alberta Department of Energy)

Fig. 2.3: Orinoco Oil Belt, EastVenezuelaBasinProvince

Although Venezuela's extra-heavy oil is easier to produce than Canada's bitumen, it is still too heavy to transport by pipeline or process in normal refineries. Lacking access to first-world capital and technological prowess, Venezuela has not been able to design and build the kind of upgraders and heavy oil refineries that Canada has. In the early 1980s the state oil company, PDVSA, developed a method of using the extra-heavy oil resources by emulsifying it with water (70% extra-heavy oil, 30% water) to allow it to flow in pipelines. The resulting product, called Orimulsion, can be burned in boilers as a replacement for coal and heavy fuel oil with only minor modifications. Unfortunately, the fuel’s high sulphur content and emission of particulates make it difficult to meet increasingly strict international environmental regulations.

However, Venezuela's oil sands crude production, which sometimes wasn't counted in its total, has increased from 125,000 bbl/d to 500,000 bbl/d between 2001 and 2006. [Fox M,2006]

USA

In the United States, oil sands resources are primarily concentrated in Eastern Utah. With a total of 32 billion barrels of oil (known and potential) in eight major deposits in the Utah counties of Carbon, Garfield, Grand, Uintah and Wayne. Currently, oil is not produced from oil sands on a significant commercial level in the United States, although the U.S. imports twenty percent of its oil and refined products from Canada, and over fifty percent of Canadian oil production is from oil sands. In addition to being much smaller than the Alberta Canada oil sands deposits, the U.S. oil sands are hydrocarbon wet, whereas the Canadian oil sands are water wet. As a result of this difference, extraction techniques for the Utah oil sands will be different than those used for the Alberta oil sands. A considerable amount of research has been done in the quest for commercially viable production technology to be employed in the development of the Utah oil sands. A special concern is the relatively arid climate of eastern Utah, as a large amount of water may be required by some processing techniques [BLM,2008].Section 526 of the Energy Independence And Security Act prohibits United States government agencies from buying oil produced by processes that produce more greenhouse gas emissions than would traditional petroleum including oil sands [Kosich,2008].

Other countries

Several other countries hold oil sands deposits which are smaller by orders of magnitude. Russia holds oil sands in two main regions [Rigzone,2006]. The Volga-Urals basins (in and around Tatarstan), which is an important but very mature province in terms of conventional oil, holds large amounts of oil sands in a shallow formation. Exploitation has not gone beyond pilot stage yet. Other, less known, deposits are located in eastern Siberia.

In the Republic of Congo, the Italian oil company Eni have announced in May 2008 a project to develop the small oil sands deposit in order to produce 40,000 barrels per day in 2014.[Eni,2008] Reserves are estimated between 0.5 and 2.5 billion barrels.

In Madagascar, Tsimiroro and Bemolanga are two heavy oil sands deposits with a pilot well already producing small amounts of oil in Tsimiroro and larger scale exploitation in the early planning phase. [Rigzone, 2007]

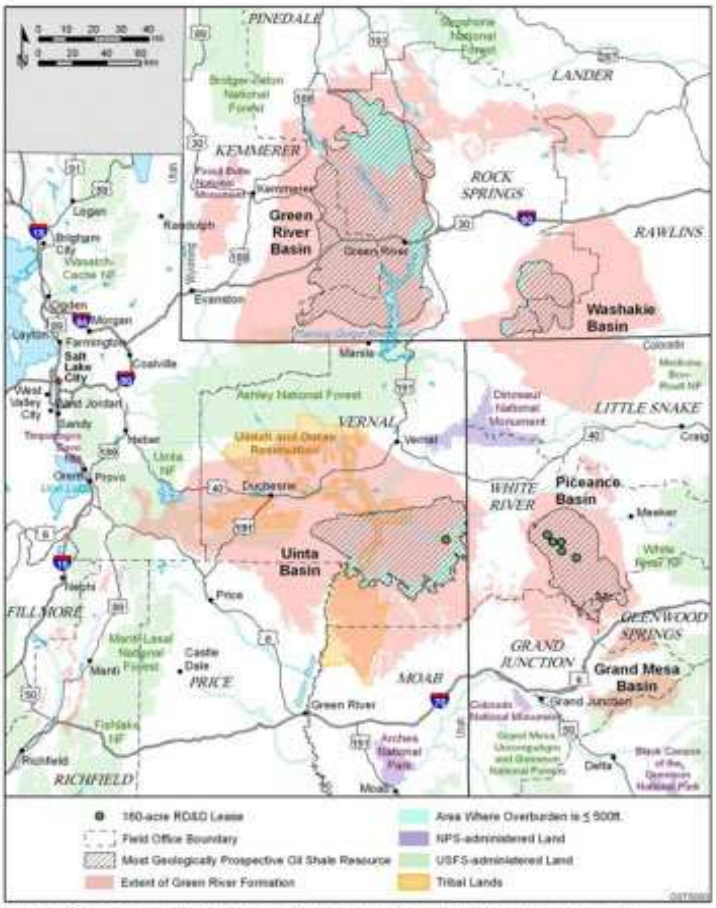

Fig. 2.4: Green River Formation Basins in Colorado, Utah, and Wyoming-USA

2.5. Heavy Oil Recovery Methods

Nowadays exploration technology is of minor importance, since large resources have already been discovered, but optimizing production technology is important. Because heavy oil, extra-heavy oil, and bitumen do not flow readily in most reservoirs, they require specialized production methods.

Any heavy oil operator faces decisions on how to develop their assets. An analysis must be done to classify the different hydrocarbon resources by production method. A prioritization is then made based on financial, marketing and environmental considerations to develop a production strategy. In all cases, proper reservoir characterization, modelling, simulation and pilot studies must be carried out. Canada, Venezuela, and the United States are leading producers of these unconventional oils.

In this part, the various methods currently used to produce heavy crude oils are presented. These methods depend on several parameters:

- Reservoir characteristics like depth, thickness, temperature, type of rock, permeability and degree of complexity linked to the sedimentology of the reservoir and its geological history.
- Whether an aquifer is present or not.
- Crude oil characteristics, including viscosity, linked to the geological history of fluids and thermodynamic conditions.

Production techniques for heavy crude oils are classified into three major categories, based first on reservoir depth, and then on whether the crude oil can be produced by pumping alone or needs the use of thermally or chemically assisted recovery methods.

Very shallow oil sands can be mined. It means that when the reservoir depth is less than 70-80 m and there is no pressure in the reservoir, mining extraction of the oil-impregnated rock is generally used; this is followed by rock-bitumen separation. In Canada, open-pit mining of shallow oil sands provides approximately 50% of the nation’s heavy oil production.

Conventional production is used when possible and economical, at least in the initial phase of heavy oil production. This is referred to as cold production. When reservoirs are unconsolidated, which is generally the case resulting from their low compaction due to limited burial during the geological history, producers complete the wells with special equipment to avoid the production of sand coming from the reservoir itself. However, it has been observed, particularly in Canada, that concomitant production of sand in some cases significantly increased the heavy oil recovery rate. This process is called CHOPS (Cold Heavy Oil Production with Sand).

Even when it is possible, cold production only allows for the recovery of a very limited portion of the oil in place, rarely more than 10%. Due to the high viscosity of crude oil, techniques have been developed which aim to reduce crude oil viscosity in order to increase its ability to flow and be produced. These include techniques for injecting steam, solvent or air, which are described in detail in this part. These techniques are constantly evolving. Thus, the development of horizontal wells has enabled new schemes for producing heavy oils and even bitumen.

2.5.1. Mining

Oil mining was first observed and recorded in the 13th century by Marco Polo. Today, the technique is used at a large scale mostly in Canada, where it accounts for 22% of the country's oil production. Canadian oil sands are recovered by truck and shovel operations; the overburden is stripped, and the oil sands are mined; then transported to processing plants where warm water separates bitumen from sand. The bitumen is diluted with lighter hydrocarbons and upgraded to form synthetic crude oil. After mining the land is refilled and reclaimed. An advantage of the method is that it recovers about 80% of the hydrocarbon. However, only approximately 20% of the reserves, or those down to about 75 m can be accessed from the surface. It is estimated that nearly 38% of Canada's oil production will come from oil sands mining by 2015. With proved reserves of 35.2 billion barrels of oil, mineable oil sands represent slightly less than total Nigerian crude oil reserves and 50% more than total US crude oil reserves. These reserves are within an area of 3,400 km^2, along the AthabascaRiver north of the city of Fort McMurray in northern Alberta in Canada.

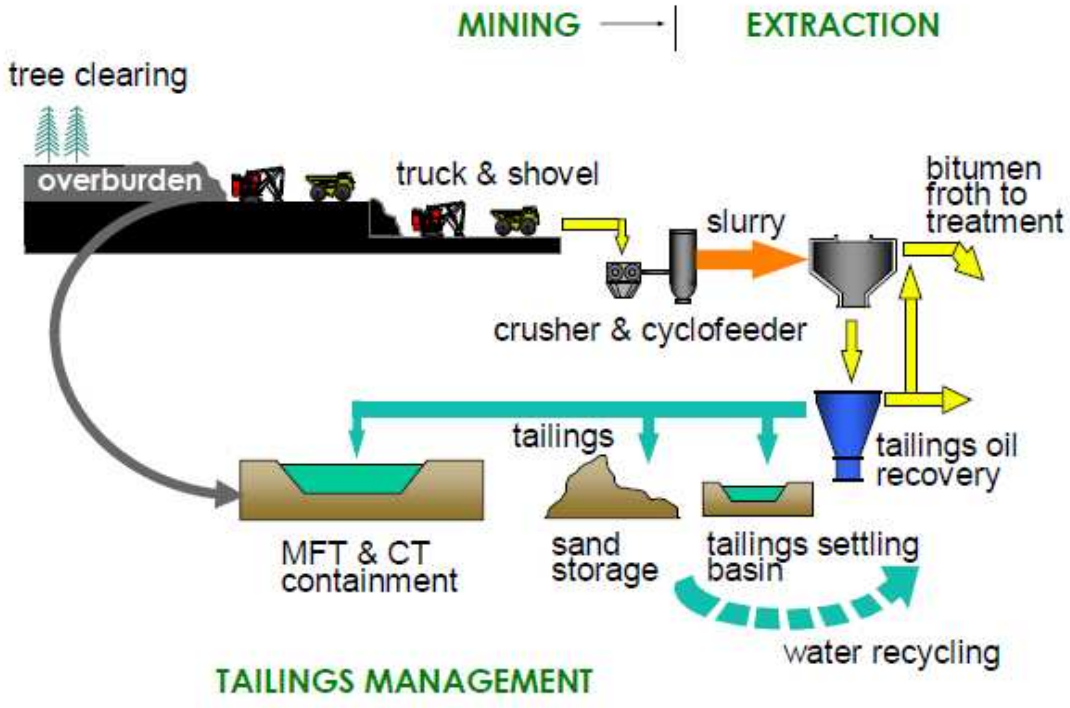

Fig. 2.5: Major Mining Based Recovery Steps

2.5.2. Cold Production

This part describes the three most commonly used methods to recover heavy and extra heavy oil at reservoir temperature. The first method is simply pumping in vertical wells. The second method is linked to the development of horizontal well technology which is now a proven and efficient technique to produce heavy and extra heavy oil. It is also widely used, regardless of oil type. As its name indicates, a third technique, called CHOPS for Cold Heavy Oil Production with Sands, favours sand production to increase the productivity of the well, followed by oil production.

2.5.2.1. Cold Production using Conventional Wells

Regardless of whether it is light or heavy, several physical phenomena occur when oil is withdrawn from a reservoir:

1) Pressure falls and oil expands.
2) Dissolved gas comes out of solution as soon as the bubble point is reached.
3) Dissolved gas flows to the wells but can also form a secondary gas cap.
4) If water is present below the oil pay, it can also flow quite rapidly to the wells.
5) Compaction of the reservoir rock is promoted, including a reduction of the pore volume.

The production mechanism associated with the first two phenomena is commonly referred to as solution-gas drive. The three others are described as gas-cap drive, water drive and compaction drive, respectively.

In heavy oil reservoirs, water drive or gas drive are not favourable since the mobility of water or gas is too high as compared to the mobility of oil. Thus the displacement efficiency is poor. On the contrary, compaction drive can have a huge impact on primary recovery of heavy oils. This is especially true when the reservoir is large and not very deep.

For many decades, most heavy oil reservoirs in California, Venezuela, Russia, etc. were produced through primary production using vertical wells until an economic limit was reached. In the 1960s, steam stimulation or flooding was used to improve oil recovery in these reservoirs. In 1990s, the implementation of horizontal wells also allowed cold production to be used to product most heavy oil reservoirs.

2.5.2.2. Cold Production Using Horizontal Wells

Horizontal wells (Figure 2.6)are differentiated from conventional wells by their larger area of contact within the reservoir. Therefore, using horizontal wells reduces the near-wellbore pressure drop that is characteristic of conventional vertical wells. This is particularly true for very thin reservoirs (a few meters thick) where a horizontal well can stay in the pay zone for the several hundred meters of its length, while a conventional vertical well will be completed only through the thickness of the reservoir.

The advantages of horizontal wells as compared to conventional wells are:

1) Increased production rates due to higher productivity.
2) Accelerated oil recovery due to these higher rates.
3) Increased oil recovery per well since very often the economic limit for producing a well is a minimum oil rate which is reached later with a horizontal well than with a vertical one.

The success of horizontal wells remained consistent since the first field-scale applications. The explosive increase in the number of horizontal wells drilled in many countries over the last two decades is remarkable. Improvements in drilling technology have led to lateral length of several kilometres with a toe placement accuracy to within a few meters.

Now "advanced wells", are also available. "Advanced wells" refers to wells that have complex geometries and architectures (Figure 2.6).

Advanced wells may be considered as a new tool in the toolbox of reservoir engineers. Instead of developing new methods to move the oil to the wellbore, the wellbore can now be cost-effectively taken to the oil by drilling as many laterals as necessary to access trapped oil. In this respect, advanced wells may be considered as an IOR (Improved Oil Recovery) technique.

2.5.2.3. Cold Heavy Oil Production with Sands (CHOPS)

In heavy oil reservoirs, promoting sand to enter the wellbore along with fluids has resulted in significant improvements in production by factors of 10 or more. [Renard G et al., 2000]. This technique is called CHOPS (Cold Heavy Oil Production with Sands) and has found numerous applications, mainly in Canada.

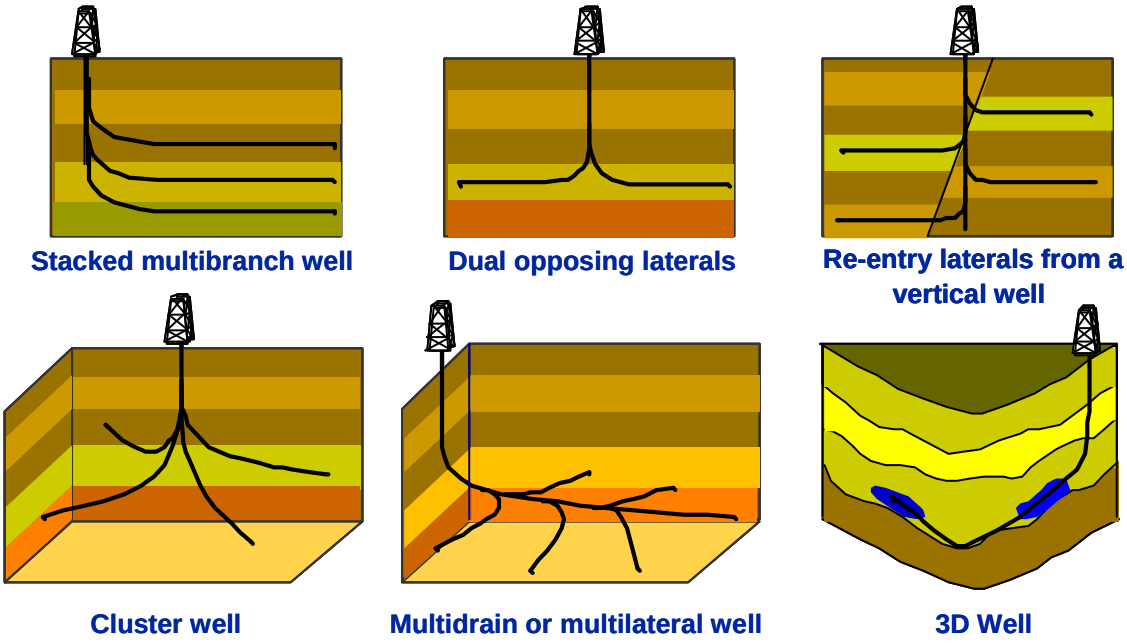

Fig. 2.6: Multilateral Well Architectures Made Possible by the Advent of Horizontal Well Technology

Four mechanisms are thought to be responsible for this surprising oil rate enhancement in CHOPS wells [Dusseault M, 2002]:

1) Fluid flow rate is increased if the sand matrix is allowed to move because the Darcy velocity relative to the solid matrix increases with matrix movement.

2) As sand is produced from the reservoir, a zone of enhanced permeability is generated and grows outward, allowing a greater fluid flux to the wellbore.

3) In a highly viscous oil, a pressure drop below the bubble point pressure leads to gas trapping and the generation of a “foamy oil” zone which is supposed to generate continuing sand destabilization and drive solids and fluids toward the wellbore.

4) Solids movement in the near-wellbore environment eliminates fines trapping, asphaltene deposition, or scale development on the formation matrix outside the casing. At the same time a large amount of sand is produced.

Voluntary sand production has been made possible by the use of Progressive Cavity Pumps (PCP). In fact, this type of pump allows for the production of effluents containing significant fraction of solids. Sand production is significant at the start of well production, possibly reaching 30 to 50% of the initial flow rate (by volume). It then gradually decreases and stabilizes at a few percent after several months. Cumulative sand production reaches several hundred – and sometimes several thousand – cubic meters after several years of production. The cause-effect relationship between sand production and improved oil productivity and

production is now understood in poorly consolidated heavy oil reservoirs in Canada [Renard G et al., 2000]: sand production drives the formation of zones of increased permeability around the wells, but the geometry of these high-permeability zones has not yet been determined well.

2.5.3. Enhanced Oil Recovery Methods

As indicated in the previous chapter, primary production of heavy and extra-heavy oils is generally limited to a few percent of Original Oil In Place (OOIP). Therefore, increasing their recovery efficiently and economically, via the implementation of specific enhanced processes, is required. The following sections describe the most salient characteristics of thermal and chemical "Enhanced Oil Recovery" processes applied by operators to increase recovery of heavy and extra-heavy oils, as well as new techniques such as SAGD (Steam Assisted Gravity Drainage) designed to recover bitumen.

2.5.3.1. Hot Fluid Injection

As indicated in Figure 2.7, high to very high viscosity of heavy oil or bitumen sharply decreases with temperature. As a general rule, and for a given increase in temperature, the more viscous the oil, the more significant its viscosity decrease. Heat injection into the reservoir via the injection of hot fluids, hot water, steam or hydrocarbon solvent is therefore one of the most widely applied techniques to decrease oil viscosity in situ and allow for better oil flow towards production wells ([Prats M, 1982];[Burger J et al., 1985];[Bavière M et al., 1991];[Sarathi PS and Olsen DK, 1992]). Reduction of oil viscosity is not the only effect of hot fluid injection. However, as indicated in Figure 2.8, viscosity reduction by heat injection is largely predominant for heavy oils.

Hot fluid injection can be performed by various methods, the details of which are described in the following sections.

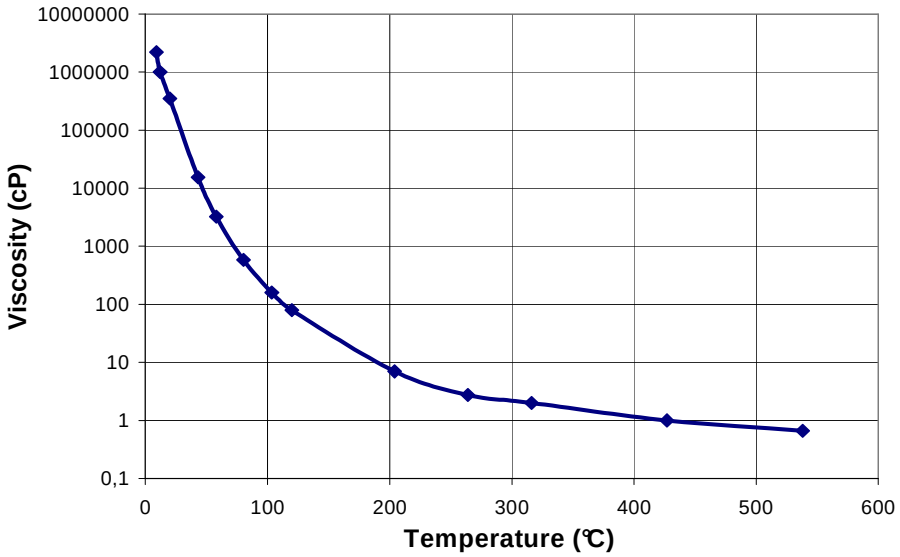

Fig. 2.7: Oil viscosity sharply decreases with temperature

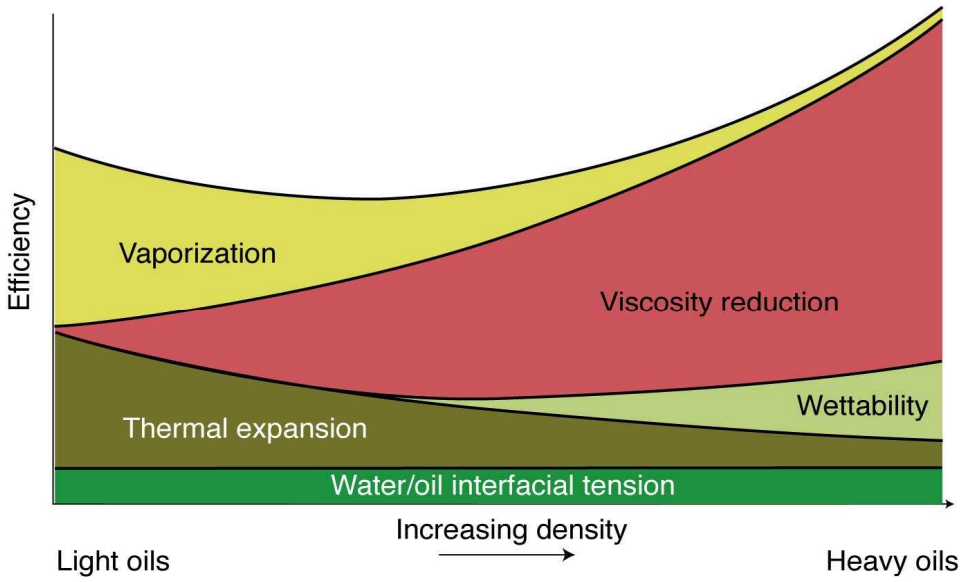

Fig. 2.8: Oil Displacement by a Hot Fluid: Contribution of Various Mechanisms [Burger *et al.*, 1985]

Hot water Injection

There has been some economic success for hot waterflooding, the most significant being at the Schoonebeek field in the Netherlands where oil viscosity at reservoir conditions is moderate. However, hot water has lower heat content than steam as the transformation of water to steam requires energy - known as latent heat - which can then be released into the reservoir as the steam condenses in order to more efficiently heat the reservoir and the fluids it contains. Furthermore, field applications of hot water flooding have been plagued by shale swelling, severe channeling and high water-to-oil ratios, generally implying low sweep efficiency. It has also been observed that the residual oil level that can be achieved with a steam flood is markedly lower than that found with hot water flood – even at the same temperature. Therefore, it seems that poor recovery efficiency makes waterflooding of very viscous crudes uneconomical even if hot water is used. For these reasons, steam injection is preferred to water injection and hot water flooding is more widely applied as a follow-up treatment to steamflooding.

Cyclic Steam Stimulation (CSS)

Steam soak - another term that is frequently used for cyclic steam stimulation (CSS) or “Huff & Puff” - was discovered as a promising production method rather accidentally in 1959 by Shell [Giusti LE, 1974] in Venezuela during early steam drive testing in the Mene Grande Tar Sands (Figure 2.9). When steam erupted at the surface due to breakdown of the overburden, the injection wells were back flowed to relieve the reservoir pressure. This resulted in high oil production rates, all the more impressive since the reservoir was unproducible by primary means.

It was concluded that injection of limited amounts of steam might be a very effective method for stimulating production of heavy-oil wells.

Following this finding, there was very rapid growth in the use of steam stimulation, particularly in several reservoirs in California: Kern River, Midway Sunset, South Belridge, San Ardo, etc, where steamflooding was used intensively afterwards.

In the CSS process, several cycles are performed in the same well, successively injector and producer. Each cycle consists of:

- An injection period - generally lasting one to three weeks - during which a slug of steam is injected into the reservoir layer.
- A soaking period of a few days during which the well is shut in to allow heat transfer from the condensing steam to the in situ fluids and rock.

- Finally, a production period allowing the well to flow back naturally and then be pumped. Production usually lasts from half a year to one year per cycle. It ends when an economic limit is reached for the oil-steam ratio or OSR, which is the ratio between the volume of oil produced and the volume of steam injected.

Usually, after two to three cycles, subsequent cycles become less effective. It is important to note that the economic limit is field-dependent.

When cyclic steam injection is used, the injection pressure is usually limited during the steam injection period to prevent formation fracturing. Imperial Oil has implemented the cyclic steam stimulation process to produce bitumen in its ColdLake field in Canada. Injection pressure is intentionally above fracturing pressure to allow steam and hot water to penetrate deeper into the reservoir. This development started with small-scale pilots in the early 1960s and has continued to large field scale, with current bitumen production in excess of 80,000 barrels per day.

Cyclic steam has been tested in horizontal wells in many reservoirs, but results have not been conclusive.

Continuous Steam Injection

Continuous steam injection - also known as steamflood or steam drive - is a process in which steam is continuously injected into one or preferentially several wells and oil is driven to separate production wells. Due to the presence of a condensable gas phase, the behavior of steam drive is very different from the behavior of water injection. The presence of the gas phase causes distillation of the light components of the oil and their movement forward toward the cold part of the reservoir. When the steam condenses, these light components do likewise, thus generating a “solvent” bank at the condensation front. Of course, oil viscosity is reduced by the temperature increase, and oil mobility is improved. Very low values of residual oil saturations (< 5%) have been reported in some field cases.

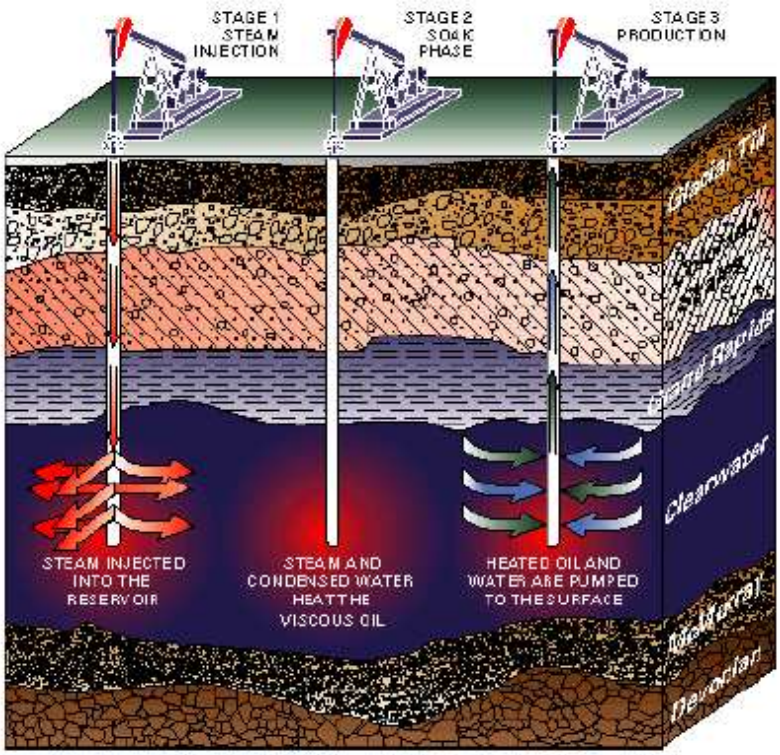

Fig. 2.9: Huff & Puff Oil Production Technology

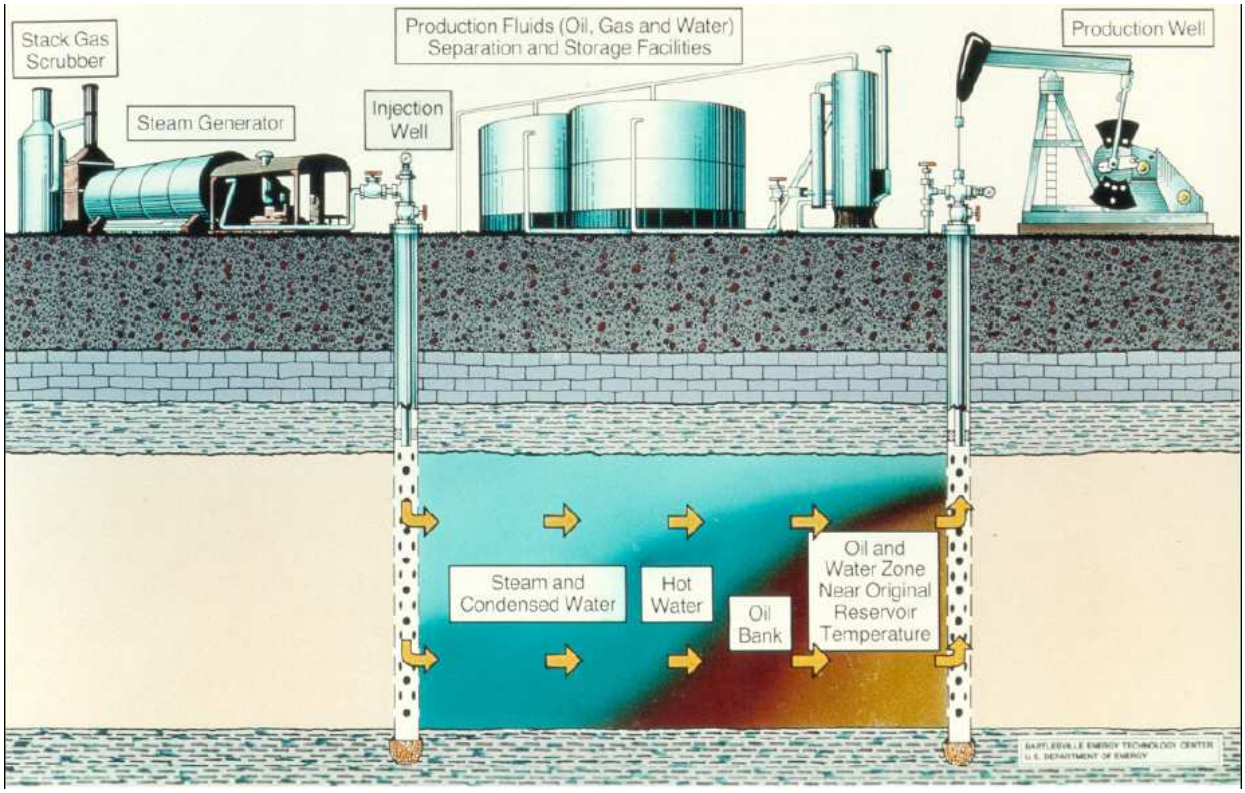

Fig. 2.10: Continuous steam injection technology

Steam Assisted Gravity Drainage (SAGD)

Butler (1981) presented an analytical model for a new horizontal steamflood technique, the steam assisted gravity drainage (SAGD) method. SAGD combined with horizontal well technology is certainly one of the most important concepts developed in reservoir engineering in the last two decades. Gravity drainage in itself is not new. However, its use to unlock heavy oil and bitumen reserves to profitable recovery was not so obvious. Butler proposed using gravitational forces assisted by steam to move oil to a production well. The geometry of SAGD, in its general form, is quite simple (Figure 2.11). This procedure relies on drilled horizontal well pairs. The well pairs are drilled horizontal, parallel and vertically aligned with each other; their length and vertical separation are on the order of 1 kilometre and 5 meters, respectively. In SAGD the growth of the steam zone is significantly affected by gravity drainage of the oil to the horizontal producer, so that the steam zone has the shape of an inverted triangle in a cross sectional view. In this model oil drains down to the production well along the sides of the steam zone.

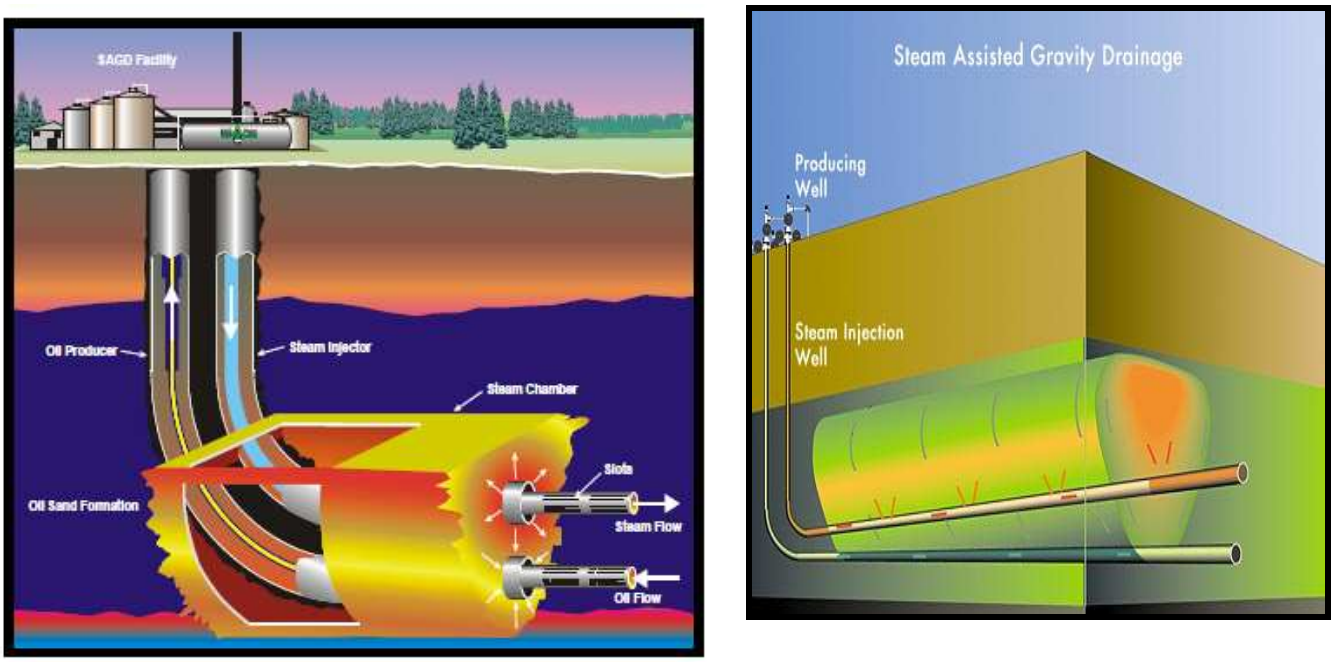

Fig. 2.11: Schematic of SAGD recovery process

Following the initial trial done in the 1980s at the UTF site (near Fort McMurray in Canada) from underground mines [Edmunds N, 1999], SAGD was first used experimentally with wells drilled from the surface in the East Senlac field in 1995 [Chakrabarty C et al., 1998]. Currently, several field-scale implementations of SAGD are currently underway in Canada.
This recovery method will be explained and discussed in details in chapter 3.

2.5.3.2. In Situ Combustion

In situ is the literal Latin term for "in place". Therefore, In Situ Combustion (ISC) is simply the burning of fuel where it exists, i.e. in the reservoir. The term ISC is applied to recovery processes in which air, or more generally an oxygen-containing gas, is injected into a reservoir, where it reacts with organic hydrocarbons acting as fuels. The heat generated is then used to help recover unburned crude (the fuel actually burned is not the crude oil but rather the carbon-rich residue resulting from thermal cracking and distillation of the residual crude near the combustion front).
With ISC, heat losses are concentrated at the fire front. ISC features thus have the potential to be more efficient and economical than the use of steam, although energy must be provided to compress the air. This energy is much lower than that required for steam generation. Moreover, the process does not require water and involves lower CO_2 emissions

2.5.3.3. Technologies in Development

There are several technologies in research, development, or pilot phase which are not yet commercial.

Polymer Injection

Waterflooding of heavy oils is often plagued by poor sweep efficiency due to the severe contrast in water and oil viscosities. To alleviate or reduce this problem, a polymer must sometimes be added to the water in order to make it more viscous.
Polymer injection is thus usually envisioned as an EOR process for which the mobility ratio between the displacing fluid (polymer solution) and displaced fluid (oil) is close to 1 (the mobility of both fluids are defined as the ratio of their effective permeability k to their viscosity μ). Thus, polymer injection has been applied in reservoirs in which oil viscosity is generally less than roughly 100 cp, the general idea being that displacing much more viscous oil would require higher-viscosity polymer solution and thus high injection pressure (higher than the reservoir fracturing pressure). The process is sensitive to temperature (polymer

degrades at high temperatures) and water salinity (high salinity reduces the polymer's viscosifying effect and thus has an impact on process economics). High permeability is also required in order to obtain sufficient injectivity for the viscous polymer solution.

With the advent of horizontal wells, it is likely that the polymer injection process could be applied in a more viscous oil reservoir where steam injection is not feasible (e.g. thin reservoirs). Recently, several pilot tests of polymer floods have been performed in the PelicanLake field [Zaitoun A et al., 1998] in Canada where the oil viscosity is roughly 1,600 cp under reservoir conditions at a depth of about 400 m. Several parallel injection and production horizontal wells have been drilled and polymer solution injected below fracturing pressure. Excellent results have been obtained to date, better than simple waterflooding in this reservoir [CNRL, 2007]. One reason for the success of this pilot test probably involves the very low effective relative permeability of the polymer solution, which was quite lower than would have been expected. The company operating the field has decided to extend the polymer flood to field scale.

Polymer flooding should thus be considered an "improved waterflooding" for heavy oil and rather than aim for a mobility ratio of 1, the target mobility ratio should be dictated only by economics.

One of the most successful polymer flood applications has been the giant Daqing field in China, where polymer flooding has been used to recover more than 300 million barrels of oil [Demin W et al., 2002] following the implementation of two successful pilots [Delamaide E et al., 1994].

CO_2 Injection

CO_2 is known for its high solubility in oils, with consequent mechanisms of oil swelling and viscosity reduction [Bavière M et al., 1991]. Therefore, CO_2 flooding has the potential to recover heavy oil, as is the case in the Bati Raman field in Turkey. On another hand, CO_2 injection can also be implemented as a single well stimulation process similar to steam Huff & Puff, as described previously. The main issue in achieving profitable applications of CO_2 flooding is its very high mobility. The lower density and viscosity of CO_2 as compared to those of reservoir oils are responsible for gravity tonguing and viscous fingering, which are more severe than in waterflooding. To limit this effect, several solutions have been investigated, such as alternating CO_2-water injection and the addition of foaming agents along with CO_2. With the advent of horizontal wells, it is likely that new well architectures will be suitable for the use of CO_2 as a good displacing agent, with the advantage of keeping a large

amount of this greenhouse gas (GHG) in situ. The issue of asphaltene precipitation for certain oils and in given thermodynamic conditions will have to be considered and carefully assessed to prevent plugging of the porous media, especially near the well bore region.

Vapor Assisted Petroleum Extraction (VAPEX)

As mentioned previously, thermal recovery processes using steam suffer from high heat losses, high water requirements, the need for extensive facilities and adverse environmental impacts. After his research on SAGD, Dr. R. Butler thus suggested using light hydrocarbon vapor instead of steam to recover extra-heavy oils or bitumen and patented a new non-thermal vapor extraction process: VAPEX [Butler RM and Mokrys IJ, 1991].

The VAPEX process is closely related to SAGD. However, in the VAPEX process, the steam chamber is replaced with a chamber containing light hydrocarbon vapor close to its dew point at the reservoir pressure. The mechanism for oil viscosity reduction is no longer the increased temperature linked to heat supplied by steam, but rather dilution by molecular diffusion of the solvent in the oil. Diluted oil or bitumen - driven by gravity - drains to the horizontal well located below the horizontal well in which the solvent is injected. If the pressure used is close to the bubble point pressure of hydrocarbons, deasphalting may in fact occur in the reservoir, leading to in situ upgrading of the oil with a substantial reduction in viscosity and heavy metal content.

A pilot test of the VAPEX process has been performed in recent years. The results of this pilot have not been officially released, but it seems that it did not perform as expected and additional research is needed to improve the process and take it to the commercial level.

Other hydrocarbons are sometimes used, in particular hot naphtha which acts via molecular and thermal diffusion, and allows for transport of the bitumen to the upgrader.

THAI and CAPRI

The Toe-to-Heel Air Injection (THAI) process [Greaves M and XiaTX, 1998] is very similar to in situ combustion. Its concept is to recover extra-heavy oil or bitumen using a vertical injector and a horizontal producer. The vertical injector is opened through the full thickness of the reservoir. Its shoe is placed close to the toe of the horizontal producer, located at the bottom of the reservoir. The combustion front generated from the vertical well should be perpendicular to the direction of the horizontal producer, and propagate through the reservoir from the toe to the heel of this well. Ahead of the combustion front, temperature is high and

oil viscosity very low. Therefore, the oil flows by gravity to the horizontal producer where it can be recovered. THAI efficiency is estimated by its inventors to be very high - up to 80 percent of the original oil in place - while partially upgrading the crude oil in situ by thermal cracking. By placing an annular layer of catalyst on the outside of the perforated horizontal well, CAPRI - an extension of THAI - has also been proposed to enhance overall upgrading of the produced crude.

THAI has many potential benefits as compared to other in situ recovery methods, e.g. SAGD. These benefits include higher resource recovery, lower capital and production costs, minimal use of natural gas and fresh water, upgraded crude oil produced, reduced diluent requirements for transport and lower greenhouse gas emissions. THAI and CAPRI have been tested at the laboratory scale, but have not yet been field-tested. A THAI field test by Petrobank is currently underway at Whitesands in Canada. Results could determine the viability of this process and its possible field-scale implementation.

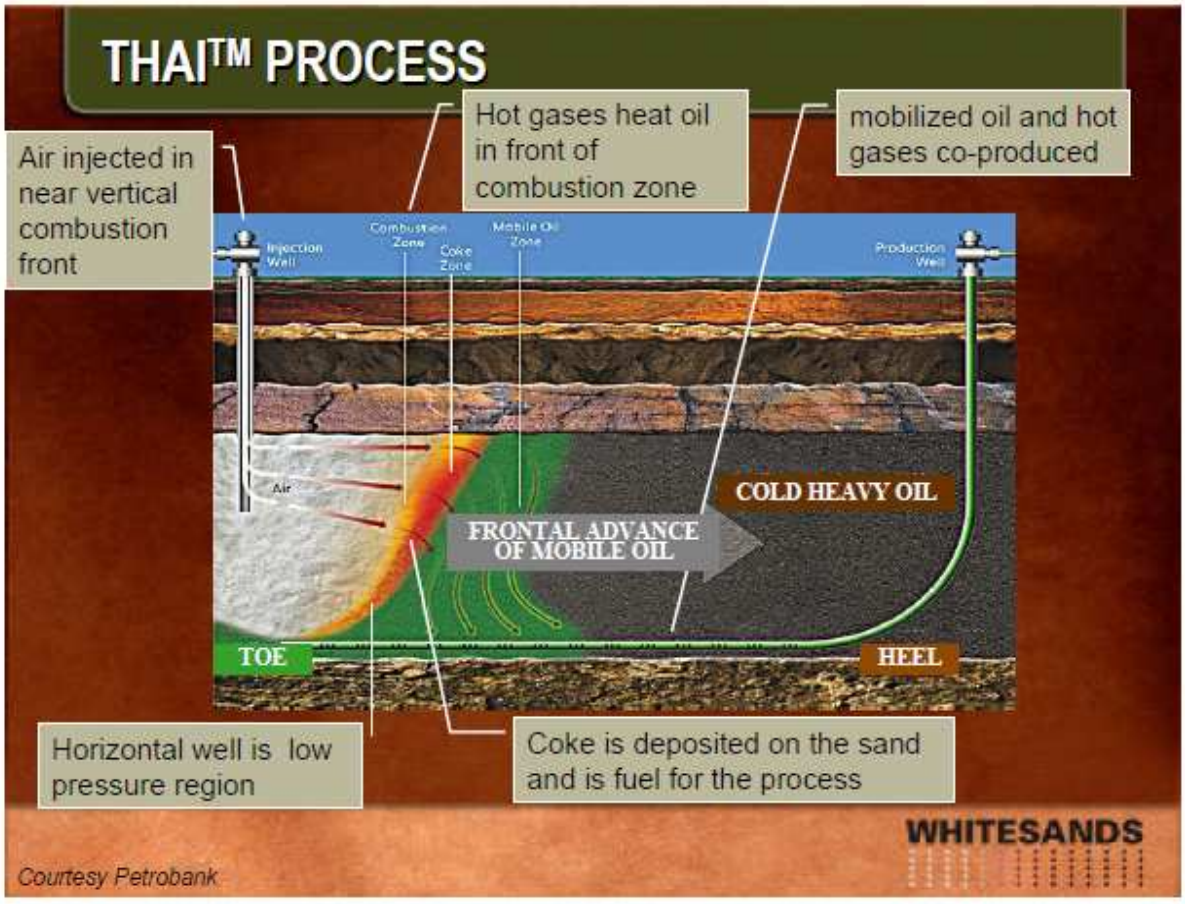

Fig. 2.12: Schematic of Thai process (Source: Courtesy Petrobank)

Hybrid Solvent and Steam Processes

By combining a solvent with SAGD, the energy requirements may be reduced, production rates increased, and recovery factor increased. In addition, capital investment, CO_2 emission, water and natural gas usage may be reduced. The solvent is injected as a vapor with the steam. Mixed with the heavy oil, it reduces the viscosity and may even provide some in situ upgrading. Pilot testing is underway in a few locations in Canada. Again, high cost and recovery of the solvent are critical to success.

2.6. Environmental Issues

Like all mining and non-renewable resource development projects, oil sands operations have an adverse effect on the environment. Oil sands projects affect: the land when the bitumen is initially mined and with large deposits of toxic chemicals; the water during the separation process and through the drainage of rivers; and the air due to the release of carbon dioxide and other emissions, as well as deforestation. Additional indirect environmental effects are that the petroleum products produced are mostly burned, releasing carbon dioxide into the atmosphere.

Air

Since 1995, monitoring in the oil sands region shows improved or no change in long term air quality for the five key air quality pollutants, carbon monoxide, nitrogen dioxide, ozone, fine particulate matter and sulphur dioxide, used to calculate the Air Quality Index. Air monitoring has shown significant increases in exceedances of hydrogen sulfide (H2S) both in the Fort McMurray area and near the oil sands upgraders.

Land

A large part of oil sands mining operations involves clearing trees and brush from a site and removing the "overburden" that sits atop the oil sands deposit. Approximately two tons of oil sands are needed to produce one barrel of oil (roughly 1/8 of a ton). As a condition of licensing, projects are required to implement a reclamation plan. The mining industry asserts that the boreal forest will eventually colonize the reclaimed lands, but that their operations are massive and work on long-term timeframes. As of 2006/2007 about 420 km^2 of land in the oil sands region have been disturbed, and 65 km^2 of that land is under reclamation. Several

reclamation certificate applications for oil sands projects are expected within the next 10 years.

Water

Between 2 to 4.5 volume units of water are used to produce each volume unit of synthetic crude oil (SCO) in an ex-situ mining operation. Despite recycling, almost all of it ends up in tailings ponds, which, as of 2007, covered an area of approximately 50 km^2. In SAGD operations, 90 to 95 percent of the water is recycled and only about 0.2 volume units of water is used per volume unit of bitumen produced. Large amounts of water are used for oil sands operations, for example Greenpeace gives the number as 349 million cubic metres per year, twice the amount of water used by the city of Calgary.

Climate change

The production of bitumen and synthetic crude oil emits more greenhouse gas (GHG) than the production of conventional crude oil, and has been identified as the largest contributor to GHG emissions growth in Canada, as it accounts for 40 million tonnes of CO_2 emissions per year. Environment Canadaclaims the oil sands make up 5% of Canada's greenhouse gas emissions, or 0.1% of global greenhouse gas emissions. It predicts the oil sands will grow to make up 8% of Canada's greenhouse gas emissions by 2015. Environmentalists argue that the availability of more oil for the world made possible by oil sands production in itself raises global emissions of CO_2.

While the emissions per barrel of bitumen produced decreased 26% over the decade 1992-2002, total emissions were expected to increase due to higher production levels. As of 2006, to produce one barrel of oil from the oil sands released almost 75 kg of GHG with total emissions estimated to be 67 mega tonnes per year by 2015.

Carbon dioxide sequestration

To offset greenhouse gas emissions from the oil sands and elsewhere in Alberta, sequestering carbon dioxide emissions inside depleted oil and gas reservoirs has been proposed. This technology is inherited from enhanced oil recovery methods, which have been in use for several decades. In July 2008, the Alberta government announced a C$ 2 billion fund to support sequestration projects in Alberta power plants (largely coal) and oil sands extraction and upgrading facilities.

Concerns of environmentalists

The environmental impact caused by oil sand extraction is frequently criticized by environmental groups such as Greenpeace. Environmentalists state that their main concerns with oil sands are land damage, including the substantial degradation in the land's ability to support forestry and farming, greenhouse gas emissions, and water use. Oil sands extraction is generally held to be more environmentally damaging than conventional crude oil, carbon dioxide "well-to-pump" emissions, for example, are estimated to be about 1.3-1.7 times that of conventional crude.

Input energy

Approximately 1.0 – 1.25 gigajoule of energy is needed to extract a barrel of bitumen and upgrade it to synthetic crude. As of 2006, most of this is produced by burning natural gas. Since a barrel of oil equivalent is about 6.117 gigajoules, this extracts about 5 or 6 times as much energy as is consumed.

Alternatives to natural gas exist and are available in the oil sands area. Bitumen can itself be used as the fuel, consuming about 30-35% of the raw bitumen per produced unit of synthetic crude.

Coal is widely available in Alberta and is inexpensive, but produces large amounts of greenhouse gases. Nuclear power is another option which has been proposed, but did not appear to be economic as of 2005. In early 2007 inCanada it was considered that the use of nuclear power to process oil sands could reduce CO_2 emissions, and they started to build a new nuclear plant at Lac Cardinal, 30 km west of the town of Peace River.

Chapitre 3

Procédé SAGD et Géomécanique du Réservoir

Le procédé SAGD (Steam Assisted Gravity Drainage) fait partie des méthodes d'injection de fluides chauds. C'est une technique de production in situ thermique qui a été conçue sur le plan conceptuel par Butler (1969) et expérimentée avec succès par Imperial en 1975.

Deux puits horizontaux parallèles superposés sont forés dans la partie basse du réservoir. La vapeur est injectée par le puits supérieur et l'huile est produite par le puits inférieur. La vapeur injectée accroît la température dans le matériau immédiatement en contact, fluidisant et mettant en mouvement le bitume. La différence de densité entre la vapeur et l'huile lourde permet à cette dernière de s'écouler par gravité vers le puits inférieur, d'où vient le terme de récupération gravitaire de l'huile. Cet écoulement des effluents (bitume et vapeur condensée) se produit le long des parois de la zone envahie par la vapeur chaude, nommée chambre de vapeur. La vapeur chaude remplace l'huile déplacée et vient de nouveau en contact avec la formation froide. La chambre de vapeur croit ainsi au cours de l'exploitation, verticalement et horizontalement.

Une phase initiale de démarrage consiste à injecter simultanément la vapeur dans les deux puits afin d'établir une connexion thermique entre eux. Cette phase peut durer quelques semaines à quelques mois. Ensuite, quand la température dans les puits producteur et injecteur est stabilisée, la mise en production est assurée par l'arrêt de l'injection de la vapeur dans le puits producteur. Après le démarrage, le brut lourd, l'eau et la vapeur condensée commence à être produits par le puits producteur inférieur. L'injection de vapeur dans le puits injecteur supérieur est continue.

Le chapitre 3 contient d'abord une description du procédé SAGD qui est basé sur le développement de la chambre de vapeur selon le modèle de Butler, avec une présentation des mécanismes de transfert de chaleur (conduction, convection) et des mécanismes de déplacement de fluides (digitation, écoulement gravitaire, émulsions). Les performances de récupération par SAGD dépendent des propriétés du réservoir comme la porosité, la

perméabilité, l'épaisseur de la couche, la teneur en gaz, la viscosité du bitume, la mouillabilité et l'hétérogénéité. Certains facteurs peuvent se montrer défavorables au SAGD : réservoirs trop profonds, hétérogénéités trop marquées, présence d'un aquifère.

Dans le procédé SAGD, de la vapeur d'eau est constamment injectée dans la formation bitumineuse. La pression de pore et la température augmentent ce qui se traduit par des changements de l'état de contrainte : l'augmentation de pression de pore diminue la contrainte effective moyenne. L'augmentation de température dilate le fluide et les grains, augmentant les contraintes horizontales alors que les contraintes verticales restent constantes. Les chemins de contrainte sont différents dans et hors de la chambre de vapeur et peuvent générer des phénomènes de cisaillement et dilatance. Des petites couches argileuses peuvent constituer des barrières imperméables et retarder l'expansion de la chambre de vapeur. L'injection de vapeur se traduit par un soulèvement du sol d'autant plus important qu'on se trouve à faible profondeur. Ce soulèvement est du à la dilatation des différentes composantes du réservoir mais aussi à la dilatance des roches peu consolidées.

D'après le modèle initial de Butler, la chambre de vapeur croît verticalement, atteint le toit du réservoir, puis croit latéralement. Le modèle analytique de Butler ne prend pas en compte la géomécanique, c'est peut être pourquoi cette description idéalisée ne correspond pas à la réalité souvent plus complexe.

Dans les premières phases du développement d'un projet SAGD, la simulation peut aider les ingénieurs à optimiser la conception du système de production, et évaluer différentes trajectoires pour les puits et le schéma de drainage. Quand le projet SAGD est mis en œuvre, une modélisation précise peut aider à optimiser la production tout au long de la vie d'un champ.

Des complétions intelligentes et une surveillance continue permettent un bon contrôle des flux d'entrées et sorties des puits en fournissant des mesures en temps réel pour la modélisation dynamique et le contrôle automatisé. Un intérêt important a été consacré à la résolution du problème d'écoulement seul en supposant un état de contrainte stable dans le système et en incorporant un terme pour rendre compte de la compressibilité du roche réservoir.

Un simulateur de réservoir conventionnel néglige l'interaction géomécanique du réservoir avec ses encaissants et suppose implicitement l'équivalence des conditions de réservoir avec

des conditions de laboratoire dans laquelle la compressibilité de la roche a été mesurée. Il en résulte une simplification grossière de la physique régissant les interactions solide-fluide.

En réalité, la mécanique des roches ou des effets géomécaniques sont intimement associés à la physique d'écoulement des fluides. Un tel couplage est un couplage dans les deux sens:

1. *Les variations de pression des fluides affectent le problème mécanique, parce que les déformations locales dépendent des contraintes effectives,*
2. *Les déformations du milieu modifient la porosité et les propriétés d'écoulement.*

Dans un simulateur de réservoir traditionnel les contraintes sont supposées rester constantes tout au long de la simulation et toutes les propriétés sont des fonctions de la pression (et de la saturation en cas d'écoulement polyphasique). La compressibilité de la roche, quantité scalaire, est utilisée pour rendre compte de la réponse complète tensorielle de l'état de contrainte et de rigidité du matériau. En réalité, ce terme la compressibilité de roche dépend des conditions locales et des conditions aux limites dans le réservoir et est également influencée par les chemins de contrainte suivis.

La modélisation géomécanique est un domaine de recherche exploré par de nombreux chercheurs pour prédire l'évolution simultanée du volume des pores et de la perméabilité du réservoir résultant de l'injection de vapeur..

Ce chapitre contient une revue des simulations numériques possibles du SAGD, avec différents schémas de couplage réservoir géomécanique

Suivant le degré de couplage entre les écoulements de fluide dans le réservoir et la géomécanique, les simulations peuvent être divisées en quatre catégories: non-couplées, découplées, couplées de manière séquentielle et totalement couplées, La solution non couplée désigne la simulation de réservoir classique, qui intègre la compressibilité de roche comme le seul paramètre à considérer dans les interactions entre les fluides et des solides.

Le découplage ou solution dite « one-way » inclut généralement l'histoire complète du temps de simulation réservoir suivie par une simulation géomécanique, mais ne prend pas en compte le retour des effets géomécaniques vers la simulation de réservoir.

Le couplage séquentiel contient à la fois le couplage explicite et le couplage itératif. Dans le couplage séquentiel, les deux ensembles d'équations sont résolus de manière indépendante,

mais l'information est transmise dans les deux sens entre les deux simulateurs. Les équations de contraintes sont résolues de manière séquentielle à chaque pas de temps ou d'itération. Ensuite, les paramètres modifiés du réservoir par le comportement géomécanique sont substituées dans les équations d'écoulement pour continuer à l'étape suivant. Le couplage séquentiel présente des avantages certains : flexibilité, modularité, facilité relative de mise en œuvre, et meilleure efficacité de calcul. Le couplage itératif est essentiellement équivalent à une méthode de Newton-Raphson modifiée. Lorsque le processus itératif converge, la solution itérative tend vers la vraie solution du problème couplé.

La simulation entièrement couplée résout simultanément les équations d'écoulement et les équations mécaniques basées sur un système de grille unifient. Toutefois, dans l'approche totalement couplée, les mécanismes hydrauliques ou géomécaniques sont souvent simplifiés par rapport aux approches conventionnelles découplées géomécanique et réservoir.

Dans l'approche couplée séquentielle les équations de la mécanique et des écoulements sont résolues séparément pour chaque pas de temps, mais l'information est transmise entre le réservoir et les simulateurs de géomécanique. Par conséquent, les problèmes de réservoir et géomécaniques doivent être reformulés en fonction du problème d'origine entièrement couplé. Contrairement à l'approche totalement couplée, le couplage séquentiel semble plus flexible et intègre les avantages du haut développement de la physique et des techniques numériques à la fois du simulateur de réservoir et le logiciel mécanique.

Étant donné la nature du pétrole lourd, les simulateurs de réservoir doivent être capable de prendre en compte une variété de comportements complexes comme le thermique, la présence de solvants ou de grandes contraintes géomécaniques.

Enfin, ce chapitre illustre l'importance de la prise en compte de la géomécanique dans le processus SAGD par deux exemples: Hangingstone et Joslyn correspondant à deux cas typiques d'exploitation en Alberta. Le cas d'Hangingstone met en évidence l'influence de barrière argileuse sur le développement de la chambre de vapeur. Le cas de Joslyn illustre un cas de rupture de la couverture sous l'effet de l'injection de vapeur.

Chapter 3

SAGD Process & Reservoir Geomechanics

3.1. Steam Assisted Gravity Drainage Process

3.1.1. Background & History

As the viscous bitumen can barely flow under reservoir conditions, the bitumen viscosity must be reduced and then a sufficient drive must be applied to the mobilized bitumen for continuous well production and in-situ recovery. Thermal recovery involving injecting hot fluids such as water and steam into the reservoir has been used for several decades to reduce viscosity and enhance the mobility of the bitumen in place. The force of gravity, which exists universally, can be utilized to drive mobilized bitumen.

Butler is the unassuming 'father' of SAGD, inventor of what has become the most commercially effective technology to extract tar-like bitumen of Alberta oil sands operations. He perfected much of the SAGD process from 1969 to 1995, when he held the first Endowed Chair in Petroleum Engineering at the University of Calgary. Butler was working with Imperial Oil Ltd. in the mid-1960s, when the company discovered a huge heavy oil deposit at ColdLake. Prior to that, he had worked on a process for mining potash deposits in Saskatchewan. It involved injecting fresh water underground, creating a large, turnip-shaped chamber and dissolving the surrounding potash and salt. The heavier brine would fall to the bottom of the chamber while the lighter injected water would rise to the top. Butler says: "I was really very impressed with the mechanism of this". He recalls he was in a restaurant enjoying a beer with a friend when he thought of injecting steam underground through one well to heat the molasses-like oil at ColdLake and create a steam chamber. The heated oil would drain to the bottom of the chamber where another well would pump it to the surface. He wrote a patent memo on his gravity drainage concept in 1969. But it was not until 1975, when Imperial moved him from Sarnia to Calgary to head up its heavy oil research effort, that he really pursued the idea. Butler figured out how much oil could be recovered by injecting

steam down one vertical well, letting the reservoir heat up and drain, then pumping the recovered oil to the surface through another vertical well. Butler concluded that the oil, trickling through sand under the force of gravity, would fall in an ever-narrowing convergent cone, and the sand would plug up the cone of the vertical well used to pump oil to the surface. To solve the problem, he would drill a horizontal production well low in the reservoir. Instead of one vertical well that drained oil into a single cone, he would create numerous drainage points along the entire length of the horizontal well to capture the oil. He says: "I could get a thousand barrels a day out of one of these wells on my paper calculations". In 1978, Butler persuaded Imperial to drill HWP1 at ColdLake – the world's first modern horizontal oil well paired with a vertical steam-injection well. The horizontal well was about 150 metres long, compared with SAGD wells today that are typically about 800 metres. But, says Butler: "The oil came out at about the right rate – I felt pretty damn good!" Butler took early retirement from Imperial and worked at the Alberta Oil Sands Technology and Research Authority for a year, where he proposed testing SAGD at AOSTRA's underground test facility (UTF) near Fort McMurray. In 1983, his appointment to the University of Calgary's Endowed Chair in Petroleum Engineering allowed him to focus his research on developing SAGD for producing bitumen from the Athabasca oil sands. He also invented a separate gravity-drainage process called VAPEX, which uses vaporized solvents instead of steam to loosen the heavy oil so it will flow.

On a map of Alberta's existing and planned SAGD projects, he points out EnCana Corp.'s advanced SAGD projects at Foster Creek and ChristinaLake, Petro-Canada's MacKayRiver project, ConocoPhillip's Surmount, Suncor's Firebag, OPTI Canada/Nexen's LongLake – in addition to more than a dozen smaller operations. In total, an estimated 600 billion barrels of oil in the Athabasca oilsands are accessible thanks to Butler's invention, with about 330 billion barrels recoverable with current techniques.

3.1.2 Actual Concept of SAGD

In conventional steamflooding, as seen in the previous chapter, the oil that is displaced by injected steam is cooled ahead by in place fluids and is hard to push towards the production well. In SAGD, the oil remains heated as it flows around the steam chamber. Butler developed the gravity drainage theory that predicts the rate at which the process will occur and confirmed the viability of the concept by lab experiments.

As Figure 3.1 illustrates, the steam is injected through the upper well and the fluids, including the condensed steam and the crude oil or bitumen, are produced from the lower one. The injected steam heats the bitumen and sands in the reservoir, and reduces the viscosity of the bitumen. The condensed steam and bitumen flow downwards towards the lower horizontal well and are recovered at the surface by artificial lift or gas lift.

Butler (1991) developed the flow equations and analytical models to predict production by the SAGD process. The key variables were the steam chamber height, oil viscosity at steam condition, oil saturation, and oil rate. In practice, the initial production was usually estimated using Butler's analytical model and reservoir simulation. It was reported that the theoretical prediction agreed well with the homogenous reservoirs and model experiments and real production (Birrell et al. 2005).

Some assumptions were made in Butler's (1981) analytical models. Heat was assumed to transfer beyond the interface by thermal conduction, and the interface was assumed to be at steam temperature. The total drainage flow was obtained using Darcy's equation and gravity driving force. One end of the interface curve remained attached to the production well and the other end spread to a vertical no-flow boundary located half way to the next adjacent wells, which indicated no interfering relation among steam chambers from neighbour well pairs.

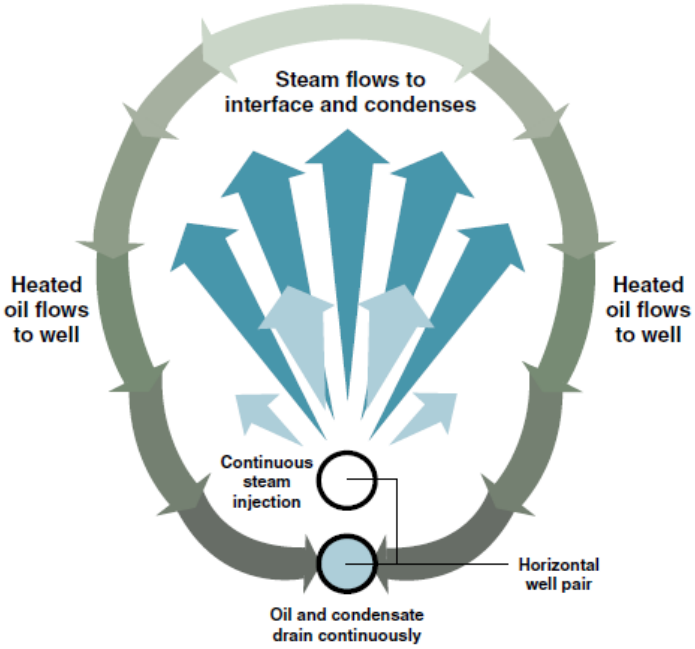

Fig. 3.1: Schematic of SAGD Process (THE WAY AHEAD-Medina, 2010)

It is commonly agreed that a steam chamber is generated and rises upwards steadily during a SAGD operation. When it touches the top of the formation, it spreads towards both sides gradually. The steam chamber's growth is mainly measured and analyzed through the temperature changes at observation wells. The unique features of SAGD are:

- Use of gravity as the primary motive force for moving oil.
- Large production rates obtainable with gravity using horizontal wells.
- Flow of the heated oil directly to the production well without having to displace uncontacted oil.
- Faster oil production response as compared to steamflooding (especially when the heavy oil is initially mobile at reservoir conditions).
- High recovery efficiency (up to 70% of OOIP) - even for bitumen.
- Low achievable Cumulative Steam Oil Ratio (CSOR) due to the large potential injection/production rates limiting the heat losses (can be lower than 2.0 m^3/m^3 with steam at 80% quality).
- Low sensitivity to limited shale intervals and interbedding.

In order to validate the concept of SAGD, the UTF project (Undergroung Test Facility) was initiated by the Alberta Oil Sands Technology and Research Authority (AOSTRA) in 1984 at Fort McMurray. The AOSTRA and nine industry partners funded and participated in this UTF project. The test consisted of three pairs of 60 m long horizontal injectors and producers, which were drilled from a tunnel. The steam injection well was placed 5 m above the producing well which was located 1-2 m above the limestone under-burden. This was the first successful field demonstration of the SAGD process and it provided sufficient data to guide the commercial application.

The SAGD process at the AOSTRA UTF had proven that the process mechanisms worked in the field as expected. The horizontal wells in Phase B were placed on production in 1988. The successful application of UTF encouraged oil operators to apply this thermal recovery to Athabasca bitumen. Since then, SAGD technology for heavy oil and bitumen recovery has been applied in full-scale commercial operations in Alberta and Saskatchewan, such as ChristinaLake by EnCana, Firebag by Suncor, MacKayRiver by Petro-Canada, Mic Mac and BurntLake by CNRL, and LongLake by OPTI Canada (Butler 2001).

Attempts to apply the SAGD process in different types of reservoirs have been made in the last decade. This technology has been widely evaluated through numerical simulations and field tested in some other countries (Sedaee 2006, Albahlani et al. 2008).

3.1.3 Implementation of the SAGD Process: Phases Involved

Four important phases during SAGD must be performed carefully in order to complete a successful operation:

3.1.3.1 Drilling and completion

Drilling must be handled carefully in order to drill the production and injection wells at a constant distance from each other, insofar as possible. For long drains in such close proximity, a new technique to pilot the wells had to be developed in order to prevent the wells from intersecting each other. The injection well is thus drilled relative to the production well.

3.1.3.2 Start-up

The start-up phase is critical for the future results of a well pair when oil viscosity is very high and does not allow initial flow of fluids (steam, water or oil) between the injector and the producer. Thus, the start-up consists in pre-heating the interval between the injection and production wells to allow the oil to flow towards the producer by gravity. This is achieved by steam circulation both in the injector and producer for a period of several weeks to several months. In the East Senlac field, oil is mobile at reservoir conditions, so it is possible to inject steam directly into the reservoir after a short preheating period.

3.1.3.3 Steam chamber monitoring

After start-up, steam injection is controlled to maintain a constant pressure in the steam chamber; total production - as well as pressure at the production well - are also monitored. The producer and injector wells can be equipped with optic fiber cables throughout the length for temperature monitoring. The temperature profiles along the wells is of great help todetermine the chamber geometry. Observation wells with thermocouples and pressuretransducers can be used to monitor pressure and temperature (Fig. 3.2)

3.1.3.4 Production

Gas lift is sometimes used to activate the production well, involving technical issues associated with the unstable phenomenon of geysering. As hot fluids are flowing to the surface, production water flashes in the tubing under lower pressure and high temperature, decreasing the average fluid density and reducing the need for gas in the gas lift. The lift rate must therefore be monitored carefully since it has a direct impact on production and thus on the operations of the well pairs.

Numerical modeling is important to evaluate and optimize an SAGD operation (Egermann P et al., 2001), as illustrated in Figure 3.3. Use of dynamic sub-gridding, with fine grid blocks to discretize the steam chamber interface, can help to decrease the high CPU time usually required to perform 2-D or 3-D SAGD computations (Lacroix S *et al.*, 2003).

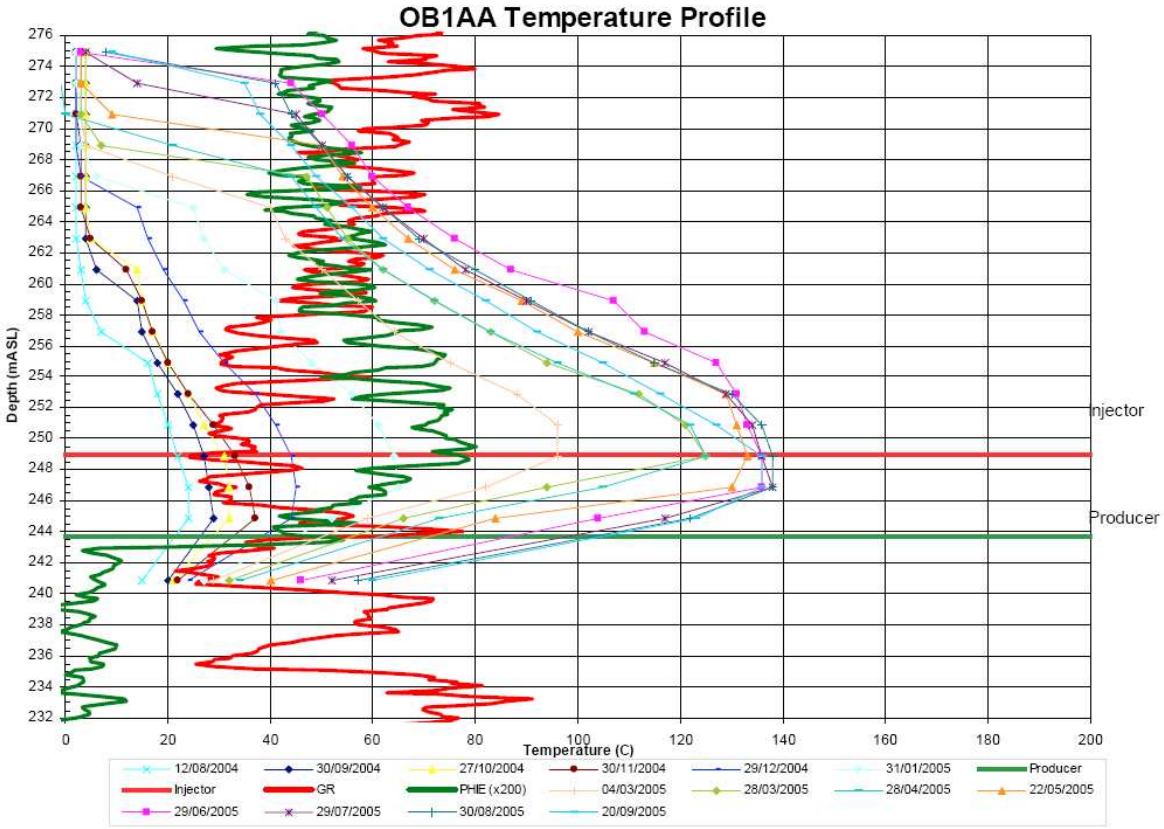

Fig. 3.2: Example of observation well temperature data (Deer Creek, 2005)

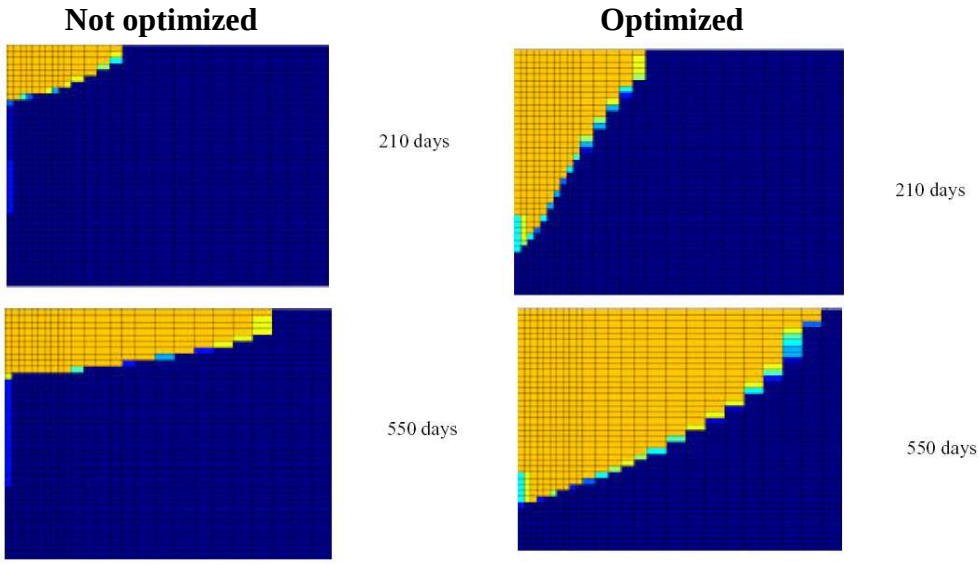

Fig. 3.3: Modeling of Celtic SAGD
Steam Saturation versus Time (2D XZ view) [Egermann P et al., 2001]

3.1.4. Well Construction

Directional-drilling technology evolution has been a key enabling factor in the commercial implementation of SAGD. Two parallel horizontal wells are drilled to vertical depths between 90 and 600 m, with 4 to 7 m of vertical offset and up to 1000 m of horizontal displacement. Due to their shallow vertical depths, some of these wells require slant drilling from the surface. Typically, the production well is drilled first and placed as close as possible to the bottom of the reservoir. In 1993, the technology to drill parallel horizontal wells was developed. The first SAGD well pair was drilled using magnetic-ranging/- guidance technology, which refers to the measurement of the relative position of one well with respect to another. It determines the distance and orientation from the well being drilled (injector) to the reference well (producer). The determination is based on measuring the magnetic signature from the target/reference well, which may be induced and measured by several methods (Grills 2002). SAGD wells must be designed to withstand the harsh environment of this process. Integrity and reliability must be balanced with the requirement to minimize capital expenditure. Typical SAGD well designs are shown in Figure 3.4. The intermediate casing is the main barrier for isolating the bottom-hole SAGD environment from the surface. Therefore, the selection of adequate cement for thermal conditions and proper thermal casing design (steel and connection selection) are critical (Kaiser 2009).

Well-completion designs can vary between operators and even within projects. The industry is still in an evaluation phase, and different completion configurations are being implemented. However, the general trend is to allow for steam injection or bitumen production at two or more points along the horizontal wellbore. As illustrated in Figure 3.4, the typical completion designs are dual parallel, or concentric, strings with tubing and annulus flow paths.

The unconsolidated nature of the sandstones in which most SAGD projects are carried out has led to the requirement of sand control in both wells. Slotted liners are the most widely used sand-control method, with standalone screens a distant second. This preference probably reflects the lower cost of slotted liners, along with research efforts (Kaiser et al. 2002) that have improved their design and performance. However, as more challenging reservoirs are targeted and more operational issues arise, the industry continues to seek other competitive sand-control options. The integrity of the production liner is crucial to avoid sand production.

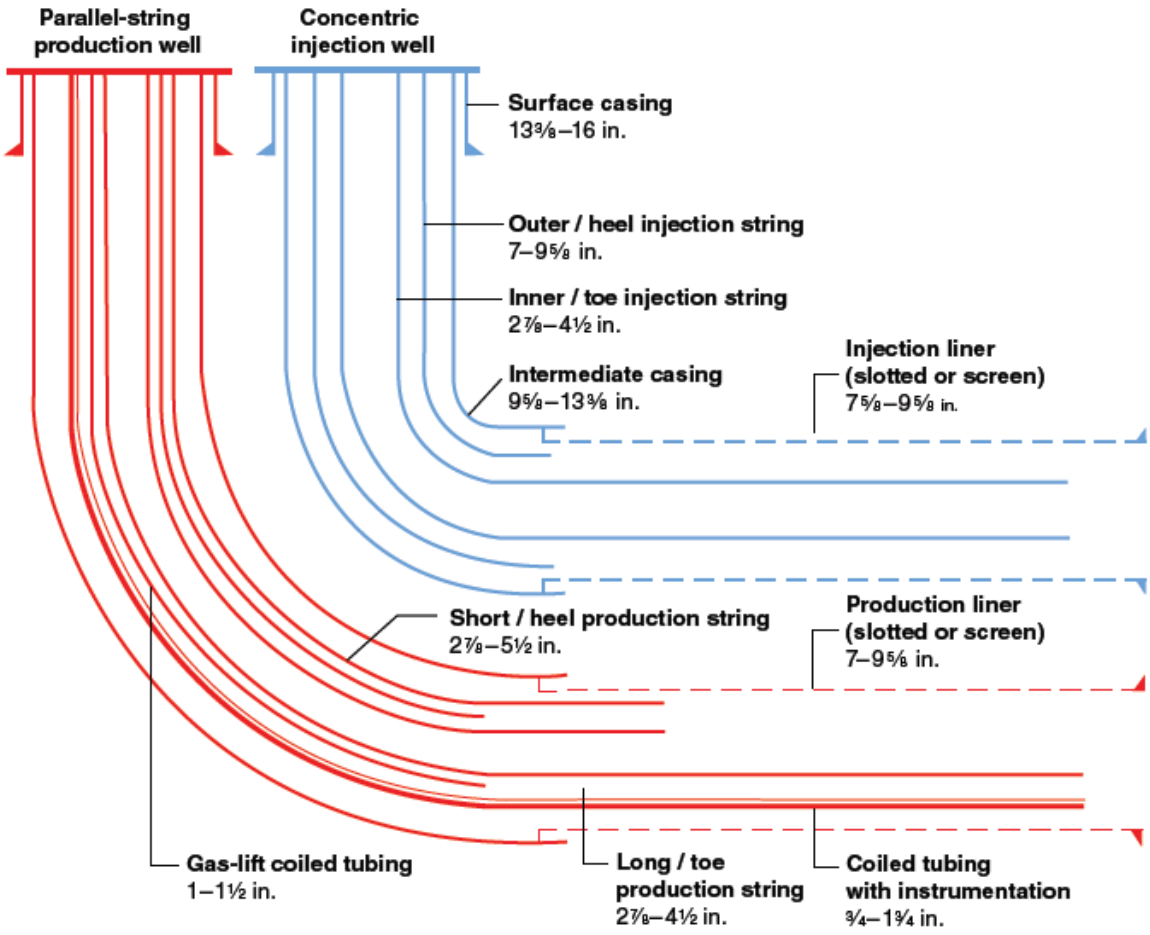

Fig. 3.4: Typical SAGD well configuration

3.1.5. Production Operations and Control

SAGD operations require monitoring strategies aimed at controlling the downhole process, to avoid operational issues and maximize efficiency and recovery. Producer wells are fitted with multiple temperature-measuring devices along the horizontal wellbore.

Thermocouples are the preferred choice because of their reliability and lower cost; however, fiber-optic technology has been field tested widely and implemented as well. Pressure monitoring is also employed in producer wells through bubble tubes, open annulus gauges, or, more recently, fiber-optic gauges. Typically, the injector wells have less instrumentation.

The main objective of temperature monitoring in the producer well is steam-trap control. The goal is to maintain the steam/liquid interface between the wells. This is achieved by managing the difference between the producer bottomhole temperature and the saturated-steam

temperature at the injector bottomhole pressure (subcool) to maintain a balance that keeps the interface between the wells. Optimum SAGD requires the steam chamber to be drained so that liquid does not accumulate over the producer—reducing production rates—but avoiding steam production because it jeopardizes the integrity of the producer well (Edmunds 1998).

Monitoring steam-chamber development is the single most important task for understanding the SAGD process and diagnosing recovery efficiency.

Along with real-time in-well monitoring, the following methods are combined to estimate steam-chamber growth:

• Fully instrumented vertical observation wells along the horizontals at each pad

• Surface-deformation measurement technologies, such as heave movements, tiltmeters, and interferometricsynthetic- aperture radar

• Seismic methods, such as 4D and microseismic mapping

• Production history matching

The steam-chamber operating pressure can also be controlled to improve efficiency and recovery. However, this will also affect the selection of the produced-fluids' lift method. During the initial SAGD operation phase, most projects operate at pressures high enough to use steam or gas lift (Medina 2010, Kisman 2001). The use of gas lift for SAGD has features that differ from its conventional applications and requires proper assessment to assure success (Medina 2010). As the SAGD project matures, the tendency is to operate at lower chamber pressure, which requires different artificial-lift methods. In recent years, R&D efforts in high-temperature mechanical-lift equipment have resulted in the ability to pump high volumes of fluids at elevated temperatures (220–260°C) with tolerance to steam, gas, and sand/fines production.

Most installations have involved "state of the art" electrical submersible pumps and metal progressive-capacity pumps.

3.1.5.1. SAGD: Favorable Factors

Factors that are favorable for SAGD include (Palmgren and Renard, 1995):

- Sufficiently thick reservoir (i.e. greater than 12 m [50 ft]) to allow the creation of the steam chamber. The well pair is located at the bottom of the reservoir, a few meters from each other.

- High permeability both in horizontal and vertical directions (i.e. greater than 1.5 Darcy). Steam chamber development needs high permeability.

Most SAGD applications are on shallow, unconsolidated sandstone reservoirs with high permeability. However, recently a significant quantity of heavy oil has been identified in Alberta's carbonate Grossmont formation, which some believe can be economically exploited with SAGD. Reservoir screening criteria have been the subject of some debate in the industry (Albahlani and Babadagli 2008). However, there is a general agreement that resource quality remains the most critical factor in SAGD project performance. Net-pay thickness, oil saturation, and porosity are the main properties required to estimate the reserve base of a project and forecast recovery factors. Vertical permeability can also influence the effectiveness of the recovery process. For example, the presence of shale layers, or breccia, within the sandstone formation can hamper the rise of the steam chamber and/or the producer/ injector communication, if located between the injector and producer wells. The overburden, or cap rock, has special relevance for most SAGD projects. It must provide a barrier to prevent the loss of steam to shallower strata or, in the worst case, to surface.

The geomechanical competence of the cap rock must be carefully assessed. If the overburden allows for leakage of steam to surface, it will be a catastrophic accident resulting in serious impact to the environment and safety. If the steam leaks to shallower strata, it would seriously affect the expansion of the chamber and, thus, thermal efficiency and ultimate recovery.

The presence of top or bottom water and/or gas caps must be considered in the SAGD development plan. Ongoing research is improving our understanding of how these fluid interfaces affect thermal efficiency bitumen recovery (Edmunds and Chhina 2001).

3.1.5.2. SAGD: Detrimental Factors

Factors that are detrimental for SAGD include:

- Reservoirs which are too thin hinder the development of an optimal steam chamber and induce highly detrimental heat losses towards the overburden. Steam chamber monitoring would also be very difficult to prevent steam breakthrough at the production well.
- Reduced vertical permeability which does not allow the flow of fluids (condensed steam and water) to the lower producer at a sufficient rate since recovery is controlled by gravity.

- Presence of significant heterogeneities. Barriers to the flow of steam or hot fluids along the steam chamber can limit process efficiency. There are no published studies on the minimum size of heterogeneities above which SAGD is no longer attractive. Numerical modeling on a case-by-case basis is required to investigate their real impact.
- High pressure associated with deep reservoirs (i.e. greater than 800 m [2,600 ft]). The higher the reservoir pressure, the higher the operating costs and the lower the latent heat of steam available to heat the rock and in place fluids.
- Presence of a bottom aquifer. However, SAGD can be successfully operated even with an aquifer present below the oil zone. Numerical modeling is required to design a project (placement of wells, flow rate for injection and production, etc.).
- Presence of a gas cap. This is qualified as a thief zone since the gas cap can act as a sink for injected steam. Here again, a project can be successfully implemented by optimizing the process via numerical modeling to determine the pressure at which it must be operated.

3.1.6. Performance and Challenges

Most companies have their own evaluation methods for SAGD performance. However, steam oil ratio (SOR) is commonly used as the key performance indicator to benchmark project efficiency.

SOR indicates the volume of steam required to produce a certain amount of oil. Although it does not truly reflect energy-use efficiency, it remains a widely used industry metric. The aim is to minimize SOR, where values in the 2.0 to 3.5 range are considered good performance. Currently, the best performing SAGD projects by this criterion are: Devon's Jackfish, Cenovus' Foster Creek and ChristinaLake, and Suncor's Firebag projects. (Medina, 2010)

Other performance indicators are bitumen production rates and recovery factors. The industry average bitumen production per well pair is between 400 and 1,000 bbls/day with ultimate recovery factors higher than 50% (Medina, 2010).

The current trend for most commercial projects is to increase the thermal efficiency and bitumen recovery of the process through enhanced techniques or SAGD variations, such as non-parallel-well geometrical configurations, additional wells, solvent injection, steam-distribution optimization, and inflow control.

Despite the successful commercial implementation of SAGD technology, the industry still has two major challenges to overcome: dependence on natural gas and environmental impact. Most SAGD projects still rely on natural gas as the energy source for producing steam.

The volatility of natural-gas prices, especially in North America, and the long-term supply uncertainty directly impact the economic performance and overall feasibility of SAGD projects.

Finally, SAGD's carbon footprint and water requirements are quite substantial, mainly due to the steam generation process. Cogeneration, brackish-water use, water recycling, and other enhancements are being implemented or considered to minimize the environmental impact of SAGD. However, additional efforts are required because more stringent regulatory requirements are likely forthcoming. Furthermore, negative perception of SAGD by a portion of the general public remains an important driving force to clean up the image of SAGD and guarantee the sustainable development of the technology.

3.1.7. Suggested Improvements to Original SAGD

As for other processes involving steam injection, SAGD suffers from the need for large volumes of water to generate steam (typical production results indicate that 1 cu. m of oil requires at least 2.5 cu. m or more - currently up to 4 cu. m - of water). Steam generation, on another hand, is a source of a large amount of CO_2 production. It has been determined that production of 16,000 m^3/d (100,000 bopd) of bitumen with an SOR of 2.5 m^3/m^3 would produce 14,300 t/d of CO_2. To reduce the amount of steam - or more generally reduce operating costs - several improvements to the SAGD process have been proposed and tested [Shin and Polikar, 2004]:

3.1.7.1. Single Well SAGD (SW-SAGD)

This technology uses a single horizontal well to inject steam and produce oil instead of two horizontal wells as in the conventional SAGD, also referred to as Dual Well SAGD. The single horizontal well is located at the base of the reservoir. Steam is injected into the insulated tubing and fluid production flows through the annulus. SW-SAGD has been tested in several Canadian fields but has not been extended to field scale and therefore its viability is still questionable.

3.1.7.2 Operational Improvements

In order to enhance operation performance and reduce the high cost associated with drilling and completion of two horizontal wells, industry has sought alternatives since the first SAGD field trial. Based on literature, most efforts were focused on the adjustment of the SAGD well configurations. Some others were trying to utilize the heat remaining in the reservoir to improve SAGD performance.

There are two methods reported in public literature related to SAGD enhancement. One is to employ specific operation schemes with a classic dual well. Another is to apply differential pressure on the wells. Two types of differential pressure (DP) occurring in the SAGD operation include the DP between the injector and producer, and the DP between pairs of SAGD wells.

SAGD performance is associated with operational conditions, which can be optimized through running numerical simulation to enhance performance in terms of oil production rate, steam-oil ratio (SOR), and cumulative steam-oil ratio (cSOR). Numerical simulation indicated that the cSOR decreased with increasing injection rate (Shin et al. 2007).

Operational optimization can be obtained through adjusting the steam injection rate and the producer liquid withdrawal rate during different SAGD operation periods. Yang et al. (2007) presented an example to quantitatively assess the uncertainty of its economic forecast on a real field case from application of experimental design to response surface generation. The results showed that the economics of this project were improved considerably through optimization. The optimum operating conditions obtained use a high initial steam rate and high production rate to develop the steam chamber. After the instantaneous steam-oil ratio reaches a certain value, both steam rate and production rate are lowered to prevent steam breakthrough to the bottom water.

In the classic SAGD, the steam is injected continuously through the injection well. There is considerable energy existing in terms of higher temperature even when steam injection is shut in after operation for some time. The steam chamber will continue to spread for a while. To efficiently utilize the existing heat in the reservoir, the concept of seasonal or cyclic exploitation was proposed for energy saving and seasonal adjustment (Birrel et al 2005). This operational strategy indicated that the oil production could be controlled through the amount of injected steam. Based on the bitumen and gas prices, the operational strategy could be adapted to gain optimal return.

Based on a numerical simulation, Vanegas et al. (2005) suggested that higher differential pressure (DP) induced higher oil flow rate peaks especially in warm regions. A preferential

flow path between the wells should have been avoided when DP was applied to the SAGD operation. This indicated that too large a DP would be detrimental to the operation (Albahlani and Babadagli, 2008).

3.1.7.3. Steam and Gas Push (SAGP)

This recovery method was introduced to enhance SAGD efficiency by adding a small amount of non-condensable gases (NCG) such as natural gas or nitrogen. The effect of the NCG is to reduce the amount of steam to be injected. However, the timing of the NCG injection is very important. When it is done during the steam chamber rising period, cumulative oil production and oil rate are decreased.

When the gas is injected during the late period of the SAGD process, the process is also referred to as SAGD Wind-down. At this time, the SOR can be reduced without severely reducing oil production since the injected NCG gases rise to the top of the reservoir and then help the steam chamber to propagate horizontally. The reservoir is still hot and the energy in place can be utilized.

Scaled model experiments and numerical simulations indicated that the NCG gas tended to accumulate in the steam front in the SAGD process. Yee et al. (2004) observed and measured for the first time a significant amount of gas that travelled ahead of the apparent top of the steam chamber.

Therefore, the presence of non-condensable gas would impede steam chamber expansion and reduce oil production in the SAGD operation. The impact of NCG gas on the SAGD operation was that the oil sands with a lower GOR were likely to be recovered more easily than those with a higher GOR. Ito et al. (2005)'s simulation study showed that steam chambers had greater height for dead oil than those for live oil with solution gas.

However, field evidence in North Tangleflags operated by Sceptre Resources (now CNRL), indicated a higher initial GOR of 11 std. m^3/m^3 did not show a negative impact on the SAGD operation when compared with classic Athabasca reservoirs that had a GOR of 1-3 std. m^3/m^3. Yee et al. (2004) and Kisman et al. (1995) advised that the presence of a moderate amount of solution gas should be beneficial to the recovery process.

There were several other publications (Bharatha et al. 2005, Canbolat et al. 2004, Gates et al. 2005) discussing the effect of non-condensable gas on SAGD performance.

3.1.7.4. Expanded Solvent SAGD (ES-SAGD)

The aim of this process is to combine the benefits of steam and solvent in the recovery of heavy oil and bitumen. In this process, the solvent is injected together with steam in a vapor phase. It condenses around the interface of the steam chamber and dilutes the oil; solvent in conjunction with heat reduces oil viscosity. ES-SAGD - also called SAP (Solvent Aided Process) - has been tested in the Senlac field and has led to promising results to lower water and energy requirements while improving oil production and SOR.

3.1.7.5. Multiple well pair operating strategy

It is practical to drill and operate more than one pair of injectors and producers in order to cover more areas and achieve systemic oil recovery. One significant issue emerges from the application of multiple well pair, which is the recovery of oil from the areas between adjacent well pairs. In the following schematic (Figure 3.5), it can be seen that the oil around and above the injection well will be easily recovered by the hot steam chamber.

However, the oil in the transition area would hardly be swept by the steam chamber especially in the lower regions of the reservoir (Albahlani, 2008).

Some operation strategies aimed at improving bitumen recovery in SAGD are being developed: Fast SAGD (Shin et al. 2005), X-SAGD (Stalder, 2005), Combination of Vertical and Horizontal Wells, Offsetting Vertical Wells, and so on. The basic concept of these strategies is to use the lateral driving force along with gravity force to move the remaining oil in the regions between the producing wells without drilling infill wells.

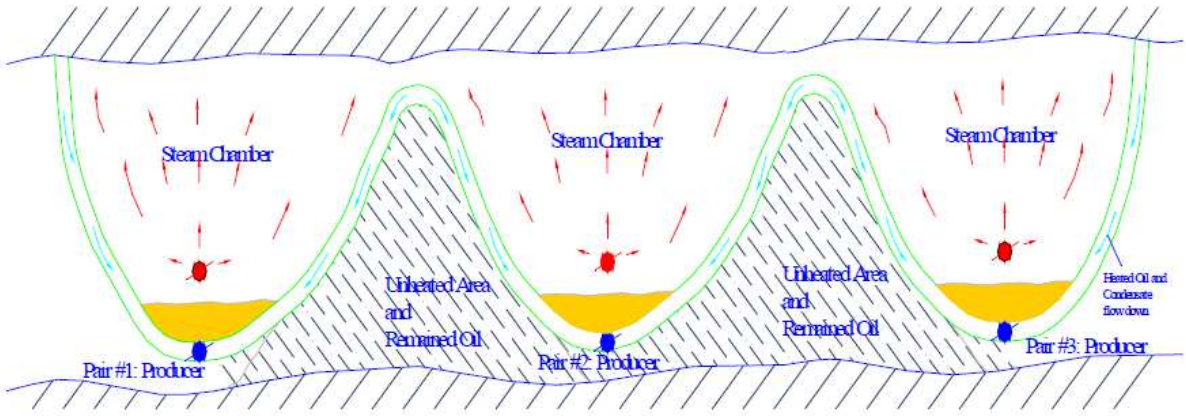

Fig. 3.5: MULTIPLE WELL PAIR SAGD

The key scheme of these strategies is to design specific well configurations in the SAGD operation area, combined with cyclic steam stimulation to utilize the existing heat in the region between the adjacent steam chambers throughout the operation and hence accelerate merging of the chambers.

Cross SAGD (X-SAGD) or L-SAGD. Stalder (2005) advised that production rate was limited to the spacing distance between the injector and producer in classic SAGD. Once the steam chamber was generated, the SAGD performance was enhanced with increasing spacing distance. The concept X-SAGD was proposed to employ specific operation strategies for steam injection through the injectors which were perpendicular to the producers. It attempted to utilize gravity and lateral drive to improve bitumen recovery.

Consequently, more oil in the formation was expected to be reached and recovered than in the classic SAGD operation. His simulation study was conducted to test the X-SAGD concept and indicated that X-SAGD had advantage over classic SAGD at lower pressure (1500 kPa) than at higher pressure (3000 kPa). However, the process of X-SAGD was expected to face some serious practical challenges: extended initialization period, low initial production rate, and complicated operations.

Fast SAGD. (Figure 3.6) In the theoretical concept of Fast-SAGD (Shin et al. 2005), the offset well was equipped and parallel to, but 50 meters away from the SAGD producer. A pair of vertically spaced, parallel, co-extensive, horizontal injection and production wells and a laterally spaced, horizontal offset well were provided in a subterranean reservoir containing heavy oil. Fluid communication was established across the span of the formation extending between the pair of wells. This concept utilized the advantages of SAGD and CSS contemporaneously as laterally spaced horizontal wells lead to faster developing fluid communication between the two well locations.

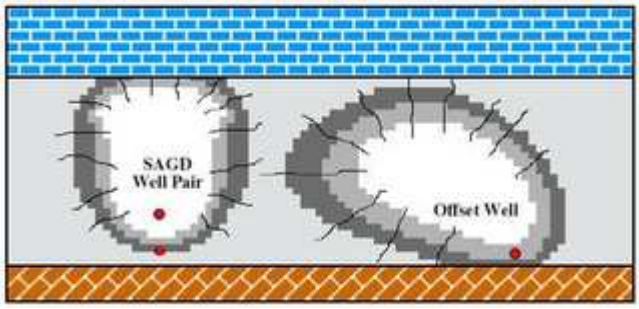

Fig. 3.6: Fast SAGD

Based on results of numerical simulation, the process yielded improved oil recovery rates with improved steam consumption. The rates of bitumen production increased and the steam-oil ratio was reduced. Shin et al. (2007) claimed Fast-SAGD was a more efficient recovery process requiring less steam and had lower operating costs to produce the same amount of bitumen.

3.2. Physics of SAGD

3.2.1. Steam Chamber Growth Mechanism

The SAGD concept is based on steam chamber development, as production is mainly from the chamber / heated oil interface. Thus, the development and analysis of the steam chamber growth and characteristics have received a great deal of attention by scientists studying SAGD. Yet it seems that the complete picture of the process of steam chamber development is not fully represented due to different processes occurring at the same time; counter-current flow, co-current flow, water imbibitions, emulsification, steam fingering and dimensional movement (lateral vs. vertical). All of these processes are related in a way due to the fact that in SAGD lighter fluid (steam) is trying to penetrate by nature to a heavier fluid (Heavy oil or Bitumen) above it. Ito and Ipek (2005) observed from field data that steam chamber grew upward and outward simultaneously like the expansion of dough during baking. It was also noticed that recent understanding of SAGD process endorses the idea that steam chamber is not connected to the producer; rather a pool of liquid exists above the production well. Gates et al. (2005) identified the advantage of having such a pool by preventing flow of injected steam into the production well.

3.2.2. Steam Fingering Theory

Butler's theory has been developed from 1969 to 1994. In 1994 from a sand pack lab experiment, Butler observed that the rise of the steam chamber doesn't advance as a flat front, rather as series of separate and ragged fingers. He referred the occurrence of these fingers to instability created by rising lighter steam below the heavy oil. Thus, understanding steam finger theory is crucial for understanding steam chamber rise processes. Depicting a rectangular boundary, Butler hypothesized steam chamber development; his description of the process can be summarized as follows:

1. Steam flows upward from lower boundary providing heat to rise reservoir temperature to steam temperature.
2. Heated material drain leaving through the lower boundary as a number of identified streams.
3. The velocity by which the residual oil leaves the system is of that steam chamber rise with.
4. Flowing hot oil and condensate leave at higher velocity because they have a downward velocity relative to the hot rock and residual oil.
5. The entering steam moves at a higher velocity than the chamber in order to pass through the lower boundary.
6. At the very top of the chamber steam fingers move into the relatively cold reservoir and heats the cold oil through conduction.

According to Ito and Ipek (2005), many observations in the UTF, Hangingstone and Surmount projects are now clearly understood by steam fingers concept. Sasaki et al. (2001) provided images where steam fingering can clearly be seen on their 2D experimental model. They also showed an increase in the ceiling instability, hence fingering, due to intermittent steam stimulation of the lower horizontal producer.

3.2.3. Co-current and Counter-current Displacement

Nasr et al. (2000) stated that the uniqueness of the SAGD recovery process lies in the salient role of moving condensing boundaries and counter-current flows. Counter-current flow between heated heavy oil and bitumen occur at the top of a rising steam chamber where steam fingers rise and heated heavy oil falls (Albahlani 2008, Butler 1994). Nasr et al. (2000) published a paper highlighting steam oil emulsion counter- current flow and rate of propagation of the steam chamber. They used a cylindrical experimental model and adiabatic control system, and CMG STARS numerical model to simulate SAGD counter-current flows and determine sensitivities of different parameters. They concluded that for a given permeability, the counter-current steam front propagation rate is a linear function of time. They observed that time taken for counter-current steam front to propagate to a specific distance is much more than time taken by a co-current front, where drainage condensate was impeding the advance of the counter-current front.

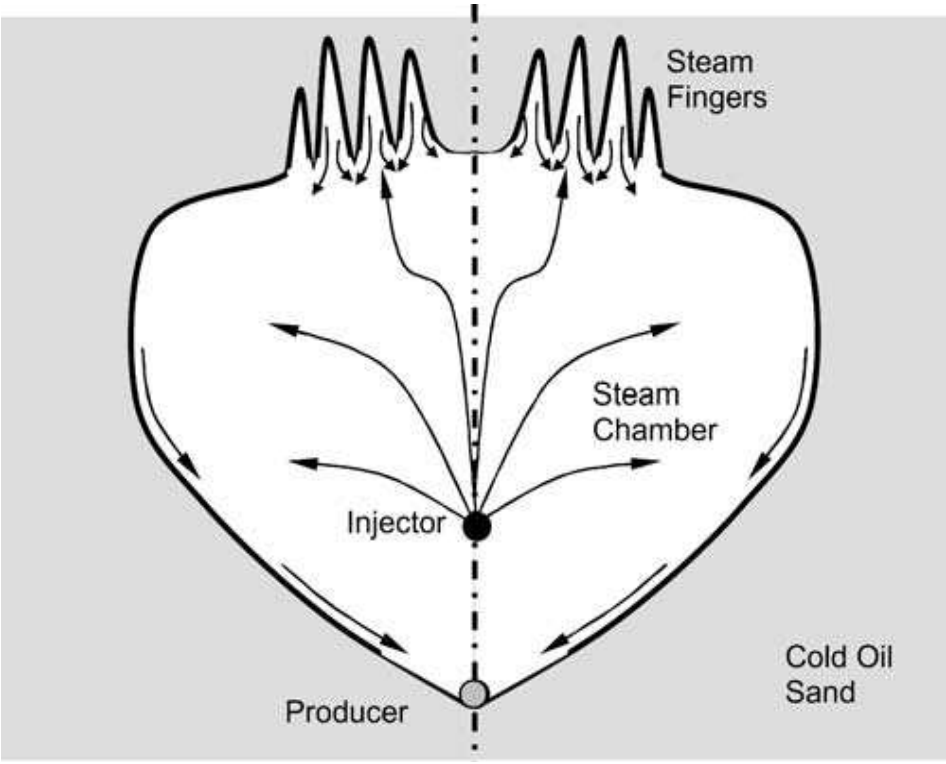

Fig. 3.7: SAGD steam chamber and exaggerated view of steam fingers.

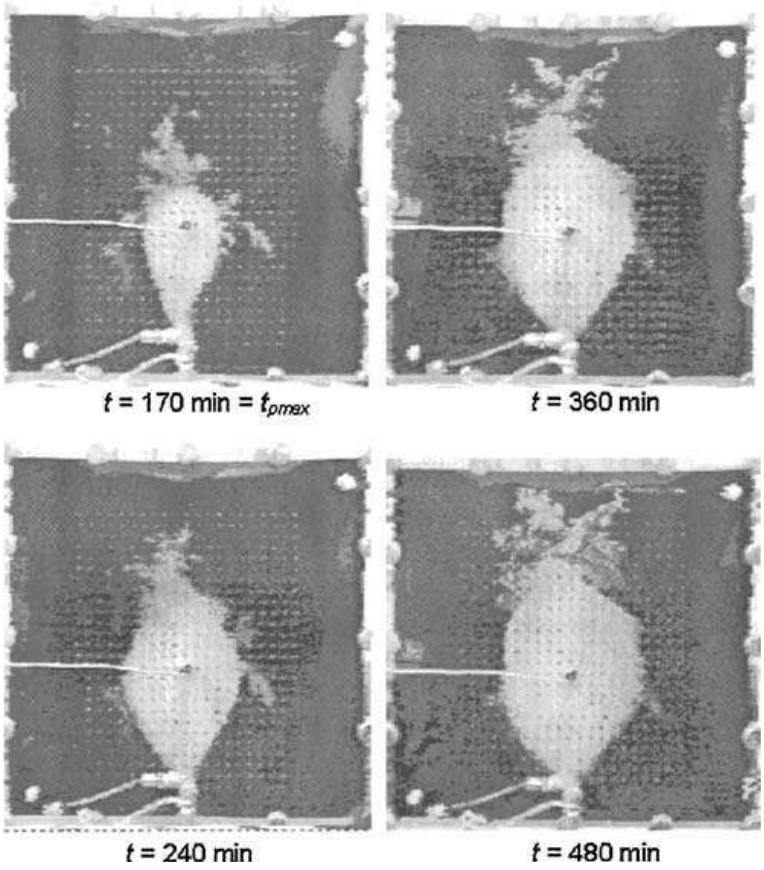

Fig. 3.8: Visualized pictures of micro-channelling at the top of the steam chamber for 300 mm×300 mm, 4.5 mm thick conventional SAGD model (Sasaki et al. 2001).

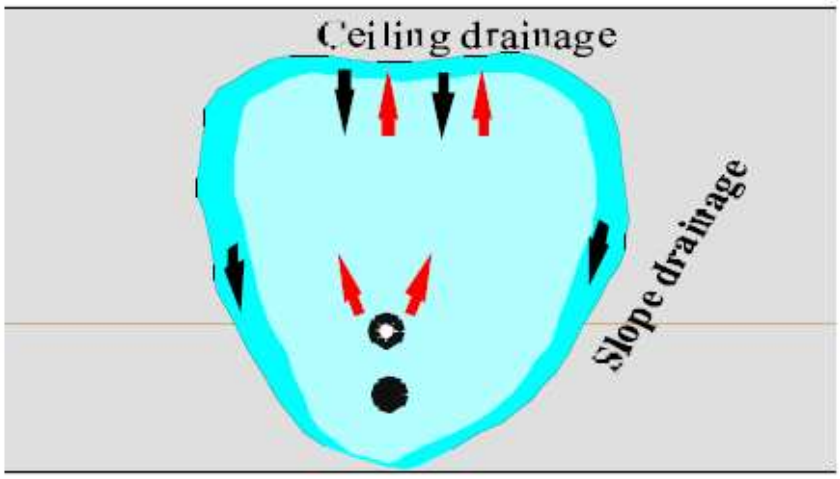

Fig. 3.9: Ceiling and slope drainage inside the steam chamber (Nasr et al, 2000)

After history matching the steam-water counter-current and co-current relative permeability curves, they found that there was a significant difference between counter-current and co-current relative permeabilities. They argued that this may be the result of a coupled flow between the phases. This observation raises a concern on whether existing numerical simulation formulations can capture this important physical analysis.

3.2.4. Heat Transfer and Distribution through Steam Chamber

Understanding the heat transfer through steam chamber is very critical. This critical understanding emerges from the fact that technically, steam chamber monitoring is applied through temperature monitoring. Furthermore, it is critical to understand SAGD thermodynamics to overcome the huge energy consumption that persists with SAGD. Farouq Ali (1997) criticized the assumption that conduction only exists in SAGD. In response to that critic Edmunds (1998) stated that based on the associated change in enthalpy, the liquid water could carry and deposit 18 % of the heat of condensation of the same water. Convection due to oil is around 1/5 of this; conduction to carry remaining 78 %. He then evaluated the convection role due to water streamline being almost parallel to isotherms to less than 5 %. This was also emphasized by Edmunds (1998) where he stated that except for the very near vicinity of the liner or anywhere live steam penetrates, heat transfer in the mobile zone is

dominated by conduction, not convection. However, Albahlani (2008) believes that with a better understanding of geomechanical effects the role of convection may be greater.

Gates et al. (2005) provided images of steam quality and temperature of the steam chamber from a simulation study. Comparing these pictures together we can clearly see that temperature is almost constant while steam quality varies significantly. This supports the claims of varying steam pressure throughout the steam chamber, i.e. steam chamber pressure is not constant. In their work, they provided a novel method for visualizing heat transfer within boundaries of steam chamber. The usefulness of this method is (as they state) that steam quality profiles provide means to examine convective heat transfer in the reservoir. Using a hypothetical example of hotwell analysis Butler (2001) provides a heat distribution table for a typical Athabasca SAGD project. Albahlani (2008) reproduced it into a pie chart as shown in Figure. 3.10. Butler comments on the outcome by stating that in general the heat remaining within the steam chamber, per unit production of oil, will be lower if the steam temperature is lower (i.e.; the chamber pressure is lower) or if the oil saturation is higher (i.e.; there is less reservoir to be heated per m^3 of oil). The later is very important in determining the relative performance to be expected from different reservoirs. High (initial) oil saturation is desirable.

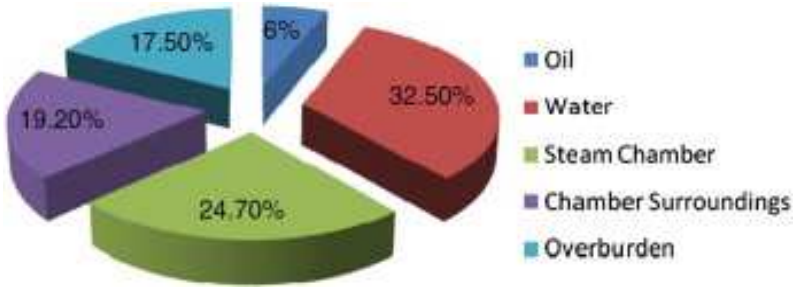

Fig. 3.10: Reproduction of Butler's (2001) heat distribution for a typical Athabasca oil SAGD project

Yee and Stroich (2004) showed that, after 5 years of Dover project, the amount of injected heat in the chamber is around 32.2 %, outside chamber is 34.7 % and 33.1 % was re-produced. It can be seen that almost one third of heat injected is re-produced. Albahlani (2008) believed that this may had a beneficial side that heat may prevent wax deposition inside the tubing and maintains a lower oil viscosity for uplifting if no emulsion is created.

3.3. Effects of Reservoir Properties on SAGD Performance

3.3.1. Porosity

Not many studies were presented to show the effect of porosity on SAGD performance. By reviewing the analytical models provided, however, one can observe that they all have the cumulative production and daily production proportional to porosity which means that higher porosity would "analytically" promote SAGD performance. This was observed in the analytical study by Llaguno et al. (2002) where they reported that accumulation properties (thickness, porosity and oil saturation) have a greater effect on SAGD performance than flow properties (permeability, viscosity, API, and reservoir pressure) (Albahlani et al. 2008).

3.3.2. Thickness

Several studies report that increase in oil production was noticed with an increase in oil pay thickness (Sasaki et al. 2001; Shin and Polikar 2007; Singhal et al., 1998; Edmunds and Chhina 2001). Edmunds and Chhina (2001) stated that zones less than 15 m thick are unlikely to be economic. Most of work done to draw this conclusion is based on the fact that thin reservoirs increase thermal losses hence higher SOR. However, this conclusion is subjected to variable understanding of what is "thick" and what is "thin". Also, the steam chamber growth behaviour –due to other geological parameters- may have an effect on such conclusions. For example, a cupcake steam chamber growth (laterally and sideways) would not see much effects of reservoir thickness, while a hand fan steam chamber growth (laterally and sideways) might take much longer time for the steam chamber to grow and complicated process such as steam fingering, emulsification, and prevailing counter current flow which may result in fluctuation/decrease of oil production. (Albahlani et al. 2008).

3.3.3. Gas Saturation

Nasr et al. (2000) studied the effect of initial methane saturation on the advancement of steam front in an experimental sand packed model. They noticed that the presence of initial methane saturation resulted in a faster movement of preset temperature values ahead of the steam front at a given time as compared to the case where there was no methane present. However, as the steam front entered into the region of methane saturation, the propagation rate declined as the methane mole fraction increased in gas phase. Canbolat et al. (2002) conducted a series of

studies on a 2D visualized model. They found that initial presence of n-butane had a positive effect on the process. They explained this by the reduction of oil viscosity due gas presence. Bharatha et al. (2005) conducted a study on dissolved gas in SAGD by means of theory and simulation. They stated in their conclusion that the effect of dissolved gas on SAGD is to reduce the bitumen production rate. They also showed that operating pressure plays a greater role in reducing the effect of dissolved gas saturation presence (Albahlani et al. 2008).

3.3.4. Permeability

McLennan et al. (2006) stated that the predicted flow performance of SAGD well pairs is sensitive to the spatial distribution of permeability. After experimental (sand packed core) and numerical model investigations, Nasr et al. (2000) noted that the effect of liquid convection ahead of the steam front can provide a better heating for the 10 Darcy permeability case than for the 5 Darcy case. They also observed that there was evidence that steam temperature inside 5 Darcy sand was lowered by about 3° C than that for 10 Darcy sand for a given steam injection temperature. They argued that this might be a result of higher capillary pressure for the 5 Darcy case. They also reported that he propagation rate of the steam front is not a linear function of permeability.

In a 2D simulation model investigating SAGD in carbonate reservoir, Das (2007) reported no significant change in production due to matrix permeability at earlier stages and faster decline for low permeability at later stages. He referred this due to the possibility of matrix production which occurs primarily by imbibition and thermal expansion. However, by looking at the examination range (10 – 50 mD) it can be seen that the range is too small to study the effect of permeability. Kisman and Yeung (1995), on the other hand found from a simulation model that decreasing the vertical permeability resulted in a significant decrease in CDOR (calendar day oil rate) and OSR initially. But an increase in both CDOR and OSR was noticed at later stages. It was also shown by Shanquiang and Baker (2006) in a 3D simulation model that decreasing permeability reduced initial oil production but later increased dramatically.

Nasr et al. (1996) showed a decrease in OSR due to decrease in permeability through their numerical modelling study. Collins et al. (2002) stated that laboratory tests on specimens of undisturbed oil sands have conclusively proven that absolute permeability increase dramatically with dilation. They also showed that shear dilation of oil sands enhance permeability in SAGD process. Shin and Polikar (2007) found that higher permeability

resulted in a higher ultimate recovery as well as lower CSOR. They also observed that fining upward sequence showed better SAGD performance due to lateral steam propagation (cupcake growth). Nasr et al. (1996) reported from 2D sand packed model that for low permeability reservoirs, the steam zone was localized around the injection well. The low permeability reduced the drainage of oil and growth of the gravity cell. Mukherjee et al. (1994) observed that the presence of low permeability zone between the injector and producer may cause water hold up between the wells where water is not well drained.

Butler (2004) studied the effects of reservoir layering. He stated that in layered reservoirs with permeability ratio less than about two, the height average permeability should be used in the Lindrain equation. He then suggested that in the situation described above, steam should be injected in the more permeable area. He also stated that if the more permeable layer is at the bottom then a steam swept zone will tend to undermine the upper layer. If the more permeable layer is at the top and the permeability ratio is greater than two, the penetration of the steam into the lower layer will be delayed and oil will move through the lower region driven by the imposed pressure gradient. Effects on oil rate are not very severe at least until the upper layer is exhausted.

3.3.5. Viscosity and API

Das (2007) studied the effect of oil viscosity in a 2D model investigating SAGD in carbonate reservoir. He found that recovery rate and injectivity improved with lower viscous oil. Shanqiand and Baker (2006) studied the effect of API on SAGD performance, clearly increasing API reduced oil production. Singhal et al. (1998) from a screening study outline the effects of viscosity on geometrical and operational parameters. For example, they advise that from viscosities less than 35000 mPa.s and thickness more than 15 m, using vertical steam injectors staggered around horizontal producers was a feasible recovery strategy. Also, relaxation of subcool constraint under certain circumstances may be feasible. They also advised that, for viscosities above 65000 mPa.s, the use of horizontal injectors and subcool constraint was determined to be critical. (Albahlani et al.;2008).

3.3.6. Heterogeneity

Albahlani et al. (2008) compiled the records produced about SAGD over the last three decades and pointed out the strengths and weaknesses in this process. Permeability is one of the most critical reservoir parameters to SAGD processes. Shale interbeds, whose

permeability is almost zero, prevent the steam chamber from expanding vertically (Figure. 3.11) and have profound effects on well productivity, oil recovery and Cumulative Steam-Oil Ratio (CSOR). (Le Ravelec et al. 2009)

Fig. 3.11: Left: steam chamber development in a homogeneous reservoir.
Right: steam chamber development in a reservoir with shale baffles of limited extent.

Birrel and Putnam (2000) refer the importance of reservoir heterogeneity to SAGD process due to the fact that the driving force for the steam rise is the gravity head. Yang and Butler (1992) studied the effect of reservoir heterogeneities on heavy oil recovery by SAGD. Their approach was to use a two dimensional sand-packed model and they limited their study to two field conditions: (1) reservoir with thin shale layers, (2) reservoir containing horizontal layers of different permeabilities. For the two layer reservoir they studied two cases: (1) high/low permeability reservoir, and (2) low/high permeability reservoir. They noticed that high/low permeability was acting like a whole high permeability reservoir. For a low/high permeability case they noticed an undermining of steam in the lower (high permeability) layer. This effect decreased with time. They then compared the cumulative oil production from the previous setup to all low permeability setup and they noticed little difference. They then studied the effect of barrier length for each case (i.e.; short horizontal barrier, and long horizontal barrier). They concluded that a long horizontal barrier decreases the production rate but in some configurations, not as much as expected. All these, confirm how SAGD is heavily dependent on a good communicating reservoir.

Chen et al. (2007) conducted a numerical simulation study on stochastic of shale distribution Near Well Region (NWR) and Above Well Region (AWR). They stated in their conclusion that drainage and flow of hot fluid within the NWR is short characteristic length and is found to be very sensitive to the presence of shale that impairs vertical permeability. The AWR affects the (vertical and horizontal) expansion of steam chamber. It is of characteristic flow

length on the order of half of formation height. SAGD performance is affected adversely only when the AWR contains long continuous shale or a high fraction of shale. They also studied the potential improvement of SAGD performance by hydraulic fracturing by identifying three cases; horizontal fracture, vertical fracture parallel to, and vertical fracture perpendicular to the well. They observed in some cases an improvement in oil steam ratio by a factor of two when a vertical hydraulic fracture is introduced. They also concluded that vertical hydraulic fractures are predicted to enhance SAGD performance more dramatically in comparison to horizontal hydraulic fracture. They finally stated that a vertical hydraulic fracture along the well direction is superior to one perpendicular to the well direction.

Zhang et al. (2005) showed 4D seismic amplitude and crosswell seismic images of steam chamber growth at the Christina Lake SAGD project which identified the effects of reservoir heterogeneity on the heated zones (Figure 3.12)

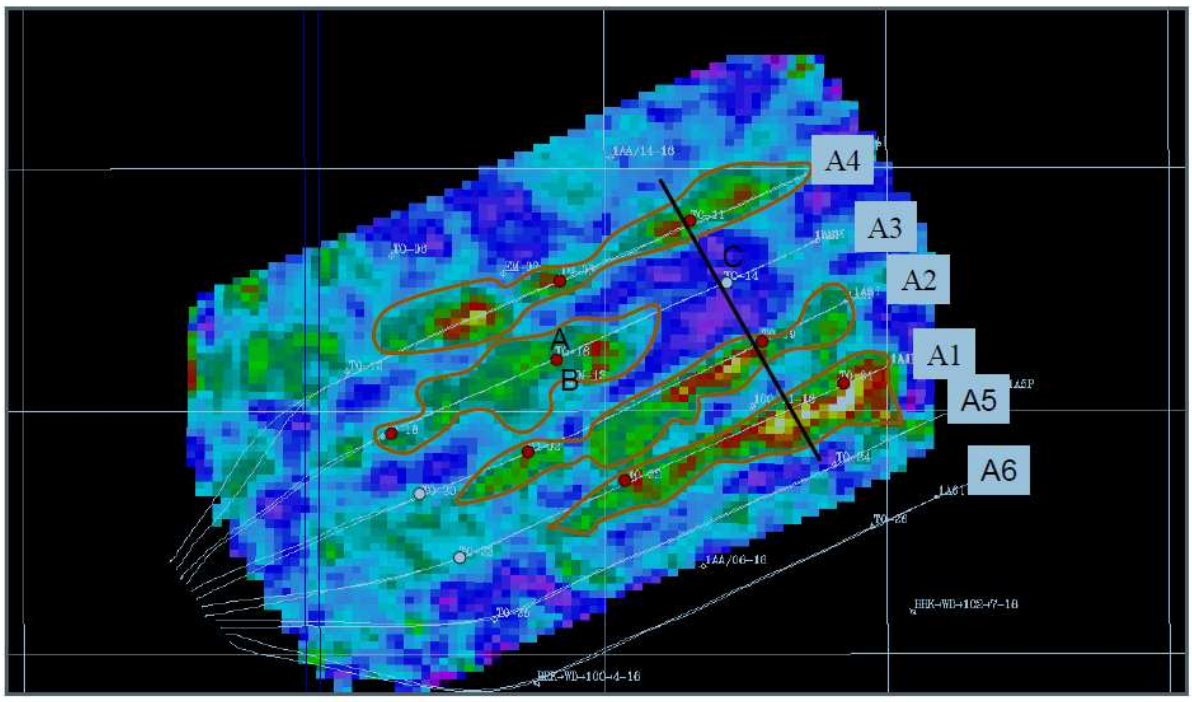

Fig. 3.12: Map view of 4D seismic amplitude difference between 2001 and 2005 (Zhang et al, 2005)

Yang and Butler (1992) showed that long reservoir barriers such as shales can cause difference in advancement velocity of the interface above and below the barrier. This difference is reduced by the drainage of heated bitumen through conduction above the barrier (Albahlani et al., 2008).

3.4 Geomechanical phenomena associated with SAGD

3.4.1 SAGD Stress Path

In the SAGD process, saturated steam is continuously injected into the bitumen-bearing formation. So, with increasing time of steam injection, the pore pressure and the temperature in the formation around the injector increase. However, both pore pressure and temperature decrease rapidly from the steam chamber values to initial reservoir values over a certain distance outwards from the steam chamber surface.

The geomechanical phenomena of volumetric straining under the combined effect of pore pressure changes (i.e., effective confining stress changes) and shear stress constitutes the primary factor influencing SAGD processes. Scott et al. (1991) outlined the effects of steam stimulation on oil sands pore volume changes. A temperature increase causes thermal expansion of sand grains and results in shear stresses. Pore pressure increase during steam injection decreases the effective confining stress and causes an unloading of the reservoir. These processes combine to result in a net change in the reservoir pore volume and permeability. Consequently, for the SAGD process, two predominant stress paths are followed within the reservoir:

1. Under initial anisotropic stress conditions ($\sigma'h \neq \sigma'v$), pore pressure increases result in equal reductions in $\sigma'v$ and $\sigma'h$. In p′-q space, the stress path is horizontal because q (= $\sigma'v$-$\sigma'h$) is unchanged along this path.
2. Following the pore pressure injection stage, increasing horizontal stresses due to thermal expansion of the reservoir within the developing steam chamber initiate an extension (relative to triaxial test configuration), a stress path where the deviatoric stress and mean effective stress increase together. These stress increases are due primarily to an increase in σ_h whileσ_v remains constant.

The possible range of these stress paths is schematically illustrated in Figure 3.13. For the SAGD process, it is the deformation response along this stress path that is of primary importance. If, under the actions of shear stress or changes in mean effective stress, reservoir deformations result in volumetric dilation or contraction, the porosity will be altered. Correctly identifying the magnitude of the stress-deformation behaviour and its resulting impact on reservoir processes is important for understanding the effectiveness of the SAGD process. Within a reservoir, the actual stress path will be a combination of the two stress paths (pore pressure effect and temperature effect).

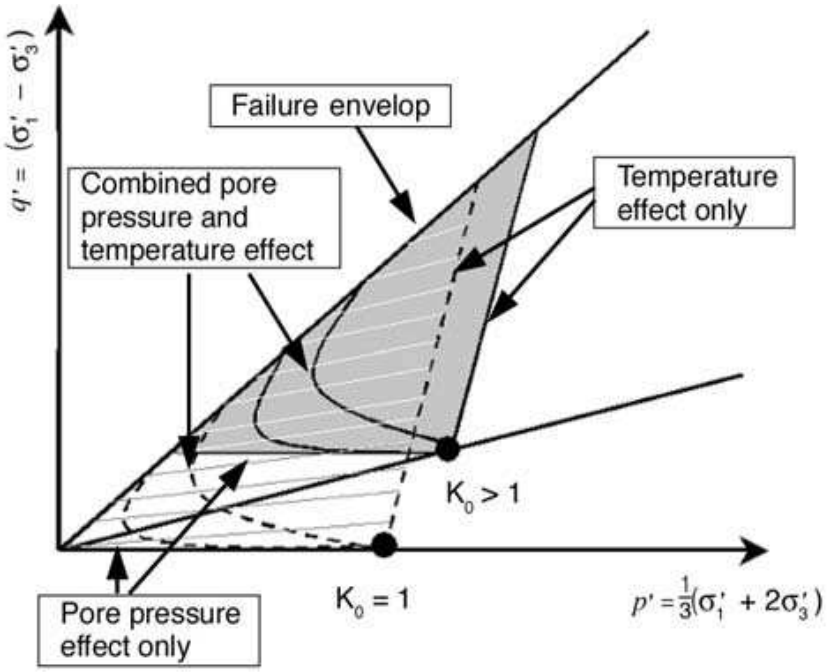

Fig. 3.13: Stress path in the SAGD process (Li et al. 2004)

[With σ′h = σ′3 & σ′v = σ′1]

It is important to note that the stress path discussion provided above is based on the principle of effective stress (total stress minus pore pressure). Consequently, it fundamentally incorporates both changes in total stress and pore pressure, regardless of the mechanism that gives rise to these changes.

3.4.2 Sand dilation around steam chambers

Several fronts develop around steam chambers (Figure 3.14). The slowest front is the steam one followed by temperature and pressure. Dilation occurs in the chamber itself because of high pressure and temperature there, but also at the periphery of the pressurized zone. A dilation front can thus also be defined. As explained in the previous section, the dilation around the steam chamber might enhance the permeability to water which accelerates the pressure and the steam progression toward the top reservoir where the confining stress is the lowest. In this scheme, the dilation is equivalent to diffused fracturing of the sand.

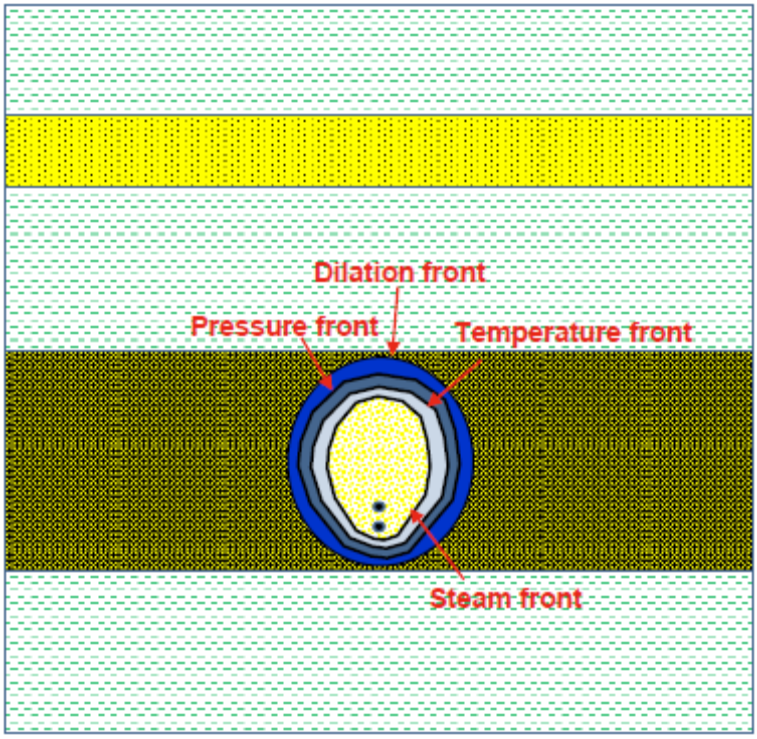

Fig. 3.14: Different fronts developing ahead of a steam chamber (TOTAL, 2010)

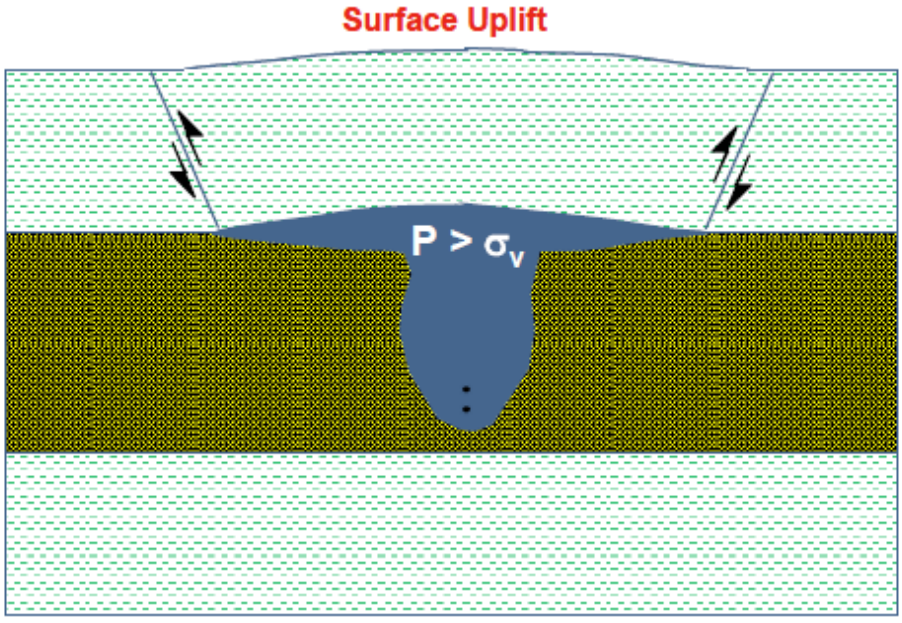

Fig. 3.15: Failure of a shale barrier by shear on the shoulders of a zone with a pressure greater than the vertical stress (TOTAL, 2010)

3.4.3 Role of shale barriers

A shale barrier might stop or at least decelerate the upward pressure transmission because of its low permeability.

In the short run, the pressure starts diffusing preferentially in the horizontal direction. The integrity of the shale barrier depends then on the surface area of the pressurized zone and on the difference between the pressure and the vertical stress. If the pressure is smaller than the vertical stress, the shale barrier will be stable. If a pressure greater than the vertical stress extends sufficiently at the base of the shale barrier, this last might fail by shear on the shoulders of the pressurized area as illustrated in Figure 3.15.

In the long run, the integrity of the barrier might be compromised due to temperature increase by heat conduction. This increase of temperature has two possible effects:

1. Shrinkage of the shale which, by reducing the confinement, might become a source of fracturing.
2. Increase of the shale pore pressure due to fluid thermal dilation.

The effect of temperature on pressure can be calculated using the coupled constitutive equation of the fluid under undrained conditions. For a shale fully water saturated, the equation is:

$$dP = \frac{1}{\phi C_w} d\varepsilon_v + 3(\alpha K)_w dT$$

With C_w and K_w, water compressibility factor and water bulk modulus. If the shale is confined and cannot deform ($d\varepsilon_v$ =0), the pore pressure might increase by several hundreds kPa/°C. In reality, the increase of pressure leads to shear failure of the shale accompanied by dilation and increase of the shale permeability.

3.5 Geomechanics-Reservoir Coupling in SAGD Process

In SAGD process, reservoir geomechanics analysis is concerned with the simultaneous study of fluid flow and the mechanical response of the reservoir. Quantification of the state of deformation and stress in the reservoir is essential for the correct prediction of a number of processes, such as recovery from compaction drive, water flooding, surface subsidence, seal integrity, hydro fracturing, sand production and well failure.

As an example of the importance of developing proper reservoir models and simulation tools integrating geomechanical effects, K. Safinya (Schlumberger) examine the Canadian case, where about 200 steam-assisted gravity drainage (SAGD) well pairs produce approximately 120,000 barrels per day – an average of about 600 b/d per well pair. The production, however, varies. While one field produces 200 b/da per well pair, a nearby field is producing 35,000 b/d from 10 well pairs. A lot could be learned by the industry if the reasons for this large variation were understood. Perhaps if accurate reservoir models (integrating geomechanics) had been built and simulation studies had been carried out, the variation and the ensuing extra costs could have been minimized. It is much more expensive to drill and test a well than to simulate it.

Here after there is an example showing the geomechanical effects of SAGD process, explained by M. Dusseault (2008):

Figure 3.16 shows a perpendicular slice of a group of SAGD chambers, as well as an axial slice of one SAGD well pair; typically, H = 20 - 35 m, W/H ≈ 3.5 - 4 and L = 750 - 1000 m.

The upper X-section is a plane-strain section. Gravity drainage takes place out at about the virgin pressure p_o, so there is no significant regional flux arising from induced pressure gradients. Steam rises under gravitational thermal segregation, moves laterally, condenses into water, and flows along with hot oil toward the producing well. Although there are no induced pressure gradients, the phase density difference $\Delta\rho$ dominates flow because of the difference in head ($\Delta\rho \cdot g \cdot z$), and the flow rate is of course proportional to the vertical permeability, an intrinsic material property.

Assuming H = 30 m, Z = 500 m with initial conditions T ~25°C, $\sigma v = \sigma h$ ~12 MPa and p_o ~5 MPa, the equilibrium T of the steam at 5 MPa is 265°C, thus ΔT ~240°C. A typical thermalexpansion coefficient of φ = 0.28–0.30 quartz sand is 8–10 x 10^{-6}/°C, and the elastic parameters are on the order of E ~3 GPa, ν = 0.25.

When a group of SAGD steam chambers under these conditions is ‘grown’, the surface of the ground rises by about 400–500 mm. However, a thermoelastic calculation, even assuming 100% of the volume of the reservoir is heated to 265°C, gives 70 mm, about 15% of the Δz_{max} measured. Because pore pressures are approximately constant, there is no confining-stress-related dilation, which would be small in any case (the compressibility effect). Therefore, the rest of the vertical heave must be the result of fabric dilation, which can only happen if high shear stresses are generated, under either hot or cold conditions. (Dusseault, 2008)

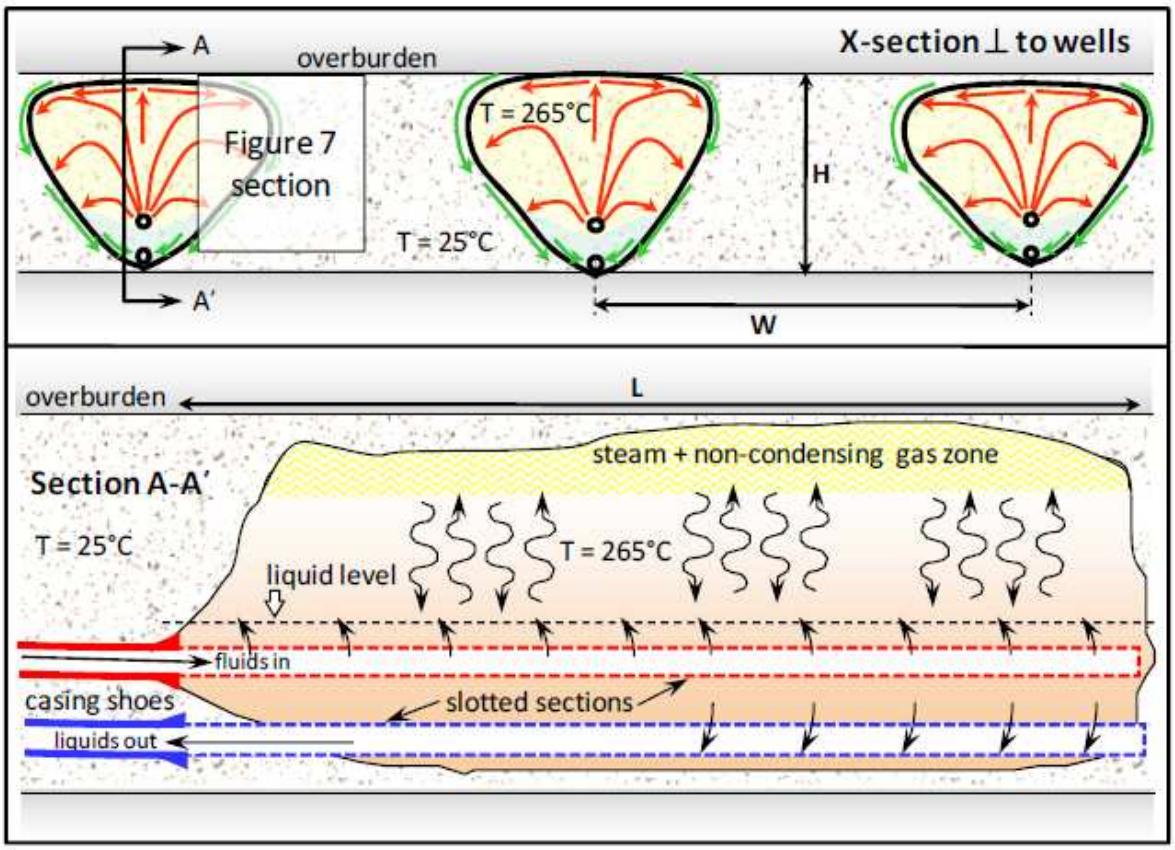

Fig. 3.16: The geometry of the SAGD process (Dusseault, 2008)

Consider the limiting case where the entire stratum is homogeneously heated to 265°C assuming that no lateral-strain in horizontal directions is possible, εx = εy = 0, the purely thermoelastic stress changes become:

$$\Delta P = 0, \quad \Delta\sigma_v = 0 \quad , \Delta\sigma_v^{'} = 0 \quad \text{so} \quad \Delta\sigma_x^{'} = \frac{E.\beta.\Delta T}{1-v}$$

Where β is the thermal expansion factor. For the parameters listed previously, this approximation gives $\Delta\sigma'_x$ ~10 MPa, or σ'_v ~7 MPa, σ'_h ~17 MPa. However, this is insufficient for shearing and dilation to develop.

Another analysis that accounts for the non-uniform distribution of strain leads to a different conclusion. The section shown in Figure 3.17 is a plane-strain slice of the SAGD process after some time.The key observation is that in advance of the thermal front, stress changes applied to the reservoir sand are compressive in the horizontal direction (approximately), but because the SAGD chamber is also expanding vertically, the vertical effective stress is diminished substantially, taking the deviatoric stress sharply into a condition of shear failure at low confining stresses. In fact, even at ΔT as low as 100°C, the vertical effective stress drops below the pore pressure value for any reasonable set of mechanical parameters.

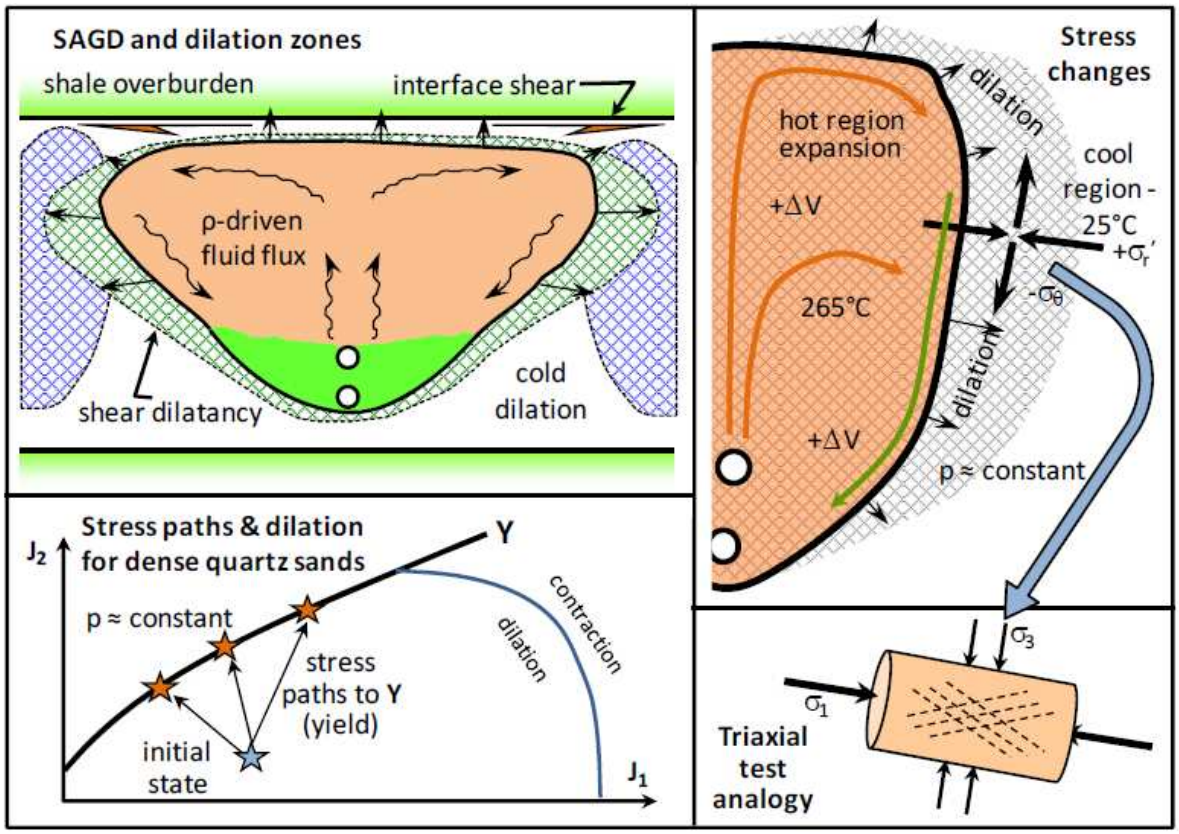

Fig. 3.17: SAGD: dilation in advance and around the expanding heated chamber (Dusseault, 2008)

This leads to dilation and changes of properties. The set of phenomena that probably take place are:

- Injection of steam leads to thermal expansion of the steam chamber in all directions.
- In advance of the chamber wall, the reservoir sand is subjected to strong compression in the horizontal direction and extension in the vertical direction.
  - Depending on properties assumed and the shape of the heated zone, changes in deviatoric stress (σ1 – σ3) can easily exceed 20 MPa.
  - Shearing takes place once the local shear yield criterion is satisfied.
  - Because of the moderate σ′3, a large amount of dilation accompanies the shearing process.
- Because of the geometry of the thermal zone and the reservoir, shear occurs throughout the reservoir, not along just a few planes; hence, general dilation ensues in advance of the thermal front.

- As the steam chamber grows, previously dilated material is progressively incorporated into it. Within the steam chamber, the compressive stresses are higher, some dilation is lost by compression – or "re-compaction", but this is small in relation to the dilation.
- The strong dilation in front of the heated zone leads to:
  - An increase in absolute permeability by perhaps x 2 to x 5 because of porosity increase.
  - Breaking up thin clay dustings on bedding planes and shale layers a few centimetres thick, further increasing permeability (especially kv, which controls gravity drainage rate).
  - The strong porosity increase (probably 4–6% locally) causes water influx (the oil is far less mobile), so the water permeability increases by at least an order of magnitude (likely much more), allowing thermal convection to develop in advance of the zone where the oil is being "melted" by the high temperature.
- These permeability increases and accelerated heat transfer mechanisms make gravity drainage much more efficient, allowing heat flux to become dominated by convection in the dilated zone in front of the steam chamber.

Again, it is worth noting that fluid flow heat flux (Fourier), and geomechanical response are intimately coupled. The mechanism of dilation-induced improvements in properties is a major reason why SAGD has proven far more successful in practice than initial simulation results suggested (Collins et al., 2002). It is also one of the reasons why petroleum engineers have to calibrate and re-calibrate non-coupled models, generating solutions formulated in terms of "pseudo-parameters" or empirically changing properties because it is impossible to make realistic predictions using virgin properties. Because large permeability enhancement related to stress-induced shearing accompanies the process, SAGD can be used in many cases where the intrinsic vertical permeability might seem too low to allow success. The SAGD process can be implemented at higher or lower pressures, provided there are no mobile water or gas zones present. If high pressure SAGD is used ($p >> p_o$ but $< \sigma v$), the rate of processes aided by dilation and permeability enhancement will be further improved. However, heat transfer through vapour phase condensation (latent heat) is reduced at higher pressure, and it will be necessary to depend more on sensible heat.

Because the temperature is higher (e.g. 296°C @ 8 MPa instead of 265°C @ 5 MPa), the oil viscosity will be lower, and this will also accelerate oil production rate.

In the absence of an understanding of geomechanics, reservoir engineers often argue that low-temperature SAGD is more efficient because of the higher enthalpy and the reduced rate of

conductive heat losses in the wellbore and reservoir. But, a higher effective stress means dilation is partially suppressed, the permeability will be lower, and the viscosity of the oil will be lower as well (e.g. at 215°C @ 2 MPa). When the coupled phenomena of thermal stress-related permeability enhancement and thermal viscosity reduction are factored in, it appears that low-Temperature SAGD is disadvantageous, compared to high-Temperature SAGD.

3.6 SAGD Numerical Simulation & Coupling

Given the nature of heavy oil, reservoir models are perhaps more important than they are for conventional plays. Reservoir simulators for heavy oil should be able to take into account a variety of complex reservoir behaviours when it is subject to heat, solvents or large gemechanical stress; in the latter case, to account properly for reservoir behaviour, non-linear geomechanical variables at a resolution of one square metre across the entire reservoir are necessary to estimate surface movement over long production periods.

In the early phase of development, simulation can help engineers optimize the design of the production system, and to evaluate various well trajectories and drainage patterns. After production begins, operators may see a wide range of results from individual wells. In that case, accurate modelling can help optimize production throughout the life of a field.

Intelligent completions and continuous monitoring enable better control of inflow and outflow from the well – providing measurements in real-time for dynamic modelling and automated control. Prior to deployment of any such system a proper optimization study should be conducted using simulation tools.

Generally, more emphasis has been given to solving the flow problem alone by assuming a constant state of stress (total stress) in the system and by incorporating a time-invariant rock compressibility term to account for the complete mechanical response of the system. Conventional simulator neglects the geomechanical interaction of a reservoir with its overburden and sideburden and implicitly assumes equivalence of reservoir conditions with laboratory conditions under which the rock compressibility was measured. This results in a crude oversimplification of the physics governing solid-fluid interactions. Solution to the coupled geomechanical problem, however, has started to evolve from a research topic to an essential component of reservoir simulation, given the enormous environmental and economic impact that the mechanical deformation of the reservoir may have.

In reality, rock mechanics or geomechanical effects are intimately coupled with fluid flow physics. Such coupling is a two-way coupling:

1. Fluid pressure variations affect the mechanical problem, because deformation is driven by the effective stress (roughly speaking, the total stress minus the pore pressure).

2. Deformation of the medium affects the flow problem in two ways:

(a) Flow properties coupling where fluid pressure affects the solid configuration and consequently porosity and permeability of the system.

(b) Pore volume coupling where effective stress induces strains in the solid skeleton resulting in pore volume changes.

In a traditional reservoir simulator stress is assumed to be constant throughout the simulation and all properties are understood as a function of pressure (and saturation in case of multiphase flow). Rock compressibility, a scalar quantity, is used to account for the complete tensorial response of the stress state and material stiffness. In reality, this rock compressibility term has been shown to be a function of the local conditions and boundary conditions on the reservoir and is also influenced by stress path.

3.6.1. Review of SAGD simulations

Computational geomechanics is a research field being explored by many researchers to predict simultaneous changes in reservoir pore volume and permeability resulting from production and injection.

A vast literature on the SAGD concept has been developed since it was first introduced by Butler and his colleagues in the late 1970s. Also the numerical simulation has been widely used by many researchers to investigate the physical process and practical operation of SAGD as well. For example, Ito and Suzuki (1996) observed a large amount of oil drains through steam chamber when geomechanical changes occur in the reservoir. They hence flagged the role of geomechanical change of formation during SAGD as very important. Li and Chalaturnyk (2003) worked on coupled reservoir-geomechanics simulation and showed a higher oil production than uncoupled simulation. They inferred this difference to take into account the enhancement of both porosity and permeability in coupled simulation. Chalaturnyk and Li (2004) presented an insight into the geomechanical effects on SAGD operations. They hypothesized that, in a SAGD process, the combination of pore pressure and temperature effects, creates a complex set of interactions between geomechanics and fluid flow. In their work, they studied, using coupled reservoir simulation, major geomechanical-

reservoir factors which include: initial in situ effective stress state, initial pore pressure, steam injection pressure and temperature, and process geometry variables such as well spacing and well pair spacing. They stated that it was difficult to be conclusive about specific geomechanical process relative to the multiphase characteristics of SAGD from a work at that stage. However, they provided some observations including enhancement of absolute permeability occurrence in significant zones of shear failure.

3.6.2. Different coupling strategies

Based on the degrees of coupling between reservoir fluid flow and oil sand geomechanics, coupled simulations can be split into four categories: non-coupled, decoupled, sequentially coupled, and fully coupled, as Chalaturnyk pointed it.

The non-coupled solution denotes the conventional reservoir simulation, which applies rock compressibility as the sole parameter to consider the interactions between the fluids and solids.

The decoupled or one-way solution usually includes the complete time history of reservoir simulation followed by a stress solution, but does not include the feedback of geomechanical effects on reservoir simulation. In one-way coupling, two separate sets of equations are solved independently and output from one simulator is passed as input to the other at certain time intervals. The information is passed only in one direction. Under specific conditions, one-way coupling can be used effectively to obtain the correct solution (Wang, 2000). Also, one can gain valuable insight into the physical situation, especially for fluid flow dominated problems. The one-way coupling approach has been successfully used by Fedrich et al., Boade et al., Sulak et al., and Cook et al. (Chen et al., 2007)

The sequentially coupled solution contains both explicitly coupled and the iteratively coupled reservoir geomechanical simulations. In sequentially coupling, the two sets of equations are solved independently, but the information is passed in both directions between the two simulators. The stress equations are solved sequentially in each time step or iteration during each time step. Then, the modified reservoir parameters by geomechanical behaviour are substituted back into the flow equation to continue the next time step. The sequentially coupling has advantages like flexibility and modularity, relative ease of implementation, and better computational efficiency. The iterative coupling is basically equivalent to the modified Newton-Raphson version of the fully coupled method. When the iterative process converges, the iterative analysis yields the true solution of the coupled problem. Settari and Walters

(1999) discussed the different methods of coupling and gave to sequentially coupling the advantage of flexibility and reliability over other methods. The sequential scheme has been used effectively by Settari and Mourtis (1998) and Rutqvist et al. (2003). Chin et al (2002) developed and implemented a parallel computing method in an iterative scheme and indicated an increase in speed of geo-mechanical computations by an order of magnitude.

The fully coupled reservoir geomechanical simulation solves the flow equation and stress equation simultaneously based on a unified grid system. However, in the fully coupled approach, the hydraulic or geomechanical mechanisms are often simplified by comparison with conventional uncoupled geomechanical and reservoir approaches. In the sequentially coupled approach, the stress and flow equations are solved separately for each time step but information is passed between the reservoir and geomechanical simulators. Therefore the reservoir and geomechanical problems have to be reformulated according to the original fully coupled problem. Contrarily to the fully coupled approach, the sequential coupling looks more flexible and benefits from the high developments in physics and numerical techniques of both the reservoir simulator and the mechanical software.

3.6.3 Is coupling too difficult?

Full coupling of all processes and non-linearities in a general framework is too difficult to implement, and may so remain for some time. Later, two examples of SAGD processes will be given; these are economically important processes that have not yet been fully analysed in a coupled manner at a realistic engineering scale. Such lacuna may be for several reasons; several of them are described here.

The problem may be computationally intractable. In structurally complex environments, reservoir analysis involving injection and production in many wells (e.g. 20–50) can easily lead to 107–108 degrees of freedom (equations), especially if there are many steep gradients in pressure, temperature, σ' and saturations (Yin et al., 2008). Also, non-linear behaviour such as shear dilation, fabric collapse, and fracture orientation changes, all combined with changes in k, Cc, and φ, make computational efforts exceptionally large. Of interest to reducing computational effort is a method combining finite elements for the reservoir with displacement discontinuity elements for the surroundings (Yin et al. 2008, see Figure 3.18). This method treats the exterior zone as elastic (not necessarily isotropic), the interior zone of reservoir rock which may undergo non-linear behaviour of various kinds (e.g. dilatancy, collapse, etc.), and an intermediate zone in which temperature and pressure changes (and

hence, stress changes coupled to ΔT and Δp) are important. Compared to classical finite element approaches, the number of degrees of freedom can be reduced by a factor of five or so.

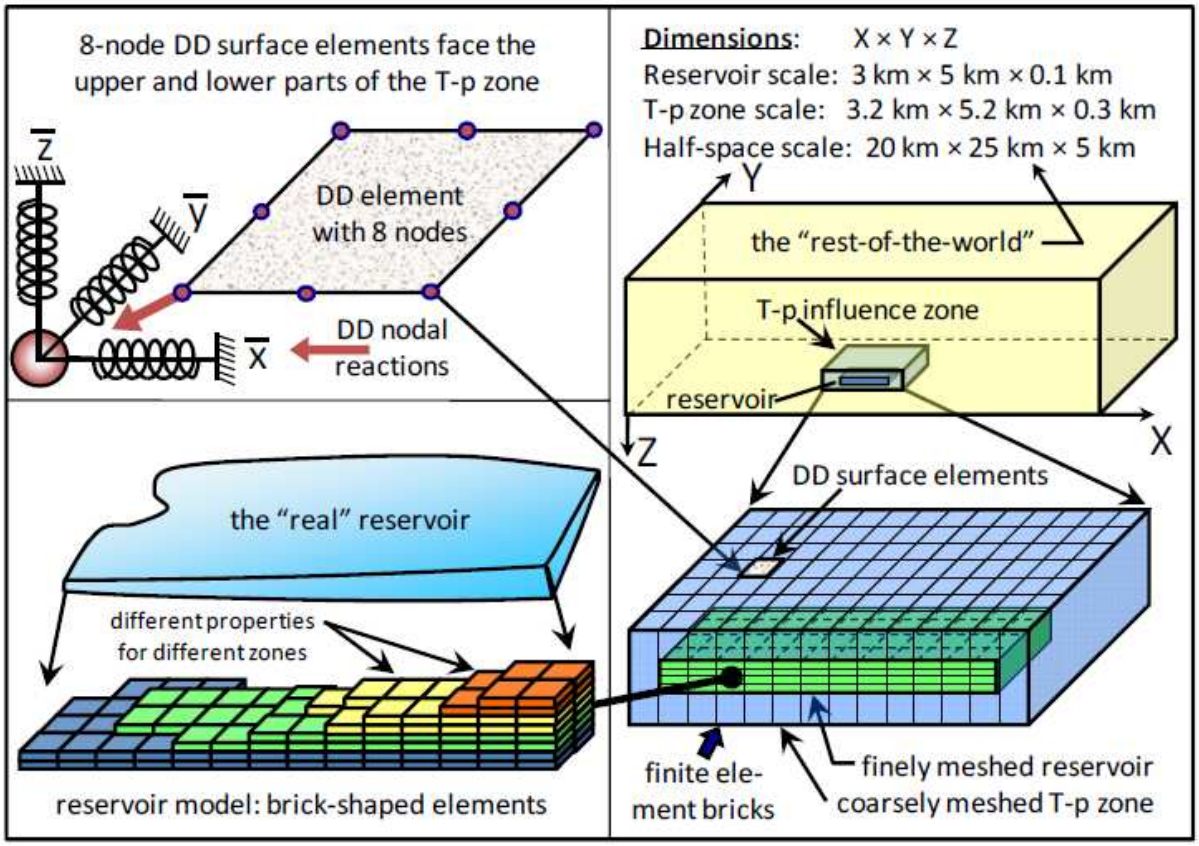

Fig. 3.18: A DD–FEM scheme for reservoir engineering analysis of tabular reservoirs (Dusseault, 2008)

Vital data may be lacking. For example, in a shale oil extraction technology that involves electrical heating and induced pyrolysis, all four basic diffusion processes are important and coupled (Darcy flux, Fourier flux, Fickian flux, Ohmic flux). Complex pyrolysis reactions are generating liquid and gaseous phases through thermal decomposition of solid kerogen, hence pressure-volume temperature behaviour is important. These changes trigger massive σ′ alterations, and fracturing takes place, in large part because shale is dehydrated (~125°C), then dehydroxylated (~400°C), with massive volume shrinkage taking place. Permeability changes of five to seven orders of magnitude develop, and reaction stochiometry over large p–T ranges in the presence of clay minerals are ill-understood. Hence, any attempt at generating a sensible coupled model is severely constrained by the lack of constitutive behaviour for the rock and fluids undergoing pyrolysis. In such cases, better-defined subsets of process will be analysed in a coupled manner, rather than trying to develop a "complete" model.

Complexity may be intense. Heterogeneity, process complexity, geometrical and constitutive uncertainty may, in aggregate, be so large that executing a coupled model in an attempt to make a prediction is unwarranted. In this situation, the proponent must decide on one of two directions: abandon the attempt at coupling and perhaps even modelling, or, treat the coupled modelling attempts not as a predictive model, but as a parametric or physics model used to gain insight into the potential magnitude of the effects or their consequences. In fact, given typical complexity of many thermal petroleum recovery processes, much coupled geomechanics modelling serves exactly this role. In the casing shear problem described later, a close correspondence between reality and predictions is rarely obtained without a substantial attempt at calibration of models to field measurements.

Coupling may not be warranted. For engineering processes, there are three levels of importance. A phenomenon of "first-order" importance will have >10% effect on the results; it must be included in design and analysis. Simple coupled models are used to assess whether this magnitude is to be expected. Phenomena of "second-order" importance, 1–15% effect, may or may not be included in coupled analysis, depending on the general level of uncertainty. For example, in foundation analysis, factors of safety are usually so high that second-order coupling effects are not analysed, although they may be noted and flagged for observation. "Third-order" processes, giving less than 1–2% on results, are not included in coupled geomechanics analysis. For example, large temperature differences associated with steam injection in oil sands give rise to induced electrical currents, but these are of no consequence to the rest of the process.

In this study, we apply the one-way (or decoupled), explicit and iterative coupling methods in order to simulate numerically the SAGD process. This simulation is performed by using PumaFlow, IFP reservoir simulator, and Abaqus as the geomechanical simulator. In chapter 5, we will explain the case study and the applied methodology in details.

3.7 Examples

In this section two examples are presented which illustrate the importance of taking into account geomechanics in SAGD process. Hangingstone and Joslyn fields are located in Northern Alberta (Canada) in the Athabasca oil sands province (Figure 3.19).

The reservoirs are made of unconsolidated sands from the fluvio-estuarine McMurray Formation. Reservoirs from this area exhibit a complex internal architecture which is

associated with heterogeneities specific to fluvial and estuarine environments. In Hanginstonearea, the top of the McMurray reservoir is at a depth of 260m in average and in Joslyn, it is at a depth from 65 to 110 m.

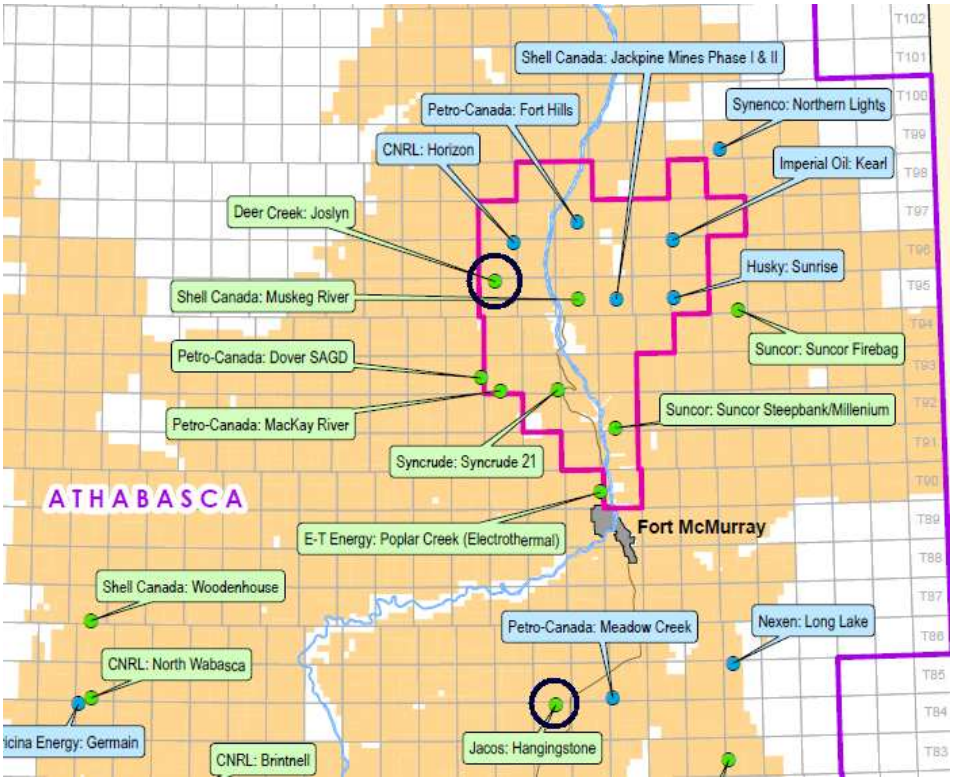

Fig. 3.19: Location of Hangingstone and Joslyn fields

3.7.1 Hangingstone study

The impact of reservoir heterogeneities on the steam chamber growth was studied by Lerat et al (2010) at IFP Energies nouvelles using data from the Hangingstone field.

Figure 3.20 shows a vertical cross section across the reservoir showing the horizontal well pair placement considered for the study. The reservoir thickness is about 50m in average, with a 20-25m net pay. The producer lies 5m above the producer. The well pair length in the reservoir is 820m.

The synthetic geological model was defined by a reservoir grid exported from the global geological grid with overburden layers. The grid was exported with porosity, permeability, saturation and lithological properties (Figure 3.21).

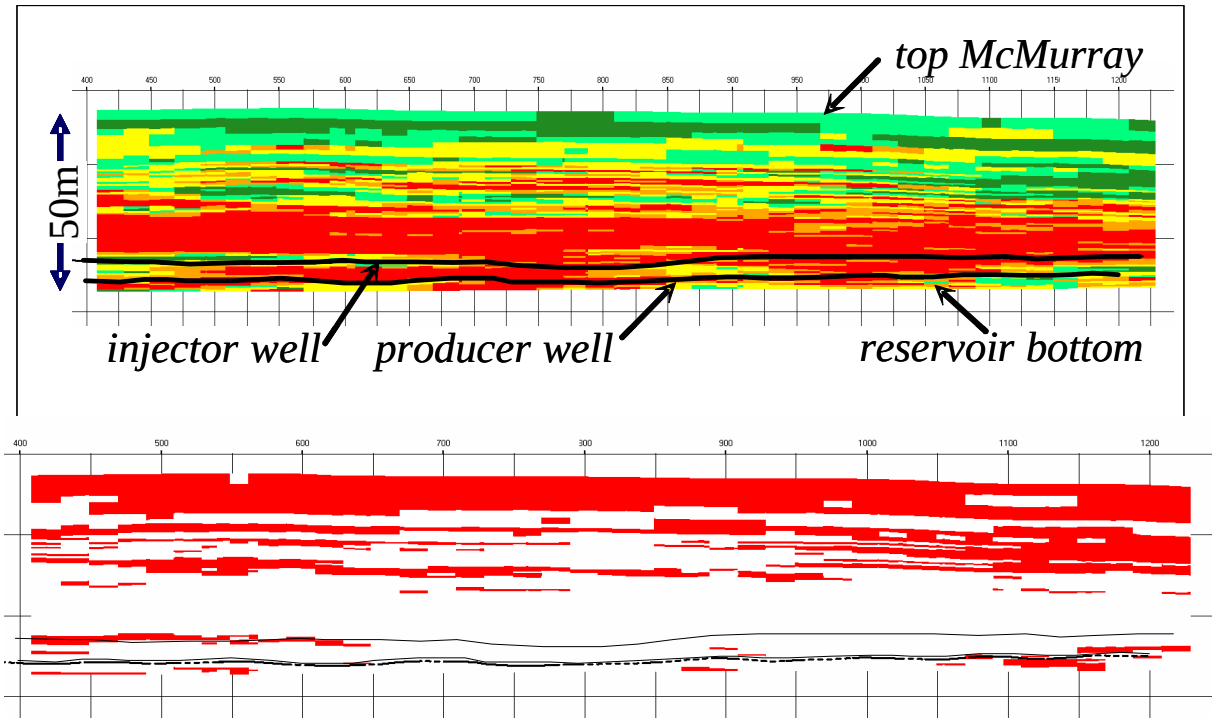

Fig. 3.20: Vertical section along the well pair: facies (upper) and horizontal permeability (lower).Permeability values: 0.01 mD (red), 3000 mD (white).

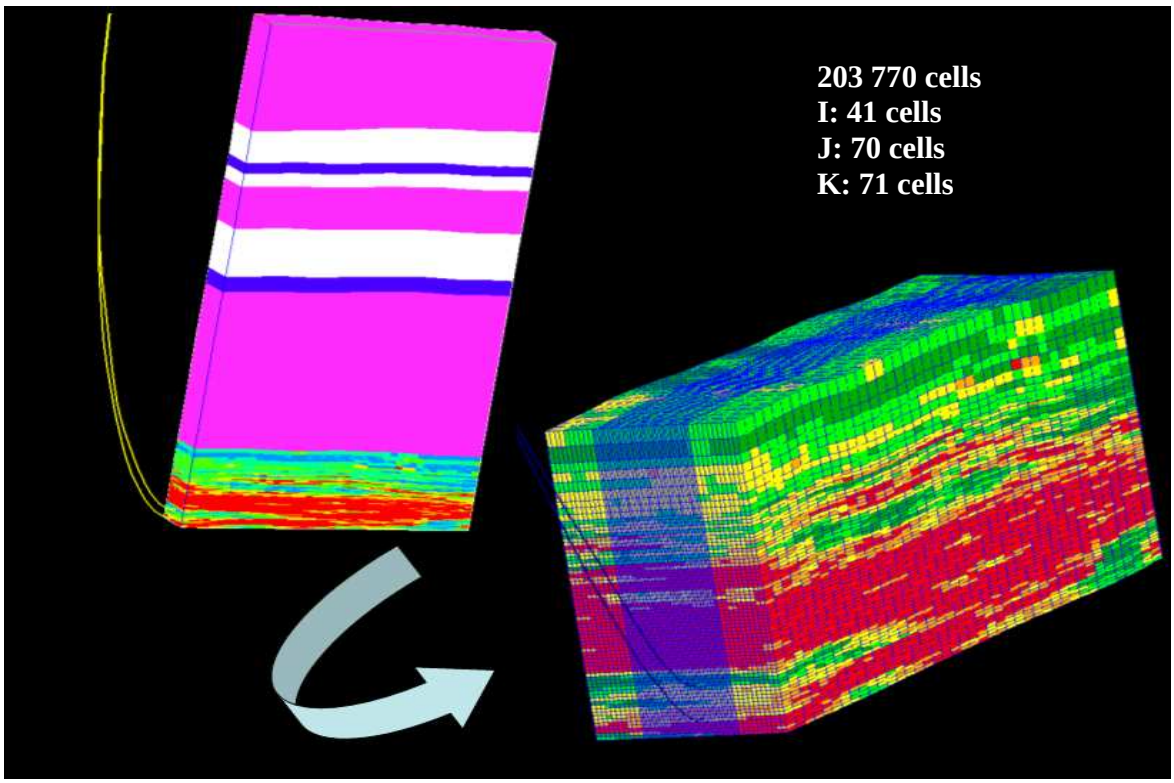

Fig.3.21: Overburden and reservoir grid (Lerat et al, 2010)

Reservoir and geomechanical computations were realized on a local SAGD grid which represents the well pair:

° Reservoir simulations with PumaFlow: evolution of pressure, temperature, oil, steam and water saturations for different stages of production

° One way coupling with a geomechanical model (Abaqus) to compute stress variations and volume strains at these stages

° Explicit coupling with an update of the permeability field in the reservoir area.

Two periods of SAGD production were studied in details: the early steam injection and later on when the steam chamber develops laterally and vertically towards the top of the reservoir. Of course, some simplifying assumptions were taken into account and unfortunately there are no in situ measurements available to validate the results.

Figure 3.21 shows the extension of the steam chamber after six months of production for the one-way coupling (upper figure) and explicit coupling (lower figure). The 3D envelope corresponds to a value of 100 °C; it means that every cell inside this domain has a temperature ranging from 100 to 280 °C.
Both indicate clearly a high degree of heterogeneity of temperature distribution along the well pair due to the presence of shale barriers were the steam chamber can not develop.

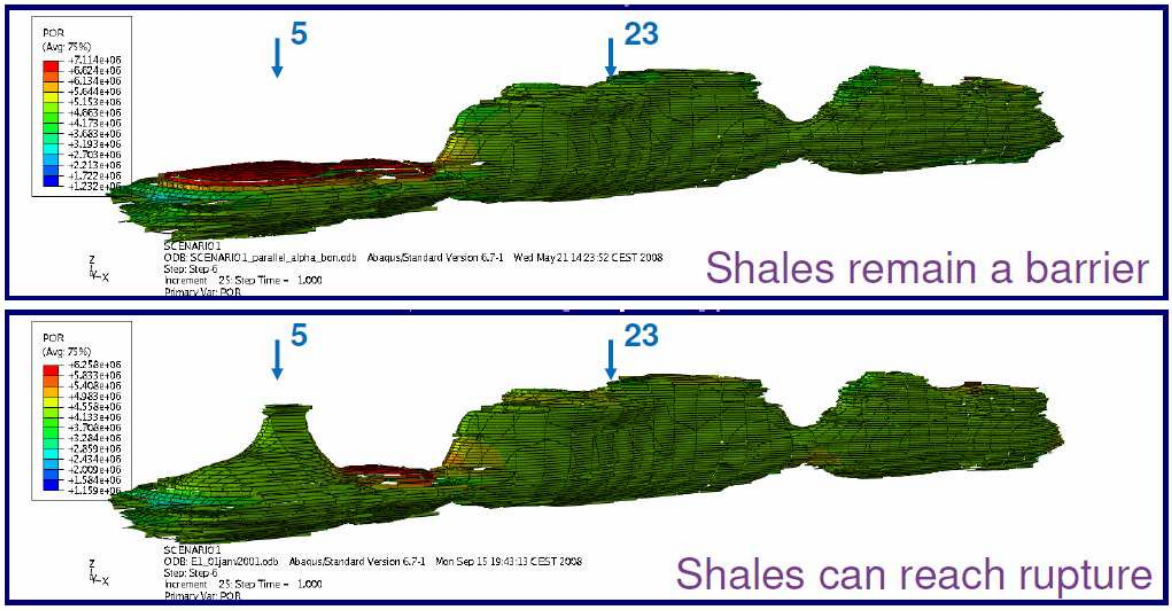

Fig. 3.22: Impact of the shale mechanical behaviour on the geometry of the steam chamber (Lerat et al, 2010)

In the case of explicit coupling where there is an update of permeability in the cells of the reservoir model from the computation of deformation and stress in the geomechanical model, some of the shale barriers are no longer impervious when heated by steam (section 5 for instance) and they fail, helping steam to move upwards and heat more reservoir. This shows that interaction between the two models through iterations is important.

3.7.2 Joslyn study

3.7.2.1 Joslyn steam release

The Joslyn field has been the scene of a steam explosion in surface in May 2006, creating a crater 150 m in diameter in the forest (Figure. 3.23 & 3.24). The release created a large vent formed by fissures approximately 3 m wide, 4 m deep, and 15 to 25 m long. A substantial amount of subsurface material, including pieces of rock up to 1 m in size, was ejected.

Several hypotheses were brought by Total to explain the Joslyn steam release:

- Shear failure at the edge of a pressurized area.
- Leakage within or around wells (e.g. through poor cementation),
- Pre-existing existing fractures or other structural feature,
- Erosion or other sedimentary feature,
- Hydraulic fracture,
- Thermal failure of shale,

All these hypothesis involve geomechanics.

Figure 3.23 shows the lay out of the 18 SAGD well pairs on the Joslyn field: 12 were on SAGD production mode, 2 were on circulation and 4 were shut after the steam release.
Figure 3.24 shows a simplified stratigraphy above Joslyn well pair 204-1.

From ground surface and downward, the formations are:

1. Clearwater shale : continuous cap rock of very low permeability
2. Wabiskau: three layers of aquifer sands, continuous shale and silts. The thickness and other properties of the upper sand and middle shale are very continuous over the area.

3. Upper McMurray bitumen filled (and occasionally gas filled) filed sands/shale alternations.

4. Upper Middle McMurray: alternation of shale and low quality sands (K < 200 md). Shale layers act as local barriers to vertical steam movement and pressure diffusion due to their low permeability.

5. Lower Middle McMurray: good oil sands providing the bulk of HC reserves, permeability of several Darcys.

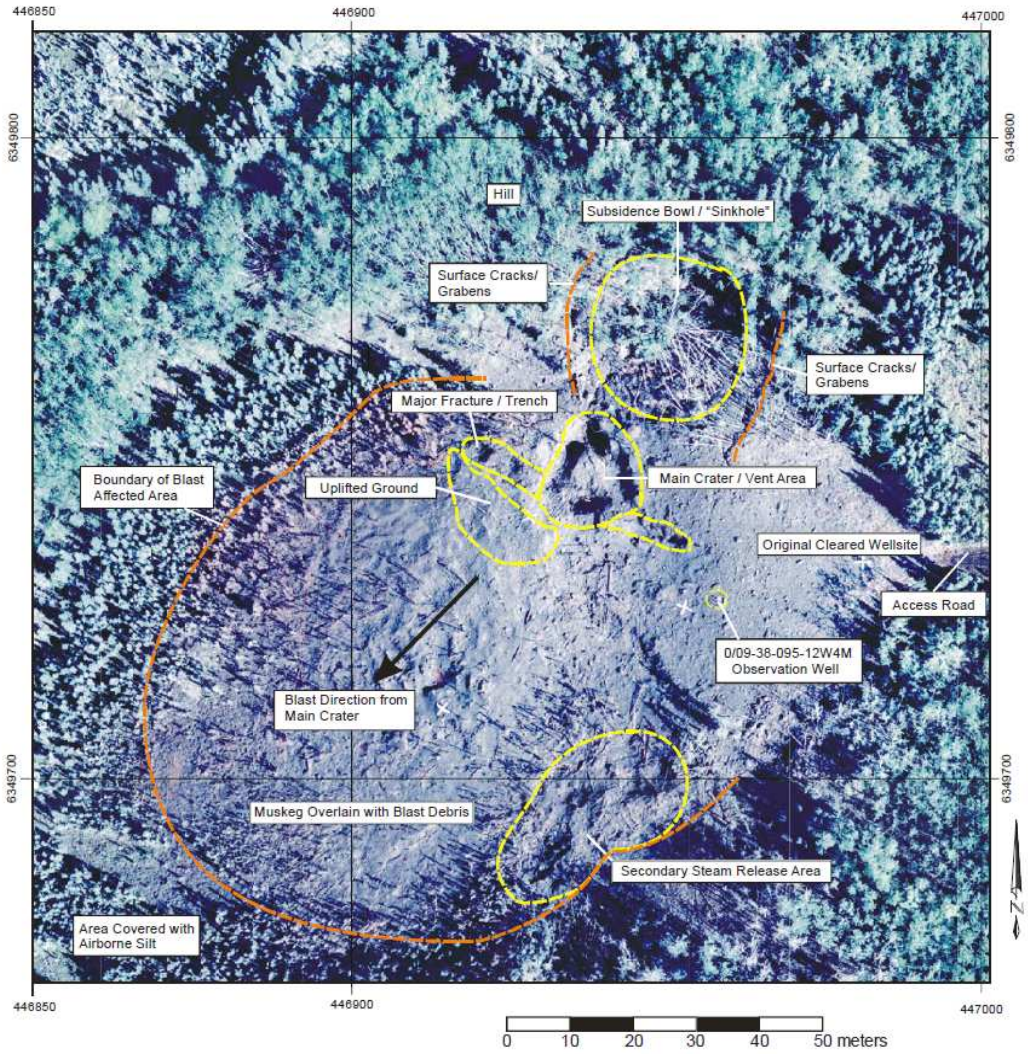

Fig. 3.23: Aerial photographies of area after steam release

Fig. 3.24: Surface photographies of area after steam release

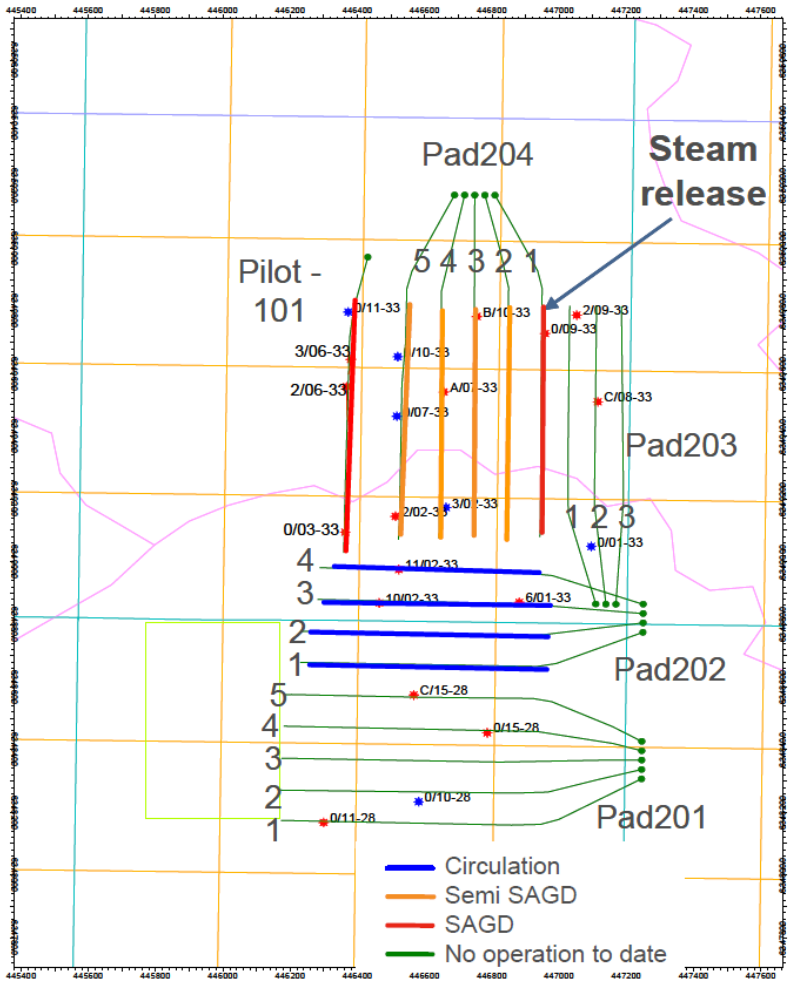

Fig. 3.25: Well Location and Status Map (@ time of steam release)

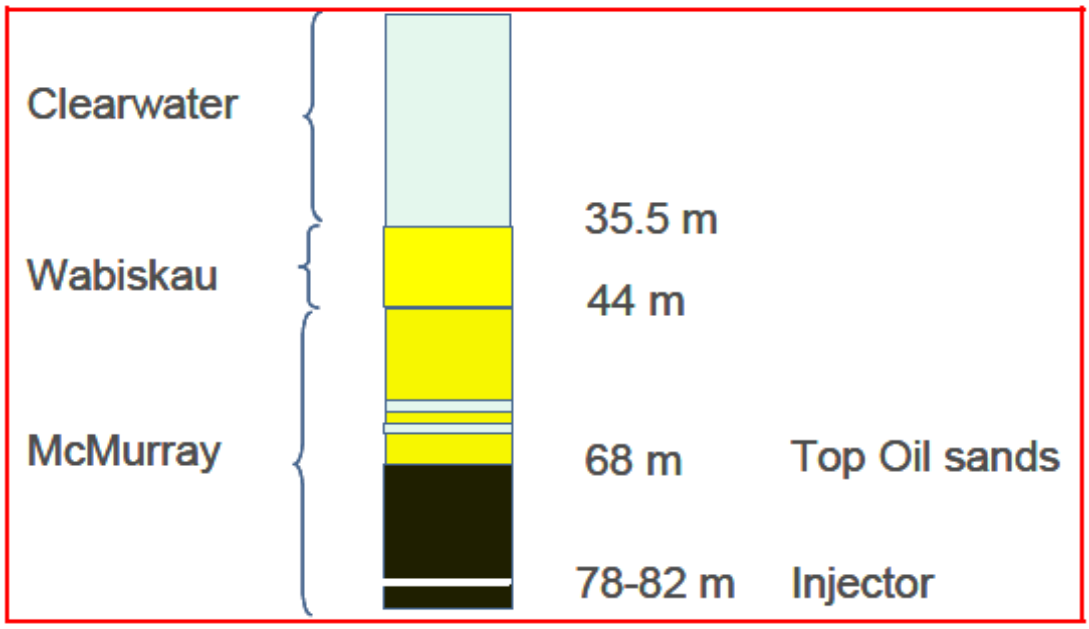

Fig. 3.26: Simplified stratigraphy above Joslyn well pair 204-1

3.7.2.2 Scenario for steam release proposed by Total

First studies performed by Total show that the down-hole pressure at the time of the steam release was much lower than the confining stress at the depth of the 204-I1P1 well pair. Such observation indicates that the steam release was not caused by the opening of a fracture originating from the well depth immediately before the steam release.

The seismic survey shot in December 2006 – January 2007 over the steam release area allowed a volume of formation affected by the steam release to be mapped. The affected volume is fully disconnected from nearby delineation, monitoring or development wells below the Top McMurray interval. Such observation supports the hypothesis that the steam release is not related to channelling around wells.

Others conclusions were drawn:

- Steam vents are observed at surface more than 30 m away from any surface well locations. Such observation supports the hypothesis that the steam release is not related to channelling around wells.

- Available data does not allow clear conclusions relative to nearby wells' cement bond quality to be drawn.

- No evidence was found, after an extensive investigation of geological and seismic data, of pre-existing seal weakness at the particular location of the Joslyn May 18th 2006 steam release.

The reservoir analysis of the SAGD behaviour of well pair 204-I1P1 suggests that some fracture(s) developed at least 4 weeks before the steam release during a phase of high steam injection/circulation pressure. A water volume of around 1000 to 2600 m^3 was stored in this fracture(s) and reservoir connected by this fracture(s) until the final catastrophic failure of the last seal.

The mechanical constraints prevailing in the Joslyn reservoir are such that tensile fractures should develop primarily in the horizontal direction. Vertical tensile fractures would have directly caused a release with no storage period. The most likely failure mechanism of shale barriers in the present context involves successive shear failures at the edge of horizontally pressurized areas.

Geomechanical analysis and modelling were performed in light of results from the previous results. The mechanical model parameters were derived from previous Joslyn geo-mechanical studies and from published data about sand and shale formations analogous to the ones encountered on Joslyn. One way coupling was performed.

The geomechanical model was used to calculate the dilation strain around steam injector as a function of the injection pressure and the size of the pressurized zone (Figure. 3.27). A pressure of 1600 kPa exceeds both the initial vertical and minimum horizontal stresses at the top of the pressurized zone.

To investigate the likelihood of shale barrier failure by shearing at their shoulders, Total built a finite element model of 60 m thick overburden. A pressure of 1800 kPa, to be compared with the overburden weight of 1560 kPa, was applied to the base of this model. The radius of the pressurized zone was changed by steps of 5 m starting from 15 m.

The plastic shear strain (or norm of plastic deviatoric strain) increases significantly when the pressure diffuses laterally at the bottom of a shale layer. When the radius of the pressurized zone reaches 45 m, plastic shear strain cuts through the whole overburden. (Figure 3.28), it means that the shear fault which cuts the shale barrier will be wide open to flow.

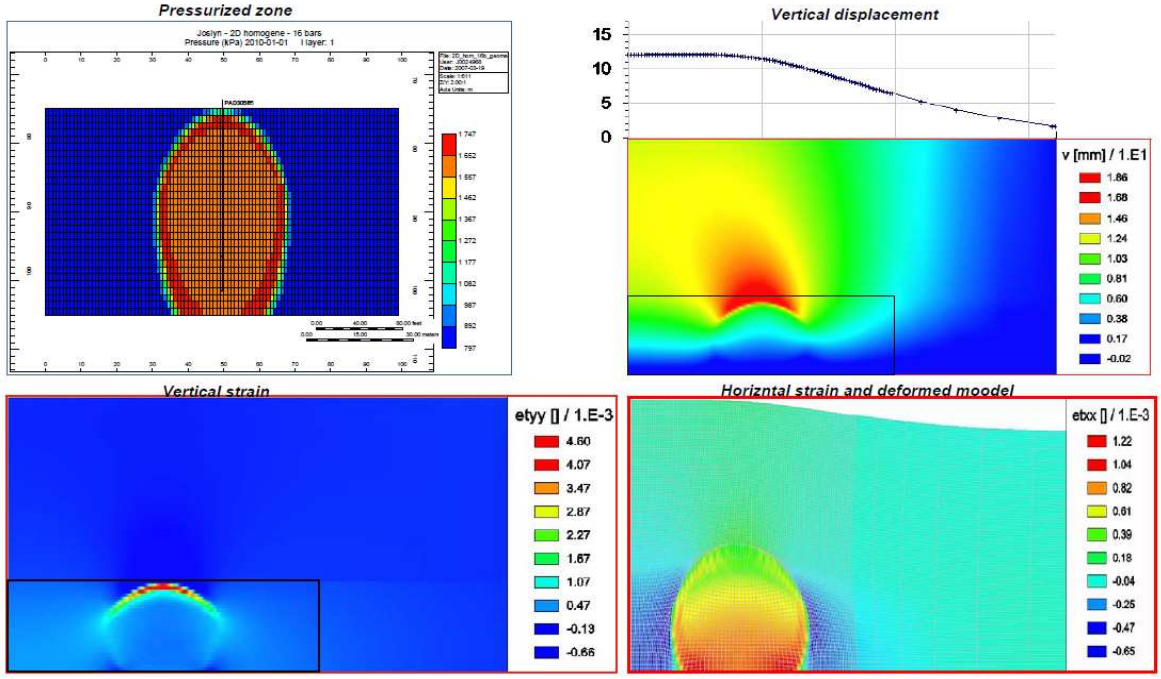

Fig.3.27: Example of geomechanical model results (Total, 2010)

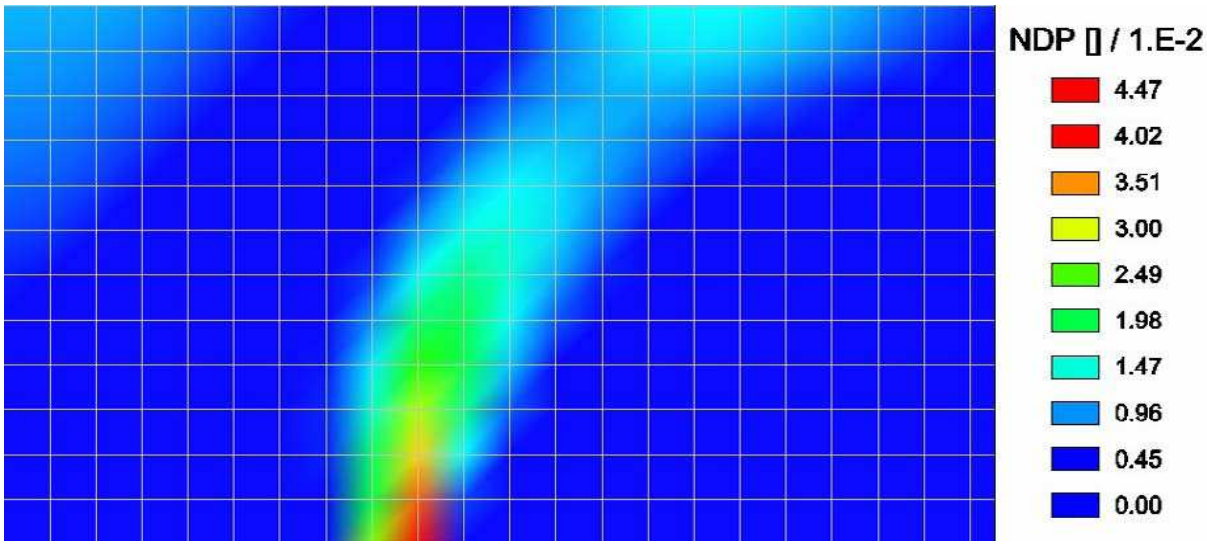

Fig. 3.28: Example of plastic strain in a 60m thick overburden under 1800 kPa pressure (Total, 2010)

Finally, from Total report, the most likely scenario for the steam release involves:

- A fast, gravity-driven, local development of a steam chamber to the top of the reservoir, probably involving sand dilation,

- A lateral extension of the pressured area below the top of the reservoir,

- A shear failure or series of successive shear failures on the edge of this pressurized area that allowed the steam to breach within the Wabiskaw reservoir,

- A significant water / steam storage in the SAGD chamber and fracture system, and a catastrophic shear failure of the ultimate, Clearwater seal leading to release of steam at surface on May 18th 2006

Chapitre 4

Modélisation physique et mathématique

Le chapitre 4 commence par une description générale du problème THM couplé avec interaction des phases fluides et du milieu poreux déformable.

Les principales inconnues pour un problème de THM couplé sont des fonctions de l'espace et le temps :

- *température T à chaque point et à chaque instant commun à toutes les phases (liquide et solide),*
- *pression interstitielle P supposée commune à toutes les phases liquides non miscibles,*
- *le vecteur déplacement de la particule squelette.*

En plus des conditions initiales et des conditions aux limites, les équations qui régissent ce problème sont de deux sortes:

1) *les lois de conservation (de masse, d'énergie, de moment angulaire,)*
2) *les lois constitutives et lois de l'Etat: lois d'état de fluide, la loi de Darcy, loi de Fourier pour la transmission d'énergie par conduction, loi de contrainte effective (Biot) et la loi de thermomécaniques ...*

Au lieu de développer un simulateur parfaitement couplé, ce qui nécessite beaucoup de temps, le choix à l'IFPEN s'est porté sur l'utilisation de deux simulateurs commerciaux existant couplés en externe par un ou des modules de liaison. Il en résulte évidemment des simplifications.

Ce chapitre présente les deux simulateurs utilisés lors de ce travail, PumaFlow simulateur de réservoir et Abaqus simulateur géomécanique. L'accent est mis sur la prise en compte des spécificités de la production thermique en SAGD.

PumaFlow est un simulateur de réservoir développé par IFPEN qui offre des solutions pour traiter la quasi totalité des cas de production d'hydrocarbures. Dans ce travail, on a utilisé

une version thermique qui prend en compte la réduction de viscosité des huiles avec l'augmentation de la température et divers phénomènes de transfert thermique et de perméabilité relative en flux multiphasique.

Cependant avec ce logiciel certains aspects ne sont pas très bien pris en compte comme ce qui concerne le squelette poreux : dilation thermique,...

Le schéma numérique utilisé est un schema en volume finis et une résolution implicite.

Le simulateur de géomécanique utilisé est ABAQUS avec un solveur généraliste qui recourt à un schéma traditionnel d'intégration implicite.

Le solveur ABAQUS/Explicit emploie un schéma d'intégration explicite pour résoudre des problèmes dynamiques ou quasi-statiques non-linéaires.

ABAQUS/CAE constitue une interface intégrée de visualisation et de modélisation pour lesdits solveurs. Chacun de ces produits est complété par des modules additionnels et/ou optionnels, spécifiques à certaines applications.

Le couplage entre un simulateur de réservoir et un simulateur de géomécanique a été un sujet de recherche à IFPEN depuis 2000. Par exemple les couplages entre Sarip, un code de réservoir, et Cesar ou entre Sarip et Abaqus ont été abordées dans une phase de recherche. Le couplage entre Sarip et Abaqus qui était basé sur la mise à jour de porosité a été utilisé par D. Bévillon (2000) afin de modéliser la subsidence d'un réservoir très compactable homogène. Dans un stade légèrement plus avancé, le couplage entre Athos (version précédente de PumaFlow) et Visage (VIP) (un simulateur de géomécanique) a été étudié par M. Mainguy et P. Longuemare en 2002. Cette étude, qui a été un couplage séquentiel (ATH2VIS), a été menée pour savoir si les changements dans les contraintes effectives résultant de l'injection d'eau froide pourraient expliquer des venues d'eau prématurées dans la production.

Le couplage (de la porosité) entre PumaFlow et Abaqus a été initialisée par S. Vidal dans le cadre d'une modélisation de stockage de CO2.

En 2007, l'étude d'une simulation couplée du processus SAGD réservoir-géomécanique a été initialisée par F. Adjemian et G. Servant G.

Cette thèse est en continuité avec les travaux précédents. Certains programmes et subroutines ont été modifiés, d'autres ont été adaptés afin d'être appliqués dans une simulation thermo-hydro-mécanique couplée. Un module de couplage entièrement automatique (PUMA2ABA) a été développé en Python pour gérer le couplage entre PumaFlow et Abaqus :

- *la pression de pore et la température déduite du modèle réservoir sont introduites dans le modèle géomécanique pour calculer un nouvel équilibre mécanique,*
- *le modèle géomécanique calcule les déformations induites dans le réservoir et donne une perméabilité actualisée qui est transférée au modèle réservoir.*

Ce module de couplage est actuellement opérationnel en approche one-way, explicite et itérative. Dans la deuxième partie de ce travail afin de réduire le temps de simulation couplée courir, la possibilité d'utiliser différents systèmes de maillage pour les modèles de réservoir et géomécanique a été étudiée et un module de transfert de champs a été mis en œuvre dans notre module de couplage réservoir-géomécanique pour faciliter l'interpolation des données entre deux simulateurs. Par conséquent ce code de couplage PumaFlow-Abaqus est complètement opérationnel en vue d'effectuer une simulation couplée sur un cas sur le terrain réel.

La méthodologie de couplage pour effectuer des simulations réservoir-géomécanique pour le procédé SAGD peut être décrite comme suit:

1. Établir les fichiers de démarrage initial pour PumaFlow et Abaqus, puis concevoir la boucle suivante pour réaliser la simulation couplée réservoir-géomécanique;

2. Extraire la distribution de la pression et de la température après chaque pas de temps de PumaFlow,

Remarque: dans ce modèle, nous avons négligé la pression capillaire. En fait, dans SAGD, la porosité du milieu considéré est très élevé (ou nous avons un rayon de pores importants), donc la pression capillaire est négligeable. Donc, en PumaFlow nous avons la même pression pour l'eau, l'huile et la vapeur qui est la pression utilisée dans Abaqus comme le chargement d'entrée.

3. Transformer la pression et la température de format de données de PumaFlow en ce qui est requis par Abaqus, y compris l'interpolation dans l'espace.

4. Exécuter Abaqus avec les données de la pression interstitielle et température mis à jour pour calculer les contraintes et les déformations, et de modifier la perméabilité.

5. Exécuter PumaFlow pour le pas de temps suivant avec le champ de perméabilité à jour.

6. Répétez la procédure depuis l'étape 2 à 5 jusqu'à la fin du temps de calcul.

Lors d'une analyse couplée, le simulateur de réservoir calcule les variations de pression interstitielle, la saturation et la température. Ces variations de la pression interstitielle et la température calculée par le simulateur de réservoir sont convertis dans des conditions limites distribués dans le simulateur mécanique. En appliquant la pression interstitielle et des conditions aux limites thermiques, le simulateur calcule l'évolution des contraintes et déformations géomécanique induites par l'exploitation de réservoir sur le réservoir et les formations adjacentes.

PUMA2ABA génère la correction du volume des pores et le nouveau champ de perméabilité, qui peuvent être utilisés dans l'étape suivante de simulation de réservoir. Le couplage séquentiel est appelé explicite si la méthodologie précédente est seulement effectué une fois pour chaque pas de temps et itérative si la méthodologie est répété jusqu'à convergence du contrainte et inconnues d'écoulement du fluide. Le couplage explicite est adapté pour mettre à jour la perméabilité alors que le couplage itérative est plus adaptée pour le mis à jour de porosité.

La méthodologie de couplage séquentiel mis en œuvre dans PUMA2ABA est réalisée avec différents pas de temps pour le simulateur réservoir et le simulateur géomécanique. Par conséquent, les pas de temps en simulateur réservoir sont des subdivisions de la période de temps (définies par l'utilisateur) sur lequel le problème géomécanique est résolu. Couplage explicite ou itératives peuvent être réalisées avec différents pas de temps pour les simulateurs réservoir et géomécanique. Notez que la méthodologie de couplage itérative ne garantit pas la convergence vers le même résultat de la méthode entièrement couplé, mais permet une forte réduction du coût de calcul.

Chapter 4

The Physical & Mathematical Model

The goal of geomechanics-reservoir coupling is to describe the role of geomechanics on the whole reservoir characterization and to predict reservoir behaviour under varying conditions of stresses and strains during various stages of exploration, development, production and completion. The purpose of this chapter is to explain a thermo-hydro-mechanical model and its application in the case of SAGD thermal heavy oil recovery.

This chapter starts with a general description of coupled THM problem with interaction of fluid phases and a deforming porous medium. Then it presents two simulators used during this work, PumaFlow the reservoir simulator and Abaqus the geomechanical simulator. In the next step, the applied simplifying assumptions and the reservoir-geomechanics coupled equations are described. In the last section of this chapter, the external coupled simulator, named PUMA2ABA, developed in this work is presented, in which the applied coupling approaches and the coupling module are detailed.

4.1 General Coupled THM Problem

In underground applications, the main unknowns for a coupled THM problem, which are functions of space and time, are:

- Temperature T assumed at each point and every moment common to all phases (fluid and solid)
- Pore pressure P assumed common to all immiscible fluid phases
- The displacement vector of the skeleton particle u

In addition to the initial conditions and boundary conditions, the equations governing this problem are of two kinds:

1) The conservation laws

- Mass conservation law (of fluid, since in poromechanics we follow the movement of skeleton)
- Energy conservation law (in our case it is mainly the thermal energy)
- Linear momentum conservation law (purely mechanical quantity).

In the simulations realized in this thesis, the first two conservation laws have been treated by the 'reservoir' software which therefore has to calculate temperature T and pressure P. The last law is managed by the 'mechanical' software in order to calculate the displacement u.

2) constitutive laws and state laws: fluid state laws, Darcy's law, Fourier's law for the energy transmission by conduction, concept of effective stress (Biot) and thermomechanical constitutive law for solid matrix ...

The complete equation system is divided into two parts:

1) The first is carried by the 'reservoir' software and requires external data such as:
   - Historical details of the current point (in our case we assumed small deformations, and only the initial geometry is used),
   - The involvement of the solid in the energy balance (we attribute a volumetric heat to the solid and we consider the Fourier law with an overall conductivity),
   - The deformability of the skeleton resulting in a variation of the porosity that occurs in both mass and energy balances and in the intrinsic permeability of the medium.
2) The second part, managed by the 'mechanical' software, requires the fields of temperature T (skeletal thermal expansion) and pressure P (Biot's theory).

It should be mention that in the realized simulations, the Ω field treated by 'mechanical' software is larger than the domain $\omega \subset \Omega$ which is treated by 'reservoir' simulator (Figure 4.1). The reservoir boundary is assumed impermeable so fluids cannot flow through the boundaries but heat losses by conduction through upper and lower boundaries are taken into account by a simplified and one-dimensional modelling of the overburden and underburden that is oriented in the vertical direction. However, the coupling process that we developed in this thesis is entirely general and is not caused by these simplifying assumptions.

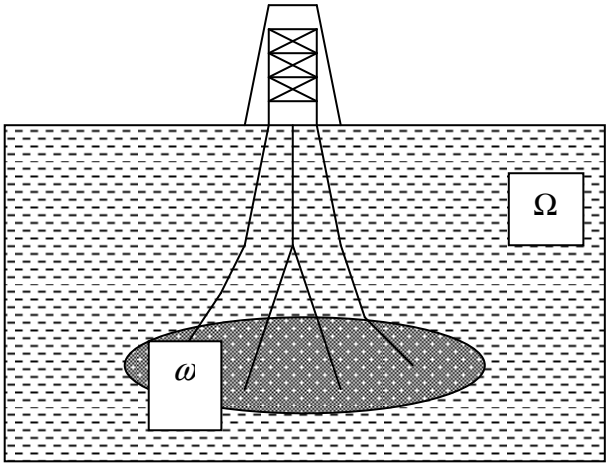

Fig. 4.1: Schema of reservoir and its country rocks

4.2 Description of Simulators

Instead of developing a fully coupled simulator, which is extremely time-consuming, this research links two separate existing commercial simulators through a coupling module.

As explained in chapter 3, the two-way or sequential coupling approach has been adopted to perform reservoir-geomechanical modelling in order to provide an understanding of the effects of geomechanical parameters on permeability and porosity. Permeability and porosity, in turn, affect the pore pressure profile and ultimately, the final recovery factor.

In this work the methodology is based on the work of Samier et al. (2008), Dean et al. (2006), Chalaturnyk (2006), Dussault (2002) and many other authors. Despite focusing on different aspects and using different methodologies, the work of these authors share two main attractive characteristics: 1) the codes of the commercial simulators need no modifications; 2) any two commercial simulators can be used, depending on the objectives and requirements of the research, allowing exploitation of their special features.

The key idea of two-way or sequentially coupled approach is the reformulation of the stress-flow coupling such that a conventional stress analysis code can be used in conjunction with a standard reservoir simulator. In this section we present PumaFlow, the reservoir simulator, and Abaqus the geomechanical simulator used in this research. The equation system in our reservoir simulator and geomechanical simulator and applied resolution method in each simulator is explained in detail in this section.

4.2.1 PumaFlow

PumaFlow is a multipurpose reservoir simulator developed at IFPEN that offers rigorous formulation of all simulation options.

Generally three possible representations of oil and gas mixture models are identified for non-isothermal modelling:

- Black oil (Live oil) model
- Dead oil model
- Compositional model

Black Oil Model

The black oil fluid model is the standard phase behaviour model most often used in petroleum reservoir simulation. It is able to predict compressibility and mass transfer effects between phases that are needed to model primary (pressure depletion) and secondary (water injection) recovery.

The term black-oil refers to the fluid model, in which water is modelled explicitly together with two hydrocarbon components, one (pseudo-) oil phase and one (pseudo-) gas phase.

This is in contrast with a compositional formulation, in which each hydrocarbon component is handled separately. The black oil flow equations consist of the conditions of thermodynamic equilibrium (which determines how the components combine to form phases), an equation of state, Darcy's law and a mass conservation equation for each component.

In the black oil model, it is assumed that the hydrocarbon components are divided into a gas component and an oil component in a reservoir at the standard pressure and temperature and that no mass transfer occurs between the water phase and the other two phases (oil and gas). The gas component mainly consists of methane and ethane.

Compositional Model

In compositional model, flow involves multicomponents and three phases, and there is mass transfer between the hydrocarbon phases (i.e., the vapour and liquid phases). In this model, a finite number of hydrocarbon components are used to represent the composition of reservoir fluids. These components associate as phases in a reservoir. Normally the model is described under the assumptions that the flow process is isothermal (i.e., constant temperature), the components form at most three phases (e.g., vapour, liquid, and water), and there is no mass

interchange between the water phase and the hydrocarbon phases. Furthermore, the diffusion/dispersion effect is neglected. A general compositional model should be stated that involves any number of phases and components, each of which may exist in any or all of these phases. While the governing differential equations for this type of model are easy to set up, they are extremely complex to solve.

Dead-Oil Model

Dead Oil model is the oil at sufficiently low pressure that contains no dissolved gas or a relatively thick oil or residue that has lost its volatile components. It means that the gas phase contains only steam water and no hydrocarbon.

The Dead Oil thermodynamic representation may be used either with vapour or without it (displacement with hot water). Oil physical properties (such as density, viscosity, enthalpy) are defined either in an explicit form (as the parameter dependence on pressure and temperature), or in the form of analytical relationships, the constants of which may be derived from multiple correlations by selecting a necessary function.

It should be noted that in case of simulation of a non-isothermal filtration, the Black Oil thermodynamic representation (with dissolved or free gas) may be used only under assumption of water vapour absence in the designed model; so Dead Oil model was used in this work in order to design a model of oil and gas properties in order to solve a non-isothermal problem with water vapour.

4.2.1.1 Thermal Dead Oil Model

In this work, we have used the Thermal version of PumaFlow in order to simulate the SAGD process.

The PumaFlow Thermal module concerns the resolution of heat transfer equations coupled with the hydrocarbon mass conservation equations using the Dead Oil model. The fluid which saturates the medium porosity is composed of three immiscible phases: one phase of liquid water (subscript w), a phase of steam (subscript s) and oil phase liquid (subscript o).

The thermal option aims at designing and simulating different thermal Enhanced Oil Recovery processes. It allows simulating steam and hot water flooding and in-situ combustion applications.

The Thermal module is based on: (a) reduction of crude viscosity with increasing temperature, (b) change of relative permeabilities for greater oil displacement, (c)

vaporization of connate water and of a portion of crudes for miscible displacement of light components, and (d) high temperatures of fluids and rock to maintain high reservoir pressure. This Thermal module can model the important physical phenomena and processes:

- Viscosity, gravity and capillary forces;
- Heat conduction and convection processes;
- Heat losses to overburden and underburden of a reservoir;
- Mass transfer between phases;
- Effects of temperature on the physical property parameters of oil, gas and water;
- Rock compression and expansion.

4.2.1.1.1 Mass Conservation and Darcy's Law

Capillary pressure

Capillary pressure is the difference in pressure across the interface between two immiscible fluids, and thus defined as:

$$P_c = P_{non\text{-}wetting\ phase} - P_{wetting\ phase} \tag{4.1}$$

Capillary pressures are generally input for the gas-oil and oil-water systems and for the gas-water system in a gas-water reservoir. They are input as a series of curves which are normalized by the programme and a series of end point values. Curves are input as tables of the referred parameter versus saturation. In PumaFlow the capillary pressures and relative permeabilities are generally defined for different "rock types" corresponding to different ranges of rock properties.

It should be mentioned that in this work, the capillary pressure has been neglected. In fact, in SAGD, porosity of the considered medium is very high (or we have an important pore radius); so the capillary pressure is negligible. Therefore in this work we have the same pressure for water, oil and steam;

$$P_w = P_s = P_o = P \tag{4.2}$$

Conservation of water components

The mass conservation law for water components reads:

$$\partial_t[\phi(\rho_w S_w + \rho_s S_s)] + \nabla \bullet [\rho_w \vec{U}_w + \rho_s \vec{U}_s] = 0 \quad (4.3)$$

Where ϕ is porosity, ρ_f is density of fluid phase f , where f returns to water by *w*, steam by *s* or oil by *o*. S_f is degree of saturation and U_f is the velocity vector.

Conservation of "hydrocarbon" components:

The mass conservation law for hydrocarbon components reads:

$$\partial_t[\phi \rho_o S_o] + \nabla \bullet [\rho_o \vec{U}_o] = 0 \quad (4.4)$$

Darcy velocity

The Darcy velocity for water and hydrocarbon components is written as:

$$\vec{U}_f = -k \frac{k_{rf}}{\mu_f} (\vec{\nabla} p + \rho_f \cdot \vec{g}) \quad \text{for} \quad f \in \{w, s, o\} \quad (4.5)$$

4.2.1.1.2 Energy Conservation

The energy conservation law reads:

$$\partial_t[(\phi(\rho_w S_w e_w + \rho_s S_s e_s + \rho_o S_o e_o)) + (1-\phi)\rho_r e_r] + \nabla \bullet [\vec{J}_q + \rho_w \vec{U}_w H_w + \rho_s \vec{U}_s H_s + \rho_o \vec{U}_o H_o] = 0 \quad (4.6)$$

Where $\overrightarrow{J_q}$ is the heat flux derived by the heat conduction law, also known as Fourier's law, which is written in form of equation (4.7), where λ is the thermal conductivity.

$$\vec{J}_q = -\lambda . \vec{\nabla} T \quad (4.7)$$

In SAGD the flow term of energy consists of convective and conductive flow.

4.2.1.1.3 Fluid Properties

Density

The fluid mass density is a function of temperature and pressure, which is given by the correlation law. The mass density of oil is given by:

$$\rho_o(P,T) = \rho_{oref}\left(1 + c\left(P - P_{ref}\right) - d\left(T - T_{ref}\right)\right) \tag{4.8}$$

Where ρ_{oref} is the density of oil at reference pressure P_{ref}, expressed in *Pa*, and reference temperature, T_{ref} expressed in °K. c is the compressibility of oil and d its coefficient of thermal expansion.

A correlation gives the water density, ρ_w, as follows:

$$\rho_w(P,T) = \rho_w(T)\left[1 + c_w(p - p_0)\right] f(C_s) \tag{4.9}$$

Where $\rho_w(T)$ is given by a correlation, C_s represents the salinity and c_w the water compressibility.

The correlation defining steam density, ρ_s, takes into account the steam compressibility ($Z(T)$) and the constant of ideal gases (R) and is given by:

$$\rho_s(P,T) = \frac{P \times 0.018016}{Z(T)RT} \tag{4.10}$$

Viscosity

The viscosity of most materials decreases as temperature increases. As it was explained in previous chapters the heavy oil viscosity decreases exponentially when temperature increases. The Andrade equation relates the viscosity to temperature as follows:

$$\mu = Ae^{\frac{B}{T}} \tag{4.11}$$

Where A and B are constants characteristic of heavy oil or other material and T is the absolute temperature. The viscosity of the heavy oil at a given temperature can be estimated by knowing the viscosity at two other temperatures. This knowledge allows calculation of the constants A and B and subsequent determination of viscosities at other temperatures. Therefore the oil viscosity in PumaFlow is defined by:

$$\mu = \mu_1 \exp[(1-\frac{T_1}{T})(\frac{T_2}{T_2 - T_1}) \ln(\frac{\mu_2}{\mu_1})] \tag{4.12}$$

The water viscosity is given by the Bingham law (for T ≤ 260°C):

$$\mu_w = \mu_w(T)(1 + 1.34C_s + 6.12C_s^2) \tag{4.13}$$

The steam viscosity is obtained by interpolation in the international tables or by the Hilsenrath formula.

Relative Permeability

In multiphase flow in porous media, the relative permeability of a phase is a dimensionless measure of the effective permeability of that phase. It is the ratio of the effective permeability of that phase to the absolute permeability. It can be viewed as an adaptation of Darcy's law to multiphase flow.

Data required for the estimation of three-phase relative permeability are two sets of two-phase data, water-oil and steam-oil. From the water-oil data we obtain both k_{rw} and k_{row}, as a function of water saturation (S_w), where k_{row} is defined as the relative permeability to oil in the oil-water two-phase system. Similarly, we obtain k_{rs} and k_{ros}as a function of S_s steam saturation. In PumaFlow the following formula is used (Stone II):

$$k_{ro}(S_w, S_s) = \max[0, k_{row\max}(\frac{k_{row}}{k_{row\max} + k_{rw}})(\frac{k_{ros}}{k_{ros\max} + k_{rs}}) - k_{rw} - k_{rs})] \tag{4.14}$$

Where:

- $k_{rw\max}$, maximum water relative permeability, $k_{rw}(S_w = 1 - S_{orw})$
- $k_{row\max}$, maximum oil relative permeability, $k_{row}(S_w = S_{wir})$
- $k_{rs\max}$, maximum steam relative permeability, $k_{rs}(S_s = 1 - S_{ors} - S_{wir})$
- S_{wir}, irreducible water saturation.
- S_{orw}, residual oil saturation to water.
- S_{ors}, residual oil saturation to steam.

4.2.1.1.4 Rock Properties

PumaFlow is a reservoir software and it deals only with fluids, however, as we have seen it needs the porosity of the skeleton and its intrinsic permeability. Also it was mentioned that the energy conservation law and the heat conduction law are global. In current version, the software can not easily impose a field history of quantities related to the skeleton and it uses the relationships that will be explained here.

Rock compressibility

The rock compressibility c_r defines the total pore volume variation against pressure (i.e. pore compressibility c_p) as:

$$c_r = \frac{1}{V_T}\frac{\partial V_T}{\partial P} \tag{4.15}$$

$$c_p = \frac{1}{\phi V_T}\frac{dV_T}{dP} = \frac{1}{\phi}c_r \tag{4.16}$$

Rock Heat Capacity and Conductivity

The rock volumetric heat capacity is computed from a linear relationship whose coefficients are user defined:

$$\rho_{oc}(T) = \rho c_1 + \rho c_2 T \tag{4.17}$$

Where ρc_1 and ρc_2 are given constants.

The thermal conductivity (in $W\ m^{-1}\ K^{-1}$) corresponds to a saturated rock and is calculated vs. temperature from a published relationship (after Somerton):

$$\lambda(T) = \lambda_{ref} + \alpha(T - T_{ref})(\lambda_{ref} - 1.42) \tag{4.18}$$

Where α is a given constant. These expressions are used for the reservoir rock.

The heat capacity and conductivity of the overlaying and underlaying strata are constant and must be user defined. They are compulsory in the thermal context.

4.2.1.1.5 Equilibrium Equations

Liquid-Vapour equilibrium state relationship

These equations state that the hydrocarbon components are constantly in equilibrium between liquid and vapour phases.

- If temperature is below the saturation temperature ($T - T_{sat}(P) < 0$) , liquefaction happens ($S_w \geq 0$) and steam saturation is equal to zero.

$$S_s \times S_w (T - T_{sat}(P)) = 0 \quad (4.19a)$$

Where T_{sat} is the temperature at which vapour phase is in equilibrium with liquid phase.

- When temperature is equal to steam saturation temperature ($T = T_{sat}$), the water phase is in equilibrium with the vapour phase.

$$S_w \geq 0 \quad , \; S_s \geq 0 \quad (4.19b)$$

- If the temperature exceeds the saturation temperature ($T - T_{sat}(P) > 0$), there is only dry steam ($S_s \geq 0$) and water saturation is zero.

$$S_s (T - T_{sat}(P)) \geq 0 \quad , \quad S_w (T - T_{sat}(P)) = 0 \quad (4.19c)$$

Closure Equation

The closure equation to define the porous media equilibrium state is:

$$S_w + S_s + S_o = 1 \quad (4.20)$$

4.2.1.1.6 The Equation System

In summary, the non-isothermal fluid flow equation system to resolve in PumaFlow are illustrated in table 4.2a:

$$\partial_t[\phi(\rho_w S_w + \rho_s S_s)] + \nabla \bullet [\rho_w \vec{U}_w + \rho_s \vec{U}_s] = 0 \quad (4.21)$$

$$\partial_t[\phi \rho_o S_o] + \nabla \bullet [\rho_o \vec{U}_o] = 0 \quad (4.22)$$

$$\partial_t[(\phi(\rho_w S_w e_w + \rho_s S_s e_s + \rho_o S_o e_o)) + (1-\phi)\rho_r e_r] + \nabla \bullet [\vec{J}_q + \rho_w \vec{U}_w H_w + \rho_s \vec{U}_s H_s + \rho_o \vec{U}_o H_o] = 0 \quad (4.23)$$

$$\vec{J}_q = -\lambda . \vec{\nabla} T \quad (4.24)$$

$$\vec{U}_f = -k \frac{k_{rf}}{\mu_f} (\vec{\nabla} p + \rho_f \cdot \vec{g}) \quad \text{for} \quad f \in \{w, s, o\} \quad (4.25)$$

$$S_s S_w (T - T_{sat}(P)) = 0 \quad (4.26)$$

$$S_w \geq 0 \ , \ S_s \geq 0 \quad (4.27)$$

$$S_s (T - T_{sat}(P)) \geq 0 \ , \ S_w (T - T_{sat}(P)) = 0 \quad (4.28)$$

$$S_w + S_s + S_o = 1 \quad (4.29)$$

Table 4.2a: Non-isothermal fluid flow equation system in PumaFlow

4.2.1.2 Initial Conditions & Boundary Conditions in SAGD

In order to have a well-posed mathematical problem, the initial and boundary conditions for the unknown fluid flow parameters (which are pressure, temperature and saturation) must be defined.

4.2.1.2.1 Initial Conditions

To assume proper initial conditions for the reservoir simulation, it is necessary to start the simulation from the only fluid distribution that can be determined reliably, which is the uniform temperature distribution in reservoir and hydrostatic equilibrium before production.
A reference pressure is assumed to be known, somewhere in the oil zone. The initial oil pressure to be deduced from this reference pressure, for initialization, is calculated using the hydrostatic law:

$$\vec{\nabla} P = \rho_o \cdot \vec{g} \tag{4.30}$$

Once the pressure initialization is done, it allows the calculation of initial water and oil saturations.
Initial water saturation is at its irreducible water saturation: $S_{w,ini} = S_{wir}$
and the oil saturation is equal to: $S_o = 1 - S_{wir}$ ($S_s = 0$, the injection has not started yet)

4.2.1.2.2 Boundary Conditions

The notations used for the boundary conditions are given in Figure 4.2.
Γ_l denotes the lateral edges of the reservoir. The upper and lower limits of the reservoir are Γu and Γd , respectively. Γi and Γp represent respectively the injector and producer wells.

- ***On*** Γ_l :

There is no flux. In other words, there is no exchange of mass or heat.

- ***On the perforations of the injection and producer wells*** (respectively, Γi and Γp):

The mass flux is characterized by:

- conditions of pressure; in this case, it is said that the well is working at imposed pressure limit (surface or bottom hole pressure); or
- Conditions of flow rate; in this case, it is said that the well is working at imposed flow rate (maximum or minimum).

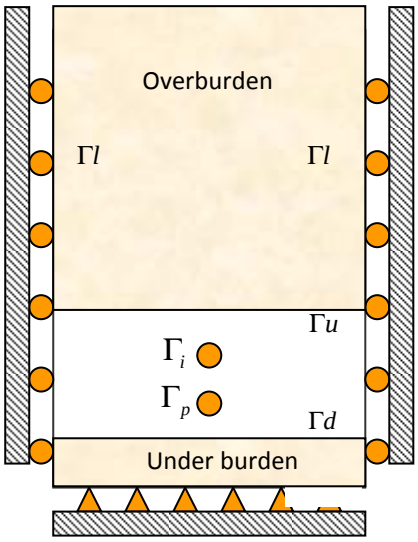

Fig. 4.2: Representation of fluid flow boundary conditions

- ***On*** Γi

The temperature of the well is specified.

- ***Thermal regulation for horizontal production wells***

Optimization of the oil production is a difficult task in the simulation of the SAGD process. To achieve a good efficiency, the presence of liquids above the producer is required. However, if this amount of liquids is too large, temperature in the vicinity of the producer is not high enough and the oil viscosity is insufficiently reduced. Besides, in the source/sink system formed by the two closely spaced horizontal wells there is a risk of short-circuiting of steam between injector and producer.

To avoid steam breakthrough at the producer, either the producer or the injector well rate must be lowered. As a consequence of rate reduction, the steam chamber moves away from the producer, inducing reduced temperatures and larger liquid volumes around the well.

The reduction of the flow rate of either well has to be initiated when temperatures in the producer well have reached a threshold slightly lower than steam temperatures.

In PumaFlow three regulation modes are available:

- In the first one (REGMET1) the producer bottom-hole pressure, at each time-step, is set to a value function of the maximum temperature, reached in well, at the previous time-step.

- In the second one (REGMET2) a temperature difference between the producer and a reference well (generally the injector) must be set, and it should be respected by reducing or increasing either the well rate of the producer or the well rate of the injector.

- In the third one (REGMET3) a maximum and a minimum temperature value are set at the producer, and the well rate of a reference well (the producer or the injector) is varied accordingly.

In this work, the second regularization method, REGMET2, has been adopted.

- ***On*** Γp

The imposed Fourier flux is equal to zero, and the temperature of the meshes of producer well is then equal to the imposed temperature to the well.

- ***On*** Γu and Γd

The overburden and underburden are assumed impervious, so fluids cannot flow through the boundaries but heat losses by conduction through upper and lower boundaries are taken into account by a simplified and one-dimensional modelling of the overburden and underburden that is oriented in the vertical direction.

4.2.1.3 Discretized Equations

In the previous section it was mentioned that our model is a coupled system which involves the mass conservation law for 2 differents components: oil and water, and also energy conservation law. This is a complex equation system and so finding an analytical solution for this equation system is not possible. In PumaFlow, these equations are discretized in space using a finite volume method.

4.2.1.3.1 The mesh

Among the meshes used in reservoir simulation, there is structured Cartesian mesh. This simple mesh method can neither denote the complex geometry of the reservoir nor take into account the presence of faults. In these cases, the Corner Point Geometry (CPG) mesh type is used where gridcells have hexahedral form. This type of mesh gives more flexibility in representation of reservoir geometry, as shown in Figure 4.3.

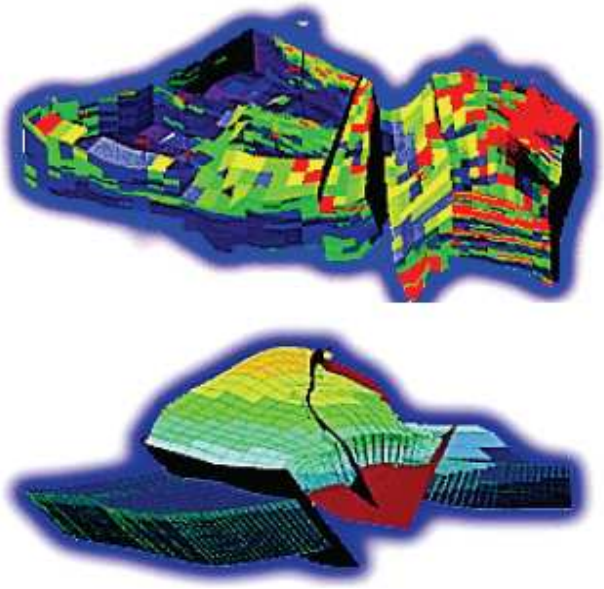

Fig. 4.3: Example of CPG mesh type

In reservoir engineering, in order to reduce the numerical diffusion to the minimum possible whithout excessive increasing of the gridcell number, the non-structured localy refined mesh is used. In our study, we use a locally refined Cartesian mesh (around the well). (See Figure 4.4).

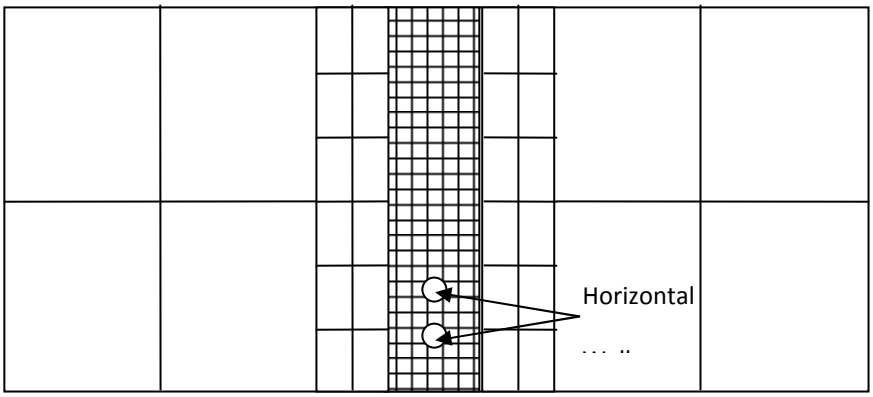

Fig. 4.4: Example of unstructured Cartesian mesh, locally refined

4.2.1.3.2 The Numerical Schemes

Several numerical schemes are available in PumaFlow. Concerning the discretization in time, the most used schemes are IMPES (implicit in time for pressure and explicit for saturation) and fully-implicit (implicit in time for all variables).

The numerical scheme used to simulate our SAGD model is the finite volume scheme with five points and implicit in time. It is unconditionally stable, contrairy to the explicit scheme. However, the values of the time steps are limited by the convergence of Newton's algorithm(used for resolution of non-linear systems). Compared to an explicit resolution, an implicit one needs more time for each time step because the linear system has more unknowns by gridcell, but the number of time steps can be reduced.

4.2.1.3.3 Resolution of the implicit scheme in time

Pressures, saturations and temperature are all involved in the equations system (See Section 4.2.1.1.6). Depending on the thermodynamic state of the gridcell (see section 4.2.1.1.5) it is possible to reduce the number of unknowns and also the number of equations of the system. Three cases are possible:

- $T = T_{sat}\ (P)$:

  There is equilibrium between water and steam phases. We can then choose the pressure and two saturations (P, S_o and S_s for example) as the principal unknowns, the third saturation (S_w) will be deduced from the two other saturations ($S_w=1-S_o-S_s$).

- $T > T_{sat}\ (P)$:

  There is dry steam. The temperature is higher than the saturation temperature and water saturation is zero. In this case, the main unknowns can be pressure, temperature and oil saturation, the steam saturation is then equal to $S_s=1-S_o$.

- $T < T_{sat}\ (P)$:

  There is only liquid water. The steam saturation is zero. The principal unknowns are then the pressure, temperature and oil saturation; therefore in this case water saturation is equal to $S_w=1-S_o$.

If we consider for example P, T and S_o as the main unknowns, the equation system can be written as: $F(X) = 0$ with $X = (P, T, S_o)$.

The discretized system is non-linear. In order to solve it, the Newton method is used. Each Newton’s iteration implies the resolution of a linear system.

4.2.2 Abaqus Description

The finite element code Abaqus was used for the geomechanical simulation part in our study. Abaqus is originally designed for non-linear stress analyses. It contains a capability of

modelling a large range of processes in many different materials as well as complicated three-dimensional geometry.

The code includes special material models for rock and soil and ability to model geological formations with in situ stresses by e.g. the own weight of the medium. Detailed information of the available models, application of the code and the theoretical background is given in the Abaqus Manuals.

In this study Abaqus is used to resolve a geomechanical problem in which we have injected the nodal pressure and nodal temperature calculated by PumaFlow. Therefore, the model of 'coupled pore fluid diffusion and stress analysis' is used, which is described in this section. Here, it should be mentioned that Abaqus is not asked to resolve the fluid and the thermal conduction part of the problem.

4.2.2.1 Coupled Pore Fluid Diffusion and Stress Model

A coupled pore fluid diffusion and stress analysis in Abaqus:

- is used to model single phase, partially or fully saturated fluid flow through porous media;
- can be performed in terms of either total pore pressure or excess pore pressure by including or excluding the pore fluid weight;
- requires the use of pore pressure elements with associated pore fluid flow properties defined;
- can be transient or steady-state; (*Note*: in this study the computation is steady-state)
- can be linear or non-linear.

4.2.2.1.1 Flow through Porous Media

Effective stress principle for porous media

A porous medium is modelled in Abaqus by the conventional approach that considers the medium as a multiphase material and adopts an effective stress principle to describe its behaviour. The simplified equation used in Abaqus for the effective stress is:

$$\sigma' = \sigma + bP\,I \tag{4.31}$$

Where σ is the total stress, P is the pore pressure and b is the Biot's coefficient. We assume that the constitutive response of the porous medium consists of simple bulk elasticity relationships for the liquid and for the soil grains, together with a constitutive theory for the

soil skeleton whereby σ' is defined as a function of the strain history and temperature of the soil:

$\sigma' = \sigma'$(strain history, temperature, state variables)

The Newton method is generally used to solve the governing equations for the implicit time integration procedure. In Abaqus, analysis of small, linearized perturbations about a deformed state is also sometimes required. For these reasons the development includes a definition of the form of the Jacobian matrix for porous media model.

Porosity, Void ratio, Saturation

The elementary volume *dV,* is made up of a volume of rock (solid material) dV_r , a volume of voids dV_v, and a volume of fluid $dV_f \leq dV_v$ that is free to move through the medium if driven.

<u>*Note*</u>: Abaqus gives the possibility to model the systems in which there may also be a significant volume of trapped wetting liquid (for example, systems containing particles that absorb the wetting liquid and swell in the process). But here in the following equations and relations the term of trapped wetting liquid is neglected.

The porosity of the medium, ϕ ,is the ratio of the volume of voids to the total volume :

$$\phi = \frac{dV_v}{dV} = 1 - \frac{dV_r}{dV} \tag{4.32}$$

Using the superscript 0 to indicate values in some convenient reference configuration allows the porosity in current configuration to be expressed as:

$$\phi = 1 - \frac{dV_r}{dV_r^0}\frac{dV^0}{dV}\frac{dV_r^0}{dV^0} = 1 - J_r J^{-1}\left(1 - \phi^0\right) \tag{4.33}$$

So that :

$$\frac{1-\phi}{1-\phi^0} = \frac{J_r}{J} \tag{4.34}$$

Where

$$J = \left| \frac{dV}{dV^0} \right| \tag{4.35}$$

is the ratio of the medium's volume in the current configuration to its volume in the reference configuration.

$$J_r = \left| \frac{dV_r}{dV_r^0} \right| \tag{4.36}$$

is the ratio of the current to reference volume for the rock.

Abaqus generally uses void ratio, $e = dV_v / dV_r$, instead of porosity. Conversion relationships are readily derived as:

$$e = \frac{\phi}{1-\phi} \quad , \quad \phi = \frac{e}{1+e} \quad , \; 1-\phi = \frac{1}{1+e} \tag{4.37}$$

4.2.2.1.2 Equilibrium Equation

Equilibrium is expressed by writing the principle of virtual work for the volume under consideration in its current configuration at time *t*:

$$\int_{\Omega} \sigma : \delta\varepsilon \cdot dV = \int_{\Gamma} \tau \cdot \delta v \cdot dS + \int_{\Omega} f \cdot \delta v \cdot dV \tag{4.38}$$

Where δv is a virtual velocity field, $\delta\varepsilon = sym(\partial \delta v / \partial x)$ is the virtual rate of deformation, σ is the Cauchy stress, τ the surface tractions per unit area, and *f* the body force per unit volume.

$$f = \rho_h g \tag{4.39}$$

Where ρ_h isthe homogenized density of the medium and gis the gravitational acceleration, which we assume to be constant and in a constant direction.

4.2.2.1.3 Constitutive Equations

A porous medium in Abaqus is considered to consist of a mixture of solid matter (rock) and voids that contain liquid attached to the solid matter. The mechanical behaviour of the porous medium consists of the responses of the fluid and rock (solid matter) to local pressure and of

the response of the overall material to effective stress. The assumption made about the rock response is discussed in this section.

Rock response

The solid matter in the porous medium is assumed to have the local mechanical response under pressure $\overline{P}$

$$\frac{\rho_r}{\rho_r^0} \approx 1 + \frac{1}{K_r}\left(S_f P_f + \frac{\overline{P}}{1-\phi} \right) - \varepsilon_r^{th} \tag{4.40}$$

Where $K_r(T)$ is the bulk modulus of this solid matter, $S_f$is the saturation of fluid, and

$$\varepsilon_r^{th} = 3\alpha_r \left(T - T_r^0 \right) - 3\alpha_{r|T^1} \left(T^1 - T_r^0 \right) \tag{4.41}$$

is its volumetric thermal strain. Here $\alpha_r(T)$ is the thermal expansion coefficient for the solid matter and T_r^0 is the reference temperature for this expansion. $\left|1 - \rho_r / \rho_r^0\right|$ is assumed to be small.

4.3 PumaFlow-Abaqus Coupling

In previous chapters we have described the motivation of conducting a coupled reservoir-geomechanics simulator, the different existing methodologies and the physical and mathematical models. In this section we intend to provide the implementation details of the coupled PUMA2ABA simulator developed as part of this research.

4.3.1 Reservoir-Geomechanics coupling background at IFPEN

The coupling between a reservoir simulator and a geomechanical simulator has been a subject of research at IFPEN from 2000. For example the couplings between Sarip, a reservoir code, and Cesar or between Sarip and Abaqus were addressed in a research phase. The coupling between Sarip and Abaqus which was based on porosity updating was used by D. Bévillon (2000) in order to model the depletion of a highly compactable homogeneous reservoir. In a slightly more advanced stage, the coupling between Athos (previous version of PumaFlow)

and Visage (V.I.P.s) (a geomechanical simulator) has been studied by M. Manguy and P. Longuemare in 2002. This study which was a sequential coupling (ATH2VIS) was conducted to find out whether the changes in effective stresses resulting from injection of cold water could explain premature watercuts in production.

The coupling (in porosity) between PumaFlow and Abaqus was initialized by S. Vidal with the purpose of modeling CO_2 storage. To quantify the geomechanical risks of CO_2 injection, the most reliable approach is to conduct the coupled geomechanical-reservoir simulations. Studies already conducted indicate possible surface uplift in case of shallow reservoir or aquifer (Rutqvist et al., 2007, Vidal-Gilbert et al., 2009).

In 2007 study of SAGD reservoir-geomechanics coupled simulation was initialized by F. Adjemian and G.Servant. Then this PhD thesis was started in order to capitalize on the results of research carried at IFPEN and enhance this work through advanced studies.

In this thesis, first the influence of the boundary conditions was studied which leaded us to neglect the presence of side-burdens in the SAGD modelling (because of the symmetry due to the presence of more than one twin-well). Briefly saying, during this thesis, after modifying some programmes and subroutines, the existent programmes were adapted in order to be applied in a thermo-hydro-mechanical coupled simulation frame-work. Then a completely automatic coupling module was developed in Python which relates PumaFlow to Abaqus with the permeability updating strategy. This coupling module is now operational using one-way or explicit or even iterative coupling approach. In the second part of this work to reduce the coupled simulation run time, the possibility of using different gridding system in reservoir model and geomechanical model was investigated and a field transfer module was implemented into our reservoir-geomechanics coupling module to facilitate the interpolation of the data between two simulators. Therefore this PumaFlow-Abaqus coupling code is completely operational in order to perform a coupled simulation on a real field case.

In this section after a brief review of development history of reservoir-geomechanics coupled simulator at IFPEN, the actual PumaFlow-Abaqus coupling simulator will be presented.

Coupling in porosity on a highly compactable reservoir

This part illustrates the iterative isothermal coupling between Sarip and Abaqus which is extracted from the thesis of D. Bévillon (2000). The coupling methodology was based on the porosity updating and was applied on a synthetic reservoir case. This work illustrated the depletion of a highly compactable homogeneous reservoir, of simplified geometry with a

producing well located in its center. The geometry of the reservoir and its finite volume mesh are shown on Figure 4.5a. The finite element mesh used in Abaqus includes the reservoir, sideburdens, overburden and underburden (Figure 4.5b). The simplified reservoir geometry and the choice of finite volume and finite element discretisation simplify data exchange between the two models. The coupling scheme is illustrated in Figure 4.6.

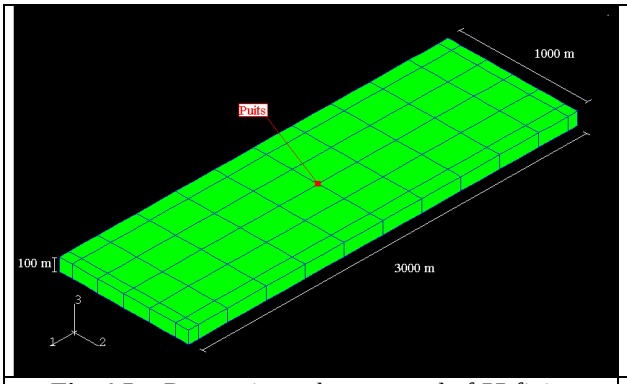

Fig. 4.5a: Reservoir mesh composed of 55 finite volume cells

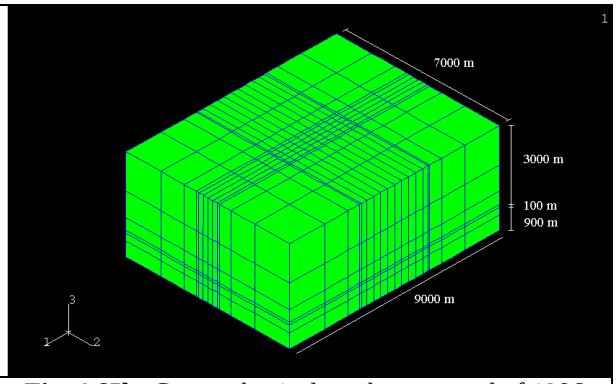

Fig. 4.65b: Geomechanical mesh composed of 1296 Q20 finite elements.

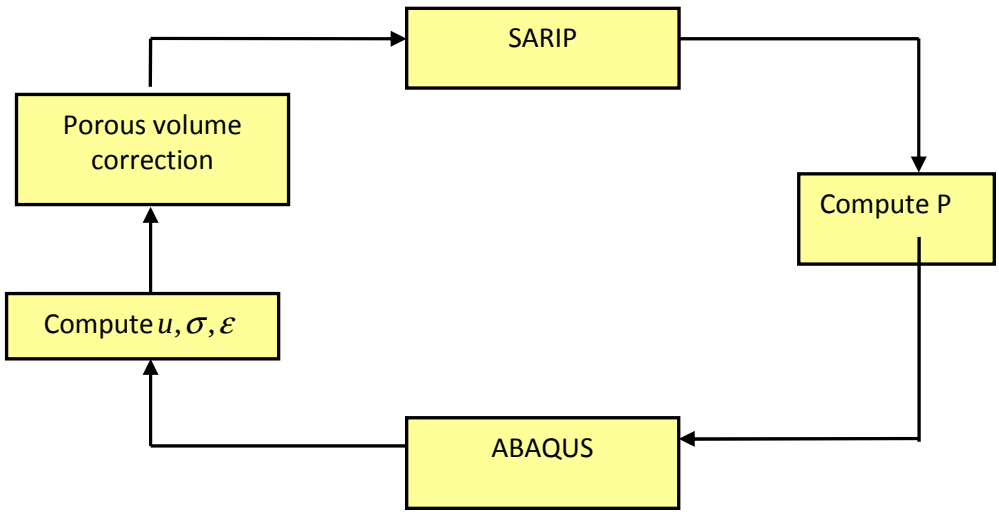

Fig.4.6: Applied coupling method by Bevillon (2000)

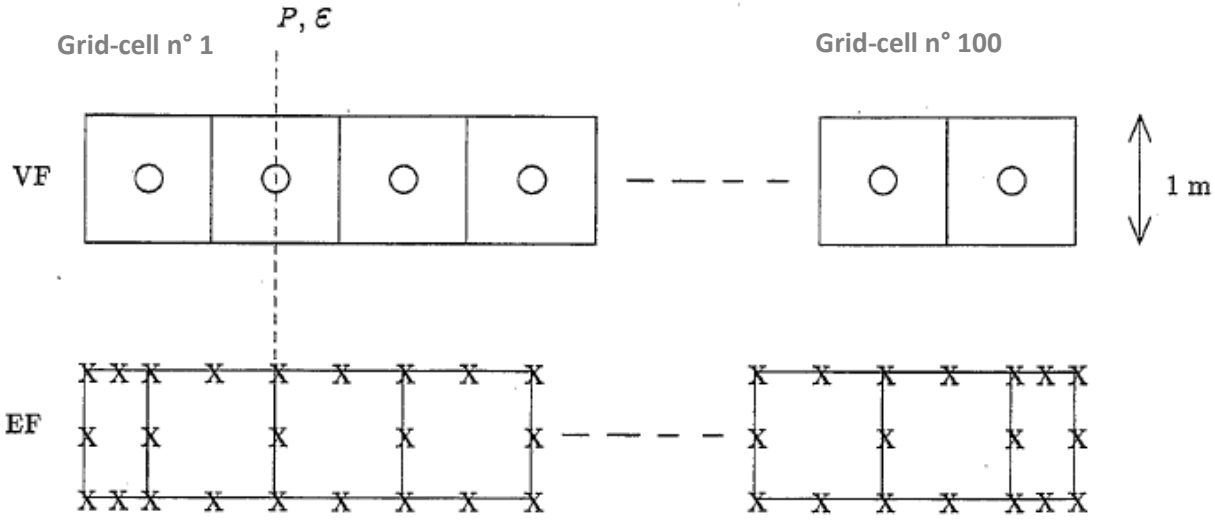

Fig 4.7: Adjustment of finite volume and finite element mesh

To avoid the use of an interpolation technique for transferring information between the reservoir and mechanical models, Bevillon adapted the reservoir grid by the mechanical grid. He chose a quadratique 20 nodes finite element mesh in displacement and linear pressure.

Finite element nodes affected by the pressures are aligned with the center of finite-volume mesh (Figure 4.7). Indeed, the pressure being considered constant over the entire height of the reservoir, only the nodes in extremities of the finite element mesh took the value of the pressure of the finite volume mesh concerned. Similarly, the finite element nodes located in the center of the reservoir grid-cells are used to determine the total strain.

Regarding the finite element nodes that are along the reservoir area, the boundary condition at zero flow requires that the pressure value in these nodes be identical to the value of the corresponding finite-volume grid-cell.

The presented methodology was implemented for modeling of a reservoir depletion consisting of a 3D geometry with porous rock and elastoplastic behavior. The results of the coupled simulations indicated compaction of the reservoir rock resulting as surface subsidence (Figures 4.8 and 4.9). After 33 years production, the vertical displacement reached a maximum value of 75 cm on the surface and in the center of the reservoir.

The comparison between the results of coupled simulation and conventional reservoir simulation confirmed that the coupling with the mechanical model allowed the representation of geomechanical effects. Besides, analytical and numerical models taking into account the reservoir and its surrounding formations (upper, lower and side layers) demonstrated that the rocks surrounding the reservoir could have a significant influence on its behaviour during

depletion. Refer to Bévillon (2000) for a numerical approach combining a reservoir model and a geomechanical model, provides a rigorous mechanical framework to describe compaction.

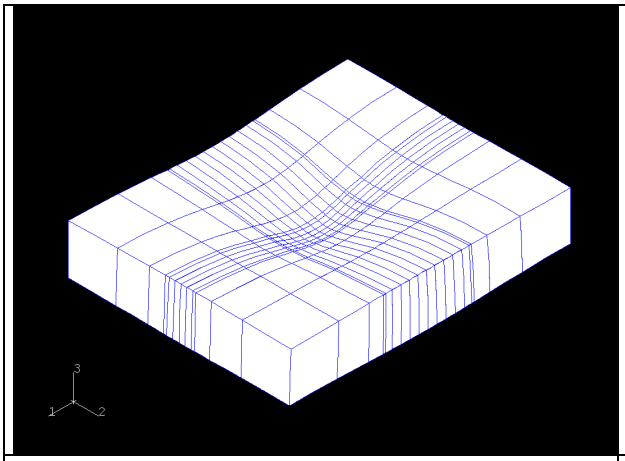

Fig. 4.8: Deforming finite element mesh after 33 years production

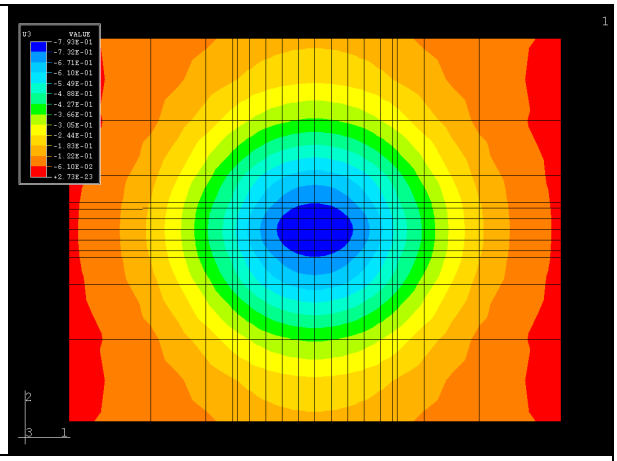

Fig. 4.9: Vertical displacement isovalues on the surface after 33 years of production

Formulations of the sequential coupling

This work was performed by M. Manguy and P. Longuemare in 2002. They proposed three formulations of the sequential coupling approach that are based on information exchanges between conventional reservoir and geomechanical simulators. For an isotropic porous medium and assuming a linear isothermal poroelastic behavior of the rock, they derive three formulations of the porosity correction that should be added to the reservoir porosity in order to correctly account for the pore volume variation predicted by the geomechanical reservoir simulator. The porosity correction depends on the pore compressibility factor used in the reservoir simulator and a mechanical contribution that can be expressed either in terms of pore volume change, volumetric strain or the mean total stress change.

They also compared a fully coupled simulation with conventional reservoir simulation and iteratively coupled reservoir simulation. The comparison is carried out on a simplified one-dimensional example for which the fluid flow problem is nonlinear and the mechanical problem is linear with the rock matrix assumed to be non compressible. For the example considered, the numerical test illustrates the importance of the geomechanical problem on the fluid flow problem and reveals that the iteratively coupled formulation proposed is as rigorous as the fully coupled simulation (Figure 4.10a and 4.10b).

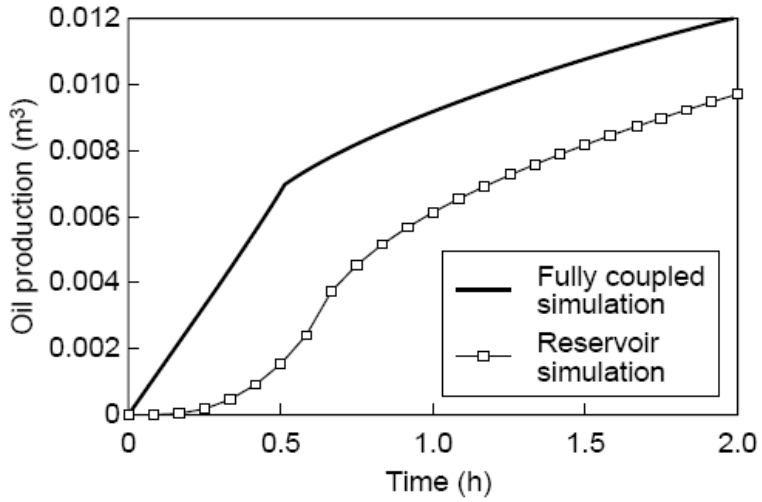

Fig. 4.10a: Comparison of the oil production for the fully coupled model and the reservoir model

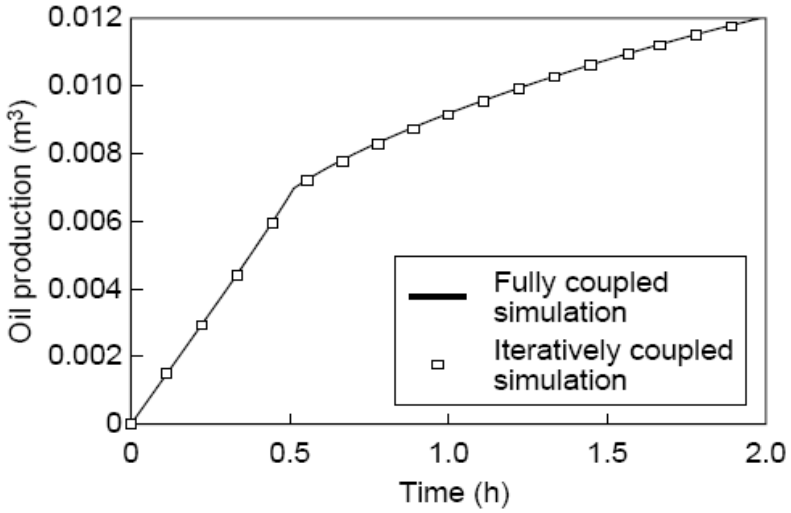

Fig. 4.10b: Comparison of the oil production obtained with the fully-coupled simulator and the iteratively coupled simulator

With this example they also illustrated the role of the pore compressibility factor in the partially coupled reservoir simulation. This parameter can be interpreted as a relaxation parameter that controls the convergence speed of the iteratively coupled process between reservoir simulation and geomechanical simulation. This parameter has to be chosen carefully in order to reduce the iteration numbers and avoid divergence of the process.

Coupling in permeability

This part illustrates the explicit coupling methodology with permeability updated using the geomechanical model of a faulted reservoir. This work was performed by Longuemare *et al.*,

(2002) using ATH2VIS (Figure 4.11) coupling module which connected Athos and Visage geomechanical simulator.

The aim of this study was to quantify geomechanical effects associated with reservoir exploitation, particularly thermal fracturing and fault and fracture permeability enhancement. The reservoir model represents a highly heterogeneous and compartmentalized limestone reservoir.

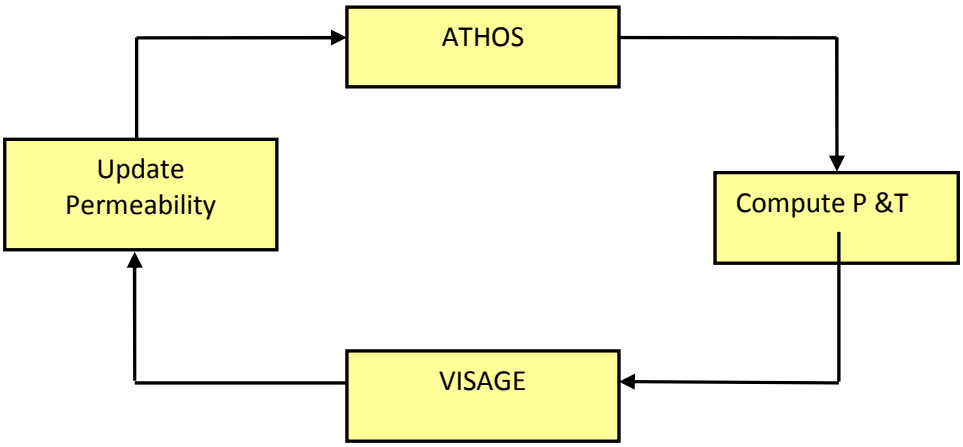

Fig.4.11: Applied coupling method by Longuemare *et al.*

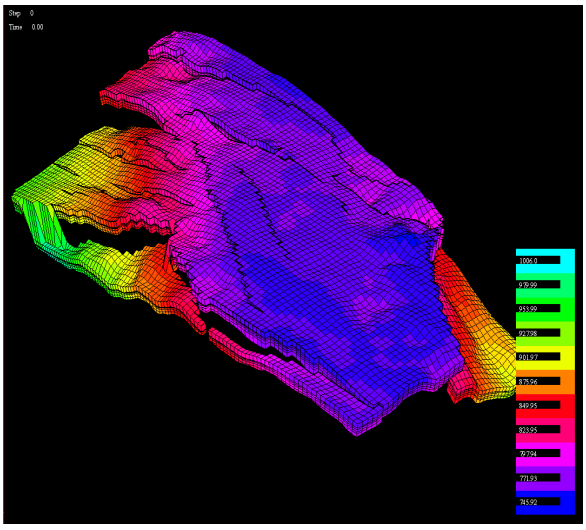

Fig. 4.12: Reservoir geometry

Figure 4.12 shows the reservoir geometry taken into account in the reservoir simulator. The reservoir model is a simple porosity model including faults whose permeability is described by transmissivity multipliers.

In the coupled ATH2VIS procedure, pore pressure and temperature variations calculated by the reservoir simulator are used in the geomechanical model as a loading for the stress and strain calculation. The geomechanical calculation requires modeling not only of the reservoir but also of its containment (over-, under- and side-burden), to apply boundary conditions and to define the thermo-hydromechanical properties of the intact rock, fracture and faults. The geometry of the geomechanical model including the reservoir and over-, under- and side-burden is shown in Figure 4.13a. In the geomechanical model, the faults act as mechanical interfaces where strain localization can occur due to stress perturbation induced by production. Figure 4.13b shows the faults that are incorporated in the geomechanical model.

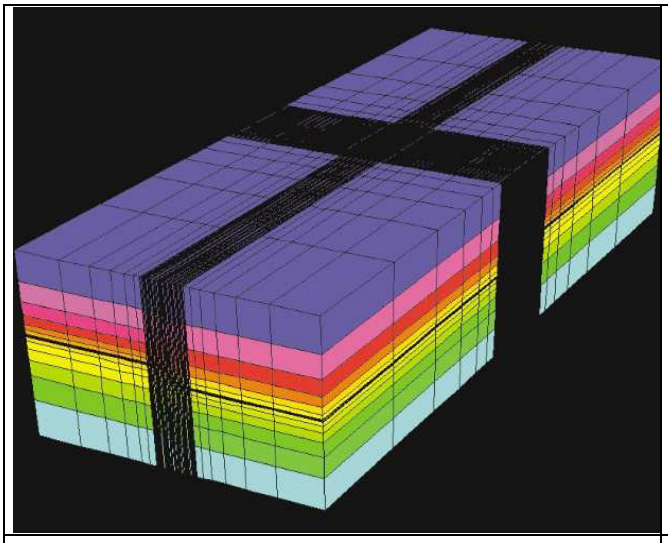

Fig. 4.13a: Geometry of the modelled structure including the reservoir

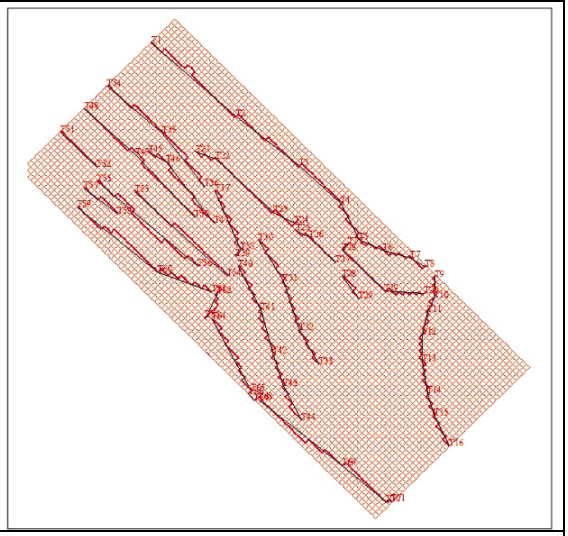

Fig. 4.13b: Mechanical description of faults

The permeability strain model is used in the “updating permeability” step of the coupled methodology. This model (Koutsabeloulis and Hope, 1998) describes fracture and fault permeability evolution as a function of normal and shear strains on fault and fracture planes. This model can be presented in a conceptual way as indicated by Figure 4.14. Different physical mechanisms are considered, which contribute to increase or decrease the joint transmissivity. The first mechanism is joint dilatation (deformation perpendicular to the joint plane) which tends to increase permeability in the direction of the joint plane. Once dilatation reaches a given magnitude, the shear strains that occur on the joint plane causes a smearing effect that reduces the joint permeability in the direction of the joint plane.

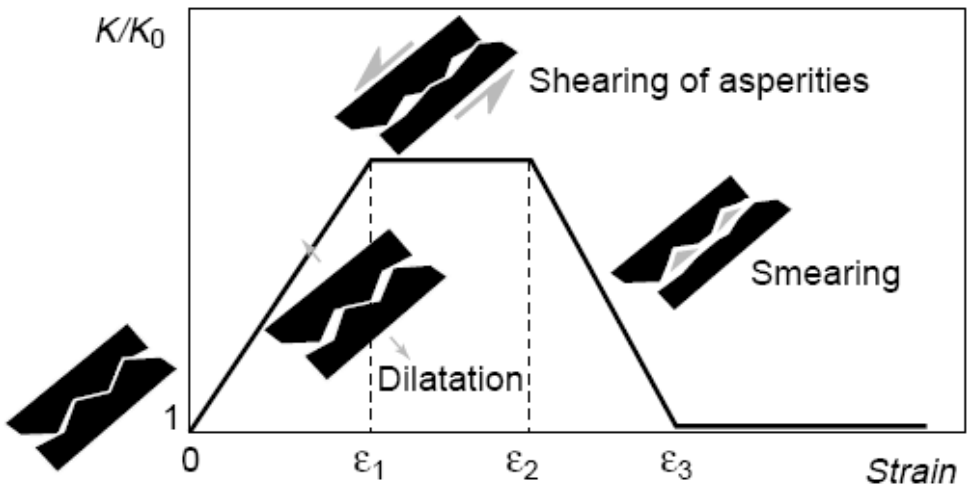

Fig. 4.14: Description the fracture and fault permeability-strain model

The results presented indicate that during reservoir exploitation, changes in pore pressure and temperature give rise to a modification of the reservoir stress equilibrium and to progressive strain localization on some faults. Only specific parts of these faults are critically stressed depending on pore pressure and temperature variations and fault strikes compared with maximum compressive stress direction. Using a fracture and fault permeability model, the progressive straining of faults is interpreted in terms of permeability enhancement in the sequentially (partially) coupled analysis.

From ATH2VIS to ATH2ABA

The coupling in porosity between Athos and Abaqus was initialized by P. Longuemare and S. Vidal. From 2002 to 2006 different internships were defined and performed at IFPEN with the purpose of ATH2ABA development and validation. This project was divided into 2 main parts: pre-processing and processing, started by construction of geomechanical model in Abaqus based on the geological formation and reservoir model constructed in Athos, then it was followed by different steps as finite-element mesh generation (reservoir and adjacent formations), definition of initial and boundary conditions, writing the Abaqus and Athos input-files, calculation of pressure by Athos and imposed in Abaqus and correction of pore volume for the coupling. Figure 4.15 shows the different steps needed to achieve coupling.

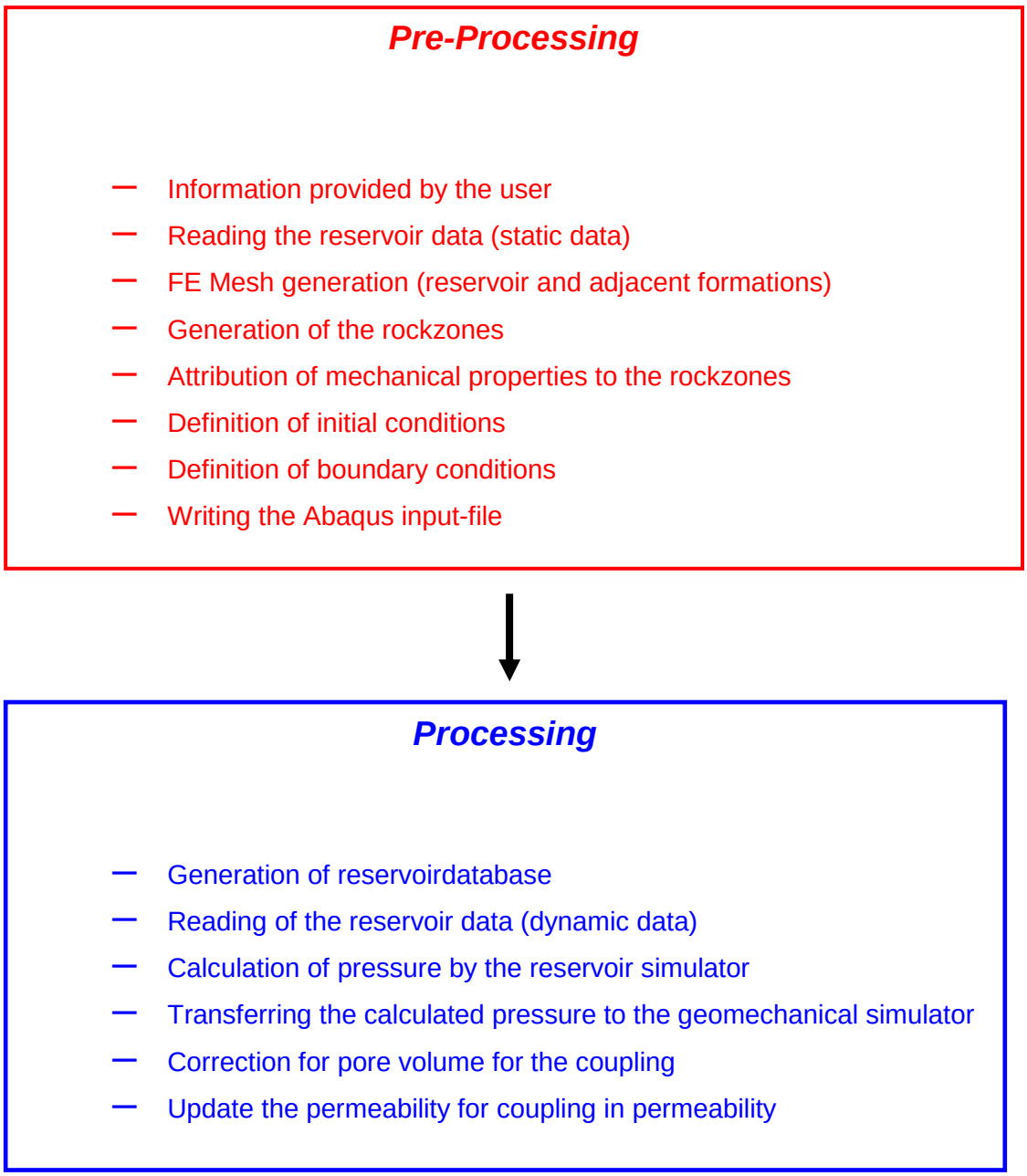

Fig. 4.15: Diagram of the coupling with the list of the various processes

To validate this coupling methodology, first it was tested on 1D case study and then it was applied on a 3D synthetic reservoir case study.

In Longuemare's work the same gridding technique was used for reservoir area in reservoir simulator and geomechanical simulator (Figure 4.16), and the linear interpolation technique was applied in order to transfer the pressure from reservoir simulator to geomechanical simulator.

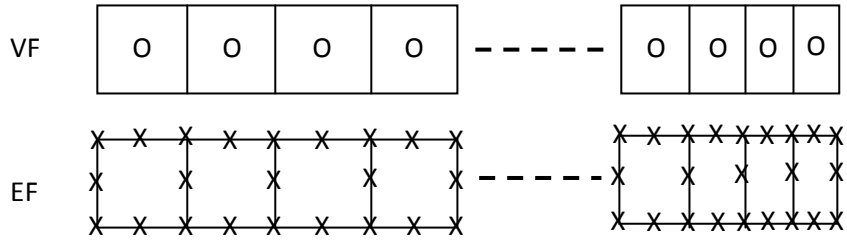

Fig 4.16: Adjustment of finite volume and finite element mesh

To model the reservoir area in Abaqus, it was necessary to use quadratic finite element (2nd order) to be able to apply the boundary conditions of pore pressure and mechanical displacements in 3 directions. Therefore, element of type C3D20RP was considered which means: Continuous, 3D, 20 nodes, Reduced Integration, Pore Pressure. Abaqus documentation encouraged to use a reduced integration with quadratic elements because it gives results which are more accurate and less costly in computing time. For mechanical modeling of the surrounded strata (side, over and under-burdens), element of type C3D20R was sufficient. Figure 4.17 illustrates numbering of nodes constituting an element in Abaqus.

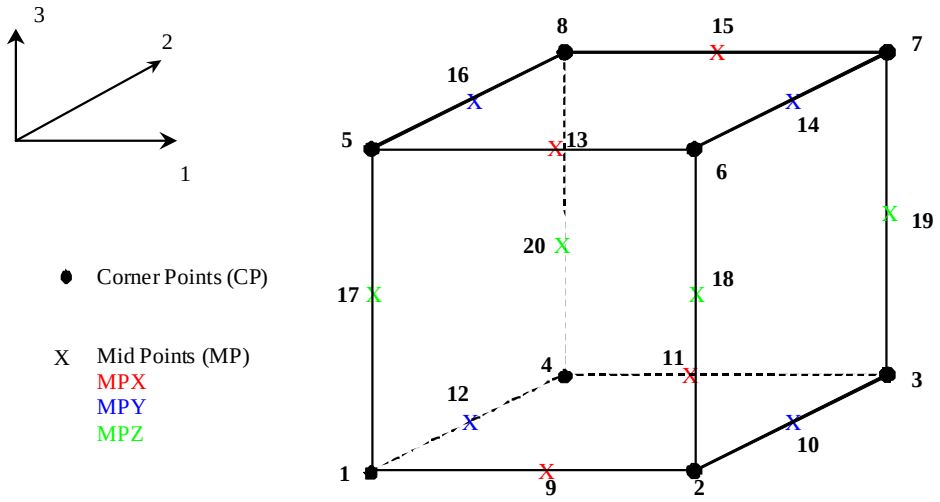

Fig. 4.17: Numbering of nodes constituting an element in Abaqus

In Athos reservoir simulator, the mesh type is CPG finite volume, (Corner Point Geometry). In the reservoir model, the grid-cells are identified by the coordinates of the eight nodes as follows (Figure 4.18):

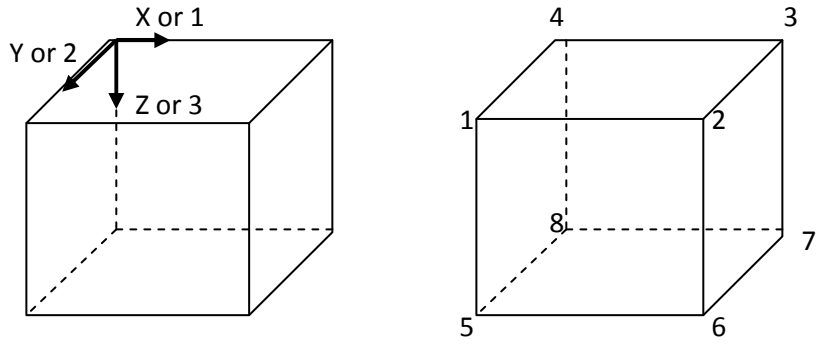

Fig. 4.18: Numbering of nodes constituting an element in Athos

In the coupled ATH2ABA procedure, pore pressure variation calculated by Athos is used in Abaqus as a boundary condition for the stress and strain calculation. The geomechanical calculation requires modeling not only of the reservoir but also of its surrounding strata (over-, under- and side-burden). In the ATH2ABA development framework, the possibility of using infinite elements for sideburdens was also studied. The ATH2ABA coupling module was used for modeling the reservoir compaction and CO_2 storage. To quantify the geomechanical risks of CO_2 injection, the most reliable approach is to conduct the coupled geomechanical-reservoir simulations. Studies already conducted by S. Vidal (2009) indicate possible surface uplift in case of shallow reservoir or aquifer.

This coupling module was also used in the frame work of 4D seismic monitoring project. In 2006 it was used in one-way by S. Vidal, and in 2009 by O. Lerat *et al*.

4D seismic can be used to track the progress of the injected fluid front (water, gas, steam, CO_2, etc.) and may play a role in optimising the injection programs.

More recently, time-lapse seismic has been applied for objectives other than monitoring saturation changes, such as pressure monitoring and compaction detection. Over the past few years, seismic monitoring has been widely used to track fluid movements (saturation effect). This approach is no longer sufficient and pressure effects must be taken into account to improve the interpretation of 4D seismic data (Landro, 1999). More precisely, the pressure effect does not concern the pore pressure alone, but also the induced geomechanical effects.

Decreasing the pore pressure in the reservoir will increase the mean effective stress; this will lead to rock compaction and increase the P-wave velocity Vp in the reservoir. The overburden and underburden will deform to fill the space created by reservoir compaction. Vp may be

reduced in these zones due to the arching effect, a phenomenon observed by Hatchell *et al.* (2004) on a North Sea field. The velocity variations in the cap rock were even greater than those observed in the reservoir.

Coupled geomechanical-reservoir simulations can be used to determine the porosity, *in situ* stresses and saturations which will then be substituted in the Gassmann equation to calculate the P- and S-wave velocity field not only in the reservoir but also in the entire block considered. The studies conducted in this field are highly promising (Vidal *et al.*, 2002, Minkoff *et al.*, 2004).

SAGD modelling by PUMA2ABA

In 2007 study of SAGD reservoir-geomechanics coupled simulation was initialized by F. Adjemian and G. Servant. This poro-thermo-mechanical simulation using First (new version of Athos) and Abaqus was performed in one-way coupling method.

Briefly saying, the work realized during this thesis can be listed as:

1. Study of work which has been carried out at IFPEN, especially the work directed by S. Vidal.
2. Testing of the existing program files of the coupling, and modifying and adapting them for taking into account the variation of temperature (SAGD process).
3. Study of the influence of the boundary conditions which leaded us to neglect the presence of side-burdens in the SAGD modelling (because of the symmetry due to the presence of more than one twin-well).
4. Construction and automation of the coupling module (script in Python) which is operational in one-way and also sequentially coupling method.
5. Comparing the results obtained by one-way approach and explicit coupling approach.
6. Evaluation of the effects of number of coupling time steps on the results of explicit coupling approach.
7. Application of different grids for reservoir and mechanical simulators where the separate grids are coupled through a field transferring technique that allows mapping fields from one grid to another by using a diffuse approximation method. The advantage of this technique is to use grids adapted to the described phenomena in both thermal fluid flow and geomechanical analyses in order to reduce computation time.

8. Automation of coupling module applicable in one-way, explicit and iterative methods with different grid system.

In this section the last version of PUMA2ABA (PumaFlow-Abaqus) coupling simulator will be presented.

The PUMA2ABA coupled reservoir-geomechanics simulator is based on the one-way and sequential coupling methodology. According to this approach, the geomechanical problem and the thermo-hydro problem (i.e. the conventional reservoir problem) are solved separately with two different simulators, but information is passed between these simulators. PUMA2ABA is the interface code between PumaFlow and the geomechanical simulator Abaqus developed by SIMULIA.

PUMA2ABA manages data exchanges between both simulators at given time intervals and run the reservoir and geomechanical simulations. With the possible use of most of reservoir and geomechanical simulation options, the PUMA2ABA interface code benefits from the high developments in physics and numerical techniques of both the reservoir simulator and the mechanical software.

4.3.2 Realised Coupling approaches

4.3.2.1 One-way Coupling

As explained in chapter 3, the decoupled or one-way coupling is the simplest coupled approach in which the pore pressure and temperature history deduced from a conventional reservoir simulation is introduced into the geomechanical equilibrium equation in the stress-strain simulator, in order to compute the new stress equilibrium (Figure 4.19).

4.3.2.2 Sequential Coupling

This coupled approach consists in executing sequentially the two reservoir and geomechanics software on compatible numerical grids, linked through external coupling modules (Figure 4.20). This module transfers relevant information between the field equations that are solved in each respective simulator. The coupling between these two simulators implies changes in reservoir petrophysics parameters as a function of volumetric strain. These functions can be estimated from laboratory data and theoretical relationships. This coupling process includes

the effects of oil and material deformation on porosity and/or permeability, and the effects of fluid pressure and temperature variation on oil sand material deformation.

The sequential coupling is described as "explicit" if the methodology is only performed once for each time step (Figure 4.20) and "iterative" if the methodology is repeated till convergence between the two models of the calculated stress and fluid flow (Figure 4.21).

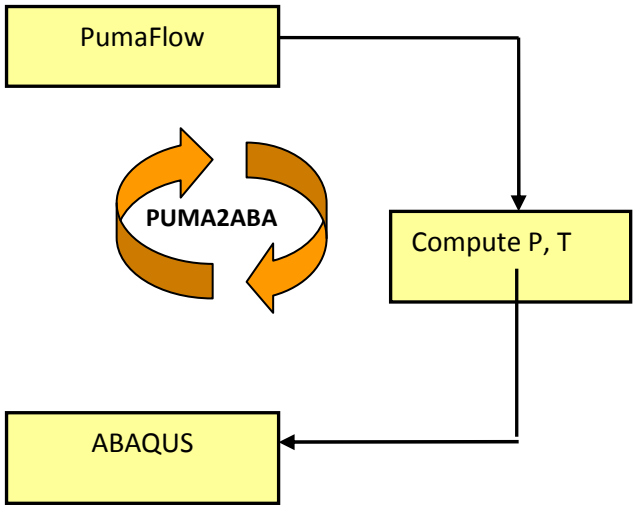

Fig.4.19: Applied one-way coupling method

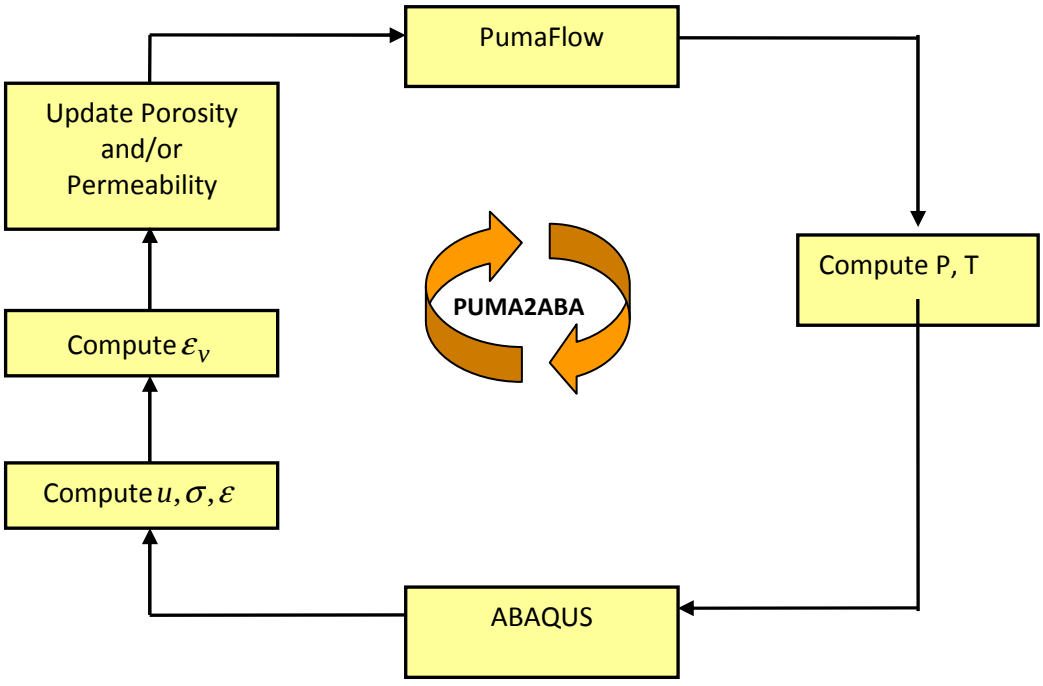

Fig.4.20: Applied explicit coupling method

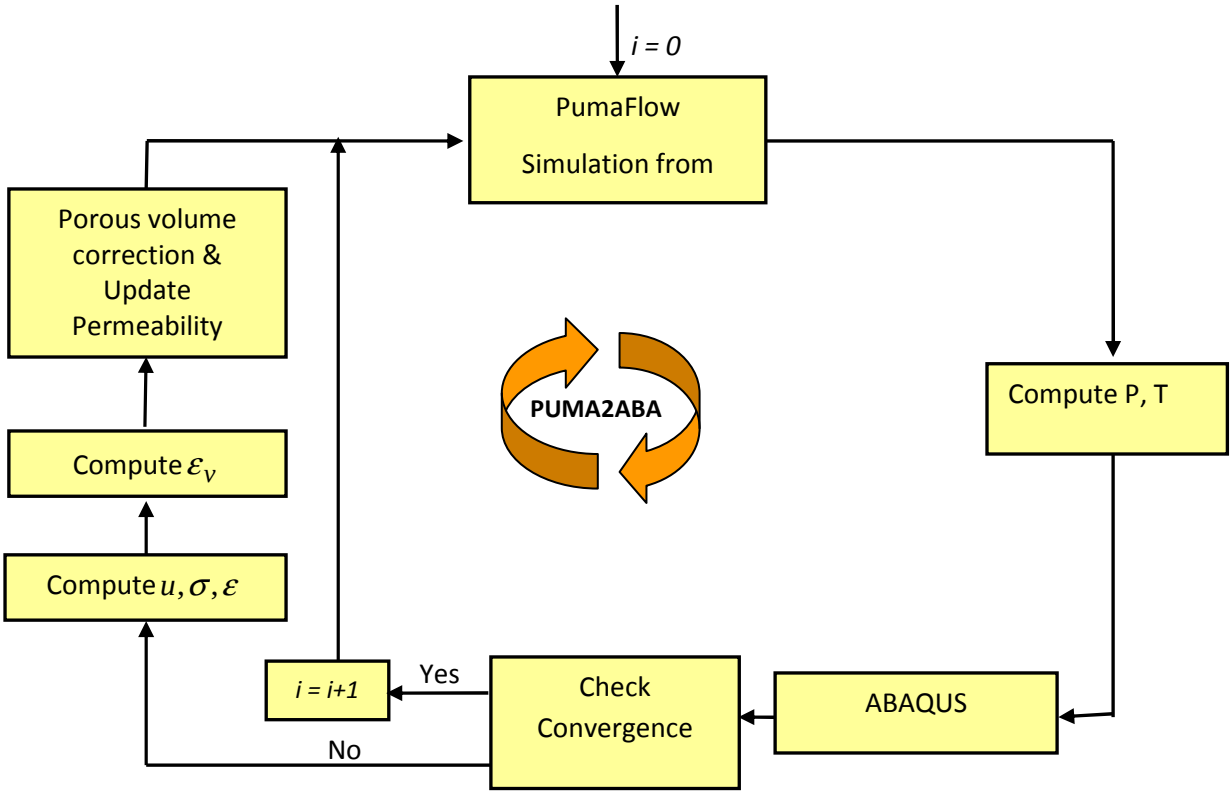

Fig.4.21: Applied iterative coupling method

4.3.3 Coupling Module

The coupled reservoir geomechanical simulation starts from PumaFlow, IFPEN reservoir simulator, and the updated pore pressures and temperatures are provided to Abaqus (Figure 4.19, 4.20 and 4.21). Because PumaFlow unknowns are located in the center of each element and finite element nodes are located in element corners, data have to be interpolated from the center of the grids to the corner. This interpolation is performed through Fortran and Python modules.

Based on the updated producing conditions and constitutive relationship, Abaqus calculates the elastic and plastic strains. Then the reservoir permeabilities are modified according to theoretical or empirical functions. Updated permeabilities are then transferred to PumaFlow at the beginning of the next time step. This data transfer is also performed by a Python module.

4.3.4 Coupling Methodology

The coupling methodology to perform reservoir-geomechanics simulations for the SAGD process can be described as follows:

1. Establish the initial start files for both PumaFlow and Abaqus, and then design the following loop to realize the coupled reservoir and geomechanical modelling;
2. After each time step of PumaFlow, extract pressure and temperature distributions
   Note: in this model, we have neglected the capillary pressure. In fact, in SAGD, porosity of the considered medium is very high (or we have an important pore radius); so the capillary pressure is negligible. So in PumaFlow we have the same pressure for water, oil and steam which is the pressure used in Abaqus as the input load.
3. Transform the pressure and temperature data format into what is required by Abaqus, including the interpolation in space.
4. Run Abaqus with updated pore pressure and temperature data to calculate stresses and strains, and modify permeability.
5. Run PumaFlow for the next time step with the updated permeability field.
6. Repeat the procedure from step 2 to 5 until the final time step is reached.

During a coupled analysis, the reservoir simulator computes pore pressure, saturation and temperature changes. The pore pressure and temperature changes computed by the reservoir simulator are converted in distributed boundary conditions in the stress simulator. Applying the pore pressure and thermal boundary conditions, the geomechanical simulator computes the evolution of stresses and strains induced by reservoir exploitation on the reservoir and the possible adjacent formations. Depending on the input keyword, PUMA2ABA generates pore volume correction and new permeability fields, which can be used in the next reservoir simulation. The sequential coupling is termed explicit if the previous methodology is only performed once for each time step or iteratively if the methodology is repeated until convergence of the stress and fluid flow unknowns. The explicit coupling is adapted for permeability update whereas the iterative coupling is more adapted for porosity changes.
Figure 4.19, 4.20 and 4.21 illustrate thedata exchanges managed by the PUMA2ABA interface between reservoir and geomechanical models during one coupling iteration.
The sequential coupling methodology implemented in PUMA2ABA is performed with different time steps for the reservoir and geomechanical simulation. Consequently, the reservoir time steps are small subdivisions of the time period (user-defined) on which the

geomechanical problem is solved. Explicit or iterative coupling can be performed with different time steps for the reservoir and geomechanical simulators. Note that the methodology of iterative coupling on large geomechanical time period does not ensure the convergence towards the same result of the fully coupled method, but allows a high reduction of the computation cost.

4.3.5 Coupling Parameters

Many researchers (Settari and Mourits 1995; Settari 2000; Thomas et al. 2002) presented the coupling parameters between reservoir flow and geomechanics. There are two main kinds of coupling parameters: one is a volume coupling related to porosity; and the other is the flow properties coupling related to permeability.

Analyzing the coupled terms in the mass conservation Equation 4.5, in reservoir model, we find porosity and permeability which are both function of the volumetric strain calculated from the geomechanics model. On the other hand, the pore pressure appears in Equation 4.5, which is calculated from the reservoir model. Therefore, we can conclude that the coupling parameters between reservoir model and geomechanics are the pore pressure and the volumetric strain.

The pore pressure can be directly used in the geomechanics model; however, using the volumetric strain in reservoir model is not direct and it is done by the different formulations of porosity and permeability.

To account for the change in porosity and permeability as a result of volumetric strains developed in the rock by temperature and pressure, the following equations can be used:

$$\frac{\Delta\phi}{\Delta t} = \left[\phi_0 C_p + (\phi_0 - b) C_s\right]\frac{\partial p}{\partial t} - b\frac{\partial \varepsilon_v}{\partial t} \tag{4.42}$$

$$\ln\frac{k_2}{k_1} = \frac{c}{\phi_1}\varepsilon_v \tag{4.43}$$

With ε_v being the volumetric strain, equation (4.42) is from Manguy and Longuemare; 2002 and the equation (4.43) is presented by Touhidi-Baghini (1998).

Generally the explicit coupling is adapted for permeability updates (equation 4.43) whereas the iterative coupling is more adapted for porosity change (equation 4.42).

Permeability updating relationship

Equation 4.43 which is a simple empirical relation for the prediction of changes in the absolute permeability during dilation is presented by Touhidi-Baghini.

This equation allows the computation of absolute permeability k_2 from its initial value k_1 , the volumetric strain ε_v and initial porosity value ϕ_1. An appropriate value for *c* has to be picked. Values of *c* are derived from the Chardabellas equation. According to Touhidi-Baghini, the values *c* = 5 and *c* = 2 appear to be appropriate to match with vertical and horizontal permeability evolutions, respectively.

Convergence criterion for iterative coupling

Porosity coupling is more complicated than permeability because it is the problem of convergence of two kinds of porosity: one provided by the reservoir simulator and the other one provided by the geomechanical simulator.

The principle of this coupling is not modification of the input parameters. After each iteration between reservoir and geomechanics simulation, we calculate a factor called C_{PV} which is porous volume correction and it defines the difference between the porous volumes obtained by reservoir and geomechanical simulators. Then another iteration is done between the two simulators using as initial porosity, the initial reservoir porosity corrected by C_{PV}. When the convergence is reached the porosity in both simulators is close to each other. In practice, the coupling module works in porous volume coupling and not in porosity.

In our applied iterative procedure the convergence criterion which is checked for every element of the reservoir simulator is:

$$\frac{\left|\phi_{g/r}(t_{i+1}) - \phi_r(t_{i+1})\right|}{\phi_0} < \delta \tag{4.44}$$

In this formula,

- $\phi_{g/r}(t_{i+1})$ is the lagrangian porosity deduced on the reservoir grid from the fields transferred by the geomechanical simulator at the end of the last iteration of the i^{th} period;

- $\phi_r(t_{i+1})$ is the lagrangian porosity evaluated by the reservoir simulator at the end of the last iteration of the i^{th} period, ϕ_0 the initial lagrangian porosity;
- δ is a user-defined value; and
- t_{i+1} is the time at the end of the i^{th} period.

If the convergence criterion is not verified the reservoir permeability is updated and the porous volume evolution is corrected in order to perform another iteration of the same period. For the studies considered in this work (chapter 5), the convergence criterion has been checked with δ equal to 10^{-3}.

Porous volume correction

Porous volume correction defines the difference between the porous volumes obtained by reservoir and geomechanical simulators. In this coupling procedure the correction of the porous volume is implicitly made. At the beginning of the new iteration of the current period, a term C_{PV} traducing the evolution of porous volume due to the geomechanical phenomena is introduced in the reservoir simulator, it reads:

$$C_{PV} = \frac{PV_{g/r}(t_{i+1}) - PV_r(t_i)}{t_{i+1} - t_i} \tag{4.45}$$

with t_i the time instance at the beginning of the i^{th} period, $PV_{g/r}(t_{i+1})$ the porous volume deduced on the reservoir grid from the fields transferred by the geomechanical simulator at the end of the last iteration of the i^{th} period, $PV_r(t_i)$ the porous volume evaluated by the reservoir simulator at the end of the i^{th} period. This loop is performed until convergence is reached. When the convergence is reached, the next period is simulated. This procedure is continued until the end of the simulation.

Furthermore, it should be noticed that the compressibility c_p used in the reservoir simulator PumaFlow, is linked with the geomechanical parameters using the following relation:

$$c_p = \left[\frac{b - \phi_0}{K_s} + \frac{b^2}{K_d} \right] \tag{4.46}$$

with b the Biot modulus, K_s the matrix bulk modulus and K_d the drained bulk modulus.

Chapitre 5

Simulations Numériques

Dans ce chapitre, nous présentons la méthodologie utilisée pour simuler le procédé SAGD.

Dans une première section, une étude d'un cas synthétique nommé 'Senlac' est présentée. Ce cas test est basé sur un réservoir réel de brut lourd, classé comme "réservoir profond", avec un historique de production bien connu. Le réservoir est supposé homogène sans aquifère actif. La technique des maillages coïncidents a été utilisée.

Le domaine considéré pour simuler le procédé SAGD dans le simulateur réservoir est un réservoir rectangulaire, avec la dimension de 147 mètres par 500 mètres par 20 mètres en X, Y et Z, respectivement. Le doublet de puits est situé sur l'axe Y et dans le milieu de l'axe X. La distance entre les deux puits est de 5 mètres. Le producteur est de 2 mètres au-dessus de la base du réservoir. Les roches environnantes ne sont pas modélisées dans le simulateur de réservoir. Les limites latérales du réservoir sont considérés comme sans flux thermique, ni flux fluide. Pour les limites latérales, cette hypothèse est faite pour représenter la symétrie supposée. Pour les limites supérieures et inférieures, cette hypothèse est liée à l'imperméabilité des roches qui se trouvent dans le haut et le bas du réservoir. Le comportement thermo-hydro-mécanique du réservoir est analysé sur une période de production de 2000 jours. Une période de préchauffage de 150 jours est d'abord modélisée. Il simule la circulation de la vapeur dans les deux puits de SAGD pour permettre une communication hydraulique et l'écoulement des fluides entre les deux puits qui n'est pas possible jusqu'à ce que la viscosité de l'huile en place n'est pas suffisamment diminué. Puis la vapeur est constamment injectée dans le puits supérieur afin de production d'huile et d'eau condensée par le puits inférieur.

Dans le modèle géomécanique, le domaine de simulation est de forme rectangulaire et ses dimensions en X, Y et Z sont de 147 mètres, 500 mètres et 800 mètres respectivement. Ce modèle inclut le réservoir entouré par des couches underburden et overburden. Les

sideburden ne sont pas représentés en raison de la symétrie supposée par la présence d'autres paires de puits horizontaux bien situés de chaque côté du domaine (plusieurs doublet de puits SAGD).

La technique des maillages coïncidents, présentée dans le chapitre 4, a été utilisée pour la modélisation du procède SAGD sur ce cas.

Dans une deuxième section, on décrit les méthodes de couplage utilisées : couplage one-way et couplage explicite.

L'influence du nombre de pas de couplage dans l'approche de couplage explicite a été étudiée. Les résultats obtenus par les différentes méthodes de couplage sont analysés et comparés : chemins de contrainte, déformation en surface, évolution des températures, des pressions et des perméabilités.

En one-way une simulation complète de 2000 jours d'écoulement fluide a été réalisée avec le simulateur de réservoir. A la fin de cette simulation, la pression et la distribution de température ont été extraites du simulateur de réservoir et présentés comme conditions aux limites dans le simulateur de géomécanique. Les contraintes et déformations dans le réservoir et les roches environnantes ont ensuite été calculées par le simulateur géomécanique à des moments choisis: 0 (initial), 150ème jour (fin de préchauffage), 300ème jour, le 1000ème 2000ème jour.

En couplage explicite la même simulation de 2000 jours avec le même historique d'injection et de production a été réalisée avec le simulateur de réservoir. Aux instants choisis, la distribution de pression et de température ont été extraites du simulateur de réservoir et présenté comme conditions aux limites dans le simulateur de géomécanique. La contrainte et déformation dans le réservoir et les roches environnantes ont ensuite été calculées par le simulateur géomécaniques à ces instants de temps sélectionné. Puis la nouvelle déformation volumique calculée par simulateur géomécanique est utilisée pour déterminer la nouvelle perméabilité pour passer au pas de temps suivant dans le simulateur de réservoir.

Ensuite pour déterminer l'influence géomécanique de l'injection de vapeur sur les variations de pression et de température dans le réservoir et sur la variation de perméabilité globale, le comportement géomécanique du réservoir a été étudié sur trois mailles différentes qui représentent trois zones différentes dans le réservoir. Les chemins de contraintes dans ces

trois mailles obtenus par les deux méthodes de couplage différentes : one-way et explicite, ont été spécifiquement étudiés.

Dans une troisième section, on aborde des techniques destinées à réduire les temps de calcul.

Après avoir analysé les différents éléments dans la littérature, plusieurs possibilités ont été envisagées:

1 / Utilisation d'une méthode intégrale pour limiter le champ d'étude (Dusseault et al, 2002, Yin et al, 2006))

2 / Utilisation de systèmes de maillages différents (maillage) pour les deux modèles (Tran et al, 2008)

La première stratégie exige des développements significatifs si le code d'éléments finis n'est pas destiné à être couplé avec des éléments frontières. Cela impose une limitation dans la modélisation puisque les roches environnantes de réservoir sont considéré élastique semi-infini. Cela peut être un facteur limitant si nous sommes intéressées à l'évolution de contrainte dans les side-burdens, par exemple lorsque la température augmente au cours du SAGD. Ces éléments nous ont amené à se concentrer sur la deuxième stratégie, qui semble être plus prometteuse.

Pour développer un système de maillage différent, ce travail a été basé sur les résultats d'une thèse de doctorat sous la direction de M. Tijani (Savignat, 2000) qui nous donne la possibilité de transférer l'information entre deux systèmes de maillage différents (méthode d'approximation diffuse).

Le fait que le type de maillage dans le simulateur de réservoir soit différent de celui du simulateur de géomécanique rend le processus de transfert des données plus compliqué. En effet dans le simulateur de réservoir une discrétisation par volumse finis est utilisée lorsque les variables de flux sont calculés au centre des grilles tandis que dans le simulateur de géomécanique une discrétisation par éléments finis est utilisée pour calculer les déplacements aux nœuds de la grille.

Si les maillages du simulateur de réservoir et du simulateur de géomécanique sont confondus, l'interpolation des données entre les deux simulateurs est simple. Après chaque pas de temps les nouvelles pressions interstitielles et températures calculées au centre des grilles du réservoir, sont transférés sur les nœuds des maillages du modèle géomécanique dans le

simulateur géomécanique. Dans ce transfert, les données sont interpolées pour passer de la discrétisation volumes finis à la discrétisation par éléments finis et inversement.

Lorsque les maillages dans les simulateurs réservoir et géomécanique ne coïncident pas, le transfert des données (température, pression, déformation volumique) entre les deux simulateurs est plus complexe. Dans ce cas, un algorithme de transfert de champ doit être utilisé pour effectuer le transfert des données à partir d'un maillage à l'autre. Cette technique est expliquée dans ce chapitre.

Cette approche de couplage, basée sur la méthode d'approximation diffuse, a été appliquée sur deux différentes études de cas synthétiques : d'abord, sur le cas test Senlac, puis sur un cas appelé Hangingstone correspondant à un réservoir peu profond.. Une méthode de couplage itératif a été appliquée sur le cas test Hangingstone. Les temps de calculs sont diminués sans altération majeure de la représentation des phénomènes physiques

Chapter 5

Numerical Simulations

In this chapter, the proposed methodology to simulate the SAGD process is presented.

In first section a synthetic case study named ‘Senlac’ is presented. This test case is constructed based on ‘Senlac’ heavy oil reservoir which is classified as a deep reservoir. The same (coincident) gridding technique, presented in chapter 4, is used for Senlac modelling.

In second section the one-way and explicit coupling methods are applied on Senlac test case. The influence of the number of coupling periods in explicit coupling approach is studied. Then a comparison between the results obtained by one-way and explicit coupling methods is done.

In third section in order to reduce the computation time an enhanced coupling method using two-grid system is presented. This coupling approach which is based on diffuse approximation method is applied on two different synthetic case studies. First it is tested on Senlac test case with different gridding (mesh size) in reservoir and geomechanical model.

The second case study is constructed based on ‘Hangingstone’ heavy oil reservoir which is a shallow reservoir comparing to Senlac. An iterative coupling method with two-grid system is applied on Hangingstone test case. The results and the computation run time are presented and compared.

5.1 Senlac case Description

The case is based on the implementation of the SAGD process in the East Senlac heavy oil reservoir located in Saskatchewan, Canada (Chakrabarty et al., 1998). It has been operated by CS Resources Limited since 1994. In July 1997, PanCanadian Petroleum Limited purchased CS Resources Limited.

The reserves of East Senlac were established with the drilling of 11 vertical wells. However, the complex nature of the reservoir, which is characterized by significant bottom or edge water and varying thickness of massive sand and interbedded transition zone within the reservoir, makes it difficult to perform reliable production forecasts under primary production. CS Resources and IFP initiated a joint geological and geophysical re-evaluation of the East Senlac pool. Using 3-D-seismic, an impedance cube was generated which demonstrated a relationship between the existing geology and seismic that was not evident from seismic amplitude data used previously. This enabled CS Resources to create a series of maps that were used to make an economic assessment of the production potential. The resulting pay thickness maps were used to develop production simulations that confirmed that the pool could support significant thermal in situ exploitation using the Steam Assisted Gravity Drainage (SAGD) process. While primary recovery had produced approximately 22 dam^3 ($1dam^3$= 1000 m^3) of oil from three horizontal wells, the SAGD process has the potential to produce more than 3180 dam^3 of crude oil over a 12–15 year period. Approximately $127dam^3$ of oil has been produced during the first 22 months of operation of the East Senlac Thermal Project.

Some aspects of the SAGD modelling and simulation by PUMA2ABA, applied on the East Senlac field are discussed in this section.

5.1.1 Reservoir Fluid Flow Model and Production History

The reservoir is assumed homogeneous without bottom aquifer. As indicated in Figure 5.1, the top of the reservoir is 730 meters deep, the initial pressure and temperature being equal to 5.2 MPa and 27°C respectively.

The domain considered to simulate the SAGD process is a rectangular reservoir, with the dimension of 147 meters by 500 meters by 20 meters in X, Y and Z directions, respectively (Figure. 5.2). The well pair is located along the Y axis and in the middle of the X axis. The distance between the two wells is 5 meters. The producer is 2 meters above the base of the

reservoir. The number and the size of grid blocks in the X , Y and Z directions is indicated in Table 5.1. As the vertical distance between the two horizontal wells was supposed to be constant, only one cell 500 meters long is used to describe the well length in the Y direction.
The surrounding rocks are not modelled in the reservoir simulator.
The lateral boundaries of the reservoir are considered with no thermal nor fluid flow. For the lateral boundaries, this hypothesis is made to represent the assumed symmetry. For the upper and lower boundaries, this hypothesis is related to the imperviousness of the rocks that are located at the top and bottom of the reservoir. Main physical properties of rock and fluids used in the reservoir fluid flow model are summarized in Table 5.2.

Production history

The thermo-hydro-mechanical behavior of the reservoir is analyzed over a 2000-days production period. A pre-heating period of 150 days is first modeled. It simulates steam circulation in the two wells of the SAGD pair to allow a hydraulic communication and flow of fluids between the two wells that is not possible till the viscosity of oil in place is not decreased enough. Then steam is constantly injected in the upper well so oil and condensed water are produced in the lower well. At the injection well, a steam flow rate is fixed at 260 m^3/day (Cold Water Equivalent) from 150^{th} to 250^{th} day, and then it is fixed at 400 m^3/day to 2000^{th} day, end of the injection/production history. At the same time, a maximum injection pressure of 8 *MPa* is set for the injection well to avoid a too high pressure in the reservoir. At the production well, a minimum pressure of 1.5 *MPa* is fixed together with a maximum production flow rate of 560 m^3/day of total liquid (oil plus condensed water).

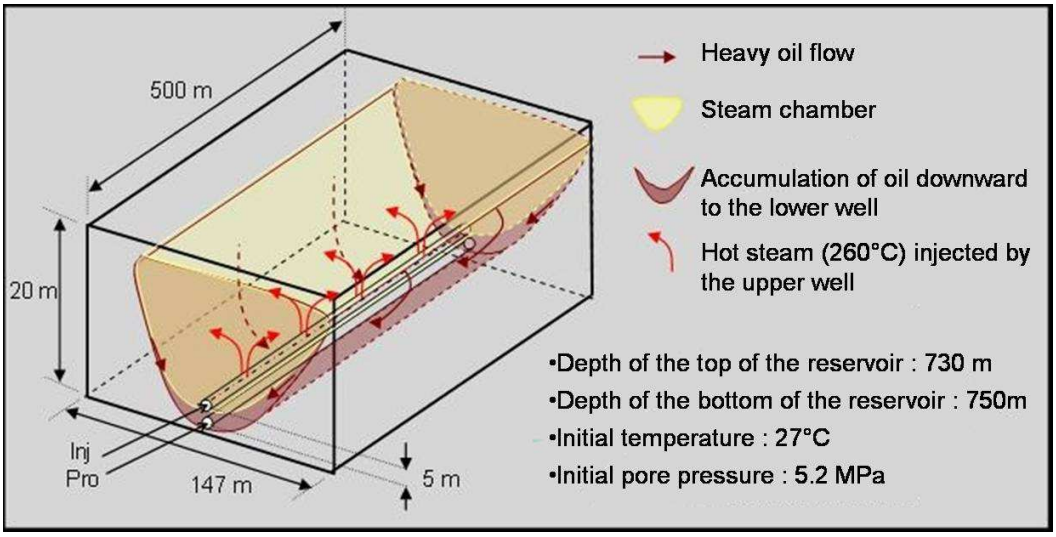

Fig 5.1: Reservoir description

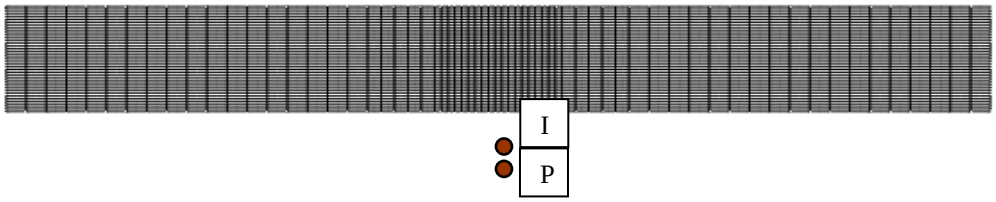

Fig 5.2: Reservoir modelled in the reservoir simulator,
location of the well-pair in the reservoir

Zone	Direction	Grid Block Number	Discretization (m)
Reservoir	X	65	18(3.) 5(2.) 19(1.) 5(2.) 18(3.)
	Y	1	500
	Z	40	0.5

Table 5.1: Number and the size of reservoir grid blocks in reservoir simulator

Properties	Value
Oil Density ($g.cm^{-3}$)	0.97
Oil viscosity at reservoir conditions ($mPa.s$)	5000
Oil viscosity at 282°C ($mPa.s$)	1.8
Porosity	0.35
Horizontal permeability (mD)	2000
Vertical permeability (mD)	1000
Rock compressibility (MPa^{-1})	3.10^{-4}
Oil compressibility (MPa^{-1})	$2.17\ 10^{-4}$
Rock heat capacity ($J.cm^{-3}.°C^{-1}$)	2.34
Rock thermal conductivity ($W.\ m^{-1}.°C^{-1}$)	2.70
Oil thermal expansion coefficient ($°C^{-1}$)	2.10^{-4}
Initial oil saturation	0.85
Irreducible water saturation	0.15
Residual oil saturation to waterflood	0.20
Residual oil saturation to steamflood	0.10

Table 5.2: Reservoir rock and fluid properties

A particular feature of SAGD is the short distance between the injection and production wells with the constant risk of steam breakthrough in the production well if a too high injection rate or production rate, or both, are set in the wells. To avoid such a condition, a special monitoring of the steam chamber has been implemented in the reservoir simulator (Egermann et al., 2001). The result of this monitoring is clearly illustrated in Figure 5.3 and Figure 5.4 that show the typical evolution of flow rates and bottom hole pressure (BHP) in the two wells. The initial steam rate imposed in the injection well between 150 and 250 days is well respected, as it is during a short period after 250 days when it is increased to 400 m^3/day. However, quite rapidly the steam front moves too closer to the production well and the

injection flow rate has to be decreased to prevent steam breakthrough, then increased again when the steam front moves away from the production well. The monitoring of the well pair to prevent steam breakthrough at the production well results therefore in variations in the steam flow rate in the injection rate during quite a long period that lasts until about 1000 days. At that time, the injection rate continuously decreases because the steam front has reached the lateral limit of the domain. Less steam can be injected and less fluid can be produced.

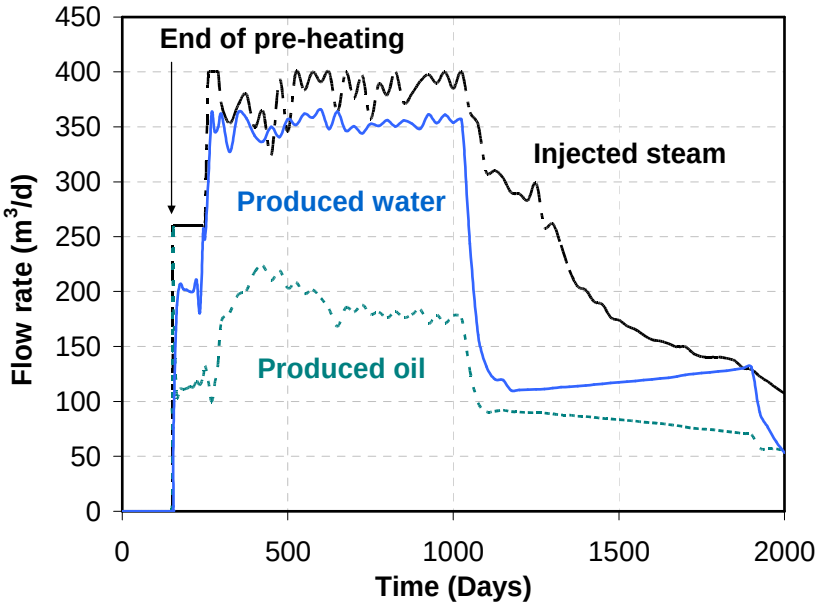

Fig.5.3: Typical evolution of injected steam rate and produced oil and water rate

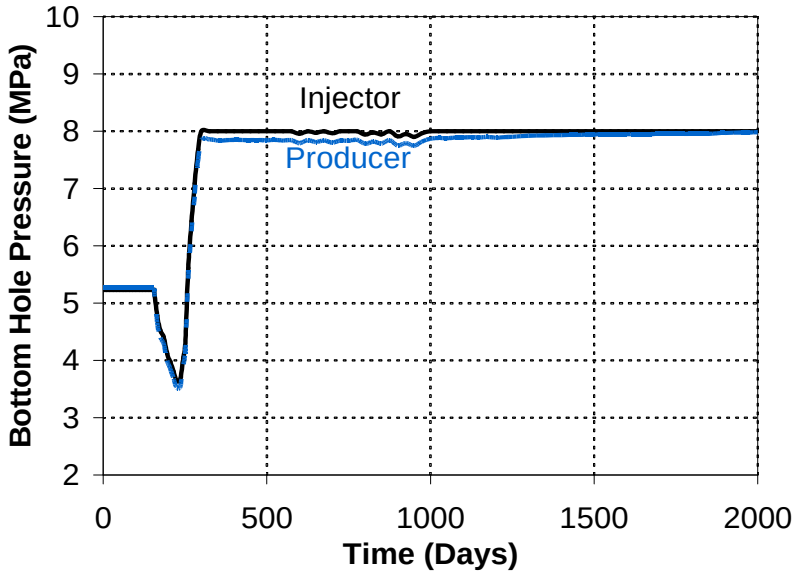

Fig.5.4: Typical evolution of BHP in injector and producer

5.1.2 Geomechanical model

In the geomechanical model, the simulated domain is rectangular and its dimensions in X, Y and Z directions are 147 meters, 500 meters and 800 meters respectively (Figure 5.5). This model includes the reservoir surrounded below by underburden layers and above by overburden layers. Sideburden rocks are not represented due to the symmetry assumed to the presence of other well pairs located on each side of the domain (multiple well pair SAGD). The size of grid blocks in the three directions is indicated in Table 5.3. The gridding system is coincident in reservoir simulator and geomechanical simulator. As the vertical distance between the two horizontal wells was supposed to be constant, only one cell 500 meters long is used to describe the well length in the Y direction.

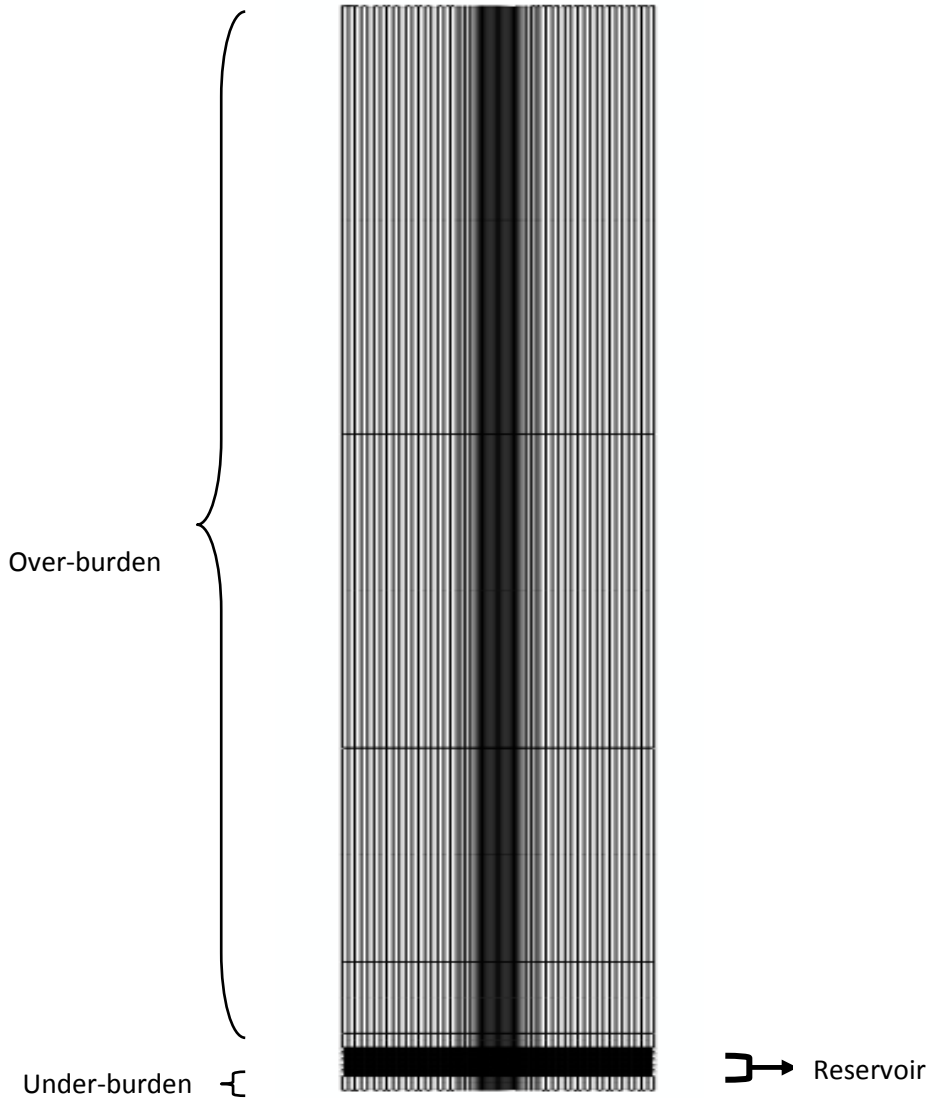

Fig 5.5: Geomechanical model (reservoir, overburden and underburden)

Zone	Direction	Grid Block Number	Discretization (m)
Overburden	X	65	18(3.) 5(2.) 19(1.) 5(2.) 18(3.)
	Y	1	500
	Z	5	1(300.) 1(220.) 1(150.) 1(50.) 1(10.)
Reservoir	X	65	18(3.) 5(2.) 19(1.) 5(2.) 18(3.)
	Y	1	500
	Z	40	0.5
Underburden	X	65	18(3.) 5(2.) 19(1.) 5(2.) 18(3.)
	Y	1	500
	Z	1	10

Table 5.3: Number of grid blocks and size for the various domains

Boundary condition

Boundary conditions in the geomechanical simulator are shown in Figure 5.6. Bottom edge of underburden is fixed. There is no displacement for the lateral sides in x and y directions. Top edge of overburden is free.

The material constitutive law (elasticity) and properties are related to the rock types present in the geomechanical domain. One mechanical rock type was assigned per zone in the overburden, underburden and reservoir. Field data was used to assign thermo-hydro-mechanical properties to each mechanical rock type. The rock properties are given in Table 5.4.

Initial conditions

Initial porosity : 0.35

Initial saturation : (=1) initially the reservoir is totally saturated

Initial pressure : we apply a vertical pore pressure gradient which varies between 4.9 MPa in top of reservoir and 5.1 MPa in bottom of reservoir.

Initial stress : the initial stress field (isotropic) which raise according to the depth is given in the Table 5.5.

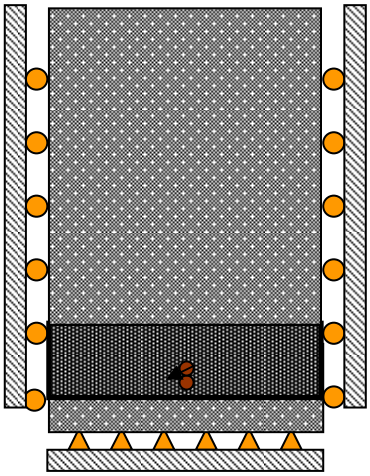

Fig.5.6: Applied boundary conditions

Properties	Reservoir	Overburden	Underburden
Density ($kg.m^{-3}$)	2320	2420	2700
Young's modulus (10^8 Pa)	3.43	2.500	10.000
Poisson's coefficient		0.3	
Biot's Coefficient		1	
Thermal expansion ($°C^{-1}$)		$2 .10^{-5}$	

Table 5.4: Thermo-poro-mechanical properties

Zone	Depth (*m*)	Stress ($10^7 Pa$)
Overburden (Total stress)	0	0
Overburden (Total stress)	-730	-1.5422
Reservoir (Effective stress)	-730	-1.051
Reservoir (Effective stress)	-750	-1.090
Under burden	-750	-1.594
Under burden	-800	-1.854

Table 5.5: Applied initial isotropic stress field

5.2 Reservoir-Geomechanics Coupled Simulation Results

In chapter 4 the applied approaches in this research were presented. As described in section 4.3, in PUMA2ABA coupled simulator the one-way coupling and the sequential coupling approaches were used.

5.2.1 One-way (Decoupled) Approach

A complete 2000-day of fluid flow simulation has been carried out with the reservoir simulator. At the end of this simulation, the pressure and temperature distribution have been extracted from the reservoir simulator and introduced as boundary condition in the geomechanical simulator. The stresses and strains in the reservoir and surrounding rocks have then been computed by the geomechanical simulator at selected times: 0 (initial), 150th day (end of pre-heating), 300th day, 1000th day and 2000th day. (Figure 5.7)

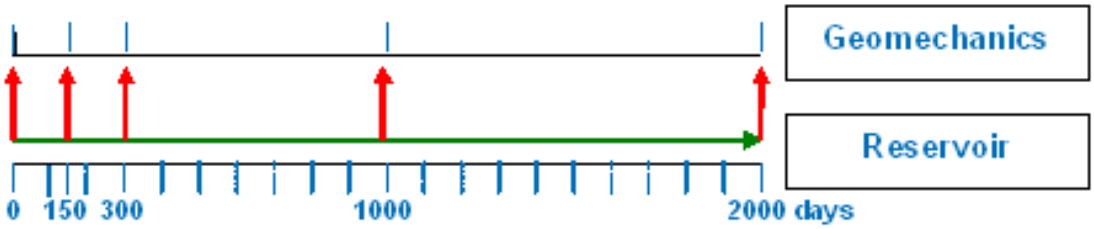

Fig 5.7: Time instants chosen to evaluate the stress state in geomechanical simulator

5.2.2 Sequential Explicit Coupling

The same 2000-day history of injection and production has been carried out with the reservoir simulator. At the selected time instants, the pressure and temperature distribution have been extracted from the reservoir simulator and introduced as boundary condition in the geomechanical simulator. The stresses and strains in the reservoir and surrounding rocks have then been computed by the geomechanical simulator at these selected time instants. Then new volumetric strain calculated by geomechanical simulator is used to compute new permeability to perform a new step with the reservoir simulator.

5.2.2.1 Comparison of 5-step and 12-step explicit coupling

In order to investigate the influence of the number of coupling periods, a sensitivity analysis has been performed. In this section, the results for two cases are compared. First coupled simulation is done in 5 coupling steps and the second simulation is realized in 12 coupling steps. (Figure 5.8)

During each coupling period, variations in pore pressure, temperature, strains and stresses were computed. As explained in previous chapters, in this explicit coupling approach, permeability in grid cells of the reservoir model have been updated at specified times after computation of stress and strain by the geomechanical simulator and modification of the permeability values according to Equation 4.101. The updated permeability was integrated in the simulation of the next period.

In 5-step explicit coupling, a first mechanical computation step (initialization) was performed to reach a mechanical equilibrium between the applied boundary conditions (regional stresses) and the initial state of stress in the reservoir. The simulation was then performed using four coupling steps at 150^{th}, 300^{th}, 1000^{th} and 2000^{th} day (end of production history).

In 12-step explicit coupling, a first mechanical computation step (initialization) was also performed in order to reach a mechanical equilibrium between the applied boundary conditions (regional stresses) and the initial state of stress in the reservoir. The simulation was then performed using eleven coupling steps, at 150^{th}, 200^{th}, 300^{th}, 400^{th}, 500^{th}, 600^{th}, 800^{th}, 1000^{th}, 1200^{th}, 1500^{th} and 2000^{th} day.

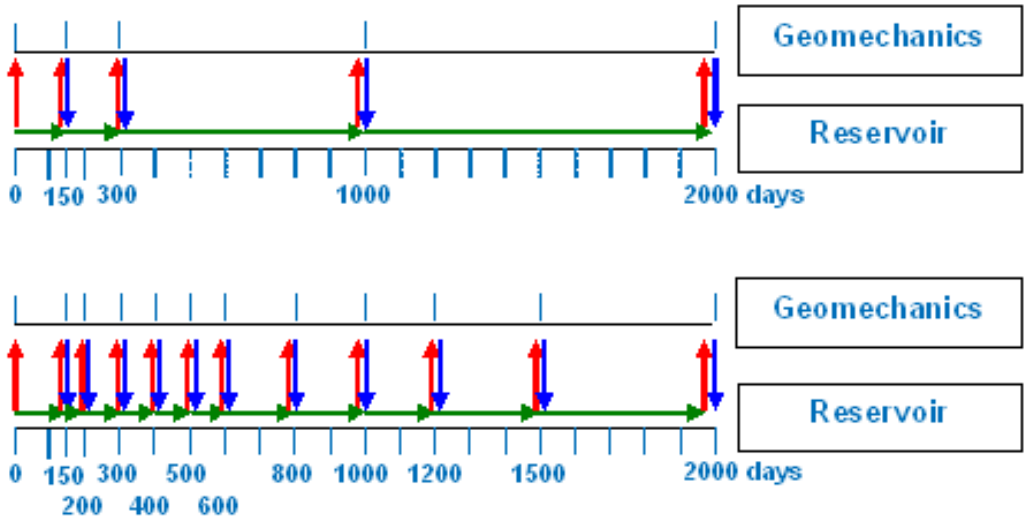

Fig 5.8: The applied coupling steps in 5-step and 12-step explicit coupling methods

Steam injection increases the pore pressure, dilates the rock skeleton and the pore fluid and modifies the in situ stresses in a complex set of interaction. Main results during the 5-steps coupling are shown on Figures 5.9 to 5.12 which give maps and curves of the state of some important parameters. For the maps presented in Figures 5.9, 5.11 and 5.12, the geometry is deformed according to calculated displacements with an amplification factor of 100.

Figure 5.9 shows that the temperature first increases above the injection well to the top of the reservoir and then extends laterally to become uniform in the upper part of the reservoir. This uniformity is related to lateral boundary conditions that were imposed on the model.

Figure 5.10 shows the evolution of the volumetric strain. It is very similar to the evolution of temperature (Figure 5.9), fast at the start of steam injection in a vertical direction above the well pair and then slower in the periphery as the steam chamber reaches the top of the reservoir.

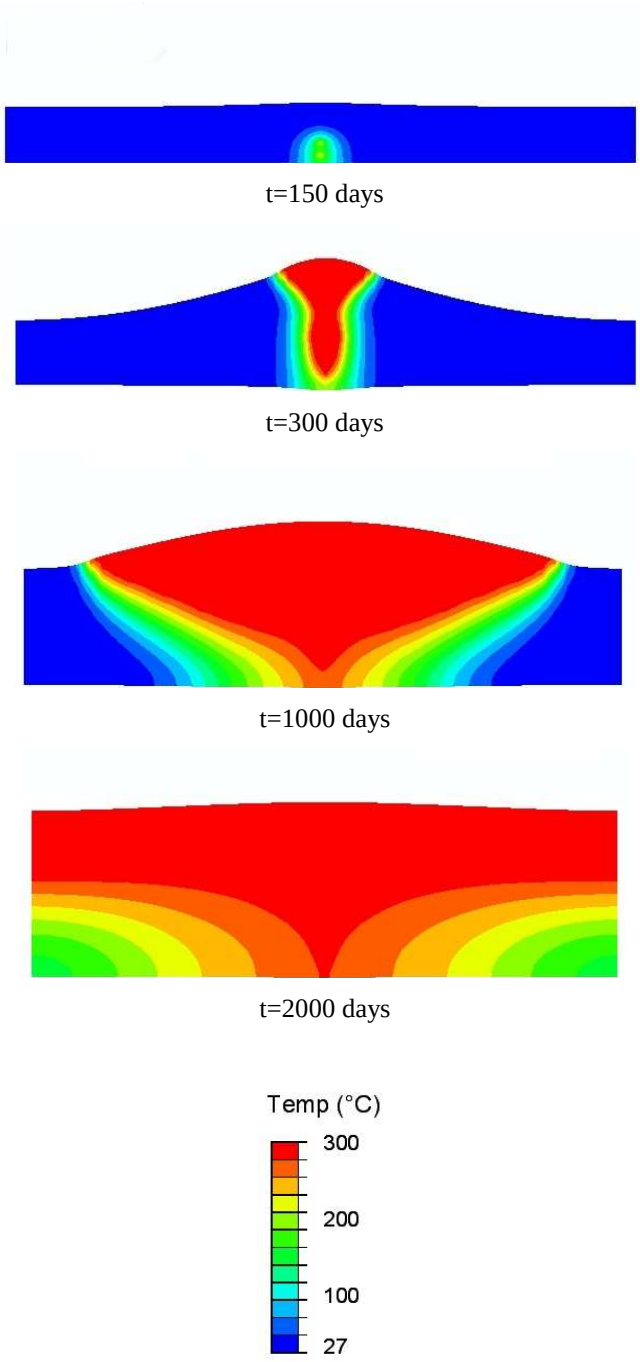

Fig.5.9: Evolution of temperature in deformed reservoir
In 5-step explicit coupling method

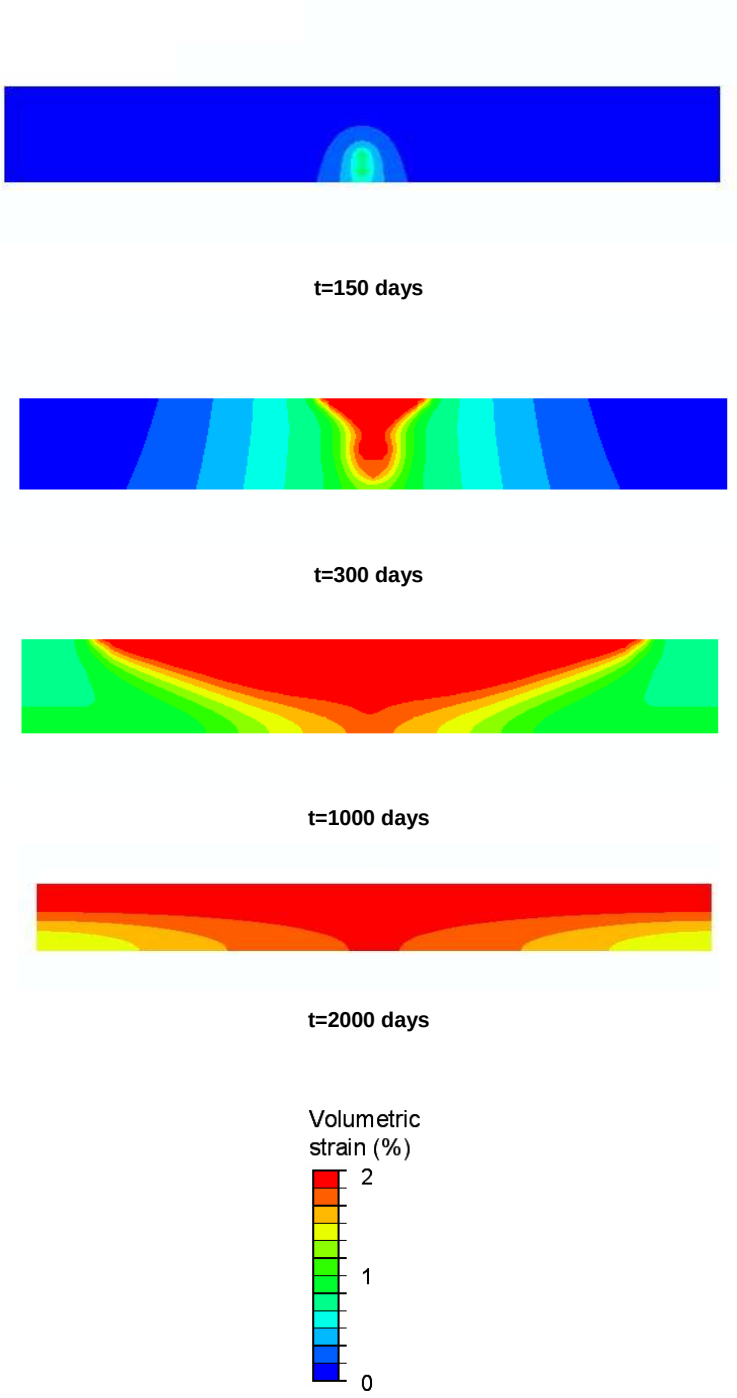

Fig.5.10: Evolution of volumetric strain in non-deformed reservoir
In 5-step explicit coupling method

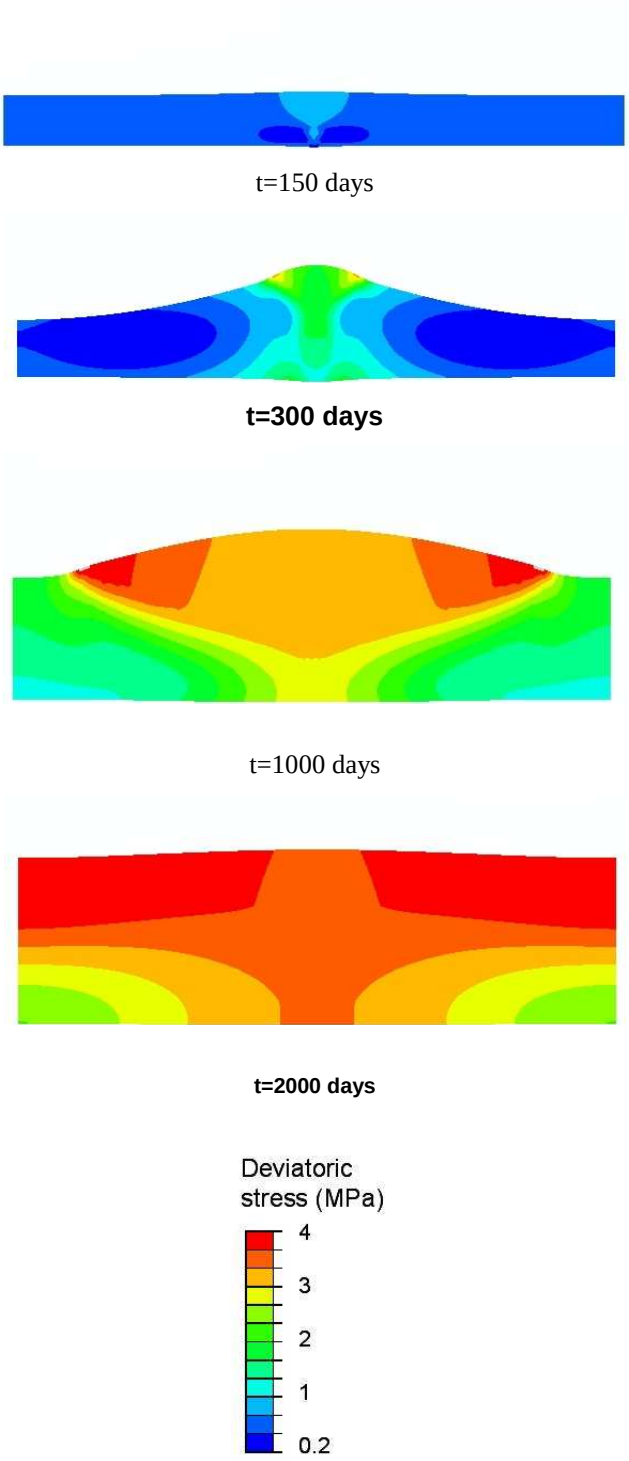

Fig.5.11: Evolution of deviatoric stress in deformed reservoir
In 5-step explicit coupling method

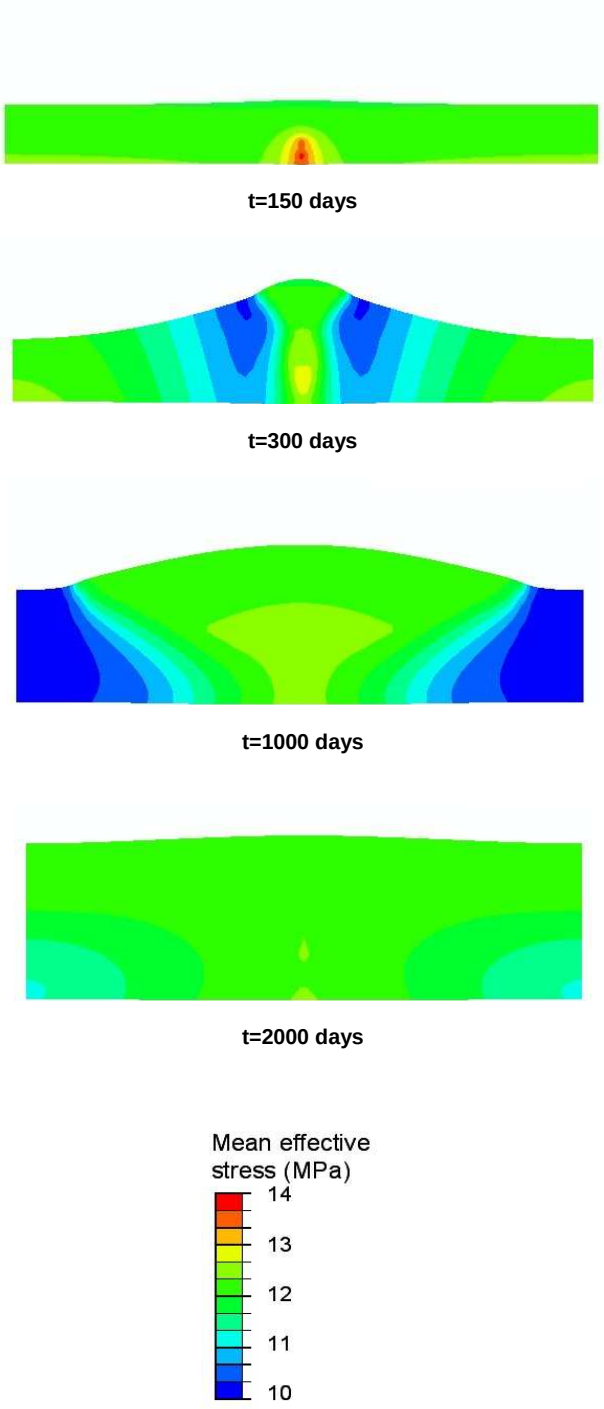

Fig.5.12: Evolution of effective mean stress in deformed reservoir
In 5-step explicit coupling method

To determine the geomechanical influence of steam injection on pressure and temperature variations in the reservoir and on overall permeability variation, the geomechanical behaviour of the reservoir have been studied in three different grid cells which represent three different zones in the reservoir. These cells are located in the same XZ plane and at the same elevation in the Z direction. Figure 5.13 shows the location of these grid cells (A, B and C). Grid cell A is placed just in the middle of the reservoir and 5.5 meters above the horizontal well injection well. Grid cells B and C are chosen farther from the wells, with the distance of 18.5 and 60 meters from the grid cell A, respectively. To analyze the geomechanical effects during SAGD process, the stress paths in these three grid cells obtained by the two different coupling methods, one-way and explicit, have been specifically studied.

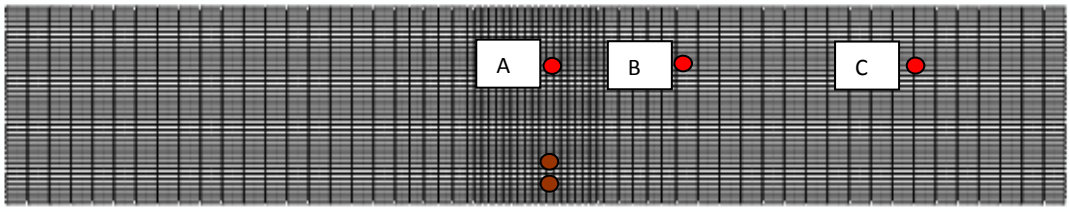

Fig 5.13: Reservoir modeled in reservoir simulator,
location of the grid cells A, B, C and well-pair in reservoir

The mean effective stress (Figure 5.12) is sensitive to pore pressure while the deviatoric stress (Figure 5.11) indicates the existence of shear stress in the reservoir. We note that the mean effective stress remains quasi unchanged when the deviatoric stress increases almost everywhere. This aspect is illustrated in Figures 5.14 and 5.15, which show the stress state at points A, B and C in a p'-q diagram. These stress paths show the evolution of the mean effective stress p' and the deviatoric stress q which are defined by,

$$p' = \frac{\sigma_v + \sigma_h + \sigma_H}{3} - p_p$$

and

$$q = \sqrt{\frac{(\sigma_v - \sigma_h)^2 + (\sigma_h - \sigma_H)^2 + (\sigma_v - \sigma_H)^2}{2}}$$

where σ_v is the vertical stress, σ_h the minimum horizontal stress, $\sigma_H$the maximum horizontal stress and p_p the pore pressure, assuming that σ_v, $\sigma_h$and σ_H are the principal stresses. It must be noticed that the sign convention of soil mechanics is considered here.

It can be seen that cell A in the middle of the reservoir has a different stress path compared to the two other cells. In fact there is a decrease of deviatoric stress (q) during the pre-heating period in grid cells B and C then an increase during the steam chamber development, while for grid cell A the deviatoric stress is always increasing.

The stress paths are globally vertical. Coupling with 12 steps clearly reveals a better identification of stress paths than with 5 steps coupling but the trend is quite the same.

An increase only in pore pressure would result in equal reduction in all effective principal stresses. In the p'-q diagram the stress path would be horizontal because deviatoric stress would be unchanged.

An only thermal expansion of the reservoir would lead in an increase of both the deviatoric stress and mean effective stress. These stress increases are essentially due to an increase in horizontal stresses.

The combination of the antagonist pore pressure increase and thermal expansion can explain the vertical stress paths observed in the model.

The fact that the final stress state is almost the same for various points is also related to lateral boundary conditions that were imposed on the model. Anisotropic initial stresses conditions certainly would change the development of stress paths, but the trend of increasing shear stress with the growth of the steam chamber would be certainly verified.

As it can be seen in Figures 5.16 and 5.17 that show the porosity and temperature variations in cells A, B and C versus time, the porosity increase corresponds exactly to the passage of the temperature front through the location of each cell, between 150 and 300 days for cell A, between 400 and 700 days for cell B and between 1000 and 1700 days for cell C. After the passage of the steam front the porosity remains constant.

The evolution of permeability in cells A, B and C is linked to the evolution of their porosity (Figures 5.18 and 5.19). The increase of 30% is very fast close to the wells and is slower far away. A greater number of steps allow a better precision of the curves as seen on Figure 5.19. Permeability in cell B increases by 30% after 1000 days for a 5 step coupling and only around 600 days for a 12-step coupling.

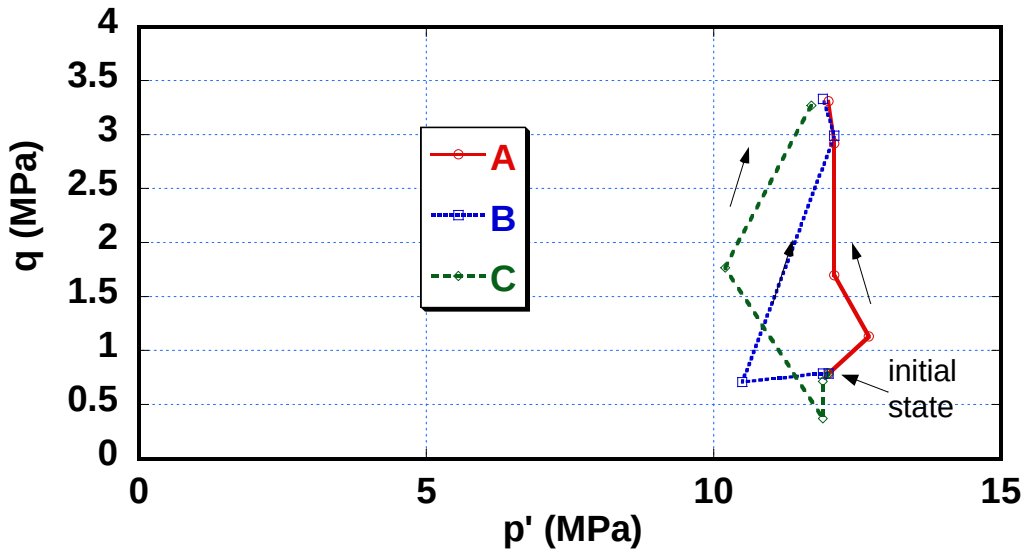

Fig.5.14: Stress path in cells A, B and C (5 step coupling)

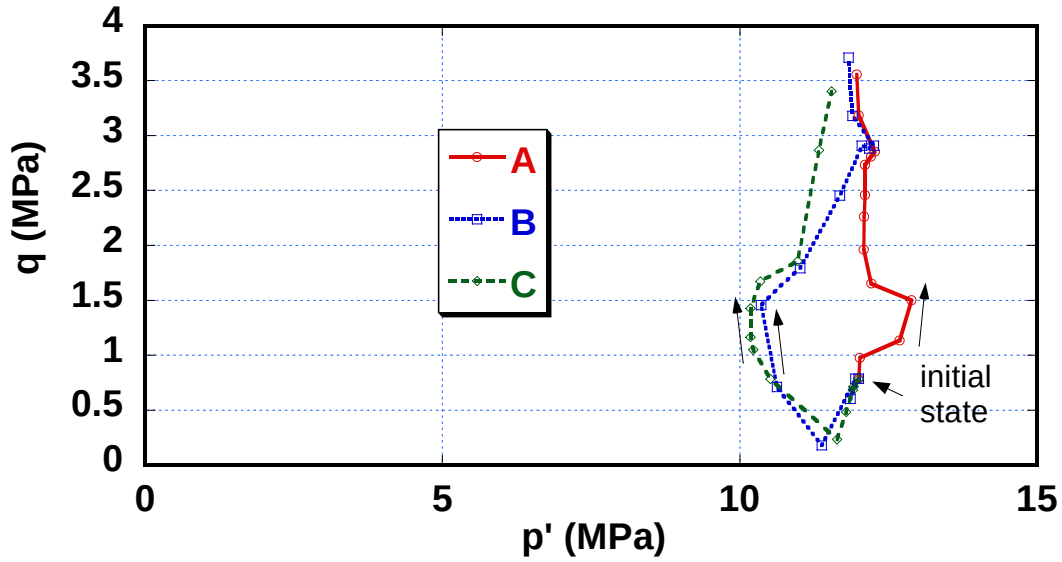

Fig.5.15: Stress path in cells A, B and C (12-step coupling)

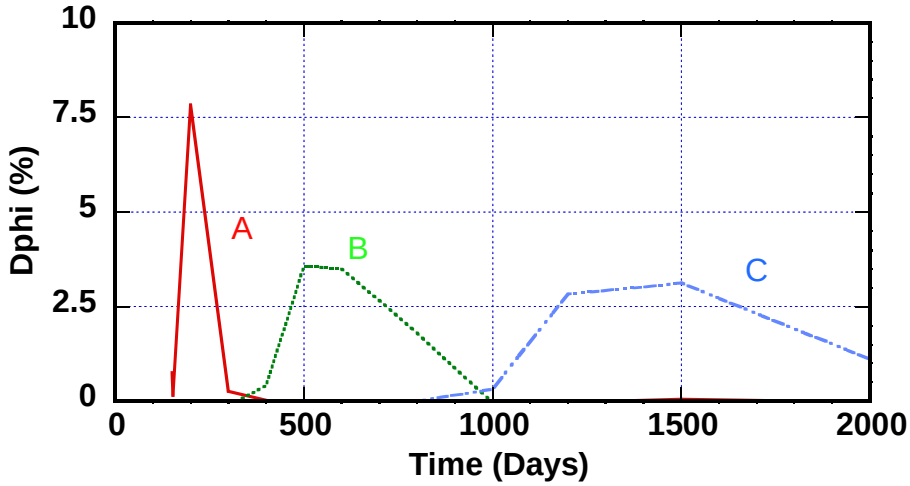

Fig.5.16: Porosity evolution in cells A, B and C
(12-step coupling)

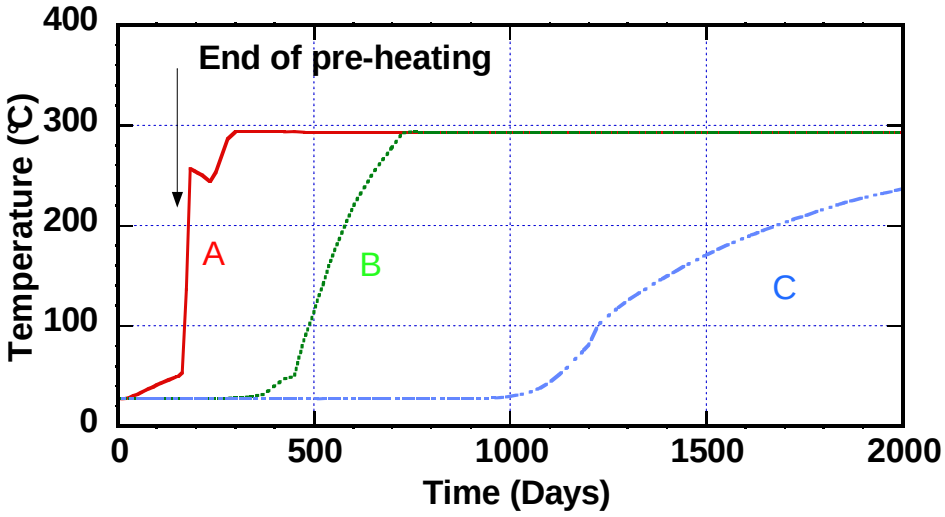

Fig.5.17: Temperature in cells A , B and C
(12-step coupling)

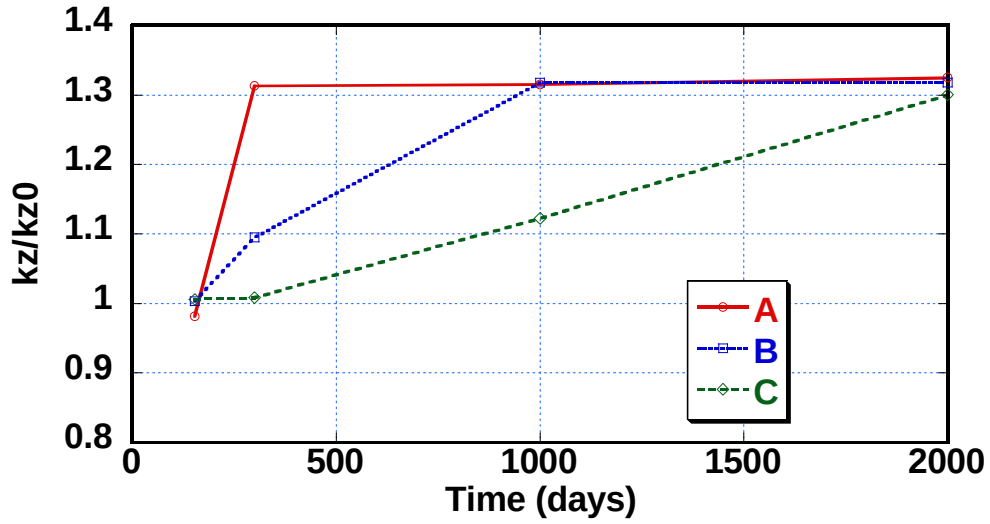

Fig.5.18: Permeability evolution in cells A,B and C
(5-step explicit coupling)

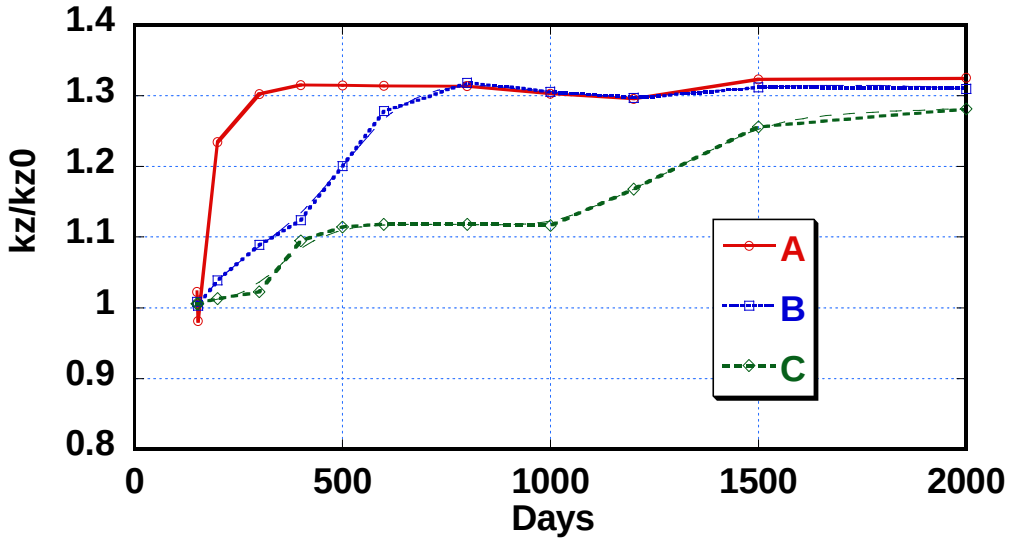

Fig.5.19: Permeability evolution in cells A, B and C
(12-step explicit coupling)

Figure 5.20 shows the vertical displacement profile of the top of the reservoir plotted at the end of each step of the 5-step coupling. As can be noticed, the uplift is very fast just above the wells, and then the uplift extends to the periphery when the steam chamber grows. It becomes almost homogeneous at the end of the 2000-day simulation. Once again, the lateral boundary conditions play an important role on this shape. Comparing the results obtained by explicit coupling (Figure 5.21), we find that the number of steps does not appear as a determining factor for the overall vertical displacement of the top of the reservoir.

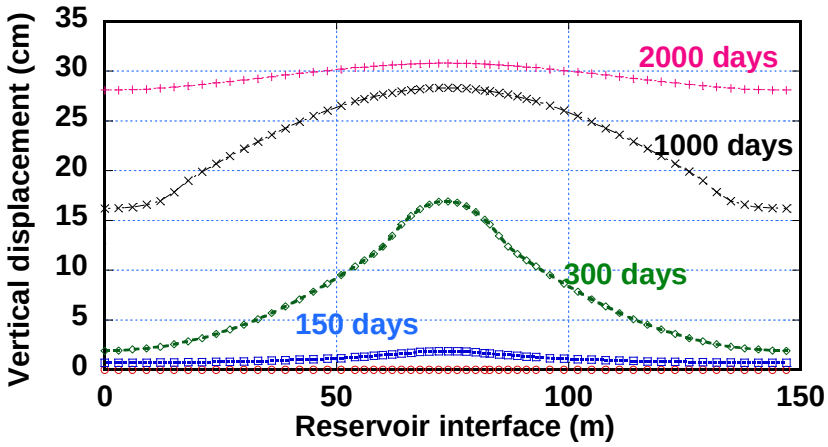

Fig.5.20: Vertical displacement profile of reservoir interface, during 2000 days (5-step explicit coupling)

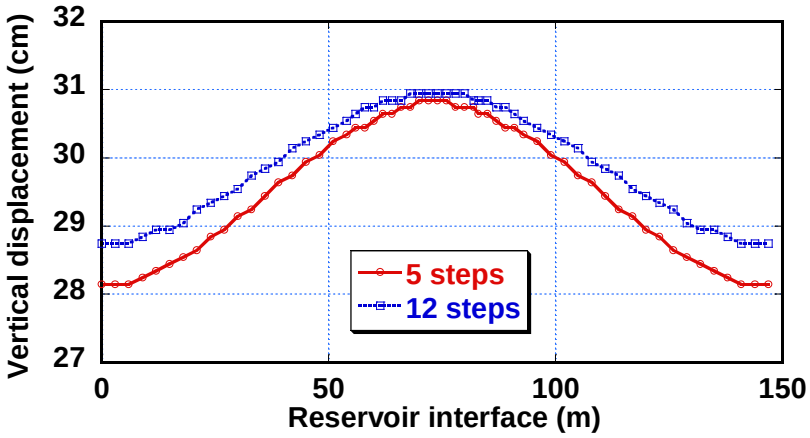

Fig.5.21: Vertical displacement profile of reservoir interface, at 2000th day

5.2.3 Comparison between one-way and explicit coupling results

In Figure 5.22 stress path computed by one-way coupling, plotted in p'-q diagram (Figure 5.22a), is compared to the stress paths resulted by the 5-step (Figure 5.22b) and 12-step (Figure 5.22c) explicit coupling approaches.

The deviatoric stress (q) obtained by 12-step and 5-step explicit coupling reaches nearly 3.8 MPa and 3.4 MPa, respectively, while in one-way approach (Figure 22.a) a maximum value of nearly 3 MPa for q is obtained. The three graphs show the difference of stress evolution that occurs when permeability changes are taken into account in the fluid flow model. With the explicit coupling the final state for the three cells are quite identical.

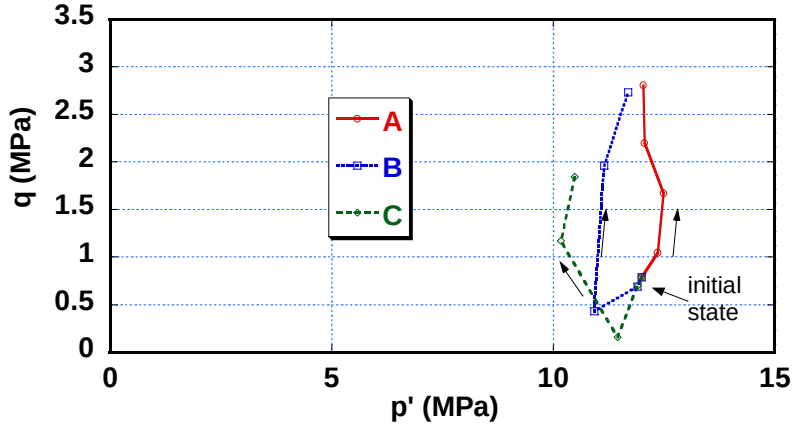

Fig. 5.22a: Stress path in cells A, B and C ;
from one-way coupling

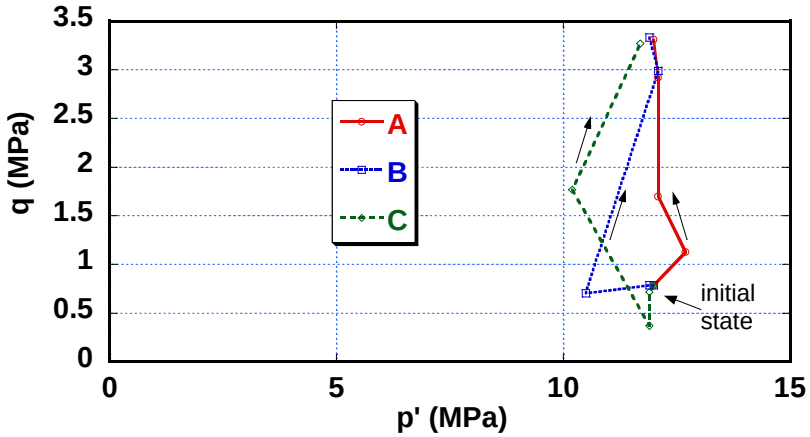

Fig.5.22b: Stress path in cells A, B and C ;
from 5 step explicit coupling

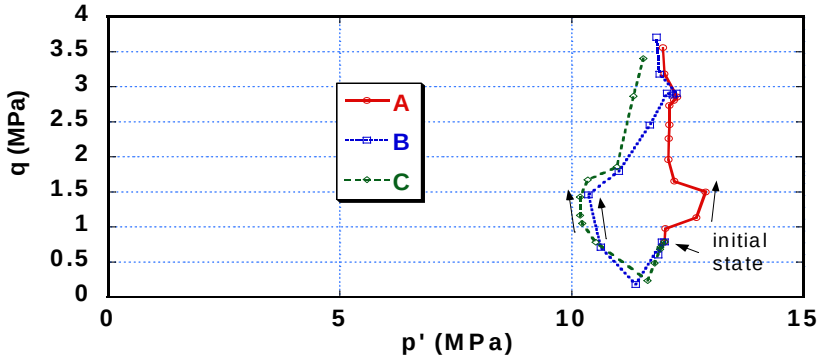

Fig.5.22c: Stress path in cells A, B and C;
From12 step explicit coupling

Figure 5.23 shows the final state vertical displacement profile of the top of the reservoir resulted by one-way, 5-step and 12-step explicit coupling approaches. As can be noticed, one way coupling while it does not allow an updating of the permeability in the grid cells of the reservoir model, gives an interesting result in terms of reservoir deformation. The explicit coupling method performing the updating of permeability shows a further 14% increase in vertical displacement at the reservoir interface compared to the one-way approach. But as explained before, it can be seen that the number of steps in explicit coupling method does not appear as a determining factor for the overall vertical displacement of the top of the reservoir.

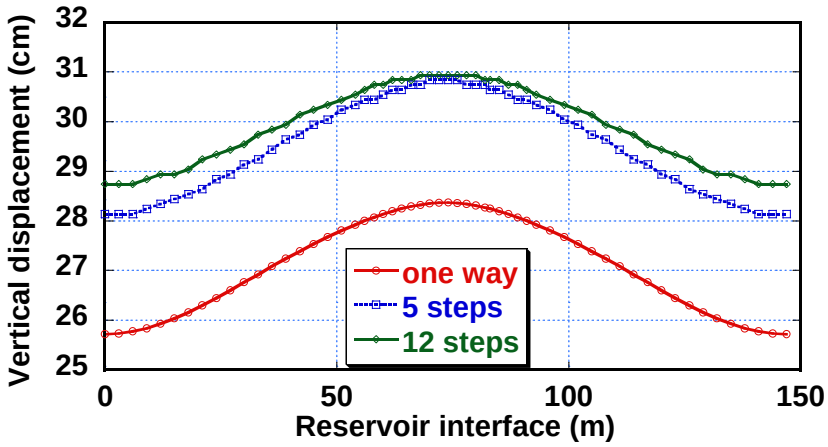

Fig.5.23: Vertical displacement profile of reservoir interface,
at 2000th day

5.3 Enhanced Coupling with Two-Grid system

One of the objectives of this thesis was to study the possibilities of simplifying the geomechanical model in order to reduce the computation run time. After analysing different elements in literature, two main pathways have been proposed:

1/ Using an integral method to limit the field of study (Dusseault et al, 2002, Yin et al, 2006))
2/ Using the different gridding system (mesh size) for two models (Tran et al, 2008)

The first strategy demands significant developments if the finite element code is not intended to be coupled with border elements. This imposes a limitation in modeling since the reservoir sideburdens are as necessarily semi-infinite elastic. This can be a limiting factor if we are interested in stress evolution in overburden, for example when the temperature rises during SAGD. These points led us to focus on second strategy which seems to be more promising.

With the perspective of developing a method with different gridding system, this work was based on the results of a Phd thesis supervised by M. Tijani (Savignat, 2000) which gives us the possibility of mapping the information between two different gridding systems (diffuse approximation method).

The fact that the grid type in reservoir simulator is different from geomechanical simulator makes the mapping process more complicated. In fact in the reservoir simulator a Finite Volume Grid discretization is used where flow variables are computed at the center of gridblocks while in the geomechanical simulator a Finite Element Grid discretization is used to compute displacements at the nodes of the grid.
If the grids in reservoir simulator and geomechanical simulator are coincident, interpolation of the data between the two simulators is simple. Updated pore pressures and temperatures computed in the center of reservoir grids, at the end of this first period, are transferred on the nodes of geomechanics grids in geomechanical simulator. In this transfer, data are interpolated to pass from finite volume discretization to finite element discretization and inversely.
When the grids in reservoir and geomechanical simulators are not coincident, passing the data (temperature, pressure, volumetric strain) between the two simulators is more complex. In this case a field transfer algorithm must be used to perform the passing of data from a grid to the other. This technique is explained in this section.

5.3.1 Diffuse approximation method

The gridding system of the case treated in section 5.2 was coincident in reservoir simulator and geomechanical simulator. As explained before, when the grids in reservoir and geomechanical simulators are not coincident, passing the data (temperature, pressure, volumetric strain) between the two simulators is more complex. In this case a field transfer algorithm must be used to perform the passing of data from a grid to the other.

The diffuse approximation method (DAM) can be used for finding estimates of a scalar field *u* from set of nodal values (Nayroles et al., 1991) (Figure 5.24). The starting point is to estimate the Taylor expansion of the studied scalar field *u* at a chosen point by a weighted least squares method which uses only the values of *u* at the nearest points.

The main advantage of this method is that it only requires sets of discretization nodes and no geometric finite elements and it is a local method. It is to note that the diffuse approximation method can be used with various weighting strategies that lead to different and interesting properties.

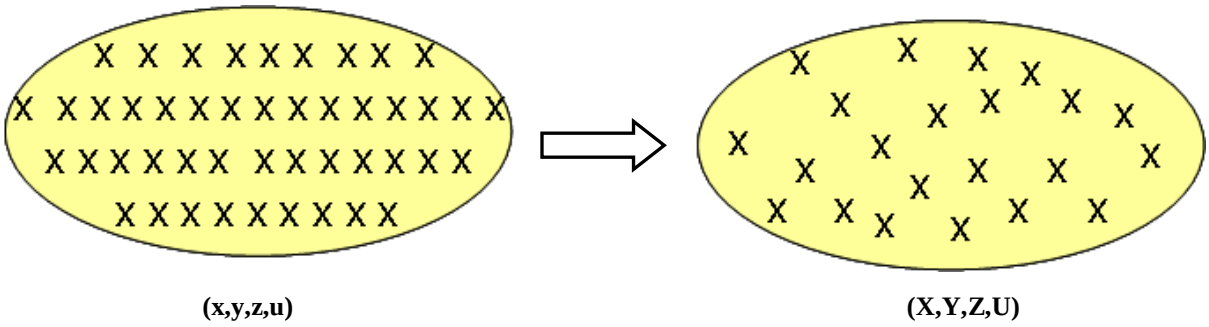

Fig.5.24: Nuage is a field transfer code which is programmed based on diffuse approximation method. Nuage needs (xi, yi, zi, u) and (Xj, Yj, Zj) to map the values of parameter u known on points (xi, yi, zi) in to points (Xj,Yj, Zj)

When the reservoir and the geomechanics grids are distinct, using the diffuse approximation method reduces the simulation run time with the results which are very close to the one-grid system as will be shown in this section. Here a code named NUAGE based on diffuse approximation method (Savignat, 2000), is used for mapping the data from reservoir grid centers to geomechanics grid nodes and vice versa (Figure 5.25).

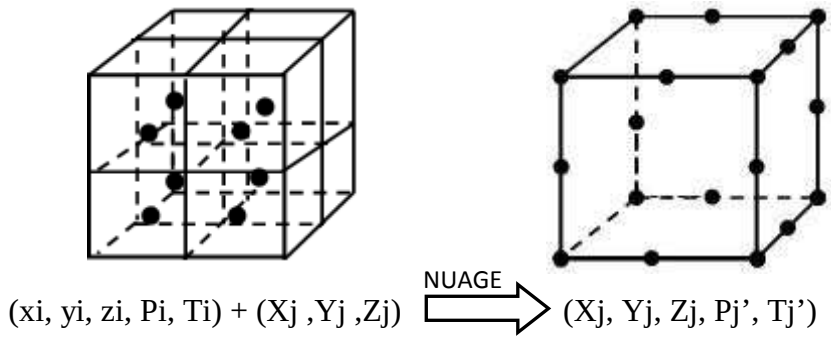

Fig.5.25: Pressure and temperature interpolation from finite volume element center toward finite element nodes. The input data for NUAGE is (xi, yi, zi, Pi, Ti) + (Xj, Yj, Zj), and the output is (Xj, Yj, Zj, Pj', Tj')

The weighting procedure used in the present scheme allows the DAM to interpolate the initial data. This scheme which is written in C gives improved mapping for discontinuous functions.
For the herein study, the data transfer is performed through a coupling module that has been developed using Fortran and Python languages which contains the mapping module (NUAGE) written in C language.
The one-way and sequentially explicit coupling schemes are illustrated in figures 5.26 and 5.27 respectively. The coupling methodology and coupling module have been explained in chapter 4, section 4.3.2, for coupling realized with the same grid systems in reservoir and geomechanics models. Comparing figures 5.26 and 5.27 with 4.21 and 4.22 shows that the same coupling methodology is applied on distinct grid (2- grid) systems between reservoir grid (RG) and geomechanics grid (GG).

5.3.2 Case study 1 (Senlac)

In this section the enhanced coupling methodology is applied on the Senlac test case presented in part 5.1. The geometry of the field in reservoir simulator and geomechanical simulator is modelled as it was presented here in part 5.1; it means construction of reservoir part in reservoir simulator (Figure 5.2), and reservoir surrounded by rocks in geomechanical simulator (Figure 5.5). In geomechanical model, the simulated domain includes the reservoir surrounded below by underburden layers and above by overburden layers. Sideburden rocks are not modelled because the treated case is assumed geometrically periodic. This assumption corresponds to the fact that in a SAGD process, it is common to use several pairs of well that are parallel and equidistant to optimize production rates. Details of the fluid flow and mechanical properties of the case study are given in Tables 5.2 and 5.4. Initial state stresses are supposed to be isotropic.

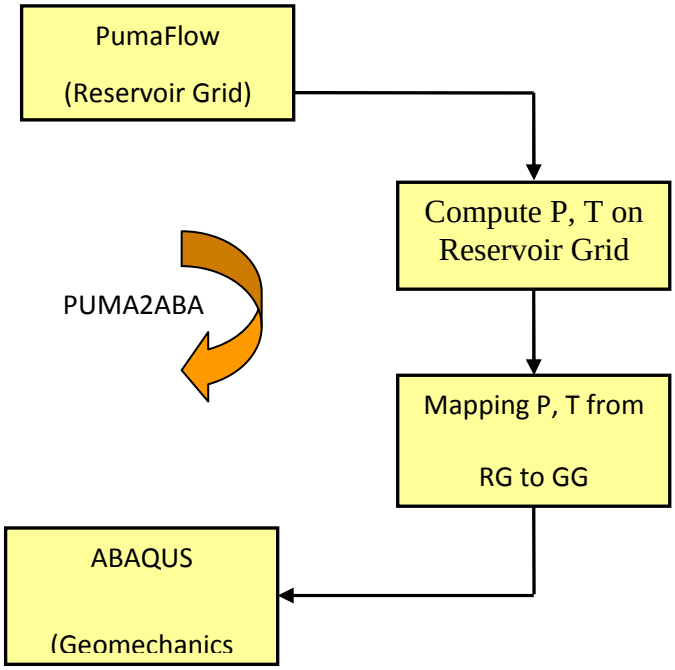

Fig. 5.26: One-way coupling architecture with distinct grid system

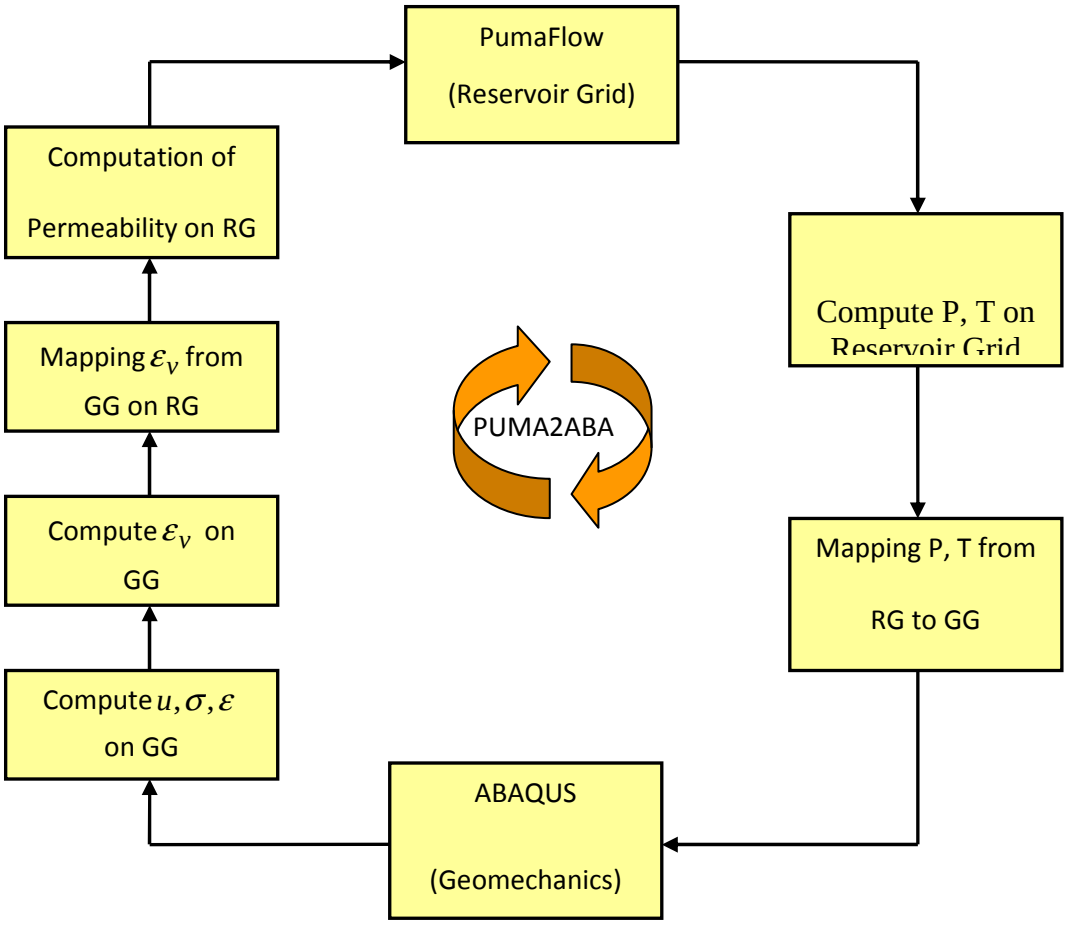

Fig. 5.27: Explicit coupling architecture with distinct grid approach

The coupling approach used is one-way simulation (figure 5.26) and here we compare three coupled simulations with different gridding (two different mesh-sizes) applied in geomechanical simulator:

1) The reservoir grid in geomechanical simulator is the same as reservoir grid in reservoir simulator,

2) The reservoir grid in geomechanical simulator is coarser than the reservoir grid in reservoir simulator,

3) The reservoir grid in geomechanical simulator is coarser than the one in the previous case,

Figure 5.28 shows the reservoir as modelled in reservoir simulator for all the three cases, with a resolution of 65x1x40 in X, Y and Z direction. Figure 5.29 illustrates the reservoir field as modelled in geomechanical simulator with:

- same grid system, where the reservoir field grid in geomechanical simulator has the same resolution as reservoir field grid in reservoir simulator, it means 65x1x40, as shown in Figure 5.29a,
- distinct grid system, where the reservoir field grid in geomechanical simulator has a resolution of 40x1x20 as shown in Figure 5.29b,
- distinct grid system in which the reservoir field grid in geomechanical simulator is coarser than the previous case. In this case the resolution of reservoir field grid in geomechanical simulator is 20x1x10 as illustrated in Figure 5.29c.

Note that in the second and the third cases, the geomechanics gridblocks of underburden and overburden are also resized and the number of gridblocks is less than the first case.

Results obtained from these three cases are compared. Here the CPU time, reservoir temperature field and reservoir interface displacement are presented.

The CPU time for the second case is 57 % less than for the first case; also the CPU time for the third case is 85 % less than the first case. It shows that the distinct grid system can save significant CPU time.

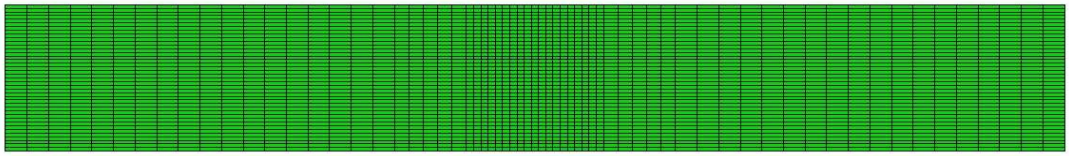

-

Fig.5.28: Reservoir field grid as modeled in reservoir simulator (147m*20m*500m)

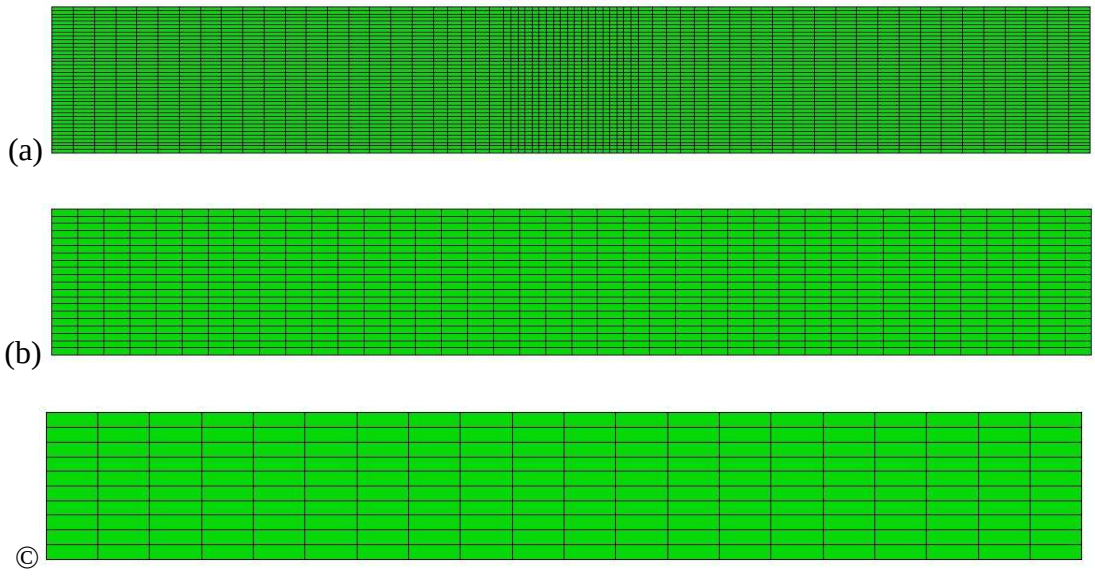

Fig.5.29: Grid as modeled in geomechanical simulator in the three different coupled simulation cases
(a) coincident reservoir-geomechanics gridding system,
(b)&(c) distinct reservoir-geomechanics gridding system

Figure 5.30 shows the temperature field in the reservoir which first increases above the injection well to the top of the reservoir and then extends laterally to become uniform in the upper part of the reservoir. This uniformity is related to lateral boundary conditions that were imposed on the model.

As can be seen, the temperature field resulted by three simulations are really similar, especially further from the wells; but the first simulation (Figure 5.30a) illustrates precisely the temperature around the wells, which is not the same in the second (Figure 5.30b) and the third (Figure 5.30c) simulation case. It shows the importance of refining the mesh around the wells, in order to have more realistic simulation results.

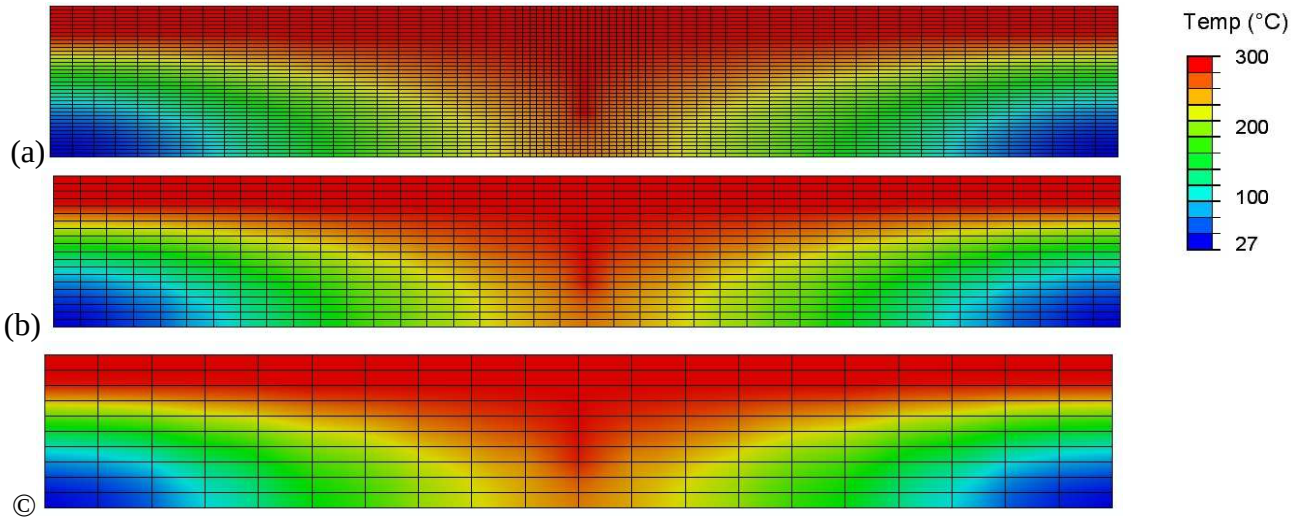

Fig.5.30: Temperature field in geomechanical simulator in three different coupled simulation cases
(a) coincident reservoir-geomechanics gridding system,
(b)&(c) distinct reservoir-geomechanics gridding system

Figure 5.31 shows the vertical displacement profile of the top of the reservoir plotted at the end of the three one-way coupling simulations explained. The uplift is very fast just above the wells, and then it extends to the periphery when the steam chamber grows. It becomes almost homogeneous at the end of the 2000-day simulation.

As can be noticed, the uplift result graph is exactly superposed in three simulations. The pink curve shows the coincident reservoir-geomechanics grid simulation results which correspond to the first test case defined. The blue and green curves illustrate the distinct reservoir-geomechanics grid simulation results which correspond to the second and third test case, respectively.

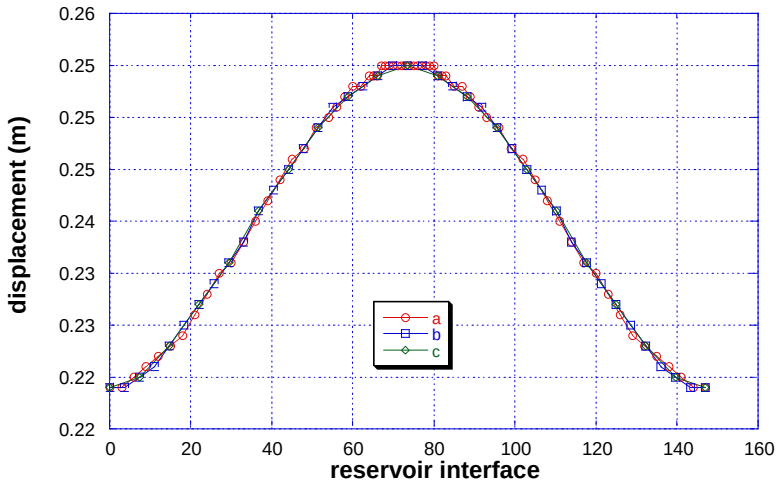

Fig.5.31: Vertical displacement profile of reservoir interface,
at the end of coupled simulation

5.3.3 Case study 2 (Hangingstone)

In this section the enhanced coupling methodology (two-grid system) is applied on a synthetic case study using iterative coupling method. The main difference of this case study is its shallowness and also its hydrostatic pressure comparing to the first case study (Senlac field case). This case study corresponds to the conditions existing on the Hangingstone field which is one of the case studies at IFP Energies Nouvelles. This test case has been constructed based on the previous case study described in section 5.1. The reservoir is assumed homogeneous. As shown in figure 5.32, the top of the reservoir is 250 meters deep, the initial pressure and temperature being equal to 2.4 MPa at the top of the reservoir and 10°C respectively.

The reservoir simulated domain is rectangular with its dimensions in the X, Y and Z directions respectively equal to 147, 500 and 20 meters (figure 5.32). The well pair is located along the Y axis and in the middle of the X axis. The distance between the two wells is 5 meters. The producer is 2 meters above the base of the reservoir.

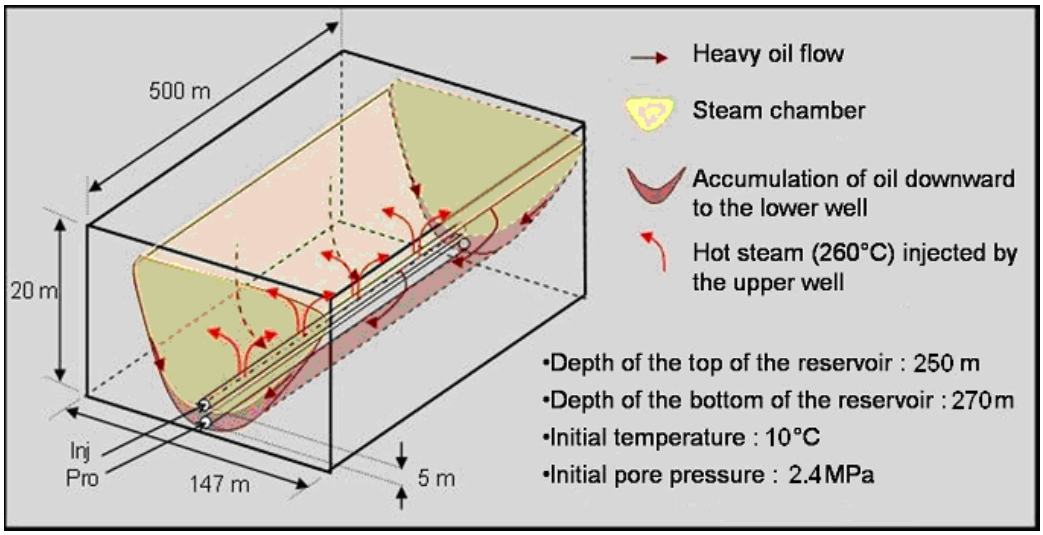

Fig. 5.32: Description of the case study

In the reservoir fluid flow simulator, the size of the grid cells in the X direction is equal to 1 meter near the wells and increased to 2 then 3 meters farther away. As the vertical distance between the two horizontal wells was supposed to be constant, only one cell 500 meters long is used to describe the well length in the Y direction. Vertical gridding in the reservoir is constant with 40 layers 0.5 meter thick. Sideburden rocks are not modelled because the treated case is assumed geometrically periodic. This assumption corresponds to the fact that in a SAGD process, it is common to use several pairs of well that are parallel and equidistant to optimize production rates. In the model associated with the reservoir simulator, fluids cannot flow through the boundaries but heat losses by conduction through upper and lower

boundaries are taken into account by a simplified and one-dimensional modelling of the overburden and underburden that is oriented in the vertical direction.

The simulations are performed over 1440 days. Similar to the case presented in production history in section 5.1.1, the first 120 days consists in pre-heating. The steam injection starts at the end of pre-heating with a maximal pressure set to 5 MPa and the production rate is controlled in order to keep the production well temperature 20°C to 35°C lower than the injection well temperature. The production well minimal pressure is set to 0.5 MPa and the steam injection temperature is about 260°C.

In the geomechanical model, the simulated domain includes the reservoir surrounded below by underburden layers and above by overburden layers. The horizontal displacement of lateral boundaries is blocked as well as all the displacements of the lower boundary. The reservoir rock and fluid properties are given by tables 5.6 and 5.7. Initial state stresses are supposed to be isotropic.

In this work we model the underground by considering a reservoir part that are modelled in both reservoir and geomechanical simulators and surrounding rocks that are only modelled in the geomechanical simulator.

The applied coupling approach is the sequentially iterative coupling method explained in section 4.3.2. The applied iterative coupling with distinct grid system is illustrated is figure 5.33.

As explained before, in iterative method, the updated pore pressures and temperatures at the end of each period are interpolated and transferred from the reservoir grid (RG) to the geomechanical grid (GG) in the geomechanical simulator. Based on the updated producing conditions and constitutive relationships, the geomechanical simulator solves the mechanical equilibrium equation.

Then the results are transferred to the reservoir grid. After this step a convergence criterion is checked. In the present procedure the convergence criterion checked for every element of the reservoir simulator is given by equation 4.44.

If the convergence criterion is not verified the reservoir permeability is updated and the porous volume evolution is corrected in order to perform another iteration of the same period. For the studies considered in this work, the convergence criterion has been checked with *CRIT* equal to 10^{-3}.

The case study aims at comparing various simulations with the same gridding for every reservoir simulations and with different gridding for the geomechanical simulations.

Properties	Reservoir	Overburden	Underburden
Density ($kg.m^{-3}$)	2320	2420	2700
Young's modulus (10^8 Pa)	3.43	2.500	10.000
Poisson's coefficient		0.3	
Biot's Coefficient		1	
Thermal expansion ($°C^{-1}$)		$2 .10^{-5}$	

Table 5.6: Thermo-poro-mechanical properties

Properties	Value
Oil Density ($g.cm^{-3}$)	0.97
Oil viscosity at reservoir conditions (*mPa.s*)	5000
Oil viscosity at 282°C (*mPa.s*)	1.8
Porosity	0.35
Horizontal permeability (*mD*)	2000
Vertical permeability (*mD*)	1000
Rock compressibility (MPa^{-1})	$2.4\ 10^{-4}$
Oil compressibility (MPa^{-1})	$2.17\ 10^{-4}$
Rock heat capacity ($J.cm^{-3}.°C^{-1}$)	2.34
Rock thermal conductivity ($W.\ m^{-1}.°C^{-1}$)	2.70
Oil thermal expansion coefficient ($°C^{-1}$)	2.10^{-4}
Initial oil saturation	0.85
Irreducible water saturation	0.15
Residual oil saturation to waterflood	0.20
Residual oil saturation to steamflood	0.10

Table 5.7: Reservoir rock and fluid properties

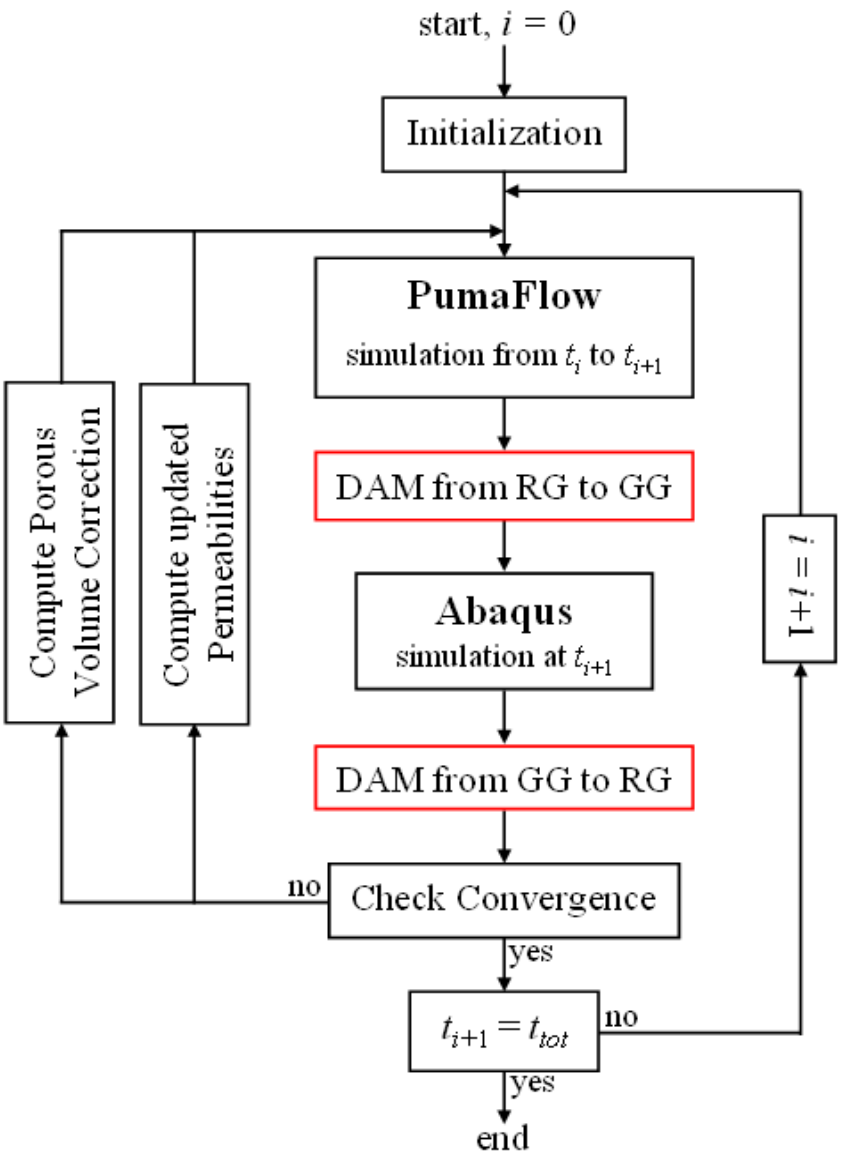

Fig. 5.33: Sequentially iterative coupling procedure architecture

The geomechanical grids are illustrated in Figure 5.34 which is made of quadratic elements. The first geomechanical grid (GG-1), shown in Figure 5.34(a), contains 6175 elements. The reservoir part (delimited by a red rectangle in Figure 5.34(a)) contains 2600 elements and is identical to the reservoir simulator grid. The second geomechanical grid (GG-2), shown in Figure 5.34(b), is coarser than the first one. It contains 2175 elements and the reservoir part (delimited by a blue rectangle in Figure 5.34(b)) contains 580 elements. The third geomechanical grid (GG-3), shown in Figure 5.34(c), is even coarser than the second one. It contains 1235 elements and the reservoir part (delimited by a blue rectangle in Figure 5.34(c)) contains 190 elements. Note that in the second and third cases, the geomechanics gridblocks of underburden and overburden are also resized and the number of gridblocks is less than in

the first case. For each considered geomechanical grid, five simulations are performed for different coupling time steps. The studied coupling time steps are 5, 10, 20, 40 and 60 days. Also, two uncoupled reservoir simulations (namely the standard compressibility simulation and the lowered compressibility simulation) are performed in order to evaluate the contribution of both geomechanical effects and compressibility effects. The difference between the standard compressibility simulation and the lowered compressibility simulation is that the standard compressibility simulation is performed with a compressibility obtained by equation (4.46) and the second simulation is performed with a ten times lowered compressibility.

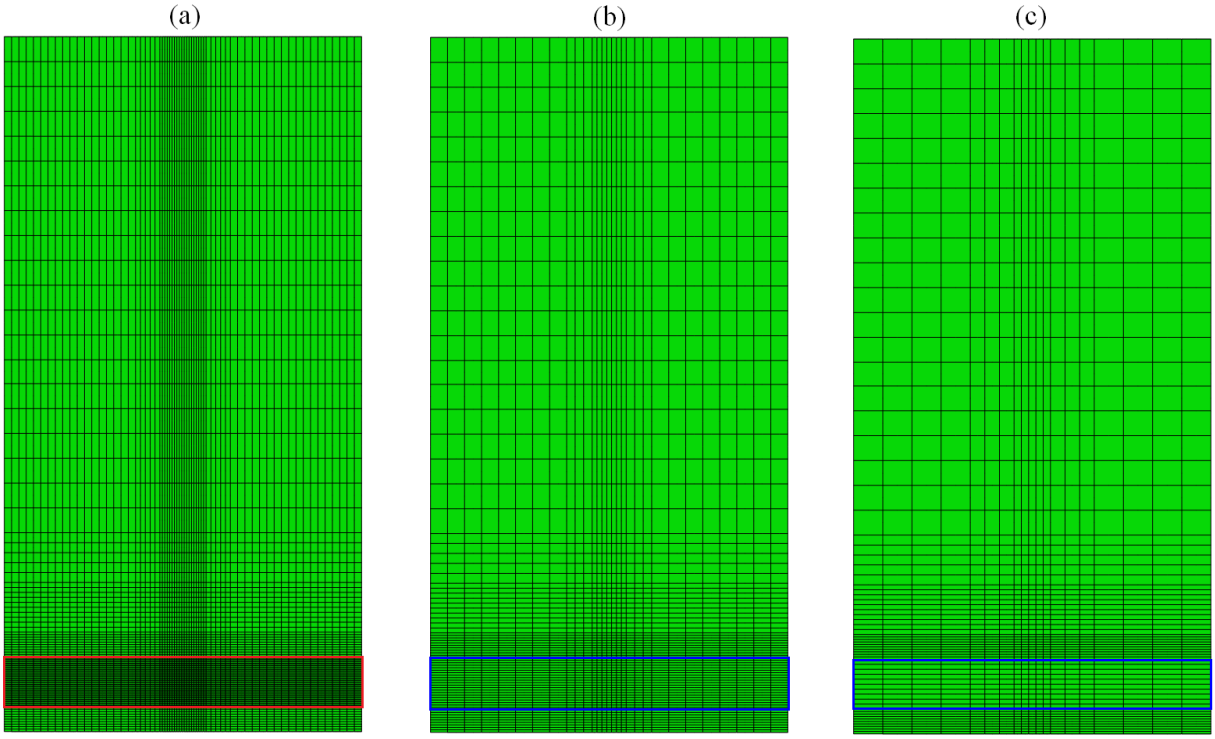

Fig. 5.34: The three geomechanical grids ((a) GG-1, (b) GG-2 and (c) GG-3)

Results

Results obtained from the fifteen coupled cases and from the two uncoupled cases are compared. First, it has to be noticed that for all the coupled simulations the coupling procedure has lead to both convergence and satisfying results.

Relevance of the results

To characterize the global response of the reservoir, cumulative oil produced at *in situ* conditions is plotted versus time on Figure 5.35 for the various simulations. On the Figure 5.35(a) the results obtained by the three considered geomechanical grids are compared together and with the results obtained by simulations in which geomechanical effects are ignored (namely the standard compressibility simulation and the lowered compressibility simulation).

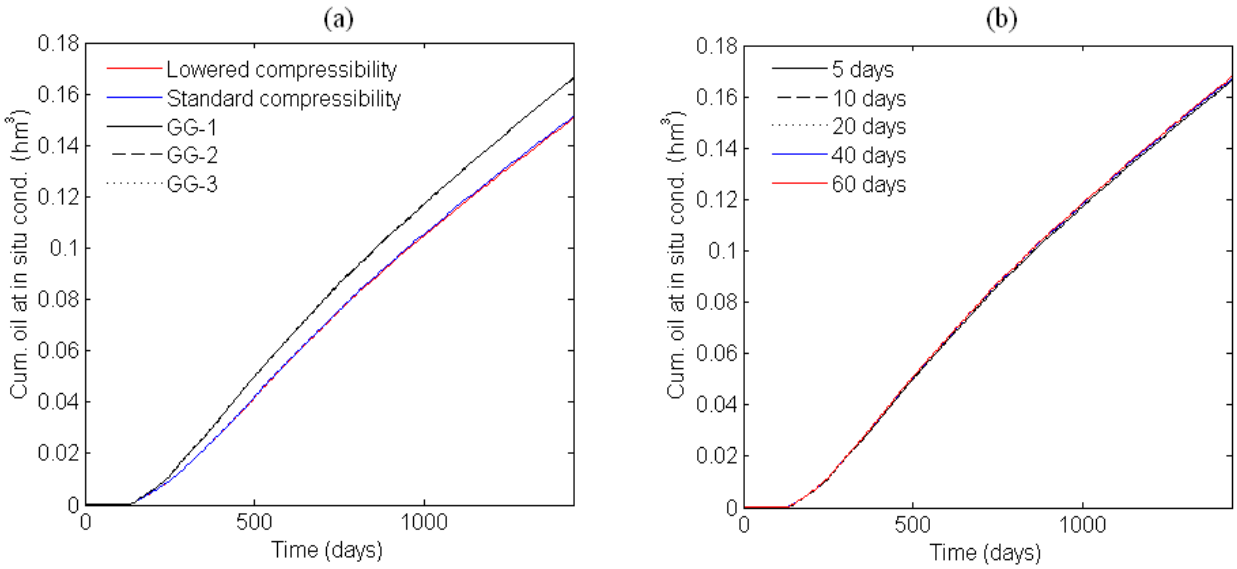

Fig. 5.35: Cumulative oil produced at in situ conditions versus time for different modeling and different spatial discretization with coupling time step of 5 days (a) and for different coupling time step with the geomechanical grid GG-1 (b)

In Figure 5.35(a), the results obtained by the three geomechanical grids are superimposed. The results obtained by the two other simulations (in which geomechanical effects are ignored) are also very close together but are different from the results obtained by the coupled simulations using the grids GG-1, GG-2 or GG-3. This clearly shows that the geomechanical effects involved in a SAGD process cannot be represented by using a simple compressibility factor. The gap between the coupled and uncoupled simulations in terms of produced oil at in situ conditions is of about 10%. This result is consistent with the one obtained by Collins et al. (2002). It also clearly shows that using a coarser grid for the geomechanical simulation than for the reservoir simulator with the proposed procedure allows to obtain relevant results in terms of oil production.

In figure 5.35(b), the results obtained with the different coupling time steps and with the geomechanical grid GG-1 are very close. It should be noticed that even the larger coupling

time steps can lead to an overestimation of the produced oil that is quite low, about 0.6%. This observation demonstrates that the results obtained through the various simulations worth computation and can legitimately be compared.

Figure 5.36 shows the temperature field in the reservoir after 750 days of simulation and with a coupling time step of 5 days for the three geomechanical grids. As it can be seen, the temperature field resulted by the three simulations are really similar. The results plotted on figures 5.36(a) and 5.36(b) are extremely close. The results plotted on figure 5.36(c) that corresponds to the coarser grid are still close to the other ones. However we can see that when a part of the thermal front arrives in an area with the coarser mesh, the shape of this numerical thermal front is influenced by the considered geomechanical mesh and associated shape functions. We can suppose that the third geomechanical grid is still satisfying but represents a limit in terms of element number reduction.

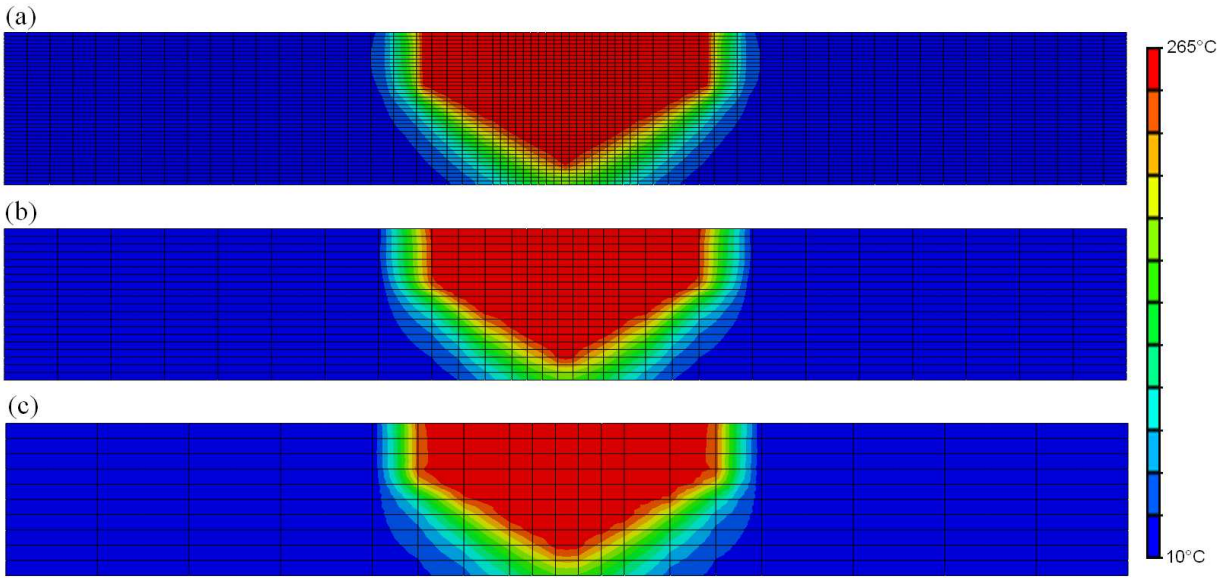

Fig. 5.36: Temperature field reconstructed on the geomechanical grids ((a) GG-1, (b) GG-2, and (c) GG-3) after 750 days of simulation and with a coupling time step of 5 days

As explained in section 5.2, in order to analyze the effects of steam injection during SAGD process, the geomechanical behaviour of the reservoir have been studied in three different grid cells which represent three different zones in the reservoir.

These cells are located in the same XZ plane and at the same elevation in the Z direction. Figure 5.37 shows the location of these grid cells (A, B and C). Grid cell A is placed just in the middle of the reservoir and 5.5 meters above the horizontal well injection well. Grid cells B and C are chosen farther from the wells, with the distance of 18.5 and 60 meters from the grid cell A, respectively.

The stress paths in three grid cells obtained by iterative coupling method have been illustrated in Figure 5.38.

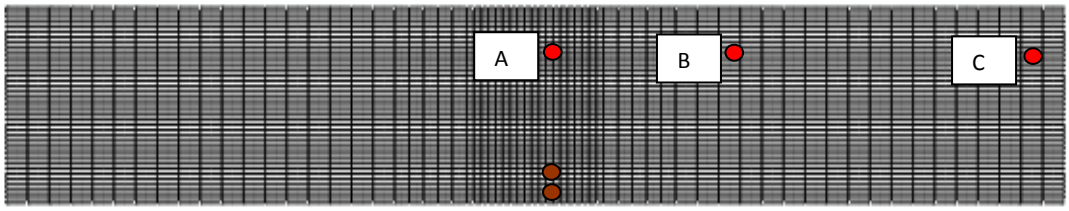

Fig 5.37: Reservoir modeled in reservoir simulator,
location of the grid cells A, B, C and well-pair in reservoir

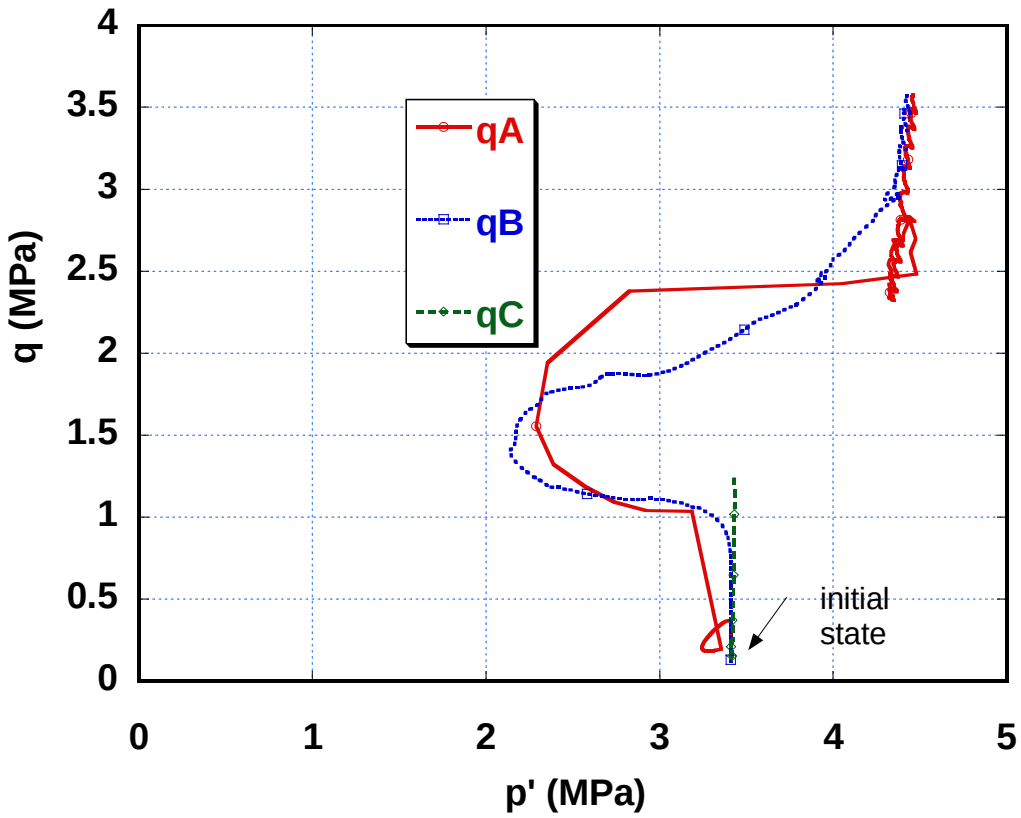

Fig.5.38: Stress path in cells A, B and C (Iterative coupling)

Comparing the stress path resulted by iterative coupling (Figure 5.38) with the stress path obtained by one-way or explicit coupling (Figures 5.14 and 5.15) shows that iterative coupling method clearly reveals a better identification of stress paths than with one-way or explicit coupling approaches but the trend is quite the same.

An increase only in pore pressure would result in equal reduction in all effective principal stresses. In the p'-q diagram the stress path would be horizontal because deviatoric stress would be unchanged.

An only thermal expansion of the reservoir would lead to an increase of both the deviatoric stress and mean effective stress. These stress increases are essentially due to an increase in horizontal stresses.

The combination of the antagonist pore pressure increase and thermal expansion can explain the vertical stress paths observed in the model.

It was mentioned that this synthetic case study represents the Hangingstone field test case and its main difference with the Senlac field case is its lower depth (250*m* against 730*m*). A comparison between the stress path evolution of these two test cases (Figure 5.38 for Hangingstone and Figure 5.15 for Senlac) shows the confinement effects related to the shallowness.

As can be seen, the deviatoric stress (q) obtained for points A and B reaches nearly 3.7 *MPa*, while for point C a maximum value of nearly 1.2 *MPa* for q is obtained. This difference of stress path is due to the steam chamber evolution. As it is illustrated by Figure 5.39 and Figure 5.40, after 1500 days of simulation the pressure front is just arrived at the zone of point C and the temperature front has not even reached at point C. It means that the zone of point C has not been swept by steam chamber which explains the difference of stress path evolution between point C and two other points. Figures 5.39 and 5.40 show also the advance of pressure front comparing to the temperature front.

The fact that the final stress state is almost the same for points A and B is also related to lateral boundary conditions that were imposed on the model. Anisotropic initial stresses conditions certainly would change the development of stress paths, but the trend of increasing shear stress with the growth of the steam chamber would be certainly verified.

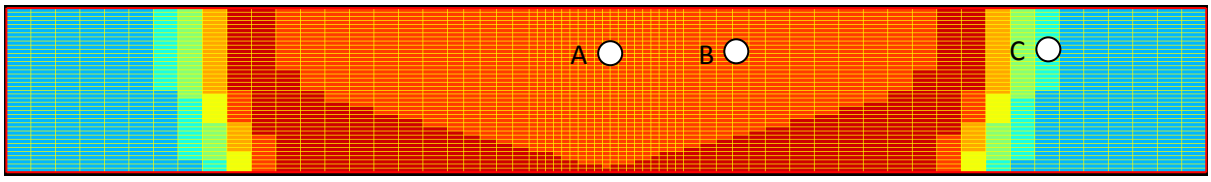

Fig. 5.39: Pressure field in reservoir at the end of simulation (1500 days)

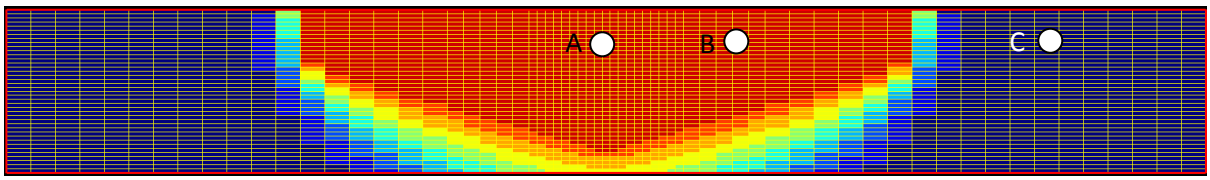

Fig. 5.40: Temperature field in reservoir at the end of simulation (1500 days)

Computation time of the simulations

In order to compare the computation time (CPU time) of the simulations, a normalized simulation CPU time is introduced. For each simulation and at the end of a time period *i*, the normalized simulation CPU time can be estimated by considering the following expression:

$$NSC(X, Dt, i) = \frac{\sum_{k=1}^{i} (Dt + DX) \times n_k}{t_{tot}}$$

with X the considered grid (GG-1, GG-2 or GG-3), Dt the coupling time step, n_k the total number of iterations performed in the period k to reach convergence and DX an equivalent geomechanical simulated time associated with the geomechanical mesh X. In the present case we take DGG-1 = 30 days, DGG-2 = 8 days and DGG-3 = 3 days and t_{tot}= 1440 days.

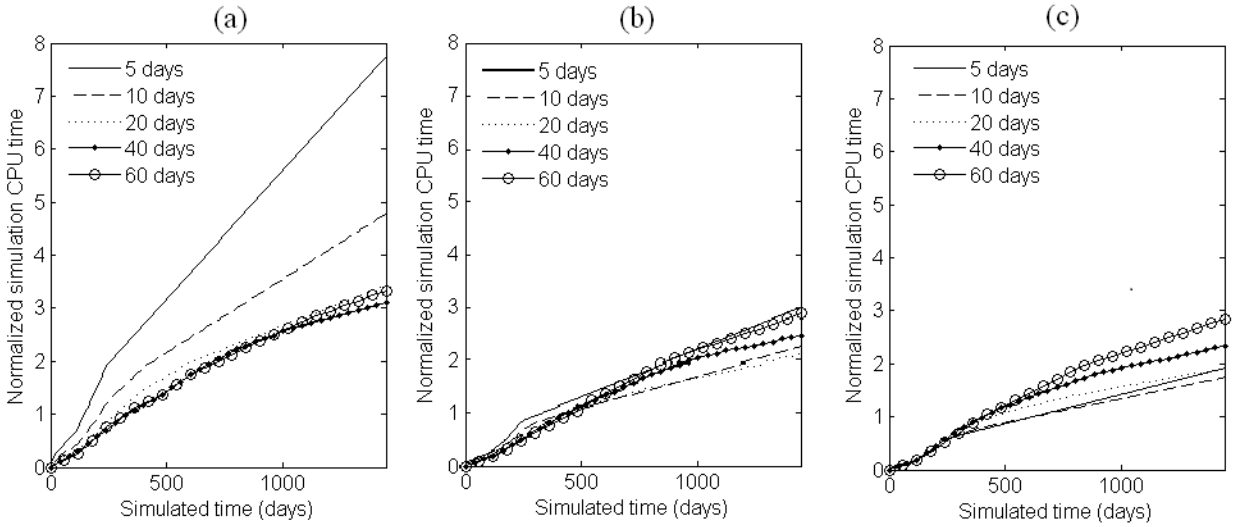

Fig. 5.41: Normalized simulation CPU time with simulated time for various coupling time step and for the three geomechanical grids (a) GG-1, (b) GG-2 and (c) GG-3

As an example, it means that the numerical cost of a geomechanical simulation with the GG-1 mesh is close to the numerical cost required to perform a simulation describing 30 days of fluid flow. The normalized simulation cost does not take into account the influence of data mapping from one grid to another because its numerical cost has appeared to be very low compared to the numerical cost of geomechanical simulations.

The values considered for the equivalent geomechanical simulation time show that using a coarser geomechanical grid clearly decreases the geomechanical simulation cost. Nevertheless it has to be noticed that this effect would probably be more significant for cases containing more elements and that it would probably also be more significant for a three dimensional

case where the increase of element size would take place in three directions (instead of only two directions in the present case).

In figure 5.41, the normalized simulation costs are plotted with simulated time for the three geomechanical grids. The results obtained for the geomechanical grids GG-1, GG-2 and GG-3 are respectively plotted on the figure 5.41(a), 5.41(b) and 5.41(c) for the five considered coupling time steps. Figure 5.41 clearly shows that it leads to more important numerical cost for every time step considered. Furthermore, as it can be seen on figure 5.41(a), the numerical cost of the total simulation increases dramatically when the finer mesh GG-1 is used with small coupling time steps (5-10 days). For this configuration the computational time is higher than for the other configuration at every step of the simulation. Figure 5.41(a) also shows that to reduce the computational time with the considered configuration, it is necessary to rarely update the transport properties considered by the reservoir simulator and that even in that case the computational time is still high. As it can be seen on figure 5.41(c), the simulations based on the geomechanical grid GG-3 and associated with small coupling time steps (5-10 days) leads to lowest computational time of the studied cases.

As shown on figure 5.42 the optimal coupling time step is not the same for the three geomechanical grids. The best coupling time step appears to decrease with the number of elements, it is 10 days for the grid GG-3, 20 days for the grid GG-2 and 40 days for the grid GG-1. Furthermore it can be seen that with the best coupling time steps, the coarser is the geomechanical grid, the faster are the simulations.

Using the proposed coupling procedure appears to be interesting because it allows performing simulations faster and updating reservoir parameters more frequently.

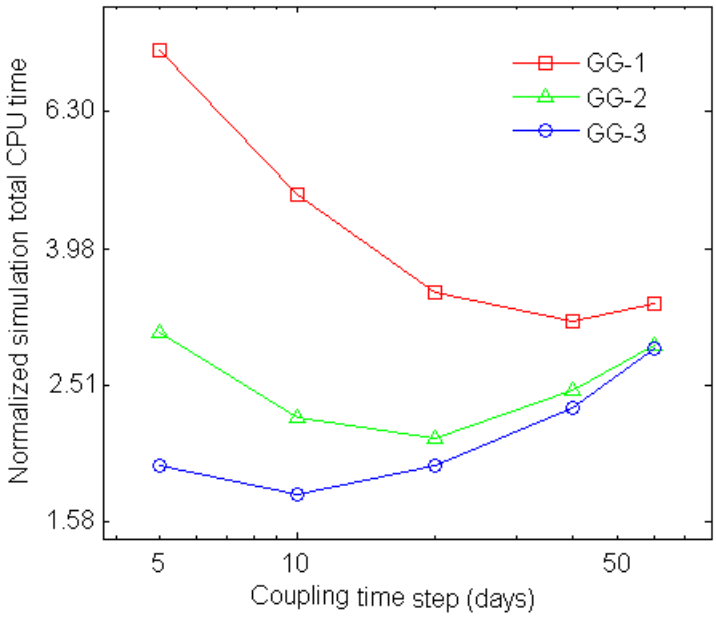

Fig. 5.42: Normalized simulation total CPU time versus coupling time step for the three considered geomechanical meshes

Chapitre 6

Conclusions

Au cours du procédé SAGD utilisé par la production des huiles lourdes, l'injection de vapeur modifie les pressions de pore et les températures dans le réservoir, ce qui modifie les contraintes effectives qui à leur tour modifient les écoulements des effluents. Une approche couplée réservoir géomécanique est requise pour modéliser la production. Cette thèse porte sur les stratégies de couplage et sur les possibilités de réduction des temps de calcul. .Le travail a été effectué sur des cas synthétiques. Plusieurs stratégies ont été étudiées pour traiter le couplage : couplage one-way, séquentiel explicite et séquentiel itératif en couplant deux logiciels commerciaux, PumaFlow logiciel réservoir et Abaqus logiciel géomécanique. Les résultats ne laissent aucun doute sur l'importance d'utiliser une approche couplée aussi efficace que possible. Les chemins de contrainte, l'évolution des perméabilités et les déformations verticales de l'interface réservoir couverture dépendent de l'approche de simulation choisie. Cependant les temps de calculs sont très élevés et les moyens de les réduire ont été recherchés, en jouant sur la géométrie du système et le type de maillage utilisé.

Si la même géométrie et le même système de maillage sont utilisés pour les deux simulateurs, les temps de calcul pour traiter un problème réel avec la prise en compte d'hétérogénéités peuvent devenir dissuasif surtout si on veut étudier l'influence de la variabilité des paramètres d'entrée. Afin de surmonter ce défi une technique d'amélioration du maillage a été utilisée dans lequel les mailles du modèle réservoir et les mailles du modèle géomécanique ne coïncident pas. Les deux maillages peuvent être affinés ou élargis dans différentes régions de façon indépendante en fonction de l'ampleur des différentes grandeurs physiques. Pour un processus de récupération thermique avec des fronts de température, pression et saturation comme le procédé SAGD, le nombre des mailles du modèle géomécanique peut être beaucoup plus petit que le nombre des grilles du réservoir, ce qui conduit à réduire le temps CPU.

Nous avons utilisé le code de transfert de champs NUAGE basé sur la méthode d'approximation diffuse. Ce code a été utilisé pour la projection des données des centres des

mailles du modèle réservoir sur les nœuds des mailles du modèle géomécanique et vice versa. D'après les résultats de ce travail nous pourrions économiser jusqu'à 85% de temps CPU, ce qui est vraiment intéressant surtout dans le cas de simulations couplées de SAGD sur un champ réel.

Chapter 6

Conclusions

Exploiting the world's heavy oil and bitumen reservoirs will gain increasing significance in the future as light oil production reaches its peak. The physical properties of these hydrocarbons require that special and expensive recovery techniques be used in their production. Thermal oil recovery methods are most commonly applied to extract such heavy oils. Given the costs of many enhanced oil recovery methods, comprehensive control of these programs during production is an essential step to ensure technically and economically successful reservoir exploitation.

SAGD programs are dominantly applied in Western Canada to produce shallow heavy oil reservoirs. The high production rate and recovery of the oil in place makes this method the most promising for heavy oil production. During a SAGD program two horizontal boreholes are drilled in a vertical plane close to the bottom of the reservoir. Through the top borehole hot steam is injected into the reservoir. Ideally, this steam then rises through the oil bearing rock matrix to the top of the formation thus forming a steam chamber. The steam condenses at the boundaries of the chamber, where it heats the oil. The viscosity of the heavy oil reduces significantly and the oil becomes mobile. As the density of the oil is larger than that of the steam the oil flows along the chamber to the bottom borehole where it is produced In the SAGD process, continuous steam injection changes reservoir pore pressure and temperature, which can increase or decrease the effective stress in the reservoir. Indeed, oil sand material strains induce changes in the fluid flow-related reservoir parameters. This is obviously a coupled problem. Therefore, coupled reservoir geomechanical simulations are required. This is particularly important for the correct prediction of oil recovery and for the correct interpretation of 4D seismic to quantify the steam chamber growth since the seismic wave velocity depends on temperature, pressure and saturations, but also on the strain and stress state of the reservoir and overburden.

This thesis dealt with the coupling between the mechanical and fluid flow problems, and the fact that the reservoir models become very computationally intensive. The main issues being investigated were (1) the coupling strategy, (2) the geometry and (3) type of gridding system. This work was performed on synthetic cases.

Coupling Approach

Several strategies were studied to deal with the coupling between fluid flow and geomechanical effects in SAGD modelling: one-way coupling, sequential explicit coupling and sequential iterative coupling.

In one-way coupling the results of the reservoir simulation are used to compute the stress and strain in reservoir with a geomechanical simulator at selected times but without feed back to the reservoir simulator. In sequential coupling a feed back is operated from the geomechanical simulator to the reservoir simulator in order to update the permeability modified by the variation of volumetric strain under pressure and temperature variations. The sequential coupling is described as "explicit" if the methodology is only performed once for each time step and "iterative" if the methodology is repeated till convergence between the two models of the calculated stress and fluid flow.

Results leave no doubt about the importance of using a coupled approach as efficient as possible. Stress path, permeability evolution and vertical displacement at reservoir interface depend on the chosen simulation approach.

The one way approach, while basic, can indicate the most mechanically stressed areas and provide a first estimation of deformation magnitude of the reservoir and surrounding layers. The explicit coupling approach allows one to roughly estimate the effect of geomechanics on reservoir flow but is less versatile than the one way coupling approach. With an explicit coupling geomechanical and reservoir simulations are interdependent and have to be performed sequentially. A comparison between the one-way simulation method and the explicitly coupled method was performed with variation in the number of coupling period. It indicates that the coupling is more important in the early period of steam chamber growth since steam strongly affects the area close to the well pair from the start of injection. It was also observed that, increasing the coupling period number affects the geomechanical behaviour evolution. Therefore it confirmed the necessity of applying an iterative coupling method in order to have a higher confidence in our analysis of reservoir production and geomechanical effects.

Compared to a fully coupled approach, iterative coupling method is still easier to apply, and gives comparable results and can lead to reduced simulation time. Nevertheless, problems related to large computer memory requirements and long CPU computation time still exist, because a geomechanical simulator normally solves a much larger number of unknowns per grid-block than a reservoir simulator does.

In order to limit the number of unknowns considered in the geomechanical simulator, the geometry of the model and the gridding type are two key issues.

Geometry

To model a reservoir-geomechanics coupled simulation, irrespective of the used gridding technique, three apparent choices exist regarding establishing the geomechanical model and reservoir model:

1. Modelling just the reservoir part in geomechanical simulator and reservoir simulator (Fig 6.1)
2. Construction of reservoir part in reservoir simulator, and reservoir surrounded by rocks in geomechanical simulator (Fig 6.2).
3. Modeling the reservoir part and the surrounding strata (here, overburden and underburden) in both simulators (Fig 6.3).

Examples of these approaches may also be found in many articles like: Settari, 2008; Lerat et al. 2009a; Shi and Durucan, 2009 and Zandi et al. 2010a.

The weakness of the first approach is the setting of an equilibrium state in the geostatic step of the geomechanical simulation.

The second approach, which was applied in our work, is the most commonly used, as we aim at a limited total number of elements in the models in order to reduce the simulation run time.

In the third approach, the reservoir surrounded by rocks is constructed in both simulators, which can result in increase of the simulation run time. Using an adapted reservoir simulator, the advantage of this method is the possibility of correctly simulating the temperature field in surrounding rocks, which is very helpful especially in the case of SAGD modelling.

Gridding

If the same geometry and gridding system is used for both simulators, due to the heterogeneity, a full-field coupled problem requires significantly more CPU time and memory than a run without coupled geomechanics calculations, which makes the coupled runs unattractive.

In order to overcome this challenge an improved gridding technique has been used in which the reservoir and geomechanical grids are not needed to be coincident. The two grids can be refined or coarsened in different regions independently according to the scale of the various physical process of interest. For typical thermal recovery process with fronts, as SAGD process, the number of geomechanics gridblocks can be much smaller than the number of reservoir gridblocks, which results in a much reduced CPU time and memory requirement (Tran et al.,2008).

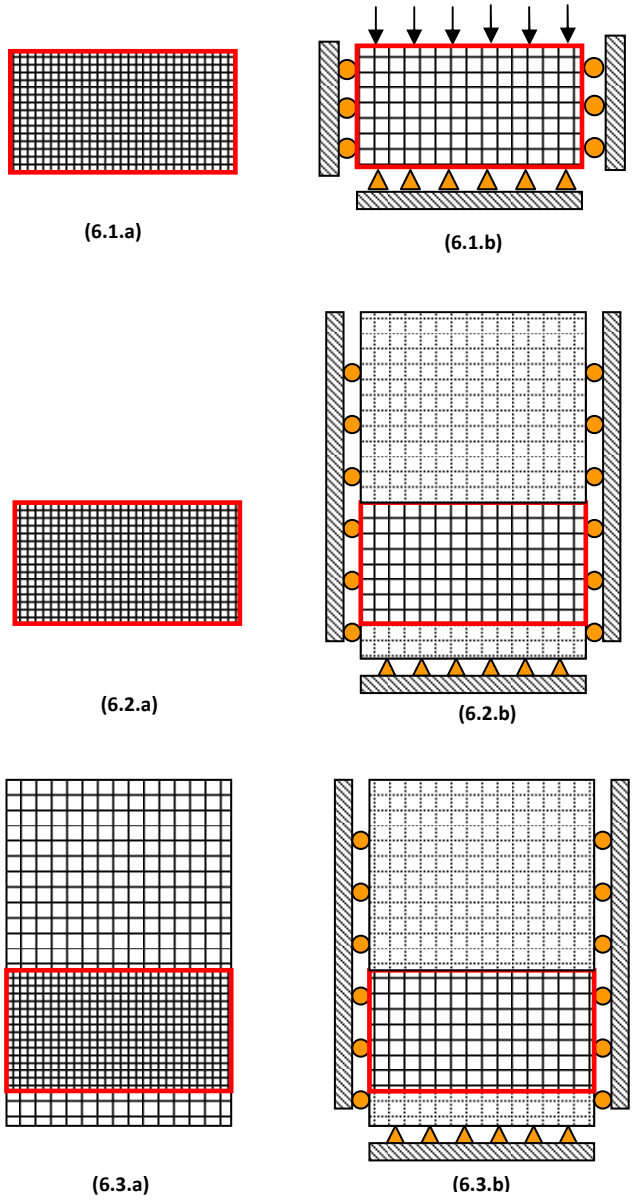

Fig.6.1-2-3: Different geometries of modeled reservoir in reservoir simulator (a) and its surrounding rocks in geomechanical simulator (b)

Here a field transfer code named NUAGE based on diffuse approximation method (Savignat, 2000) was used for mapping the data from reservoir grid centres to geomechanical grid nodes and vice versa. Using the diffuse approximation method, when the reservoir and the geomechanics grids are distinct, reduces the simulation run time with the results which are very close to the one-grid system as it has been shown in this work.

It has been shown that the sequential iterative coupling approach combined by coincident and separate grid systems has lead to a similar description of the considered process.

Furthermore, the presented procedure has appeared successful to reduce significantly the computational time. It also has to be noticed that, observed reduction in computational time comes with a decrease of the optimal coupling time steps. It means that the proposed coupling method can lead to a more frequent updating of the transport properties considered by the reservoir simulator with a lower computational cost.

Using the distinct gridding system we could save up to 85 % of CPU time, which is really interesting especially in the case of a real field SAGD coupled simulation.

When a large reservoir field is simulated, it is recommended that a coarse (low-resolution) geomechanics grid be used to obtain approximate results before applying a fine (high-resolution) geomechanics grid to get the desired accuracy.

Future research directions

The analyses and results presented in this thesis could be extended to accommodate the following points.

In order to use the field transfer code for mapping the reservoir data into the geomechanics grid in the case of a heterogeneous case study, some issues should be considered:

- How to choose the finite element and finite volume grid size,
- How to define the constitutive law for geomechanical model when it includes heterogeneities, considering both elastic and/or plastic behaviours,
- What are the variables to be transferred when there are material heterogeneities,
- Finally, how to update the petrophysical properties in the reservoir model after the geomechanical calculation. In other words, what about the downscaling?

References

Albahlani, A.M. and Babadagli, T., 2008, A Critical Review of the Status of SAGD: WhereAre we and What Is Next? Paper SPE 113283 presented at the SPE Western Regionaland Pacific Section AAPG Joint Meeting, Bakersfield, California, 29 March–2 April.

Bavière, M., 1991, Basic Concepts in Enhanced Oil Recovery Processes. Critical Reports on Applied Chemistry, Vol. 33, Elsevier Applied Science.

Bévillon D., 2000, Couplage d'un modèle de gisement et d'un modèle mécanique. Application à l'étude de la compaction des réservoirs pétroliers et de la subsidence associée, PhD dissertation, IFP - Université des Sciences et Technologies de Lille.

Bharatha, S., Yee, C.T., and Chan, M.Y., 2005, Dissolved gas effects in SAGD, Paper 2005-176, 56th Annual Tech. Meet., Calgary, Canada.

Biot, M.A., 1941, General Theory of Three Dimensional Consolidation. J. Appl. Phys. Vol. 12, 155-164.

Birrel, G.E., Aherne, A.L., andSeleshanko, D.J., 2005, Cyclic SAGD - economic implications of manipulating steam injection rates in SAGD projects – re-examination of the Dover project. Journal of Canadian Petroleum Technology, 44.

Birrell G. E. and Putnam P. E., 2000, A study of the Influence of Reservoir Architecture on SAGD steam chamber Development at the Underground Test Facility, Northeaster Alberta , Canada , Using a Graphical Analysis of Temperature Profiles, Paper 2000-104. CIPC. Calgary, Canada.

BLM, Bureau of Land Management, 2008, U.S. Department of the Interior. Tar sands basics. Argonne National Laboratory.

Burger, J., Souriaux, P., Combarnous, M., 1985, Thermal Methods of Oil recovery. Gulf Publishing Co., Houston. Editions Technip.

Butler, R.M., 2004, The behaviour of non-condensible gas in SAGD, JCPT, Vol. 43, No.1.

Butler, R., Jiang Q., and Yee C., 2001, The Steam and Gas Push (SAGP), Recent Theoretical Developments and Laboratory Results Using Layered Models , *JCPT*, Vol. 40, No.1.

Butler, R., 1994, Steam-Assisted Gravity Drainage: Concept, Development, Performance and Future. JCPT 33 (2): 44–50.

Butler, RM. and Mokrys, IJ., 1991, A New Process (VAPEX) for Recovering Heavy Oils Using Hot Water and Hydrocarbon Vapour. JCPT, Vol. 30, No. 1, 97-106.

Butler, R.M., 1991, Thermal Recovery of Oil and Bitumen.Prentice Hall.

Canbolat, S., Akin,S., and Kovscek, A.R., 2002, A study of Steam-Assisted Gravity Drainage Performance in the Presence of Non condensable Gasses, SPE 75130, *SPE/DOE Imp. Oil Rec. Sym.,* Tulsa ,Oklahoma, USA.

Chakrabarty, C., Renard, G., Fossey, J.-P., and Gadelle, C., 1998, SAGD Process in the East Senlac Field: From Reservoir Characterization to Field Application. Paper 132 presented at the 1998 UNITAR Conference, Beijing, China, 27-31 October

Chalaturnyk, R.J. and Li, P., 2004, When is it important to consider geomechanics in SAGD operations, JCPT, Vol. 42, No.4.

Chalaturnyk, R. J., 1996, Geomechanics of SAGD in Heavy Oil Reservoirs.PhD dissertation, Department of Civil Engineering, University of Alberta, Alberta.

Chen, Q., Gerristen, M.G., and Kovscek, A.R., 2007, Effects of reservoir heterogeneities on the SAGD process, SPE 109873, Aniheim, USA.

CNRL, 2007, Canadian Natural Resources corporate presentation, Feb. 2007. http://www.cnrl.com/client/media/1242/1413/w_corppresfeb.pdf, p. 23.

Collins, P.M., Carlson, M.R., Walters, D.A., and Settari, A., 2002, Geomechanical and Thermal Reservoir Simulation Demonstrates SAGD Enhancement Due to Shear Dilation. Paper SPE 78237 presented at the SPE/ISRM Rock Mechanics Conference, Irving, Texas, 20-23 October.

Coussy, O., 1995, Mechanics of Porous Continua.Wiley, New York.

Das, S., 2007, Application of thermal recovery processes in heavy oil carbonate reservoirs, SPE 105392, Bahrain.

Dean, R.H., Gai, X., Stone, C.M. and Minkoff, S.E. (2006) A comparison of techniques for coupling porous flow and Geomechanics, SPE Journal 2006, 11(1), pp. 132–140.

Delamaide, E., Kalaydjian, F., 1996, A Technical and Economical Evaluation of Steam Foam Injection Based on a Critical Analysis of Field Applications. SPE 35692 , (presented at the 1996 SPE Western Regional Meeting, Anchorage, 22-24 May).

Delamaide, E., Corlay Ph., Demin, W., 1994, Daqing Oil Field: The Success of Two Pilots Initiates First Extension of Polymer Injection in a Giant Oil Field", SPE 27819 (presented at the 1994 SPE/DOE IOR Symposium, Tulsa, 17-20 April).

Demin W, Jiecheng C, Junzheng W, Gang, W (2002) Experiences Learned After Production of More Than 300 Million Barrels of Oil by Polymer Flooding in Daqing Oil Field. SPE 77693 (presented at the 2002 SPE ATCE Conference, San Antonio, 29 Sept. – 2 Oct.).

Dussault, M.B., 2008, Coupling geomechanics and transport in petroleum engineering, SHIRMS, Perth, Western, Australia.

Dusseault, M.B. and Rothenburg, L. (2002) Deformation analysis for reservoir management, In Oil and Gas Science and Technology - Revue de l'IFP, Vol. 57, No. 5, pp. 539–554.

Edmunds, N. and Chhina, H., 2001, Economic Optimum Operating Pressure for SAGD

Projects in Alberta. JCPT 40 (12): 13–17.

Edmunds N., 1999, On the Difficult Birth of SAGD (Steam Assisted Gravity Drainage). JCPT, Vol. 38, No. 1, Jan., p. 14-17.

Edmunds, N., 1998, Investigation of SAGD Steam Trap Control in Two and Three Dimensions. Paper SPE 50413 presented at the SPE International Conference on Horizontal Well Technology, Calgary, 1–4 November.

Egermann, P., Renard, G., and Delamaide E., 2001, SAGD Performance Optimization Through Numerical Simulations: Methodology and Field Case Example.,Paper SPE 69690 presented at the SPE ITOHOS Symposium, Porlamar, Margarita Island, Venezuela, 12-14 March.

Eni, 2008, Eni and the Republic of Congo launch a new integrated model of cooperation.

Farouq-Ali, S.M., 1997, Is there life after SAGD, JCPT 97-06-DAS, Vol. 36, No.6.

Fox M, Wilpert, G., 2006, International Energy Agency increases Venezuela's oil production estimates, maybe. Venezuelan Analysis.

Gates, I. D. and Chakrabarty, N., 2005, Optimization of Steam-Assisted Gravity Draining in McMurray Reservoir, Paper No. 2005-193, 6th *CIPC (56th Ann. Tech. Meet.),* Calgary, Canada.

Giusti, L. E., 1974, CSV makes steam soak work in Venezuela field. Oil and Gas Journal, Nov., p. 88-93.

Government of Alberta., 2008, Alberta's Oil Sands: Opportunity, Balance.

Greaves, M., Xia, TX., 1998, Preserving Downhole Thermal Upgrading Using 'Toe-to Heel' ISC – Horizontal Wells Process (presented at the 7th UNITAR International Conference on Heavy Crudes and Tar Sands, Beijing, 27-30 Oct.).

Grills, T., 2002, Magnetic Ranging Technologies for Drilling Steam Assisted Gravity Drainage Well Pairs and Unique Well Geometries-A Comparison of Technologies. Paper SPE 79005 presented at the SPE International Thermal Operations and Heavy Oil Symposium and International Horizontal Well Technology Conference, Calgary, 4–7 November.

Guy, N., Zandi, S., Ferrer, G., Baroni, A., Renard, G., Nauroy, JF., 2011, Numerical coupling of geomechanics and thermal reservoir flow using separate grids, COMGEO II (2nd International Symposium on Computational Geomechanics), Cavtat, Dubrovnik, Croatia

Huc, A., 2010, Heavy Crude Oils: from Geology to Upgrading - An Overview. Technip Editions, Paris.

Ito, Y. and Chen, J., 2009, Numerical History Match of the Burnt LakeSAGD Process. Paper CIM 2009-004 presented at the Canadian International Petroleum Conference (CIPC) 2009, Calgary, Alberta, 16-18 June.

Ito, Y., and Ipek, G., 2005, Steam-fingering phenomenon during SAGD process, SPE/PS-CIM/ CHOA 97729, Calgary, Canada.

Ito, Y. and Suzuki, S., 1996, Numerical Simulation of the SAGD Process in the Hangingstone Oil Sands Reservoir.Proc., 47th ATM of the Petroleum Society of CIM, Calgary, Alberta, 10-12June.

Jeannin, L., Mainguy, M., and Masson, R., 2005, Comparison of Coupling Algorithms for Geomechanical-Reservoirs Simulations. Proc., U.S. Rock mechanics symposium, Alaska ROCKS 2005, Anchorage, USA, 25-29 June. Paper ARMA/USRMS 05-677.

Kaiser, T., 2009, Post-Yield Material Characterization for Thermal Well Design. SPEJ 14 (1): 128–134. SPE 97730.

Kaiser, T.M.V., Wilson, S., and Venning, L.A. 2002, Inflow Analysis and Optimization of Slotted Liners.SPE Drill.&Compl. 17 (4): 200–209. SPE 80145.

Kisman, K.E., 2001, Artificial Lift: A Major Unresolved Issue for SAGD. JCPT 42 (8): 39-45.

Kisman, K. and Yeung, K.C., 1995, Numerical study of the SAGD process in the Burnt Lake oil sands lease, SPE 30276, Calgary, Canada.

Kosich, Dorothy, 2008, Rapeal sought for ban on U.S. Govt. use of CTL, oil shale, tar sands-generated fuel. Mine Web

Lacroix, S., Renard, G., and Lemonnier, P., 2003, Enhanced Digital Simulations through Dynamical Sub-Gridding. Proc., 2003 CIM Annual Meeting, Calgary, 10 June, Paper CIM 2003-87.

Lerat, O., Adjemian, F., Auvinet, A., Baroni, A., Bemer, E., Eschard, R., Etienne, G. et al. 2009, Modelling of 4D Seismic Data for the Monitoring of the Steam Chamber Growth During SAGD Process. Proc., Canadian International Petroleum Conference 2009, Calgary, Alberta, Canada, 16-18 June, Paper 2009-095.

Lerat, O., Adjemian, F., Auvinet, A., Baroni, A., Bemer, E., Eschard, R., Etienne, G. et al. 2009, 4D Seismic Modelling Applied to SAGD Process Monitoring. Proc., 15th European Symposium on Improved Oil Recovery, Paris, France, 27-29 April, Paper B14.

Le Ravalec, M., Morlot, C.,Marmier, R., Foulon, D., 2009, Heterogeneity impact on SAGD process performance in mobile heavy oil reservoirs, Revue IFP, Vol.64, No.4.

Li, P., Chalaturnyk, R.J., and Tan, T.B., 2006, Coupled reservoir geomechanical simulations for SAGD process, JCPT, Vol. 45, No.1.

Llaguno, P., Moreno, F., Gracia, R., and Méndez Escobar, E., 2002, A Reservoir Screening Methodology for SAGD Application , Paper 2002-124, *CIPC* , Calgary Canada.

Longuemare, P., Mainguy, M., Lemonnier, P., Onaisi, A., Gérard, Ch., and Koutsabeloulis, N. 2002, Geomechanics in Reservoir Simulation: Overview of Coupling Methods and Field Case Study. Oil & Gas Science and Technology 57(5): 471-483 .

Mainguy, M. and Longuemare, P., 2002, Coupling fluid flow and rock mechanics: Formulations of the partial coupling between reservoir and geomechanical simulators, Revue IFP, Vol. 57, No.4.

McLennan, J.A. and Deutsch, C.V., 2005, Ranking geostatistical realizations by measures of connectivity, SPE/PS-CIM/CHOA 98168, Heavy oil symposium, Calgary, Canada.

McLennan, J.A. and Deutsch, C.V., Garner, D., Wheeler, T.J., Richy, J.F., and Mus, E., 2006, Permeability modelling for SAGD process using minimodels, SPE 103083, SPE Ann. Tech. Conf. and Exh., Texas, USA.

Medina, M., 2010, SAGD: R&D for unlocking unconventional heavy oil resources, Journal of THE WAY AHEAD, vol. 6, No. 2.

Mukherjee, N.J., Edmunds, N.R., and GITTINS, S.D., 1994, Impact and mitigation of certain geological and process factors in the application of SAGD at AOSTRA’s UTF, Paper No. HWC94-51, SPE/CIM/CANMET, Calgary, Canada.

Nasr, T.N., Law, D.H.S., Golbeck, H., and Korpany, G., 2000, Counter-current aspect of the SAGD process, JCPT, Vol. 39, No.1.

Nasr, T.N., Golbeck, H., and Lorimer, S., 1996, Analysis of SAGD process using experimental/numerical tools, SPE 37116, Calgary, Canada.

Nayroles, B., Touzot, G. & Villon, P., 1991, The diffuse approximation. C. R. Acad. Sci. Paris, Serie II, Vol. 313, 293-296.

Palmgren, C., Renard, G., 1995, Screening Criteria for the Application of Steam Injection and Horizontal Wells.presented at the 1995 European IOR Symposium, Vienna, May.

Prats M., 1982, Thermal Recovery. SPE monograph Volume 7, SPE of AIME, Dallas.

Rigzone. Summer, 2006, RigzoneReporter_HeavyOil_Russia.pdf

Rigzone. March, 2007, Madagascar Oil raises $85M for exploration, opens new head office".

Rutqvist, J., Borgesson, L., Chijimatsu, M., Kobayashi, A., Jing, L., Nguyen, T.S., Noorishad, J., and Tsang, C.-F. 2001. Thermohydromechanics of Partially Saturated Geological Media: Governing Equations and Formulation of Four Finite Element Models. Int J Rock Mec Min Sci 38(1): 105-127.

Samier, P., Onaisi, A., and Fontaine, G., 2003, Coupled Analysis of Geomechanics and Fluid Flow in Reservoir Simulation. Paper SPE 79698 presented at the Reservoir simulation Symposium, Houston, 3-5 February.

Sarathi PS, Olsen DK.,1992, Practical Aspects of Steam Injection Processes – A Handbook for Independent Operators. NIPER-580 (DE92001070), IIT Research Institute, Bartlesville.

Sasaki, K., Akibayashi, S., Yazawa, N., Doan, Q. T., and Farouq Ali, S. M., 2001, Experimental Modeling of the SAGD Performancer, SPE 69742.

Savignat, J.M., 2000, Approximation Diffuse Hermite et ses Applications, PhD Dissertation, Mines Paris Tech, Paris.

Scott, G. R., 2002, Comparison of CSS and SAGD Performance in the Clearwater Formation at Cold Lake, SPE/PS-CIM/CHOA 79020, *SPE/PS-CIM/CHOA Int. Thml. Opr. And Heavy Oil Sym. And Int. Horz. Well Tec. Conf.*, Calgary, Canada.

Sedaee, B., Rashidi, F., 2006, Application of the SAGD to an Iranian Carbonate Heavy-Oil Reservoir (SPE-100533). In: SPE Western Regional/AAPG Pacific Section/GSA Cordilleran

Section Joint Meeting, Anchorage, May 8–10.

Settari, A. &Mourits, F.M., 1998, A Coupled Reservoir and Geomechanical Simulation System. SPE J. Vol. 3(3), 219-226.

Shanqiang, L., and Baker, A., 2006, Optimizing horizontal well steam simulation strategy for heavy oil development, SPE 104520, USA.

Shi, J.Q. & Durucan, S. 2009, A coupled reservoir-geomechanical simulation study of CO2 storage in a nearly depleted natural gas reservoir.Energy Procedia, Vol. 1, 3039-3046.

Shin, H. and Polikar, M., 2005, Optimizing the SAGD Process in Three Major Canadian Oil-Sands Area, SPE 95754, *SPE ANN. Tec. Conf. and Exh.*, Dallas, USA.

Shin, H., Polikar, M. 2004.Review of Reservoir Parameters to Optimize SAGD and Fast SAGD Operating Conditions. CIM 2004-221 (presented at the 2004 CIM Annual Meeting, Calgary, 8-10 June).

Singhal, A K., Ito, Y., and Kasraie, M., 1998, Screening and Design Criteria for Steam Assisted Gravity draining (SAGD) Projects' , SPE 50410, *SPE Int. Conf. on Horz.l Well Tec.*, Calgary, Canada.

Stalder, J L., 2007, Cross SAGD (XSAGD) – An Accelerated Bitumen Recovery Alternative, SPE 97647.

Total E&P Canada Ltd, 2010, Surface Steam Release of May 18, 2006, Joslyn Creek SAGD Thermal Operation. ERCB Staff Review and Analysis.

Touhidi-Baghini, A., 1998, Absolute Permeability of McMurray Formation Oil Sands at Low Confining Stresses, PhD dissertation, Department of Civil Engineering, University of Alberta, Alberta.

Tran, D., Buchanan, L. & Nghiem, L., 2008, Improved Gridding Technique for CouplingGeomechanics to Reservoir Flow. Proceedings of the Annual Technical Conference and Exhibition, Denver, Colorado, USA, 21-24 September.

Vidal-Gilbert, S., Nauroy, J.F. & Brosse, E., 2009, 3D GeomechanicalModelling for CO2 Geologic Storage in the Dogger Carbonates of the Paris Basin. Int. J. of Greenhouse Gas Control, Vol. 3, 288–299.

Vidal-Gilbert, S. and Tisseau, E., 2006, Sensitivity Analysis of GeomechanicalBehaviour on Time-lapse Seismic Velocity Modelling. Paper SPE 100142 presented at the SPE Europec/EAGE Annual Conference and Exhibition, Vienna, Austria, 12–15 June.

Vidal-Gilbert, S., Assouline, L., 2005, Description générale du calcul couplé Athos-Abaqus construction du modèle géomécanique, Rapport interne IFP, Direction Mécanique Appliquée.

Wang, J., Walters, D., Settari, A., and Wan, R.G., 2006, An Integrated Modular Approach to Modeling Sand Production and Cavity Growth with Emphasis on the Multiphase Flow and 3D Effects. Proc., U.S. Rock mechanics symposium, Golden ROCKS 2006, Colorado, USA, 17-21 june. Paper ARMA/USRMS 06-906.

Wang, Y. and Dusseault, M.B., 2003, A coupled conductive-convective thermo poroelastic solution and implications for wellbore stability, J. Petroleum Science and Engineering 38, pp. 187–198.

Yang, G. and Butler, R. M., 1992, Effects of reservoir heterogeneities on heavy oil recovery by steam-assisted gravity drainage.

Yee, C.T. and Stroich,A., 2004, Flue Gas Injection into a Mature SAGD Steam Chamber at the Dover Project (Formerly UTF) , Journal of Canadian petroleum Technology, Vol.43, No.1.

Yin, S., Rothenburg, R. and Dusseault, M.B., 2008, Analyzing Production-Induced Subsidence using Coupled Displacement Discontinuity and Finite Element Methods, Computer Methods in Engineering Sci., 469(1), pp. 1–10.

Zaitoun A, Tabary R, Fossey JP, Boyle T., 1998., Implementing a Heavy-Oil Horizontal-Well Polymer Flood in Western Canada. (presented at the 7th UNITAR International Conference on Heavy Crudes and Tar Sands, Beijing, 27-30 Oct.).

Zandi, S., Renard, G., Nauroy, J.F., Guy, N. & Tijani, M., 2010, Numerical Modelling of Geomechanical Effects during Steam Injection in SAGD Heavy Oil Recovery.Proceedings of the EOR Conference at Oil & Gas West Asia, Muscat, Oman, 11-13 April.

Zandi, S., Renard, G., Nauroy, J.F., Guy, N. & Tijani, M., 2010, Numerical Coupling of Geomechanics and Fluid Flow during Steam Injection in SAGD.Proceedings of the Improved Oil Recovery Symposium, Tulsa, USA, 24-28 April.

Zandi, S., Guy, N., Ferrer, G., Renard, G. & Nauroy, J.F., 2010, Coupled Geomechanics and Reservoir Modelling in SAGD Recovery. Proceedings of the 12th European Conference on Mathematics of Oil Recovery, Oxford, UK, 6–9 September.

Zhang, W., Youn, S., and Doan, Q., 2005, Understanding Reservoir Architectures and Steam Chamber Growth at Christina Lake, Alberta, By using 4D Seismic and Crosswell Seismic Imaging' , SPE/PS-CIM/CHOA 97808, PS2005-373, Heavy Oil Sym., Calgary, Canada.

APPENDIX

SPE 129250

Numerical modelling of geomechanical effects during steam injection in SAGD heavy oil recovery

S. Zandi, SPE, IFP; G. Renard, SPE; J.F. Nauroy, SPE; N. Guy; M. Tijani, ENSMP

This paper was prepared for presentation at the SPE EOR Conference at Oil & Gas West Asia held in Muscat, Oman, 11–13 April 2010.

Abstract

Steam Assisted Gravity Drainage (SAGD) is a thermal process that has found wide application in high permeability heavy oil or bitumen reservoirs, mainly in the Western part of Canada.

In this process, steam injection continuously modifies reservoir pore pressure and temperature, which can change the effective stress in the reservoir, resulting in a complex interaction of geomechanical effects and multiphase flow in the cohesionless porous media. Quantification of the state of deformation and stress in the reservoir is therefore essential for the correct prediction of reservoir productivity but also for the interpretation of 4D seismics used to follow the development of the steam chamber. On another side, this quantification is crucial for the evaluation of surface uplift, risk of loss of seal integrity, hydro fracturing and well failure. Simultaneous study and analysis of interrelated geomechanics and fluid flow in the reservoir are thus crucial for the management of the process at different stages.

The objective of this paper is to show the importance of taking into account the role of geomechanics in the numerical modelling of SAGD and to provide a better description of the rock contribution to fluid flow in this process. A geomechanics-reservoir partially coupled approach is presented that allows to iteratively take the impact of geomechanics into account in the fluid flow calculations and therefore performs a better prediction of the process. The proposed approach is illustrated on a realistic field case.

Introduction

SAGD is now a well established process for the recovery of heavy oil and bitumen in sufficiently permeable porous media (Huc et al., 2010). Its prediction performance by numerical simulation is essential since it is an integral component in the design and management of this process at field scale. A conventional reservoir modelling approach is generally used (Egermann et al., 2001; Ito and Chen, 2009). However, this approach while computing multiphase flow in porous media is not conceived to adequately take into account and modelize the ongoing coupled fluid-solid interactions during injection-production because of using a simplified formulation for porosity and a static absolute permeability during simulations. Unfortunately, this assumption is not valid for unconsolidated oil sand materials, because of their high sensitivity on pore pressure and temperature variations (Chalaturnyk, 1996; Lerat et al., 2009a).

In the SAGD process, continuous steam injection changes reservoir pore pressure and temperature, which can increase or decrease the effective stress in the reservoir. Indeed, oil sand material strains induce changes in the fluid flow-related reservoir parameters. This is obviously a coupled problem. Therefore, coupled reservoir geomechanical simulations are required. This is particularly important for the correct interpretation of 4D seismic to quantify the steam chamber growth since the seismic wave velocity depends on both temperature, pressure and saturations, but also on the vertical deformation of the reservoir and overburden.

Theoretical and practical difficulties have prevented coupled geomechanical models from being used routinely in oil and gas reservoir simulation studies. Some of the faced challenges are the complex mechanical behaviour of geomaterials, the strong coupling between the mechanical and fluid flow problems, and the fact that the reservoir models become very computationally intensive. As a result, the modelling of coupled flow and geomechanics is relatively new to the oil industry.

Coupling Approach

A SAGD process induces a modification of the effective stress in the underground. Effective stress changes are possible in such process because the injected steam changes reservoir pore pressure and temperature. Geomechanical effects related to the modification of the effective stress have been the object of numerous studies. For example, it has been shown that in the SAGD process, geomechanical effects can influence production rates (Ito and Suzuki, 1999; Collins et al., 2002; Lerat et al., 2009b) or seismic analysis results (Vidal-Gilbert and Tisseau, 2006; Lerat et al., 2009a). In order to describe the SAGD process considering geomechanics, several numerical methods have been investigated (Chalaturnyk, 1996; Settari and Mourits, 1998; Rutqvist et al., 2001; Longuemare et al., 2002; Samier et al., 2003; Jeannin et al., 2005; Wang et al., 2006; Rutqvist et al., 2002; Vidal et al., 2009). These methods are associated to different theoretical frameworks that are based on different sets of simplifying hypothesis (Zandi et al., 2010). Therefore, the existing coupling methods cover a wide range of problematics and can involve various computational costs. Four kinds of methods can be distinguished: the non-coupled, the one-way, the sequentially coupled and the fully coupled methods.

The computationally low cost approach is to consider a conventional reservoir model that takes into account thermal effects. In this approach, commonly named non-coupled, the mechanical equilibrium is not solved. The non-coupled approach does not take into account geomechanical effects in the reservoir. This approach only relates porosity to pressure to describe pore compressibility. Therefore, it does not seem to be an adequate approach to study geomechanics influence on a SAGD enhanced recovery.

The one-way solution considers the mechanical equilibrium by transferring the reservoir simulator results to a geomechanical simulator. This approach allows a calculation of the stress in the reservoir and surrounding rocks. Nevertheless, when this solution is considered, the fluid flow remains unaffected by geomechanical effects. The one-way approach still can be an efficient tool to predict if and where geomechanical effects can appear.

In the sequentially coupled approach, the stress and flow equations are solved separately for each time step but information is passed between the reservoir and geomechanical simulators. Two different kinds of sequentially coupled solution can be distinguished. The explicit solution represents a lower computational cost and can be efficient if an elastic mechanical behavior is considered. The iterative solution represents an important computational cost. This coupling method is adequate to describe non-linear mechanical behaviour because the iterative procedure relies on a convergence criterion considering the whole problem.

The fully coupled approach simultaneously solves the whole set of equations that govern the thermohydromechanical problem. It yields to consistent descriptions, but the hydraulic or geomechanical mechanisms are often simplified by comparison with conventional uncoupled reservoir and geomechanical approaches. Furthermore, the numerical cost of solving totally coupled problems can be important.

In this paper, a SAGD process is modelised and an elastic mechanical behavior is considered for rocks. Therefore, a sequentially and explicitly coupled approach is chosen (Zandi et al., 2010). The sequentially coupled approach is based on an external coupling between conventional reservoir and geomechanical simulators. For that purpose, PumaFlow that is a finite volume reservoir simulator, developed by IFP, is coupled with ABAQUS, the finite element geomechanical simulator developed by SIMULIA. The stress and flow equations are solved separately for each time step but information is transferred between the reservoir and geomechanical simulators. The fluid flow simulator is executed over the first time step of the calculation. Then, as shown in Fig. 1, the pressure and temperature fields are transferred to the geomechanical simulator to evaluate the displacements and stress state. The volumetric strain, depending on displacement is extracted from the geomechanical simulation results.

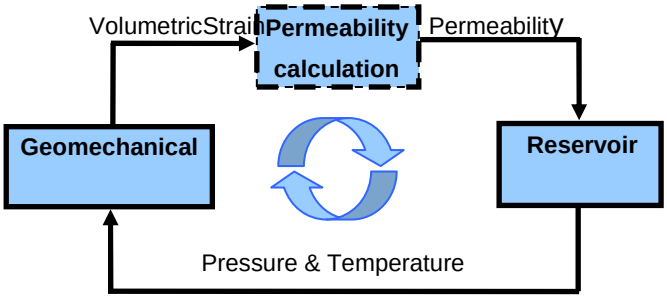

Fig.1: Schematic of the data transfer procedure

The volumetric strain is then transferred to a routine that calculates the permeability and that is based on a relation deduced by Touhidi-Baghini (1998) from laboratory results. The used relationship reads,

$$\ln\frac{k_1}{k_2} = \frac{c}{\phi_0}\varepsilon_v \qquad (1)$$

where k_0 is the initial absolute permeability, k_1 is the absolute permeability, ϕ_0 is the initial porosity, ε_v is the volumetric strainand c is a constant. It must be noted that, according to Touhidi-Baghini, the values c = 5 and c = 2 appear to be appropriate to respectively match with vertical and horizontal permeability evolutions for oil sands. Once the permeability has been calculated, it is introduced in the reservoir simulator data to perform another step of coupling. This loop is repeated for every defined time step until the end of the simulation.

To perform the coupling loop automatically, Fortran and Python based routines have been developed. These routines are able to both tranfer the fields from finite volume discretization to finite element discretization and update the permeability values in the reservoir simulator.

To perform pertinent and numerically efficient calculations with the presented tool, chosing the number of coupling time step is a crucial issue. In the next section, the sensitivity to the number of time steps is studied for a realistic case of SAGD application.

Case Description

The case is based on the implementation of the SAGD process in a heavy oil reservoir located in Saskatchewan, Canada (Chakrabarty et al., 1998). The reservoir is assumed homogeneous without bottom aquifer. As indicated in Fig. 2, the top of the reservoir is 730 meters deep, the initial pressure and temperature being equal to 5.2 MPa and 27°C respectively.

Geomechanical model

In the geomechanical model, the simulated domain is rectangular and its dimensions in X, Y and Z directions are 147 meters, 500 meters and 800 meters respectively (Fig. 2). This model includes the reservoir surrounded below by underburden layers and above by overburden layers (Fig. 3). Sideburdens rocks are not represented due to the symmetry assumed to the presence of other well pairs located on each side of the domain (multiple well pair SAGD). The size of grid blocks in the three directions is indicated in Table 1. As the vertical distance between the two horizontal wells was supposed to be constant, only one cell 500 meters long is used to describe the well length in the Y direction.

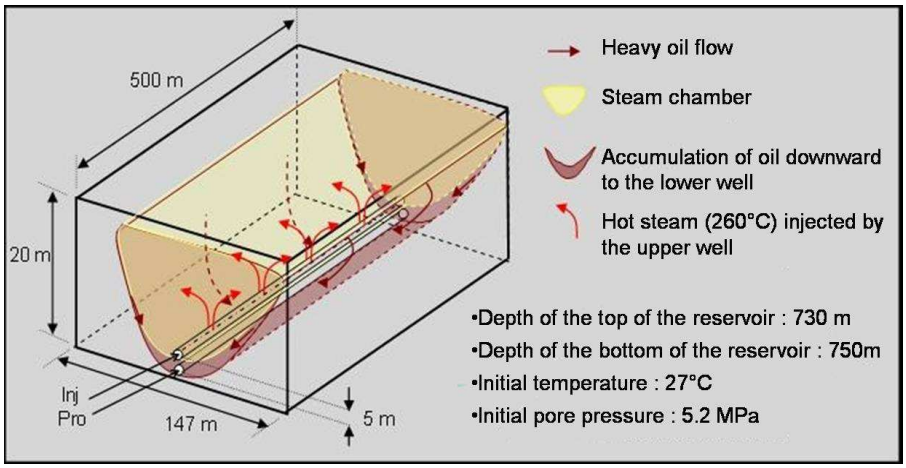

Fig.2: Reservoir dimensions

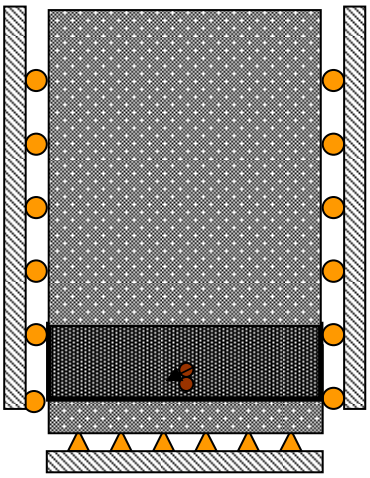

Fig.3: Applied boundary conditions

Zone	Direction	Grid Block Number	Discretization (m)
Overburden	X	65	18(3.) 5(2.) 19(1.) 5(2.) 18(3.)
	Y	1	500
	Z	5	1(300.) 1(220.) 1(150.) 1(50.) 1(10.)
Reservoir	X	65	18(3.) 5(2.) 19(1.) 5(2.) 18(3.)
	Y	1	500
	Z	40	0.5
Underburden	X	65	18(3.) 5(2.) 19(1.) 5(2.) 18(3.)
	Y	1	500
	Z	1	10

Table 1: Number of grid blocks and size for the various domains

Boundary conditions in the geomechanical simulator are shown in Fig. 3. Bottom edge of underburden is fixed. There is no displacement for the lateral sides in x and y directions. Top edge of overburden is free.

The material constitutive law (elasticity) and properties are related to the rock types present in the geomechanical domain. One

mechanical rock type was assigned per zone in the overburden, underburden and reservoir. Field data was used to assign thermo-hydro-mechanical properties to each mechanical rock type. The rock properties are given in Table 2.

Properties	Reservoir	Overburden	Underburden
Density (kg/m^{-3})	2320	2420	2700
Young's modulus (10^{8} Pa)	3.43	2.500	10.000
Poisson's coefficient		0.3	
Biot's Coefficient		1	
Thermal expansion (℃ $^{-1}$)		2 10^{-5}	

Table 2: Thermo-poro-mechanical properties

Reservoir Fluid Flow Model

The domain considered to simulate the SAGD process is a rectangular reservoir, with the dimension of 147 by 500 by 20 meters (Fig. 2). The well pair is located along the Y axis and in the middle of the X axis. The distance between the two wells is 5 meters. The producer is 2 meters above the base of the reservoir. The size of grid blocks in the x and z directions is identical to the size of grid blocks in the geomechanical model, indicated in Table 1.

The surrounding rocks are not modelised in the reservoir simulator, the lateral boundaries of the reservoir are considered with no thermal nor fluid flow. For the lateral boundaries, this hypothesis is made to represent the assumed symmetry. For the upper and lower boundaries, this hypothesis is related to the imperviousness of the the rocks that are located at the top and bottom of the reservoir. Main physical properties of rock and fluids used in the reservoir fluid flow model are summarized in Table 3.

Properties	Value
Oil Density (g.cm^{-3})	0.97
Oil viscosity at reservoir conditions (mPa.s)	5000
Oil viscosity at 282℃ (mPa.s)	1.8
Porosity	0.35
Horizontal permeability (mD)	2000
Vertical permeability (mD)	1000
Rock compressibility (bar^{-1})	3 10^{-4}
Oil compressibility (bar^{-1})	2.17 10^{-4}
Rock heat capacity (J.cm^{-3}.℃ $^{-1}$)	2.34
Rock thermal conductivity (W. m^{-1}.℃ $^{-1}$)	2.70
Oil thermal expansion coefficient (℃ $^{-1}$)	2 10^{-4}
Initial oil saturation	0.85
Irreducible water saturation	0.15
Residual oil saturation to waterflood	0.20
Residual oil saturation to steamflood	0.10

Table 3: Reservoir rock and fluid properties

The thermo-hydro-mechanical behaviour of the reservoir is analyzed over a 2000-days production period. A pre-heating period of 150 days is first modelized. It simulates steam circulation in the two wells of the SAGD pair to allow a hydraulic communication and flow of fluids between the two wells that is not possible till the viscosity of oil in place is not decreased enough. Then steam is constantly injected in the upper well so oil and condensed water are produced in the lower well. At the injection well, a steam flow rate is fixed at 260 m^3/day (Cold Water Equivalent) from 150 to 250 days, then it is fixed at 400 m^3/day to 2000 days, end of the injection/production history. At the same time, a maximum injection pressure of 8 MPa is set for the injection well to avoid a too high pressure in the reservoir. At the production well, a minimum pressure of 1.5 MPa is fixed together with a maximum production flow rate of 560 m^3/day of total liquid (oil plus condensed water).

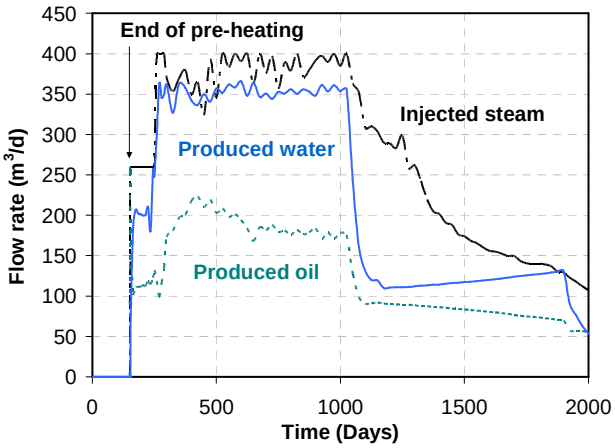

Fig.4: Typical evolution of injected steam rate and produced oil and water rate

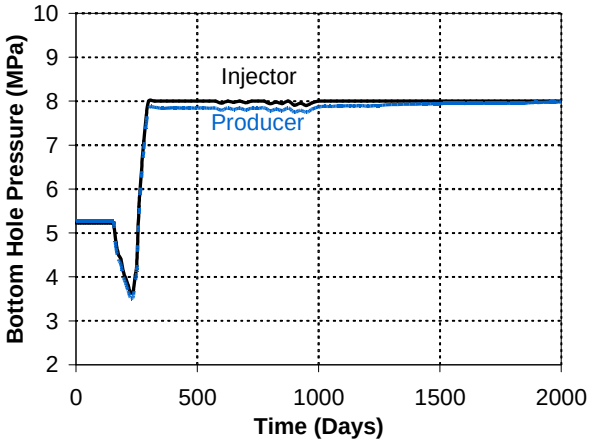

Fig.5: Typical evolution of BHP in injector and producer

A particular feature of SAGD is the short distance between the injection and production wells with the constant risk of steam breakthrough in the production well if a too high injection rate or production rate, or both, are set in the wells. To avoid such a condition, a special monitoring of the steam chamber has been implemented in the reservoir simulator (Egermann et al., 2001). The result of this monitoring is clearly illustrated in Fig. 4 and Fig. 5 that show the typical evolution of flow rates and bottom hole pressure (BHP) in the two wells. The initial steam rate imposed in the injection well between 150 and 250 days is well respected, as it is during a short period after 250 days when it is increased to 400 m3/day. However, quite rapidly the steam front moves too closer to the production well and the injection flow rate has to be decreased to prevent steam breakthrough, then increased again when the steam front moves away from the production well. The monitoring of the well pair to prevent steam breakthrough at the production well results therefore in variations in the steam flow rate in the injection rate during quite a long period that lasts until about 1000 days. At that time, the injection rate continuously decreases because the steam front has reached the lateral limit of the domain. Less steam can be injected and less fluid can be produced.

Fluid Flow and Geomechanical Coupling Simulation Results

To determine the geomechanical influence of steam injection on pressure and temperature variations in the reservoir and on overall permeability variation, the geomechanical behaviour of the reservoir have been studied in three different grid cells which represent three different zones in the reservoir. Fig. 6 shows the placement of these cells (A, B and C) located at the same elevation in the grid. Grid cell A is placed just in the middle of the reservoir and 5.5 meters above the horizontal well pair. Grid cells B and C are chosen farther from the wells, with the distance of 18.5 and 60 meters from the grid cell A, respectively.

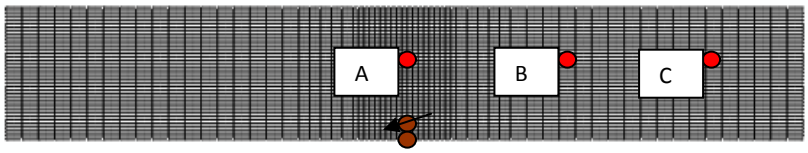

Fig 6: Reservoir modeled in reservoir simulator, location of the grid cells A, B, C and well-pair in reservoir

Comparison of 5-step and 12-step explicit coupling

In order to investigate the influence of the number of coupling periods, a sensitivity analysis has been performed. In this paper, the results for two cases are compared. First coupled simulation is done in 5 coupling steps and the second simulation is realized in 12 coupling steps.

During each coupling period, variations in pore pressure, temperature, strains and stresses were computed. The updated reservoir cell permeabilities are determined using the permeability-strain model which was defined in Eq. 1. The updated permeability was integrated in the simulation of the next period.

In 5-step explicit coupling, a first mechanical computation step (initialization) was performed to reach a mechanical equilibrium between the applied boundary conditions (regional stresses) and the initial state of stress in the reservoir. The simulation was then performed using four coupling steps at 150, 300, 1000 and 2000 days (end of production history).

In 12-step explicit coupling, a first mechanical computation step (initialization) was also performed in order to reach a mechanical equilibrium between the applied boundary conditions (regional stresses) and the initial state of stress in the reservoir. The simulation was then performed using eleven coupling steps, at 150, 200, 300, 400, 500, 600, 800, 1000, 1200, 1500 and 2000 days.

Steam injection increases the pore pressure, dilates the rock squeleton and the pore fluid and modifies the in situ stresses in a complex set of interaction. Main results during the 5-steps coupling are shown on Figs. 7 to 12 which give maps and curves of the state of some important parameters. For the maps presented in Figs. 7, 8 and 9, the geometry is deformed according to calculated displacements with an amplification factor of 100.

Fig. 7 shows that the temperature first increases above the injection well to the top of the reservoir and then extends laterally to become uniform in the upper part of the reservoir. This uniformity is related to lateral boundary conditions that were imposed on the model

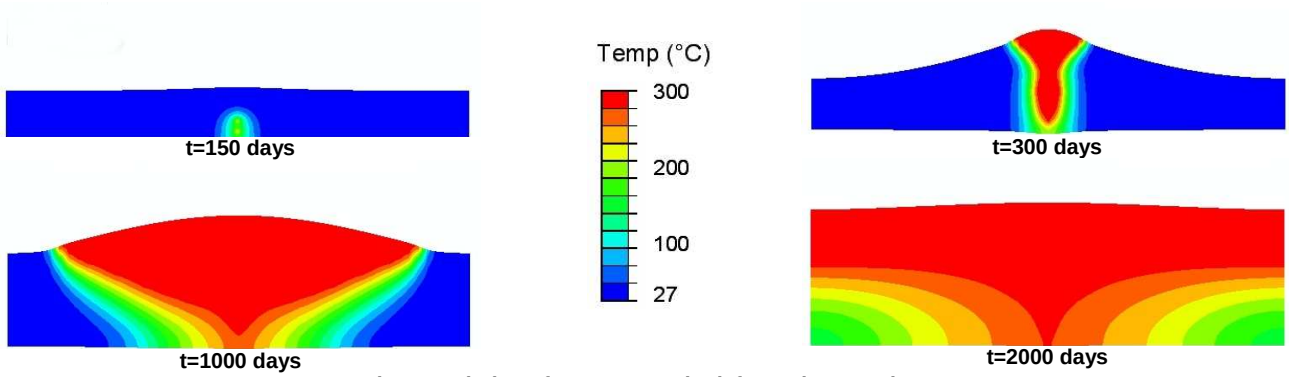

Fig.7: Evolution of temperature in deformed reservoir

Figs. 8 and 9 show the evolution of the mean effective stress p' and the deviatoric stress q which are defined by,

$$p' = \frac{\sigma_v + \sigma_h + \sigma_H}{3} - p_p \qquad (2)$$

and

$$q = \sqrt{\frac{(\sigma_v - \sigma_h)^2 + (\sigma_h - \sigma_H)^2 + (\sigma_v - \sigma_H)^2}{2}} \qquad (3)$$

where σ_v is the vertical stress, σ_h the minimum horizontal stress, $\sigma_H$the maximum horizontal stress and p_p the pore pressure, assuming that σ_v, $\sigma_h$and σ_H are the principal stresses. It must be noticed that the sign convention of soil mechanics is considered here.

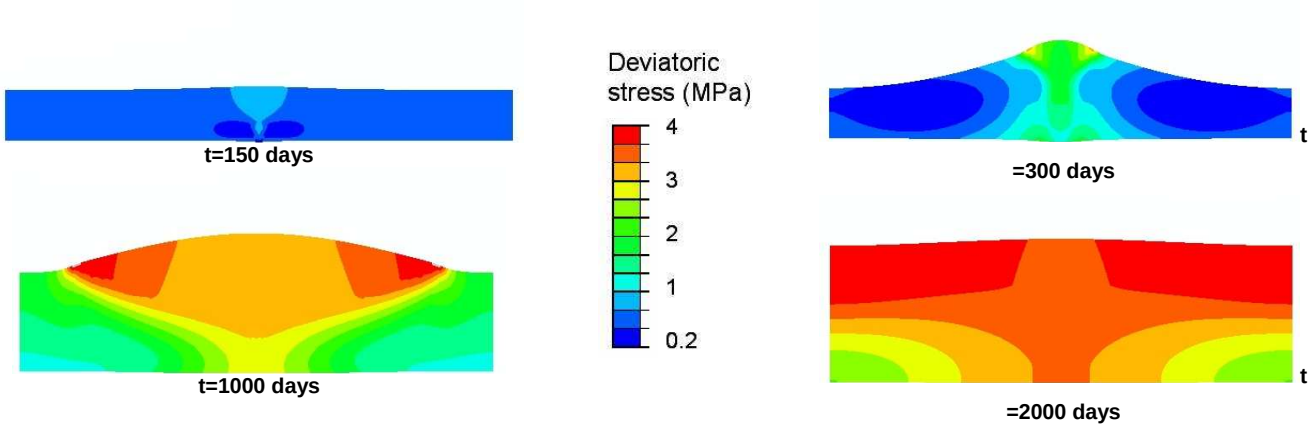

Fig.8: Evolution of deviatoric stress in deformed reservoir

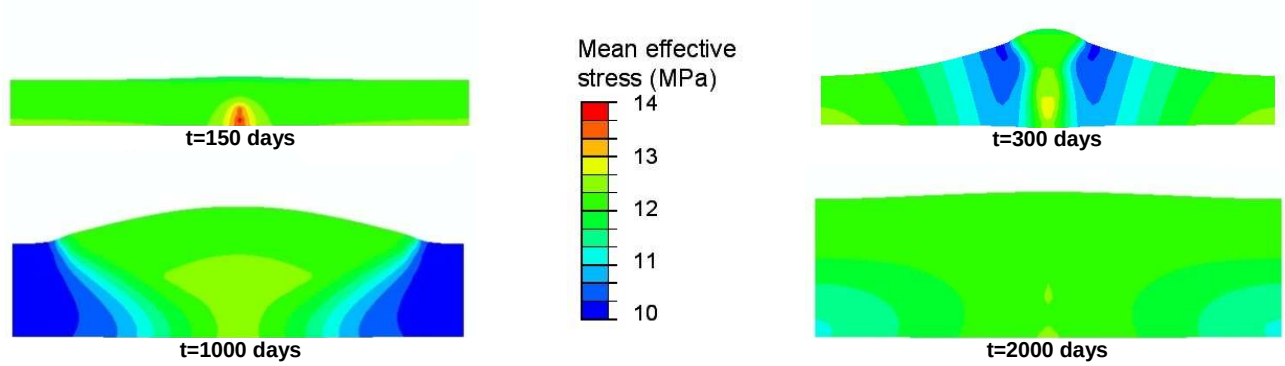

Fig.9:Evolution of effective mean stress in deformed reservoir

The mean effective stress (Fig. 9) is sensitive to pore pressure while the deviatoric stress (Fig. 8) indicates the existence of shear stress in the reservoir. We note that the mean effective stress remains quasi unchanged when the deviatoric stress increases almost everywhere. This aspect is illustrated in Figs. 10 and 11, which show the stress state at points A, B and C in a *p'-q* diagram. The stress paths are globally vertical. Coupling with 12 steps clearly reveals a better identification of stress paths than with 5 steps coupling but the trend is quite the same.

An increase only in pore pressure would result in equal reduction in all effective principal stresses. In the *p'-q* diagram the stress path would be horizontal because deviatoric stress would be unchanged.

An only thermal expansion of the reservoir would lead in an increase of both the deviatoric stress and mean effective stress. These stress increases are essentially due to an increase in horizontal stresses.

The combination of the antagonist pore pressure increase and thermal expansion can explain the vertical stress paths observed in the model.

The fact that the final stress state is almost the same for various points is also related to lateral boundary conditions that were imposed on the model. Anisotropic initial stresses conditions certainly would change the development of stress paths, but the trend of increasing shear stress with the growth of the steam chamber would be certainly verified.

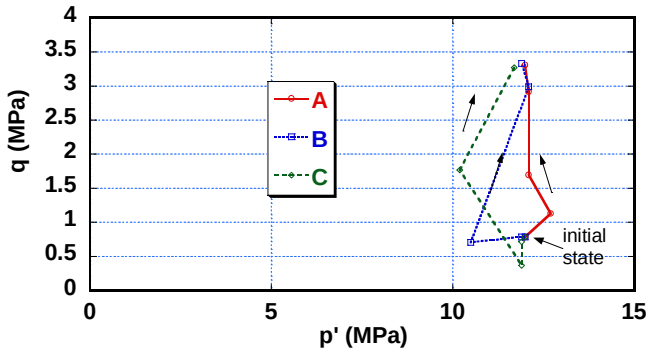

Fig.10: Stress path in cells A, B and C (5 step coupling)

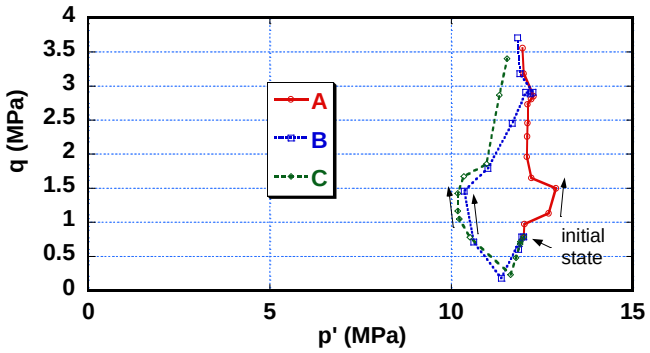

Fig.11: Stress path in cells A, B and C (12-step coupling)

Fig. 12 shows the evolution of the volumetric strain. It is very similar to the evolution of temperature (Fig. 7), fast at the start of steam injection in a vertical direction above the well pair and then slower in the periphery as the steam chamber reaches the top of the reservoir.

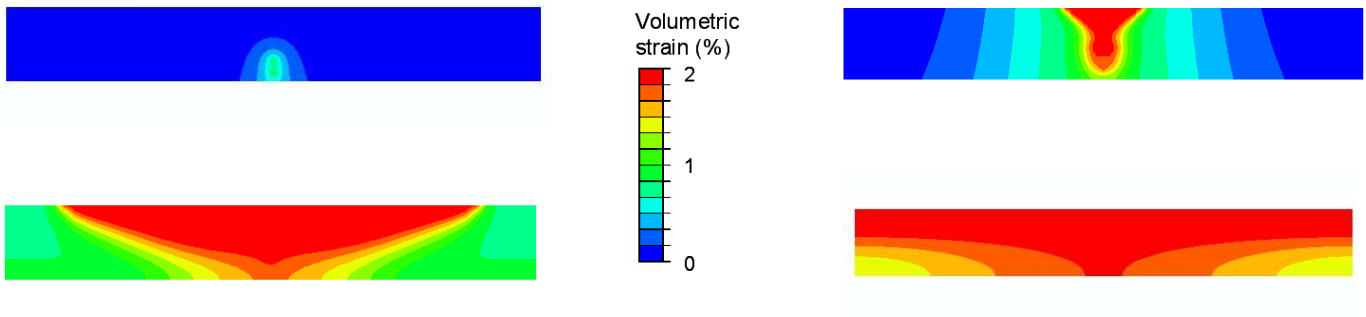

Fig.12: Evolution of volumetric strain in non-deformed reservoir

As it can be seen in Figs. 13 and 14 that show the porosity and temperature variations in cells A, B and C versus time, the porosity increase corresponds exactly to the passage of the temperature front through the location of each cell, between 150 and 300 days for cell A, between 400 and 700 days for cell B and between 1000 and 1700 days for cell C. After the passage of the steam front the porosity remains constant.

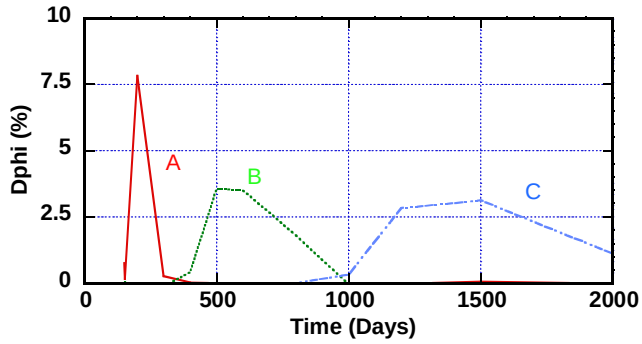

Fig.13: Porosity evolution in cells A, B and C (12-step coupling)

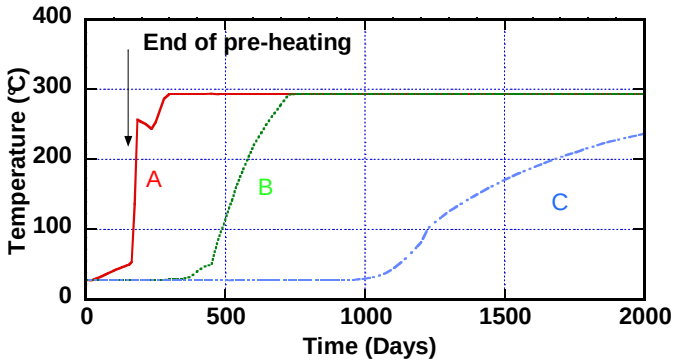

Fig.14: Temperature in cells A , B and C (12-step coupling)

The evolution of permeability in cells A, B and C is linked to the evolution of their porosity (Figs. 15 and 16). The increase of 30% is very fast close to the wells and is slower far away. A greater number of steps allows a better precision of the curves as seen on Fig. 16. Permeability in cell B increases by 30% after 1000 days for a 5 step coupling and only around 600 days for a 12-step coupling.

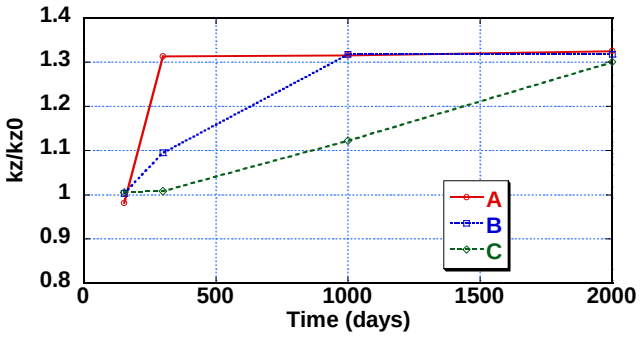

Fig.15: Permeability evolution in cells A,B and C (5-step explicit coupling)

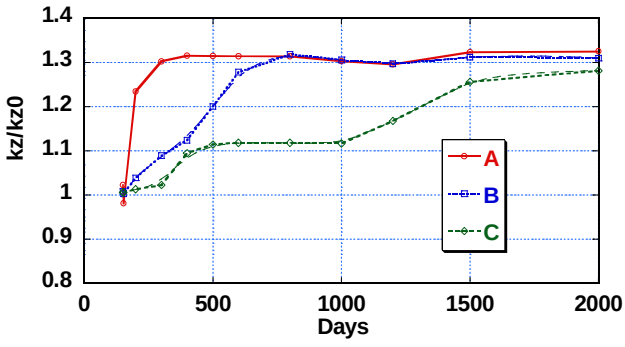

Fig.16: Permeability evolution in cells A, B and C (12-step explicit coupling)

Fig. 17 shows the vertical displacement profile of the top of the reservoir plotted at the end of each step of the 5-step coupling. As can be noticed, the uplift is very fast just above the wells, then the uplift extends to the periphery when the steam chamber grows. It becomes almost homogeneous at the end of the 2000-days simulation. Once again, the lateral boundary

conditions play an important role on this shape. The number of steps does not appear as a determining factor for the overall vertical displacement of the top of the reservoir (Fig. 18).

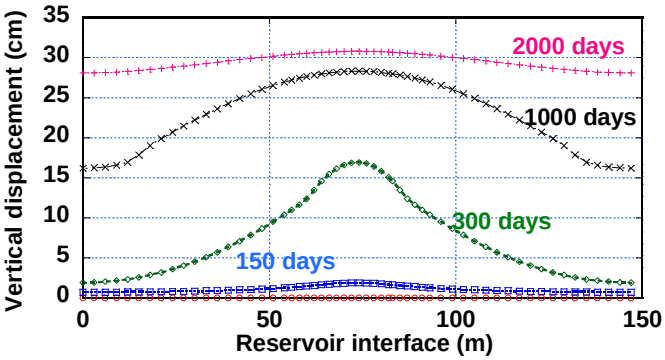

Fig.17: Vertical displacement profile of reservoir interface, during 2000 days (5-step explicit coupling)

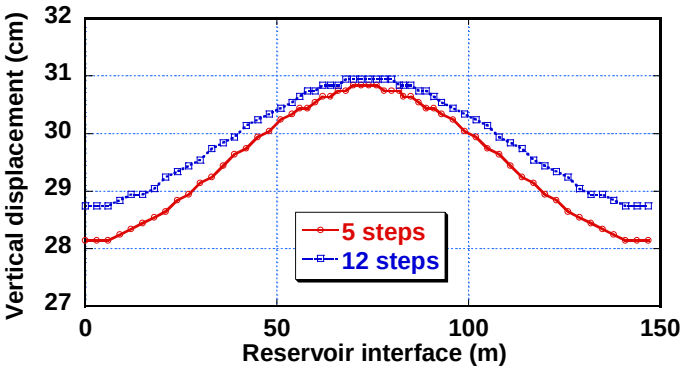

Fig.18: Vertical displacement profile of reservoir interface, at 2000th day

Conclusion

Modeling of geomechanical effects during the operation of the SAGD process is required for several reasons, mainly to ensure that injection steam pressure and temperature increases do not affect the stability of the reservoir and caprocks and also help to interpret repeated 4D seismic surveys. This demands understanding the evolution of the mechanical behaviour of the reservoir-caprock system, through reservoir fluid flow-geomechanical coupled simulations.

In this paper, an explicit reservoir-geomechanics coupling approach is presented. Results acquired at selected time steps are transferred from one simulator to the other through a coupling module.

The proposed approach has been applied on data taken from a Canadian heavy oil field. Two different numbers of time steps for the coupling, 5 and 12, have been tested and compared. They show that there is a strong variation of permeability in the reservoir reached by the steam chamber accompanied by a considerable deformation of the volume affected by the injected steam. These variations must be taken into account both for the performance prediction of SAGD but also for the interpretation of repeated 4D seismic surveys. The comparison with different numbers of time steps for the coupling indicates also that the coupling is more important in the early period of steam chamber growth since steam strongly affects the area close to the well pair from the start of injection.

Compared to a fully coupled approach, explicit coupling is easier to apply and gives comparable results. Depending on the geomechanical simulator used, problems related to large computer memory requirements and huge CPU computation time can exist. Our effort now is to work on the reduction of CPU time by using distinct grids for the fluid flow simulator and geomechanical simulator, and to apply the proposed approach to heterogeneous media in which the coupling is likely to be more necessary.

Acknowledgements

The authors wish to thank Guillaume Servant (now at EDF) who initiated this work. They would also like to acknowledge Elisabeth Bemer, Florence Adjemian, Axelle Baroni and Gilles Ferrer from IFP for their help and useful discussions.

Nomenclature

c_p	Pore compressibility factor
k_0	Initial absolute permeability
k_1	Absolute permeability
ε_v	Volumetric strain
ϕ_0	Initial porosity
ϕ	Porosity
p'	Mean effective stress
p_0	Initial pore pressure
p_p	Pore pressure
q	Deviatoric stress
σ_h	Minimum horizontal stress
σ_H	Maximum horizontal stress
σ_v	Vertical stress

References

Chakrabarty, C., Renard, G., Fossey, J.-P., and Gadelle, C. 1998. SAGD Process in the East Senlac Field: From Reservoir Characterization to Field Application. Paper 132 presented at the 1998 UNITAR Conference, Beijing, China, 27-31 October

Chalaturnyk, R. J. 1996. Geomechanics of SAGD in Heavy Oil Reservoirs. PhD dissertation, Department of Civil Engineering, University of Alberta, Alberta.

Collins, P.M., Carlson, M.R., Walters, D.A., and Settari, A. 2002. Geomechanical and Thermal Reservoir Simulation Demonstrates SAGD Enhancement Due to Shear Dilation. Paper SPE 78237 presented at the SPE/ISRM Rock Mechanics Conference, Irving, Texas, 20-23 October.

Egermann, P., Renard, G., and Delamaide E. 2001. SAGD Performance Optimization Through Numerical Simulations: Methodology and Field Case Example.,Paper SPE 69690 presented at the SPE ITOHOS Symposium, Porlamar, Margarita Island, Venezuela, 12-14 March.

Huc, A. 2010. Heavy Crude Oils: from Geology to Upgrading - An Overview. Technip Editions, Paris. In press.

Ito, Y. and Chen, J. 2009. Numerical History Match of the Burnt Lake SAGD Process. Paper CIM 2009-004 presented at the Canadian International Petroleum Conference (CIPC) 2009, Calgary, Alberta, 16-18 June 2009.

Ito, Y. and Suzuki, S. 1996. Numerical Simulation of the SAGD Process in the Hangingstone Oil Sands Reservoir. Proc., 47th ATM of the Petroleum Society of CIM, Calgary, Alberta, June 10-12.

Jeannin, L., Mainguy, M., and Masson, R. 2005. Comparison of Coupling Algorithms for Geomechanical-Reservoirs Simulations. Proc., U.S. Rock mechanics symposium, Alaska ROCKS 2005, Anchorage, USA, 25-29 june. Paper ARMA/USRMS 05-677.

Lerat, O., Adjemian, F., Auvinet, A., Baroni, A., Bemer, E., Eschard, R., Etienne, G. et al. 2009. Modelling of 4D Seismic Data for the Monitoring of the Steam Chamber Growth During SAGD Process. Proc., Canadian International Petroleum Conference 2009, Calgary, Alberta, Canada, 16-18 June, Paper 2009-095.

Lerat, O., Adjemian, F., Auvinet, A., Baroni, A., Bemer, E., Eschard, R., Etienne, G. et al. 2009. 4D Seismic Modelling Applied to SAGD Process Monitoring. Proc., 15th European Symposium on Improved Oil Recovery, Paris, France, 27-29 April, Paper B14.

Longuemare, P., Mainguy, M., Lemonnier, P., Onaisi, A., Gérard, Ch., and Koutsabeloulis, N. 2002. Geomechanics in Reservoir Simulation: Overview of Coupling Methods and Field Case Study. Oil & Gas Science and Technology 57(5): 471-483 .

Rutqvist, J., Borgesson, L., Chijimatsu, M., Kobayashi, A., Jing, L., Nguyen, T.S., Noorishad, J., and Tsang, C.-F. 2001. Thermohydromechanics of Partially Saturated Geological Media: Governing Equations and Formulation of Four Finite Element Models. Int J Rock Mec Min Sci 38(1): 105-127.

Samier, P., Onaisi, A., and Fontaine, G. 2003. Coupled Analysis of Geomechanics and Fluid Flow in Reservoir Simulation. Paper SPE 79698 presented at the Reservoir simulation Symposium, Houston, 3-5 February.

Settari, A. and Mourits, F.M. 1998. A Coupled Reservoir and Geomechanical Simulation System. SPE J 3(3): 219-226. SPE-50939-PA.

Touhidi-Baghini, A. 1998. Absolute Permeability of McMurray Formation Oil Sands at Low Confining Stresses. PhD dissertation, Departement of Civil Engineering, University of Alberta, Alberta.

Vidal-Gilbert, S., Nauroy, J.-F., and Brosse, E. 2009. 3D Geomechanical Modelling for CO2 Geologic Storage in the Dogger Carbonates of the ParisBasin. Int J of Greenhouse Gas Control 3: 288–299.

Vidal-Gilbert, S. and Tisseau, E. 2006. Sensitivity Analysis of Geomechanical Behaviour on Time-lapse Seismic Velocity Modelling. Paper SPE 100142 presented at the SPE Europec/EAGE Annual Conference and Exhibition, Vienna, Austria, 12–15 June.

Wang, J., Walters, D., Settari, A., and Wan, R.G. 2006. An Integrated Modular Approach to Modeling Sand Production and Cavity Growth with Emphasis on the Multiphase Flow and 3D Effects. Proc., U.S. Rock mechanics symposium, Golden ROCKS 2006, Colorado, USA, 17-21 june. Paper ARMA/USRMS 06-906.

Zandi, S., Renard, G., Nauroy, J.-F., Guy, N., and Tijani, M. 2010. Numerical Coupling of Geomechanics and Fluid Flow During Steam Injection in SAGD. Paper SPE 129739 presented at the Imroved Oil Recovery Symposium, Tulsa, USA, 24-28 April.

SPE 129739

Numerical Coupling of Geomechanics and Fluid Flow during Steam Injection in SAGD

S. Zandi, SPE, IFP; G. Renard, SPE; J.F. Nauroy, SPE; N. Guy; M.Tijani, ENSMP

This paper was prepared for presentation at the 2010 SPE Improved Oil Recovery Symposium held in Tulsa, Oklahoma, USA, 24–28 April 2010.

Abstract

The Steam Assisted Gravity Drainage (SAGD) process is a thermal enhanced oil recovery (EOR) method that appears tremendously successful, especially for bitumen.

SAGD process results in a complex interaction of geomechanics and multiphase flow in cohesionless porous media. In this process, continuous steam injection changes reservoir pore pressure and temperature, which can increase or decrease the effective stress in the reservoir. Quantification of the state of deformation and stress in the reservoir is essential for the correct prediction of reservoir productivity, seal integrity, hydro fracturing and well failure. In SAGD process, the analysis of reservoir geomechanics is concerned with the simultaneous study of fluid flow and mechanical response of the reservoir.

The objective of this paper is to show the importance of taking into account the role of geomechanics in SAGD numerical modeling and to provide a better description of the rock contribution to fluid flow in the SAGD process. Therefore, we introduce a geomechanics-reservoir partially coupled approach, which allows a better predictive description of the SAGD process to be performed.

The results of numerical simulations show that the classical treatment of deformation of reservoir through the rock compressibility in the conventional reservoir theory is not a rigorous framework to represent the evolution of high porous rock strains that play a significant role in the performance of SAGD.

Introduction

Steam Assisted Gravity Drainage (SAGD) combined with horizontal well technology is certainly one of the most important concepts developed in reservoir engineering in the last two decades (Huc et al., 2010). Many factors interact during this thermal process such as changes in oil viscosity, fluid saturations, pore pressure and stresses. Another important aspect is that the performance of heavy-oil production by SAGD is affected by reservoir heterogeneities (Lerat et al., 2009a). Numerical modeling is therefore important to both evaluate and optimize a SAGD operation (Egermann et al., 2001; Lacroix et al., 2003). Most significantly, pressure and temperature variations during SAGD induce stress changes in the reservoir and in the surrounding media. These modifications of the stress state may imply deformations which can in turn have an impact on reservoir production (Lerat et al., 2009b).

The objectives of this work are 1/ to emphasize the necessity of solving the coupled fluid flow and geomechanical effects that prevail during steam injection in the SAGD process, 2/ to present the various possible options to cope with this difficult issue of coupling fluid flow and geomechanics, 3/ to describe in more details two of these options with their benefits and drawbacks, and 4/ finally illustrate them on an example.

Why coupling?

In the SAGD process, continuous steam injection changes reservoir pore pressure and temperature, which can increase or decrease the effective stress in the underground. Indeed, oil sand material (skeleton and pores) strains induce changes in the fluid flow-related reservoir parameters. To take into account the geomechanical effects due to stress changes in and around the reservoir, fluid flow must be solved in a way that can predict the evolution of stress dependant parameters such as porosity, pore compressibility and permeability. In a SAGD operation, several geomechanical effects are considered as being of

significative influence. For example, laboratory tests have revealed that permeability can be strongly increased by shear stress modification (Touhidi-Baghini, 1998). This geomechanical phenomenon has been investigated through numerical simulations in numerous studies (Ito and Suzuki, 1999; Collins et al., 2002; Lerat et al., 2009b). Another example of geomechanical effect, concerning the seismic behaviour of the underground, has been given by Vidal-Gilbert and Tisseau (2006). They have shown that seismic behaviour of the underground is influenced by stress redistribution mechanisms like arching effect. The overburden stress state has appeared to be a first order parameter to consider in a seismic analysis. Thus, it is important to take into account mechanically induced volumetric strain modification and stress redistribution in the reservoir and surrounding rocks in order to perform 4D seismic analyses that are a very useful tool for SAGD monitoring (Lerat et al., 2009a). In order to represent more precisely the importance of the coupled simulation for a SAGD numerical analysis, a thermo-hydro-mechanical model is formulated on the basis of Biot's theory (Biot,1941).

Constitutive equations in linear poroelasticity

Darcy's law describes the motion of the fluid in porous rocks, whereas in the present study, the mechanical behavior of rock is governed by the equations of linear and isotropic elasticity considering infinitesimal transformations.

In a general form, following the theory of porous media presented by Biot and completed by Coussy (1995), the diffusity equation that links pressure variation and stress can be written as,

$$\frac{1}{M}\frac{\partial p}{\partial t} - 3\alpha_m \frac{\partial T}{\partial t} - \frac{k}{\mu}\Delta p = -b\frac{\partial \varepsilon_v}{\partial t} \tag{1}$$

where M is Biot's modulus, b the Biot's coefficient, α_m is the differential thermal expansion coefficient, T the temperature, t the time, k the intrinsic permeability of the porous media, μ the dynamic fluid viscosity, p the pore pressure and ε_v is the volumetric strain. The Biot's modulus M is related to the rock and fluid characteristics,

$$\frac{1}{M} = \frac{\phi_0}{K_f} + \frac{b-\phi_0}{K_s} \tag{2}$$

where ϕ_0 is the initial porosity, K_s is the matrix bulk modulus and K_f is the fluid bulk modulus. The Biot's coefficient b is related to the matrix and to the drained bulk modulus K_d by the Biot's relation,

$$b = 1 - \frac{K_d}{K_s} \tag{3}$$

which is close to 1 for incompressible grains.

The differential thermal expansion coefficient α_m reads,

$$\alpha_m = \phi_0 \alpha_f + \alpha_\phi \tag{4}$$

where α_f is the fluid thermal expansion coefficient and α_ϕ the pore thermal expansion coefficient. Considering an isotropic and elastic behaviour for rocks under small transformations, the mechanical equilibrium reads,

$$G\Delta u + \left(K_d + \frac{G}{3}\right) grad\left(div(u)\right) + \rho_h g = b \cdot grad(p) + 3\alpha_d K_d \cdot grad(T) \tag{5}$$

with G the shear modulus, u the displacement, ρ_h the homogeneised density, α_d the drained thermal expansion coefficient and g the gravity vector. This framework is complete but performing the simulations with respect to all the introduced interactions can involve a very high computation cost. This problem of computation cost is particularly important when the calculation of the stress state in the reservoir and surrounding rocks is required because meshes containing numerous elements must be used. That is why this full description is commonly simplified in conventional thermal reservoir models.

Constitutive equations in a conventional thermal reservoir model

The stress variations associated with reservoir production may be extremely high in poorly consolidated reservoirs. Consequently, the porosity, compressibility and permeability of the reservoir rock are likely to vary while the reservoir is producing. Conventional thermal reservoir simulators assume that these parameters depend only on the fluid pressure and temperature, but do not depend on stress variations.

Incorporating Darcy's law in the fluid mass conservation equation for a single-phase fluid, we obtain,

$$\frac{\partial\left(\phi\rho_f\right)}{\partial t} - div\left[\rho_f \frac{k}{\mu} grad(p)\right] = 0 \tag{6}$$

with ϕ the porosity and ρ_f the fluid density. In a conventional reservoir simulator, it is a common practise to introduce a pressure dependency to the reservoir porosity.
A typical equation for porosity is,

$$\phi = \phi_0 \left[1 + c_p \left(p - p_0\right)\right] \tag{7}$$

where p_0 is the pressure at which the porosity is equal to ϕ_0 and c_p is the pore compressibility factor. It must be noticed that the pore compressibility factor is commonly chosen constant or variable according to pressure and/or temperature in reservoir models. According to Eq. 7 and assuming a linear constitutive behaviour, the reservoir porosity linearly depends on the pore pressure and the pore compressibility. In conventional reservoir simulators, a compressible fluid is described by considering that its density depends on the pore pressure and temperature. The linearized form of the fluid state law is,

$$\rho_f \left(p,T\right) = \rho_{f0} \left[1 + c_f \left(p - p_0\right) - 3\alpha_f \left(T - T_0\right)\right] \tag{8}$$

where ρ_{f0} is the fluid density at (p_0,T_0), and c_f is the fluid compressibility. Introducing Eqs. 7 and 8 in Eq. 6, and linearizing the obtained equation yields the following hydraulic diffusivity equation,

$$\phi_0 \left(c_f + c_p\right)\frac{\partial p}{\partial t} - \frac{k}{\mu}\Delta p - 3\phi_0 \alpha_f \frac{\partial T}{\partial t} = 0 \tag{9}$$

This is the common form of the hydraulic diffusivity equation for traditional reservoir models where global stress is assumed to be constant and pore compressibility accounts for the entire mechanical response of the system. This equation is used with boundary and initial conditions to predict pressure and temperature variations in the reservoir.

From linear poroelasticity to conventional reservoir model

In case of non-thermal analysis, the conventional reservoir framework can be recovered from linear poroelasticity through simplifying assumptions (Mainguy and Longuemare, 2002). In this section, commonly made hypotheses are used to show the difference between poroelasticity and conventional reservoir approach and to point out thermal analysis particularity.

First, through considering that the rock matrix is incompressible (i.e., $K_s \rightarrow \infty$), Eqs. 2 and 3 give,

$$\frac{1}{M} \approx \phi_0 c_f \tag{10}$$

and

$$b \approx 1. \tag{11}$$

Then, considering that the pore and bulk volume variations are equal for an incompressible matrix and neglecting Eq. 5 (global stresses are supposed to be constant), the following relationship can be written,

$$b \cdot \frac{\partial \varepsilon_v}{\partial t} \approx \phi_0 c_p \frac{\partial p}{\partial t}. \tag{12}$$

Finally, introducing Eqs. 10, 11 and 12 in Eq. 1 leads to,

$$\phi_0 \left(c_f + c_p\right)\frac{\partial p}{\partial t} - \frac{k}{\mu}\Delta p - 3\phi_0 \alpha_f \frac{\partial T}{\partial t} = 3\alpha_\phi \frac{\partial T}{\partial t} \tag{13}$$

that still differs from Eq. 9.

Comparing Eq. 13 and Eq. 9, it is clear that, for thermal analysis, the term in the right hand side of Eq. 13 is neglected in the fluid flow simulator. It means that pore sensivity to thermal loading is ignored in a conventionnal reservoir model. This approximation can change the evaluation of the state of stress and deformation. Futhermore, it must be noticed that this approximation superimposes to usual approximations that allow to deduce Eq. 13 from Eq. 1.

Indeed, another difference between the two introduced frameworks is that a conventional reservoir model does not take into account the mechanical equilibrium corresponding to Eq. 5 and the matrix compressibility. These approximations can significantly biased the evaluation of stress state and volumetric strain in and around the reservoir, which can influence the underground seismic behavior.

Another point that is not discussed in the presented framework is the modification of permeability that can be induced by stress state changes. This phenomenon is not taken into account in both of the frameworks presented. Nevertheless, solutions have been developed to simulate this phenomenon. The permeability is commonly linked with volumetric strain. Under such an assumption, it is clear that a correct quantification of volumetric strain is required to make an accurate evaluation of permeability modification.

Therefore, during SAGD numerical simulation, by applying Eq. 9, which is used in conventional reservoir simulators, we do not take into account the global stress and strain modification associated with the steam injection. Therefore, coupled reservoir geomechanical simulation is required.

Coupling strategies

In SAGD process, reservoir geomechanical analysis is concerned with the simultaneous study of fluid flow and geomechanical response of the reservoir. To solve the coupling between fluid flow and geomechanics, different approaches have been envisioned (Chalaturnyk, 1996; Settari and Mourits, 1998; Rutqvist et al., 2001; Longuemare et al., 2002; Samier et al., 2003; Jeannin et al., 2005; Wang et al., 2006). Based on the degrees of coupling between reservoir fluid flow and geomechanics, the simulations can be divided into four categories: non-coupled, decoupled, sequentially coupled, and fully coupled (Chalaturnyk, 1996; Wang et al., 2006).

The non-coupled approach denotes the conventional reservoir simulation, which does not solve mechanical equilibrium considering stress redistribution associated with Eq. 5. The basic approach applies rock compressibility as the only parameter to consider the interactions between the fluids and solids. This solution does not appear to be a good one to simulate SAGD operation because it does not allow describing geomechanical effects on seismic response in the underground or mechanically induced modification of intrinsic permeability. Nevertheless, an enhanced non-coupled approach can be performed to describe mechanically induced modification of intrinsic permeability. The principle is to deduce volumetric strain from pressure changes, temperature changes and initial state by using multipliers and without solving the mechanical equilibrium (*i.e.*, considering the global stress as constant) in order to evaluate permeability changes (Samier et al., 2003). This approach is more complete than the conventional reservoir model but cannot be used to evaluate stress redistribution, which is important to characterize entire underground seismic behavior. Furthermore, for both of these methods, the pore thermal expansion is neglected.

The decoupled or one-way solution usually considers the simulation of the complete time history of the recovery process, followed by a stress solution by using a geomechanical simulator, but does not incorporate the feedback of geomechanical effects into the reservoir model. In this approach, the pore pressure and temperature history issued from a fluid flow simulation is introduced as input into the geomechanical equilibrium equation. In practice, the pore pressure and temperature computed by reservoir simulation, using Eq. 9, is introduced in Eq. 1 to deduce the stress and displacement. This coupling is easy to implement, gives quick results and still includes some interesting physics (Vidal et al., 2009). This approach represents a moderate computation cost. Furthermore, using the one-way approach, geomechanical simulation can be performed using different mechanical parameters when reservoir simulation is finished. This solution can also give a good approximation of stress state and volumetric strain in the complete geological model of the reservoir and of the surrounding strata because it takes Eq. 5 into account. With this approach, the use of enhanced 4D seismic monitoring considering geomechanical effects is possible. Furthermore, the one-way solution can be useful to locate and evaluate the risk of rock fracturing because it considers both Eq. 5 and pore thermal expansion for the stress and strain state calculation. Nevertheless, it must be noticed that the one-way solution does not take into account the effect of mechanically induced modification of intrinsic permeability into the reservoir model, since no feedback exists towards this model from the geomechanical simulator.

The sequentially coupled solution contains both explicitly coupled and iteratively coupled reservoir geomechanical simulations. In this approach, the stress and flow equations are solved separately for each time step but information is passed between the reservoir and geomechanical simulators. The stress equations are solved sequentially at the end of each time period or iteration. Then, the modified reservoir parameters by geomechanical behavior are substituted back into the flow equation to continue the next time period. The sequential coupling is described as “explicit” if the methodology is only performed once for each end of period of time and as “iterative” if the methodology is repeated until convergence of the stress and fluid flow problem under a given criterion. The computation cost of sequentially coupled solution depends on the number of fluid flow-geomechanics interactions that are taken into account. In order to simulate a SAGD operation, taking only into account the effect of mechanically induced modification of intrinsic permeability can be a good solution. Therefore, a sequentially coupled approach can be used when the mechanical behavior of rocks is elastic. An iteratively coupled approach is clearly more rigorous when the mechanical behavior of rocks is non-linear but can induce a strong increase in computation cost. Then, the sequentially coupled approach, considering both explicitly and iteratively coupled solutions, allow describing both mechanically induced modification of intrinsic permeability and geomechanical effect on seismic behaviour of the whole underground. This method also allows quantifying the evolution of porous medium thermal expansion.

In the fully coupled simulation, the flow and mechanical equations are solved simultaneously on a unified grid system. Usually in this coupled approach, the hydraulic or geomechanical mechanisms are often simplified by comparison with the conventional reservoir approach. In general, two different kinds of fully coupled simulators can be considered, the first one is based on the reservoir simulator and the second type is based on the geomechanical simulator. Often, with fully coupled simulator of the first kind (based on reservoir simulator), it is only possible to perform a simulation considering simplified mechanical behavior for rocks. With the second type of fully coupled simulator, it is possible to perform a simulation considering a mono-phasic fluid or bi-phasic fluid with simplifying assumptions. Therefore, applying both types of fully coupled method to perform a SAGD simulation of reservoir with all surrounding strata, has a very high computation cost.

Concerning the fully coupled and iteratively coupled solutions, it must be mentioned that full and iterative couplings can lead to different results using the same physical description (Samier et al., 2003). Nevertheless the iteratively coupled method

solves the problem rigorously (i.e., with respect to the physic behavior induced by the used formulations) if iterated to full convergence (Wang et al., 2006). However, the mentioned difference cannot be a good criterion of choice.

Considering the difficulties involves in a fully coupled approach, the numerical modeling of SAGD is proposed using a more convenient and easier method presented here. This method is the explicit coupling approach that is furthermore compared to the one-way (or decoupled) approach on a synthetic reservoir case. For that purpose PumaFlow which is a finite volume reservoir simulator, developed by IFP, is coupled with ABAQUS, the finite element geomechanical simulator developed by SIMULIA. Coupling modules have been developed to allow the fully automatic coupling between the two models on compatible numerical grids.

The Applied Coupling Approaches

One-way Approach

In the one way coupling, only the right branch of the iterative loop shown in Fig. 1 is considered. The pore pressure and temperature fields in the reservoir are calculated by the fluid flow simulator over the full injection-production history. Then pore pressure and temperature fields are introduced in the geomechanical simulator that performs the computation of stresses and displacements at specified times. In this approach, there is no feed back to the fluid flow simulator to update porosity and permeability values in the reservoir grid. This one-way coupling is easy to implement and still can give an appropriate approximation of the reservoir deformation.

Explicit Coupling

The explicitly coupled approach consists in executing sequentially the two models, linked through external coupling modules (Fig. 1). The fluid flow simulator is executed first over a first period. Updated pore pressures and temperatures computed at the end of this first period are transferred to the geomechanical simulator. In the transfer, data are interpolated to pass from finite volume discretization to finite element discretization and inversely. For the herein study, the data transfer is performed through a coupling module that has been developed using Fortran and Python languages.

Based on the updated producing conditions and constitutive relationships, the geomechanical simulator calculates the elastic strains. Then the reservoir permeabilities are modified according to theoretical or empirical functions (between volumetric strain and permeability). Updated grid block permeabilities are then transferred to the fluid flow simulator for the execution of the next time period. This data transfer between the two simulators is also performed by a fortran and Python based module.

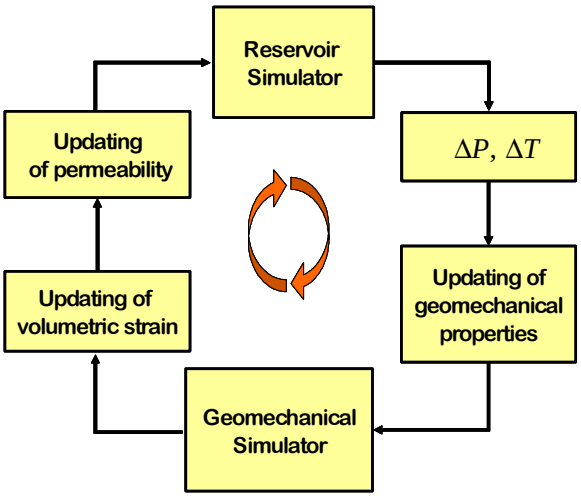

Fig.1: Schematic of the coupled system architecture

Coupling Relationship between permeability and volumetric strain

A simple and empirical relationship is proposed by Touhidi-Baghini (1998) for predicting the evolution of the absolute permeability changes induced by stress changes. This simple relationship linking permeability changes to volumetric strain reads,

$$\ln\frac{k_1}{k_0} = \frac{c}{\phi_0}\varepsilon_v \quad (14)$$

This equation allows the computation of absolute permeability k_1 from its initial value k_0, the volumetric strain ε_v and the initial porosity value ϕ_0. An appropriate value for the constant c has to be picked. According to Touhidi-Baghini, the values c = 5 and c = 2 appear to be appropriate to match with vertical and horizontal permeability evolutions, respectively.

Example of coupling on a synthetic case

Case Description

The case is based on the implementation of the SAGD process in a heavy oil reservoir located in Saskatchewan, Canada (Chabrabarty et al., 1998). The reservoir is assumed homogeneous without bottom aquifer. As indicated in Fig. 2, the top of the reservoir is 730 m deep, the initial pressure and temperature being equal to 5.2 MPa and 27°C respectively.

The simulated domain is rectangular with its dimensions in the X, Y and Z directions respectively equal to 147, 500 and 20 meters (Fig. 2). The well pair is located along the Y axis and in the middle of the X axis. The distance bewteen the two wells is 5 m. The producer is 2 m above the base of the reservoir.

In the reservoir fluid flow simulator, the size of the grid cells in the X direction is equal to 1 meter near the wells and increased to 2 then 3 meters farther away. As the vertical distance between the two horizontal wells was supposed to be constant, only one cell 500 m long is used to describe the well length in the Y direction. Vertical gridding in the reservoir is constant with 40 layers 0.5 meter thick.

In the geomechanical model, the simulated domain includes the reservoir surrounded below by underburden layers and above by overburden layers (Fig. 3). Sideburdens rocks are not modelised because the treated case is assumed geometrically periodic. This assumption corresponds to the fact that in a SAGD process, it is common to use several pairs of well that are parallel and equidistant to optimize production rates. Details of the mechanical properties of the different rock layers are given in Zandi et al. (2010). Initial state stresses are supposed to be isotropic.

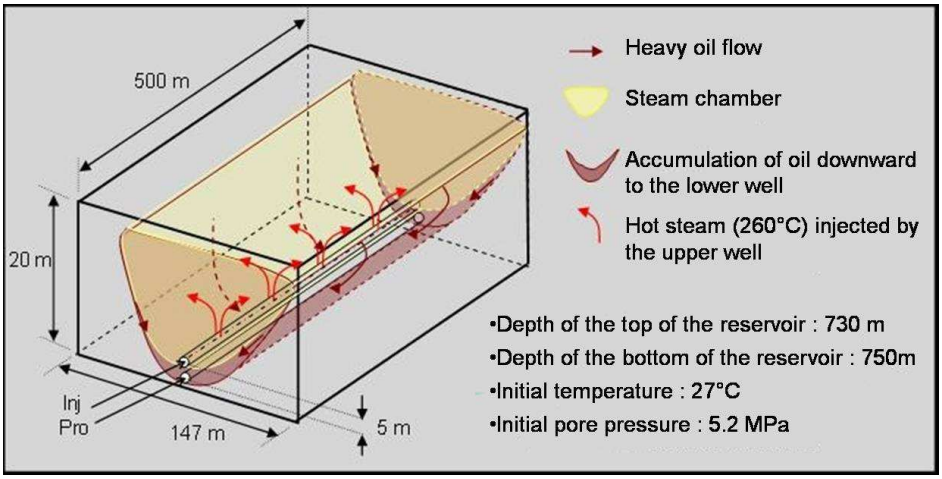

Fig 2*:* Reservoir description

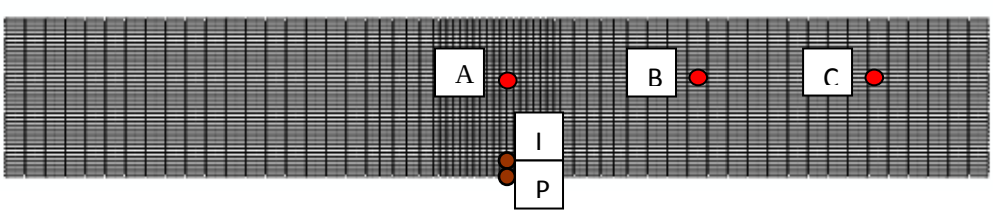

Fig 4: Reservoir modeled in the reservoir simulator, location of the grid cells A, B, C and well-pair in the reservoir

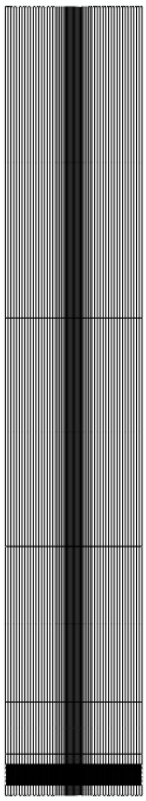

Fig 3:Geomechanical model (reservoir, overburden and underburden)

Operating conditions

The thermo-hydro-mechanical behaviour of the reservoir is analyzed over a 2000-days production period. A pre-heating period of 150 days consisting in steam circulation in the two wells of the SAGD pair is simulated first to allow the hydraulic communication and flow of fluids between the two wells to be efficient. This communication is not possible till the viscosity of oil in place is not decreased enough. Then steam is constantly injected in the upper well and oil plus condensed water produced in the lower well. At the injection well, a steam flow rate is set to 260 m^3/day (Cold Water Equivalent) from 150 to 250 days, then to 400 m^3/day to 2000 days, end of the injection/production history. At the same time, a maximum injection

pressure of 8 MPa is set in the injection well to avoid a too high pressure in the reservoir. At the production well, a minimum pressure of 1.5 MPa is set together with a maximum production flow rate of 560 m^3/d of total liquid (oil plus condensed water). A particular feature of SAGD is the short distance between the injection and production wells with the constant risk of steam breakthrough in the production well. To avoid such a condition, a special monitoring of the steam chamber has been implemented in the reservoir simulator (Chakrabarty et al., 1998). The result of this monitoring is clearly illustrated in Fig. 5 that shows the typical evolution of flow rates in the two wells. The initial steam rate imposed in the injection well between 150 and 250 days is well respected, as is this rate during a short period after 250 days when it is increased to 400 m^3/d. However, quite rapidly the steam front moves too closer to the production well and the injection flow rate has to be decreased to prevent steam breakthrough, then increased again when the steam front moves away from the production well. The monitoring of the well pair to prevent steam breakthrough at the production well results therefore in variations in the steam flow rate in the injection rate during quite a long period that lasts until about 1000 days. At 1000 days, the injection rate continuously decreases because the steam front has reached the lateral limit of the domain. Less steam can be injected and less fluid can be produced.

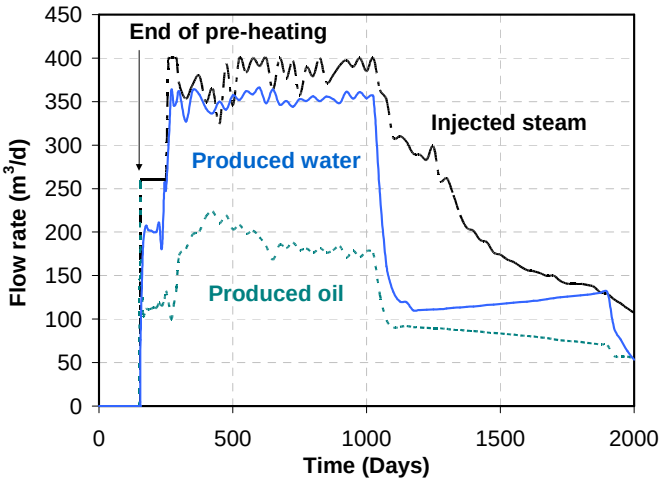

Fig.5: Evolution of injected steam rate and produced oil and water rates versus time (one-way coupling)

Fluid Flow and Geomechanical Coupling Simulation Results

To determine the geomechanical influence of steam injection on pressure and temperature variations in the reservoir and on overall permeability variation, the geomechanical behaviour of the reservoir have been studied in three different grid cells. These cells are located in the same xz plane and at the same elevation in the z direction. Fig. 4 shows the location of these grid cells (A, B and C). Grid cell A is placed just in the middle of the reservoir and 5.5 meters above the horizontal well injection well. Grid cells B and C are chosen farther from the wells, with the distance of 18.5 and 60 meters from the grid cell A, resepectively. To analyze the geomechanical effects during SAGD process, the stress paths in these three grid cells obtained by the two different coupling methods, one-way and explicit, have been specifically studied.

One-way (Decoupled) Approach

A complete 2000-days of fluid flow simulation have been carried out with the reservoir simulator. At the end of this simulation, the pressure and temperature distribution have been extracted from the reservoir simulator and introduced as boundary condition in the geomechanical simulator. The stresses and strains in the reservoir and surrounding rocks have then been computed by the geomechanical simulator at selected times: 0 (initial), 150th day (end of pre-heating), 300th day, 1000th day and 2000th day.

Stress path computed from one-way coupling is plotted on p'-q (deviatoric stress versus mean effective stress) diagram in Fig. 6 for the three grid cells A, B and C. The arrows show the path followed during the evolution of stress at the three different grid cells in the reservoir. The final state is quite similar for cells A and B, but different for cell C. At the same time the paths are quite different for the three cells with a decrease of deviatoric stress (q) during the pre-heating period in grid cells B and C then an increase during the steam chamber development, while for grid cell A the deviatoric stress is always increasing.

Explicit (Sequential) Coupling

The same 2000-days full history of injection and production has been simulated but as already explained, in this explicit coupling approach, permeability in grid cells of the reservoir model have been updated at specified times after computation of stress and strain by the geomechanical simulator, and modification of the permeability values according to Eq. 14.

The explicitly coupled approach has been tested applying different coupling step number. Here we introduce the case of five coupling step number. These coupling times are the same as for the one-way approach: 0 (initial), 150th day (end of pre-heating), 300th day, 1000th day and 2000th day. The first mechanical computation (initialization) is performed to reach a mechanical equilibrium between the applied boundary conditions (regional stresses) and the initial state of stress in the reservoir.

Stress path computed from explicit coupling is plotted on p'-q diagram in Fig. 7 for the three grid cells A, B and C. As before, cell A in the middle of the reservoir has a different stress path compared to the two other cells. The deviatoric stress (q) obtained by explicit coupling reaches nearly 3.4 MPa, while in one-way approach (Fig. 6) a maximum value of nearly 3 MPa for q is obtained. The two graphs show the difference of stress evolution that occurs when permeability changes are taken into account in the fluid flow model. With the explicit coupling the final state for the three cells are quite indentical.

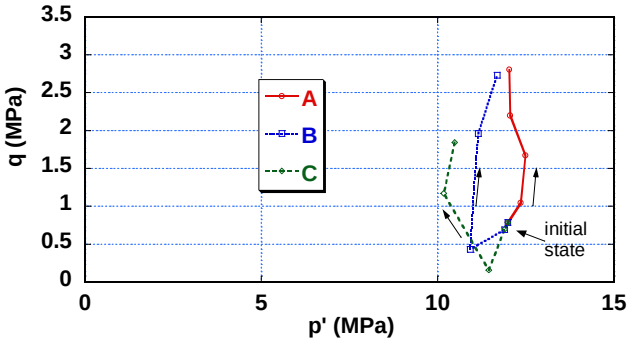

Fig. 6: Stress path in cells A, B and C ; from one-way coupling

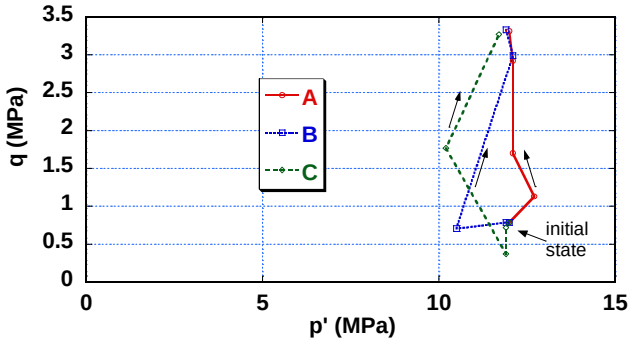

Fig.7: Stress path in cells A, B and C ; from 5 step explicit coupling

Figs. 8 and 9 show the typical evolution of pore pressure and temperature in the three selected grid cells. In the space occupied by the steam chamber, pressure and temperature are related by the water vapor pressure curve. Close to the well pair (cell A) the build up in temperature is rather sharp since the steam front arrives there quite rapidly. This build up becomes slower as the grid cells are farther from the well pair. Temperature is affected first by the flow of heated oil that is drained downward along the steam chamber from the top of the reservoir. Applying coupled method and compared to one way approach, no important modification was seen in pressure and temperature evolution. The coupling mainly affects the porosity and permeablility fields. The decrease in pressure from 150 days, at the end of the pre-heating period, and 250 days is due to the liquid rate at the production well that is greater than the steam rate at the injection well. From 250 days, the steam injection rate becomes greater than the production rate. Therefore pressure increases gradually to reach the maximum pressure allowed in the injection well. From that time, and to the end of the modeling, the system is either under this pressure limit or under the maximum allowed flow rate in the injection well as depicted in Fig. 5.

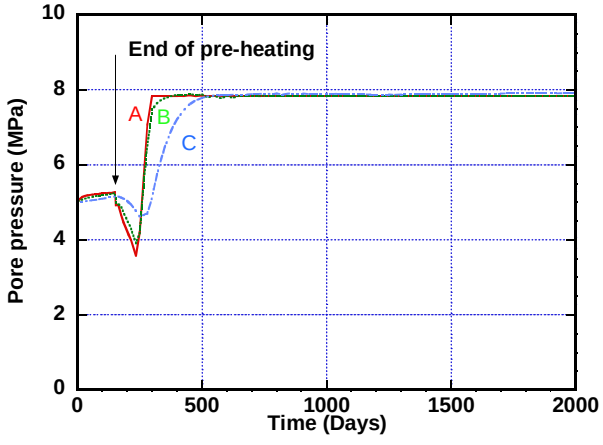

Fig.8: Pore pressure in cells A , B and C ; from one-way method

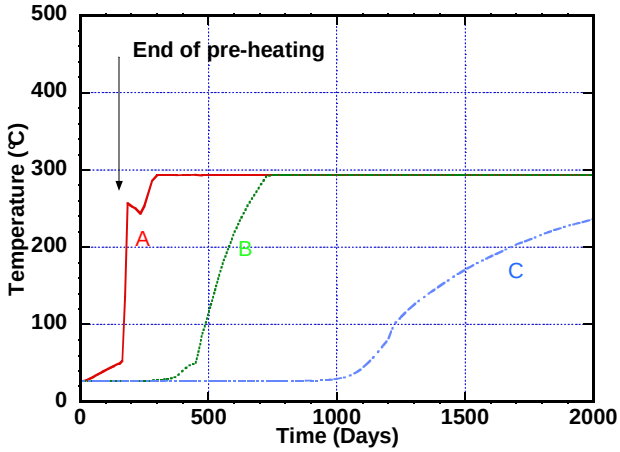

Fig.9: Temperature in cells A , B and C ; from one-way method

Fig. 10 illustrates the permeability evolution in the cells A, B and C during explicit coupling simulation. An increase of 30% is finally observed in the three grid cells. In this particular case of a homogeneous reservoir this increase while important does not impact greatly the evolution of the steam chamber. In the case of an heterogeneous reservoir with the presence of

impermeable barriers, the evolution of permeability can have a more dramatic impact on fluid flow and steam chamber development (Lerat et al., 2009a). This particular point is a topic of future study.

Fig.11 shows the vertical displacement profile of the reservoir interface plotted at the end of the 2000 days simulation for the two approaches. As can be noticed, one way coupling while it does not allow an updating of the permeability in the grid cells of the reservoir model, gives an interesting result in terms of reservoir deformation. Coupling with the geomechanical model and performing this updating of permeability shows a further 14% increase in vertical displacement at the reservoir interface compared to the one-way approach.

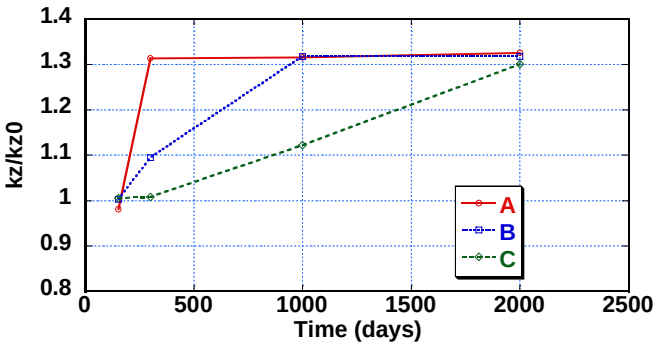

Fig.10: Vertical permeability evolution in cells A,B and C during explicit coupling

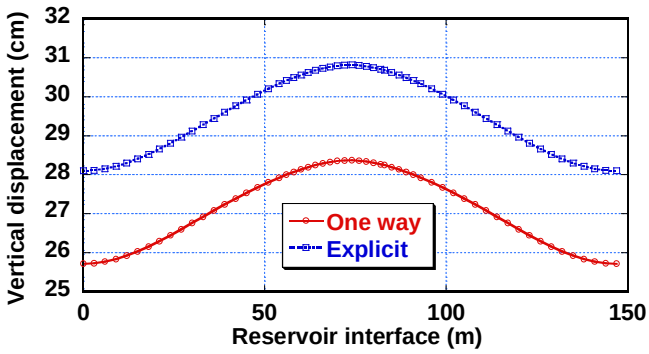

Fig.11: Vertical displacement profile of reservoir interface, at 2000 days

Conclusions

In this paper, we have described the strategies to deal with the coupling between fluid flow and geomechanical effects in the modeling of SAGD. A synthetic but realistic case has been used to compare the two approaches that were finally chosen, i.e. one way in which the results of the fluid flow model are used to compute stress and strain in the reservoir with a geomechanical model at selected times but without feed back to the fluid flow model and the explicit coupling in which a feed back is operated from the geomechanical model to the fluid flow model in order to update the permeabilities modified by the variations of porosity and strain under pressure and temperature variations.

Results leave no doubt about the importance of using a coupled approach as efficient as possible. Stress path, permeability evolution and vertical displacement at reservoir interface depend on the chosen simulation approach.

The one way approach, while basic, can indicate the most mechanically stressed areas and provide a first estimation of deformation magnitude of the reservoir and surrounding layers. The explicit coupling approach is more accurate but also much more time consuming. Our future work will focus on heterogenous media and on solutions to reduce the computation time so that 3D coupled studies can be achieved in a reasonable time.

Acknowledgements

The authors wish to thank Guillaume Servant (now at EDF) who initiated this work. They would also like to acknowledge Elisabeth Bemer, Florence Adjemian, Axelle Baroni and Gilles Ferrer from IFP for their help and useful discussions.

Nomenclature

α_d	Drained thermal expansion coefficient
α_f	Fluid thermal expansion coefficient
α_ϕ	Pore thermal expansion coefficient
α_m	Differential thermal expansion coefficient
b	Biot's coefficient
c_f	Fluid compressibility factor
c_p	Pore compressibility factor
ε_v	Volumetric strain
G	Shear modulus
k	Intrinsic permeability
k_0	Initial absolute permeability
k_1	Absolute permeability
K_d	Drained bulk modulus
K_f	Fluid bulk modulus (K_f=1/c_f)
K_s	Matrix bulk modulus
μ	Fluid dynamic viscosity
p	Pore pressure
p_0	Initial pore pressure
ϕ	Porosity
ϕ_0	Initial porosity
ρ_f	Fluid density
ρ_{f0}	Initial fluid density
ρ_h	Homogeneised density
T	Temperature
T_0	Initial temperature
t	Time
u	Displacement
$grad$	Gradient operator
div	Divergence operator
Δ	Laplacian operator

References

Biot, M.A. 1941. General Theory of Three Dimensional Consolidation. *J Appl Phys***12**: 155-164.

Chakrabarty, C., Renard, G., Fossey, J.-P., and Gadelle, C. 1998. SAGD Process in the East Senlac Field: From Reservoir Characterization to Field Application. Paper 132 presented at the 1998 UNITAR Conference, Beijing, China, 27-31 October.

Chalaturnyk, R. J. 1996. Geomechanics of SAGD in Heavy Oil Reservoirs. PhD dissertation, Department of Civil Engineering, University of Alberta, Alberta.

Collins, P.M., Carlson, M.R., Walters, D.A., and Settari, A. 2002. Geomechanical and Thermal Reservoir Simulation Demonstrates SAGD Enhancement Due to Shear Dilation. Paper SPE 78237 presented at the SPE/ISRM Rock Mechanics Conference, Irving, Texas, 20-23 October.

Coussy, O. 1995. *Mechanics of Porous Continua*. Wiley, New York.

Egermann, P., Renard, G., and Delamaide E. 2001. SAGD Performance Optimization Through Numerical Simulations: Methodology and Field Case Example.,Paper SPE 69690 presented at the SPE ITOHOS Symposium, Porlamar, Margarita Island, Venezuela, 12-14 March.

Huc, A. 2010. *Heavy Crude Oils: from Geology to Upgrading - An Overview*. Technip Editions, Paris. In press.

Ito, Y. and Suzuki, S. 1996. Numerical Simulation of the SAGD Process in the Hangingstone Oil Sands Reservoir. *Proc.*, 47th ATM of the Petroleum Society of CIM, Calgary, Alberta, June 10-12.

Jeannin, L., Mainguy, M., and Masson, R. 2005. Comparison of Coupling Algorithms for Geomechanical-Reservoirs Simulations. *Proc.*, U.S. Rock mechanics symposium, Alaska ROCKS 2005, Anchorage, USA, 25-29 june. Paper ARMA/USRMS 05-677.

Lacroix, S., Renard, G., and Lemonnier, P. 2003. Enhanced Digital Simulations through Dynamical Sub-Gridding. *Proc.*, 2003 CIM Annual Meeting, Calgary, 10 June, Paper CIM 2003-87.

Lerat, O., Adjemian, F., Auvinet, A., Baroni, A., Bemer, E., Eschard, R., Etienne, G. et al. 2009. Modelling of 4D Seismic Data for the Monitoring of the Steam Chamber Growth During SAGD Process. *Proc.*, Canadian International Petroleum Conference 2009, Calgary, Alberta, Canada, 16-18 June, Paper 2009-095.

Lerat, O., Adjemian, F., Auvinet, A., Baroni, A., Bemer, E., Eschard, R., Etienne, G. et al. 2009. 4D Seismic Modelling Applied to SAGD Process Monitoring. *Proc.*, 15th European Symposium on Improved Oil Recovery, Paris, France, 27-29 April, Paper B14.

Longuemare, P., Mainguy, M., Lemonnier, P., Onaisi, A., Gérard, Ch., and Koutsabeloulis, N. 2002. Geomechanics in Reservoir Simulation: Overview of Coupling Methods and Field Case Study. *Oil & Gas Science and Technology***57**(5): 471-483 .

Rutqvist, J., Borgesson, L., Chijimatsu, M., Kobayashi, A., Jing, L., Nguyen, T.S., Noorishad, J., and Tsang, C.-F. 2001. Thermohydromechanics of Partially Saturated Geological Media: Governing Equations and Formulation of Four Finite Element Models. *Int J Rock Mec Min Sci***38**(1): 105-127.

Samier, P., Onaisi, A., and Fontaine, G. 2003. Coupled Analysis of Geomechanics and Fluid Flow in Reservoir Simulation. Paper SPE 79698 presented at the Reservoir simulation Symposium, Houston, 3-5 February.

Settari, A. and Mourits, F.M. 1998. A Coupled Reservoir and Geomechanical Simulation System. *SPE J***3**(3): 219-226. SPE-50939-PA.

Touhidi-Baghini, A. 1998. Absolute Permeability of McMurray Formation Oil Sands at Low Confining Stresses. PhD dissertation, Departement of Civil Engineering, University of Alberta, Alberta.

Vidal-Gilbert, S., Nauroy, J.-F., and Brosse, E. 2009. 3D Geomechanical Modelling for CO2 Geologic Storage in the Dogger Carbonates of the Paris Basin. *Int J of Greenhouse Gas Control***3**: 288–299.

Vidal-Gilbert, S. and Tisseau, E. 2006. Sensitivity Analysis of Geomechanical Behaviour on Time-lapse Seismic Velocity Modelling. Paper SPE 100142 presented at the SPE Europec/EAGE Annual Conference and Exhibition, Vienna, Austria, 12–15 June.

Wang, J., Walters, D., Settari, A., and Wan, R.G. 2006. An Integrated Modular Approach to Modeling Sand Production and Cavity Growth with Emphasis on the Multiphase Flow and 3D Effects. *Proc.*, U.S. Rock mechanics symposium, Golden ROCKS 2006, Colorado, USA, 17-21 june. Paper ARMA/USRMS 06-906.

Zandi, S., Renard, G., Nauroy, J.-F., Guy, N., and Tijani, M. 2010. Numerical Modelling of Geomechanical Effects During Steam Injection in SAGD Heavy Oil Recovery. Paper SPE 129250 presented at the EOR Conference at Oil & Gas West Asia, Muscat, Oman, 11-13 April.

P019

Coupled Geomechanics and Reservoir Modelling in SAGD Recovery

S. Zandi (IFP), N. Guy (IFP), G. Ferrer (IFP), G. Renard (IFP), J.F. Nauroy (IFP)

Abstract

Reservoir geomechanics can play an important role in hydrocarbon recovery mechanism. In SAGD process, reservoir geomechanics analysis is concerned with the simultaneous study of fluid flow and the mechanical response of the reservoir under steam injection. Accurate prediction of geomechanical effects during steam injection will assist in modeling the SAGD recovery process and making a better design of process and production equipment. Reservoir-geomechanics coupled simulation is still an important research topic. To perform this kind of simulation, a solution is to use a finite element based simulator to describe geomechanics and a finite volume based simulator to describe fluid flow. Mostly, its application is limited to the use of identical grids, i.e. one-grid system, for both reservoir flow and geomechanical deformation. While it is necessary to have a fine grid for the simulation of the fluid flow, especially at the steam front, it can be envisioned to use a coarser grid to evaluate the geomechanical deformations. In this paper, a field transfer algorithm based on diffuse approximation method is used for mapping the data between the two simulators with separate-grid systems. In the present case, the number of elements in the geomechanics grids is reduced, so the simulation run time reduces while the results are very close to using a one-grid system.

Introduction

In the SAGD process, continuous steam injection changes reservoir pore pressure and temperature, which can increase or decrease the effective stress in the underground. Therefore, in SAGD process, reservoir geomechanics analysis is concerned with the simultaneous study of fluid flow and the mechanical response of the reservoir. Indeed, oil sand material (skeleton and pores) strains induce changes in the fluid flow-related reservoir parameters. To take into account the geomechanical effects due to stress changes in and around the reservoir, fluid flow must be solved in a way that can predict the evolution of stress dependent parameters such as porosity, pore compressibility and permeability. In a SAGD operation, several geomechanical effects are considered as having a significant influence. For example, laboratory tests have revealed that permeability can be strongly increased by shear stress modification (Touhidi-Baghini, 1998). This geomechanical phenomenon has been investigated through numerical simulations in numerous studies (Ito and Suzuki, 1999; Collins et al., 2002; Lerat et al., 2009b).

The work presented in this paper was performed in the framework of a study on reservoir-geomechanics coupling methods conducted at IFP.. SAGD coupled thermo-hydro-mechanical modeling is conducted using PumaFlow, the inner reservoir simulator of IFP, and Abaqus as the geomechanical simulator. Simulations of the SAGD process were applied on a synthetic but realistic case study that has previously been described (Zandi et al., 2010a). Also, some sensitivity studies on the impact of key parameters on the results of coupled modeling have been done (Zandi et al., 2010b).

We had to apply the coupled methodology on a real case. Considering the reservoir mesh size that is required to simulate the case study, the application of developed coupled methodology is very time-consuming (Lerat et al., 2009a). It is to note that a geomechanical simulator normally solves a much

larger number of unknowns per element than a reservoir simulator does. If the same (coincident) grid is used for both simulators, a full-field coupled problem requires significantly more CPU time and memory than the run without coupled geomechanics calculations, which makes the coupled runs unattractive (Tran et al., 2008).

In order to reduce the coupled simulation run time, separate-reservoir/geomechanics grid systems have to be used. Here we present the methodology of this reservoir/geomechanics coupling approach with separate grid systems. With this approach, geomechanics grid or reservoir grid can be refined or coarsened in different regions independently according to the scale of various physical processes of interest (Tran et al., 2008).

1. SAGD reservoir - geomechanics coupling strategies

1.1. Approach

To solve the coupling between fluid flow and geomechanical problems, different approaches can be used (Settari and Mourits, 1994, Longuemare et al., 2002, Jeannin et al., 2006).
The fully coupled approach simultaneously solves the whole set of equations that govern the thermo-hydro-mechanical problem. It yields to consistent descriptions, but the hydraulic or geomechanical mechanisms are often simplified by comparison with conventional uncoupled reservoir and geomechanical approaches.
The sequentially coupled approach is based on an external coupling between conventional reservoir and geomechanical simulators. The stress and flow equations are solved separately for each time step but information is transferred between the reservoir and geomechanical simulators (Fig.1). This approach has the advantage of being flexible and benefits from the latest developments in physics and numerical techniques for both reservoir and geomechanical models. Different coupling levels can be achieved for the sequentially coupled methodology. The sequential coupling is described "explicit" if the methodology is only performed once for each time step and "iterative" if the methodology is repeated till convergence between the two models of the calculated stress and fluid flow.
The decoupled or "one way coupling" is the simplest partially coupled approach in which the pore pressure history and temperature history issued from a conventional reservoir simulation is introduced as input into the geomechanical equilibrium equation to deduce the stress and deformation. This coupling is easy to implement and still includes some interesting physics (Vidal and al, 2009).
In the one way coupling, only the right branch of the iterative loop shown in Fig.1 is considered. The pore pressure and temperature fields in the reservoir are calculated by the fluid flow simulator over the full injection-production history. Then pore pressure and temperature fields are interpolated and transferredfrom the reservoir grid blocks into the geomechanics grid nodes of the geomechanical simulator that performs the computation of stresses and displacements at specified times. In this approach, there is no feed back to the fluid flow simulator to update porosity and permeability values in the reservoir gridblocks. .
The explicit coupling approach consists in executing sequentially the two models, linked through external coupling modules (Fig.1). The fluid flow simulator is executed first over a first period. Updated pore pressures and temperatures at the end of this first period are interpolated and transferred into the geomechanics grid in the geomechanical simulator.
Based on the updated producing conditions and constitutive relationships, the geomechanical simulator calculates the strains. Then the reservoir permeability is modified according to theoretical or empirical functions (between volumetric strain and permeability). Updated grid block permeabilities are then transferred to the fluid flow simulator for the execution of the next time period.
A simple and empirical relationship is proposed by Touhidi-Baghini (1998) for predicting the evolution of the absolute permeability changes induced by stress changes. This simple relationship linking permeability changes to volumetric strain reads,

$$\ln\frac{k_1}{k_0} = \frac{c}{\phi_0}\varepsilon_v$$

This equation allows the computation of absolute permeability k_1 from its initial value k_0, the volumetric strain ε_v and the initial porosity value ϕ_0 An appropriate value for the constant c has to be picked. According to Touhidi-Baghini, the values c = 5 and c = 2 appear to be appropriate to match with vertical and horizontal permeability evolutions, respectively.

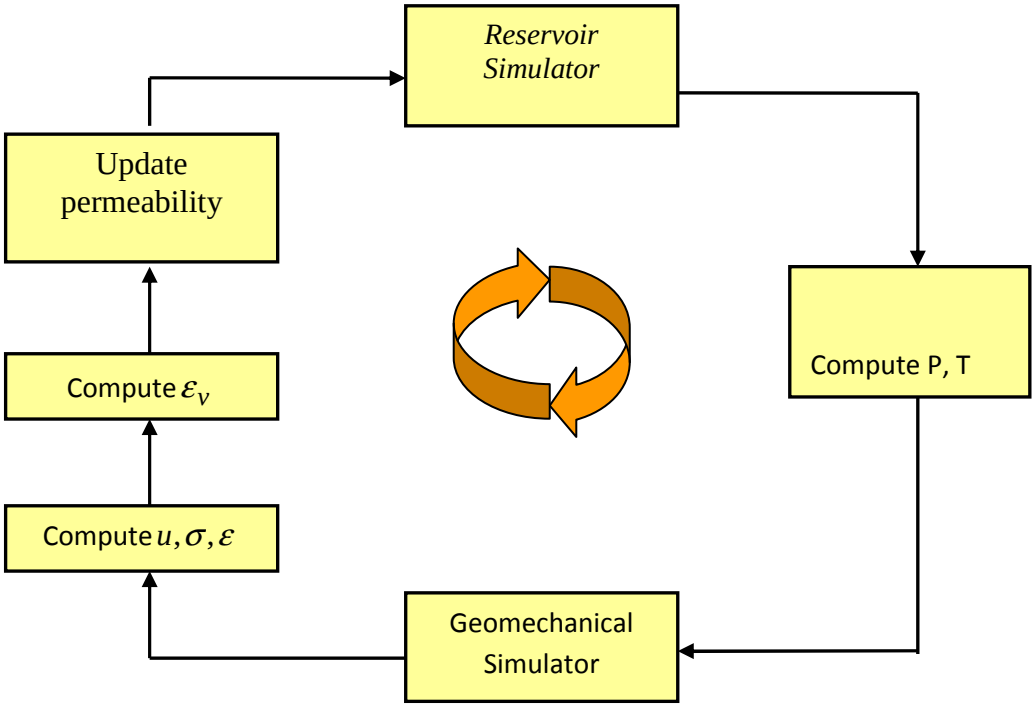

Fig.1: Coupled system architecture

SAGD coupled simulations using one-way coupling and explicit coupling methods were presented in Zandi et al.2010a and Zandi et al. 2010b.

1.2. Geometry

To model a reservoir-geomechanics coupled simulation, irrespective of the used gridding technique, three apparent choices exist regarding establishing the geomechanical model and reservoir model:

1. Modeling just the reservoir part in geomechanical simulator and reservoir simulator (Fig 2.1)
2. Construction of reservoir part in reservoir simulator, and reservoir surrounded by rocks in geomechanical simulator (Fig 2.2).
3. Modeling the reservoir part and the surrounding strata (here, overburden and underburden) in both simulators (Fig 2.3).

Examples of these approaches may also be found in many articles like: Settari, 2008; Lerat et al. 2009a; Shi and Durucan, 2009 and Zandi et al. 2010a.
The weakness of the first approach is the setting of an equilibrium state in the geostatic step of the geomechanical simulation.
The second approach is the most commonly used, as we aim at a limited total number of elements in the models in order to reduce the simulation run time.
In the third approach, the reservoir surrounded by rocks is constructed in both simulators, which can result in increase of the simulation run time. Using an adapted reservoir simulator, the advantage of this method is the possibility of correctly simulating the temperature field in surrounding rocks, which is very helpful especially in the case of SAGD modeling.

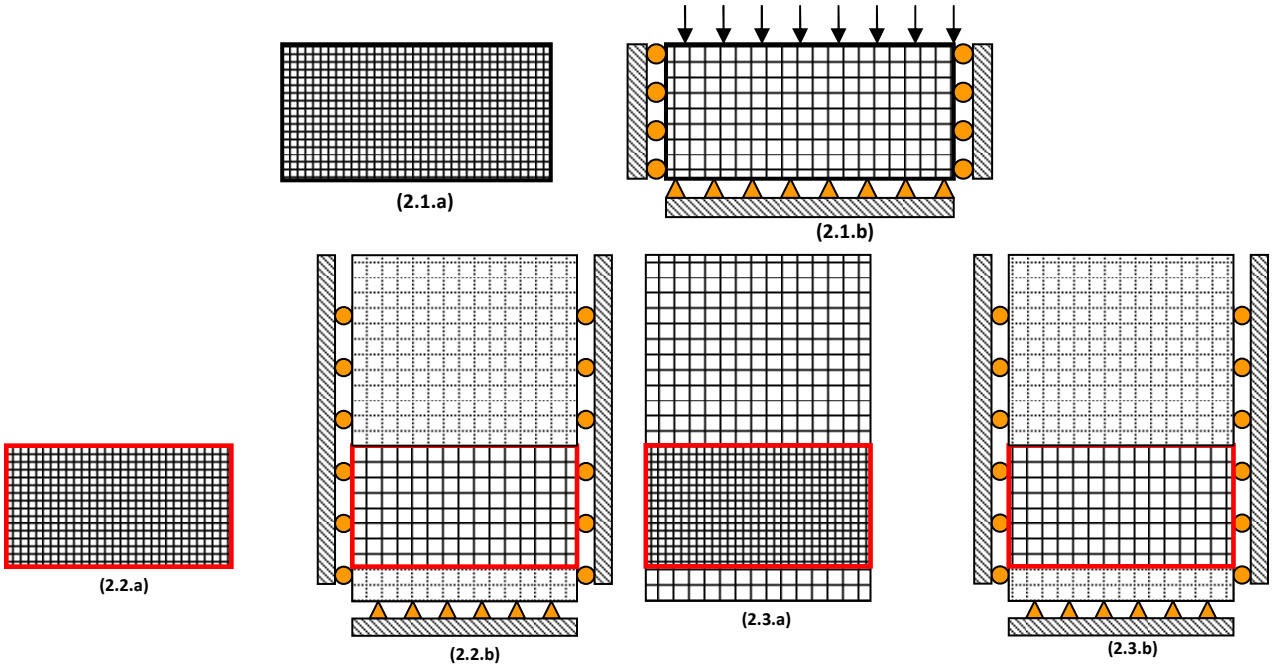

Fig.2: Different geometries of modeled reservoir in reservoir simulator and its surrounding rocks in geomechanical simulator (b)

1.3. Gridding

Coupling between a geomechanics grid and a reservoir grid is an important issue when those grids are not the same (coincident) but are used to refer to the same spatial domain in a simulation (Tran et al., 2008). The result of coupled solution will depend upon the mapping of information between the two grids.

The fact that the grid type in reservoir simulator is different from geomechanical simulator makes the mapping process more complicated. In fact in the reservoir simulator a Finite Volume Grid discretization is used where flow variables are computed at the center of gridblocks while in the geomechanical simulator a Finite Element Grid discretization is used to compute displacements at the nodes of the grid.

If the grids in reservoir simulator and geomechanical simulator are coincident, interpolation of the data between the two simulators is simple. Updated pore pressures and temperatures computed in the center of reservoir grids, at the end of this first period, are transferred on the nodes of geomechanics grids in geomechanical simulator. In this transfer, data are interpolated to pass from finite volume discretization to finite element discretization and inversely.

When the grids in reservoir and geomechanical simulators are not coincident, passing the data (temperature, pressure, volumetric strain) between the two simulators is more complex. In this case a field transfer algorithm must be used to perform the passing of data from a grid to the other.

Here a code named NUAGE based on diffuse approximation method (Savignat, 2000) , is used for mapping the data from reservoir grid centers to geomechanics grid nodes and vice versa. The diffuse approximation method (DAM) can be used for finding estimates of a scalar field φ from set of nodal values (Nayroles et al., 1991). The starting point is to estimate the Taylor expansion of the studied scalar field φ at a chosen point by a weighted least squares method which uses only the values of φ at the nearest points. The main advantage of this method is that it only requires sets of discretization nodes and no geometric finite elements and that it is a local method. It is to note that in the diffuse approximation method can be used with various weighting strategies that lead to different and interesting properties. Using the diffuse approximation method, when the reservoir and the geomechanics grids are distinct, reduces the simulation run time with the results which are very close to the one-grid system as will be shown later.

The weighting procedure used in the present scheme allows the DAM to interpolate the initial data. This scheme which is written in C gives improved mapping for discontinuous functions. For the herein study, the data transfer is performed through a coupling module that has been developed using Fortran and Python languages which contains the mapping module (NUAGE) written in C language.

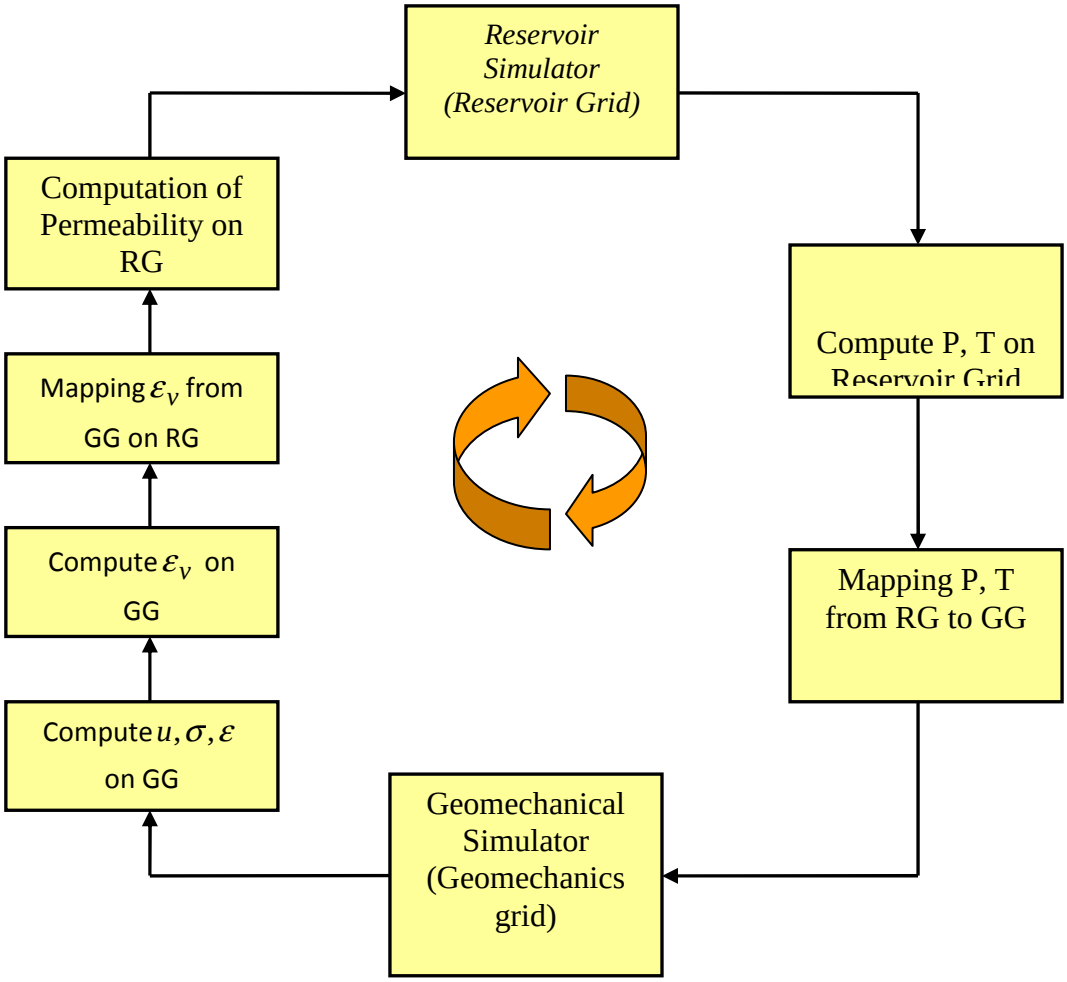

Fig.3: Coupled system architecture with distinct grid approach

2. Application of Two-Grid system

This test case is based on a synthetic study data presented in Zandi *et al*, 2010b, which is an implementation of the SAGD process in a heavy oil reservoir located in Saskatchewan, Canada (Chabrabarty *et al.*, 1998). The reservoir is assumed homogeneous without bottom aquifer. The top of the reservoir is 730 m deep, the initial pressure and temperature being equal to 5.2 MPa and 27°C respectively.

The reservoir simulated domain is rectangular with its dimensions in the X, Y and Z directions respectively equal to 147, 500 and 20 meters (Fig. 4). The well pair is located along the Y axis and in the middle of the X axis. The distance between the two wells is 5 m. The producer is 2 m above the base of the reservoir.

In the reservoir fluid flow simulator, the size of the grid cells in the X direction is equal to 1 meter near the wells and increased to 2 then 3 meters farther away. As the vertical distance between the two horizontal wells was supposed to be constant, only one cell 500 m long is used to describe the well length in the Y direction. Vertical gridding in the reservoir is constant with 40 layers 0.5 meter thick.

In the geomechanical model, the simulated domain includes the reservoir surrounded below by underburden layers and above by overburden layers. Sideburden rocks are not modeled because the

treated case is assumed geometrically periodic. This assumption corresponds to the fact that in a SAGD process, it is common to use several pairs of well that are parallel and equidistant to optimize production rates. Details of the mechanical properties of the different rock layers are given in Zandi et al. (2010a). Initial state stresses are supposed to be isotropic.

So as explained, the geometry of the field in reservoir simulator and geomechanical simulator is modeled using the second method presented here in part 1.2., it means construction of reservoir part in reservoir simulator, and reservoir surrounded by rocks in geomechanical simulator (Fig 2.2). The coupling approach used is one-way simulation andhere we compare three coupled simulations with different gridding in geomechanical simulator:

1) The reservoir grid in geomechanical simulator is the same as reservoir grid in reservoir simulator,
2) The reservoir grid in geomechanical simulator is coarser than the reservoir grid in reservoir simulator,
3) The reservoir grid in geomechanical simulator is coarser than the one in the previous case,

Fig. 4 shows the reservoir as modeled in reservoir simulator for all the three cases, with a resolution of 65x1x40 in X, Y and Z direction.

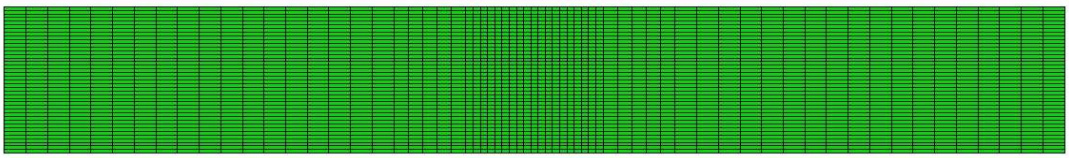

Fig.4: Reservoir field grid as modeled in reservoir simulator

Fig. 5 illustrates the reservoir field as modeled in geomechanical simulator with:

- same grid system, where the reservoir field grid in geomechanical simulator has the same resolution as reservoir field grid in reservoir simulator, it means 65x1x40, as shown in Fig.5a,
- distinct grid system, where the reservoir field grid in geomechanical simulator has a resolution of 40x1x20 as shown in Fig. 5b,
- distinct grid system in which the reservoir field grid in geomechanical simulator is coarser than the previous case. In this case the resolution of reservoir field grid in geomechanical simulator is 20x1x10 as illustrated in Fig. 5c.

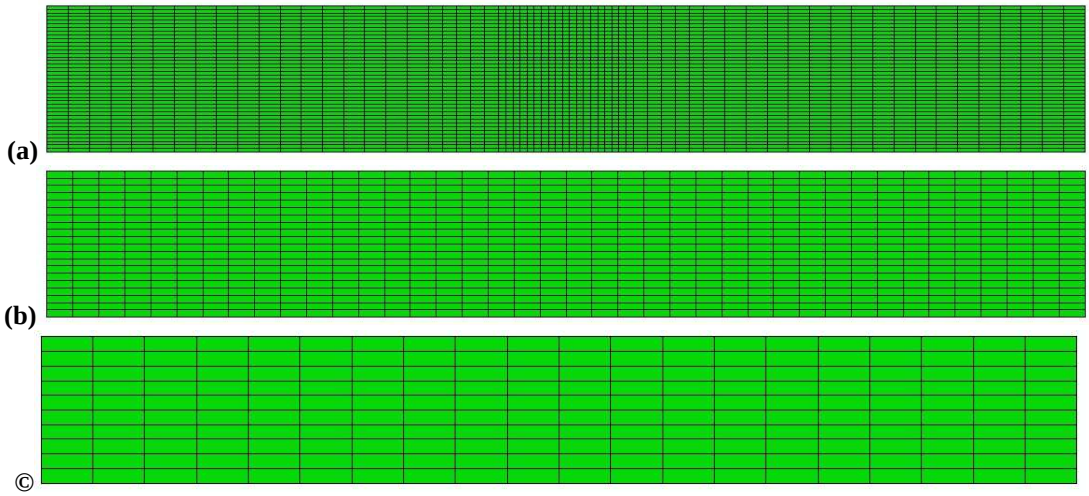

Fig.5: Grid as modeled in geomechanical simulator in the three different coupled simulation cases
(a) coincident reservoir-geomechanics gridding system,
(b)&(c) distinct reservoir-geomechanics gridding system

Note that in the second and the third cases, the geomechanics gridblocks of underburden and overburden are also resized and the number of gridblocks is less than the first case.
Results obtained from these three cases are compared. Here the CPU time, reservoir temperature field and reservoir interface displacement are presented.

The CPU time for the second case is 57 % less than for the first case; also the CPU time for the third case is 85 % less than the first case. It shows that the distinct grid system can save significant CPU time.

Fig. 6 shows the temperature field in the reservoir which first increases above the injection well to the top of the reservoir and then extends laterally to become uniform in the upper part of the reservoir. This uniformity is related to lateral boundary conditions that were imposed on the model.

As can be seen, the temperature field resulted by three simulations are really similar, especially further from the wells; but the first simulation (Fig. 6a) illustrates precisely the temperature around the wells, which is not the same in the second (Fig. 6b) and the third (Fig. 6c) simulation case. It shows the importance of refining the mesh around the wells, in order to have more realistic simulation results.

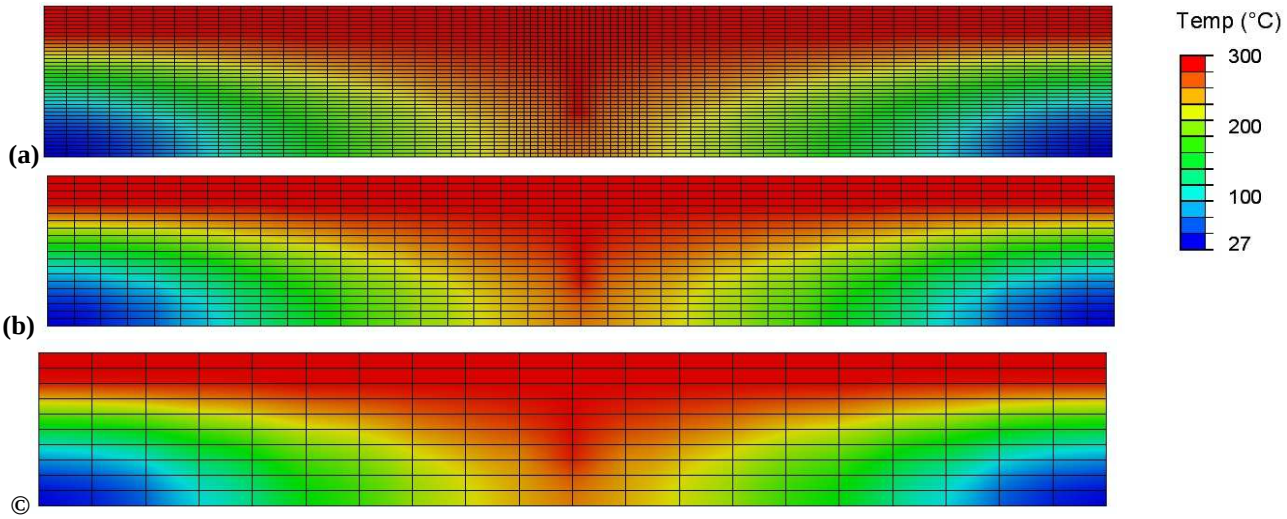

Fig.6: Temperature field in geomechanical simulator in three different coupled simulation cases (a) coincident reservoir-geomechanics gridding system, (b)&(c) distinct reservoir-geomechanics gridding system

Fig.7 shows the vertical displacement profile of the top of the reservoir plotted at the end of the three one-way coupling simulations explained. The uplift is very fast just above the wells, then it extends to the periphery when the steam chamber grows. It becomes almost homogeneous at the end of the 2000-day simulation.

As can be noticed, the uplift result graph is exactly superposed in three simulations. The pink curve shows the coincident reservoir-geomechanics grid simulation results which correspond to the first test case defined. The blue and green curves illustrate the distinct reservoir-geomechanics grid simulation results which correspond to the second and third test case, respectively.

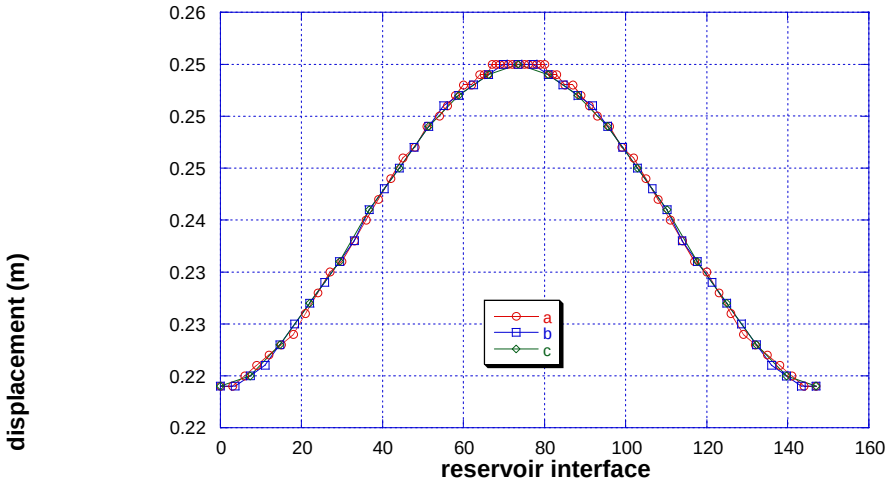

Fig.7: Vertical displacement profile of reservoir interface, at the end of coupled simulation

Conclusion

This paper presents the implementation of an integrated field transfer module into an existing reservoir-geomechanics coupled simulation code, used for SAGD process modeling.

The different coupling approaches, different coupling geometries and two different gridding systems are discussed.

The one-way coupling approach combined by coincident and distinct grid systems was used to simulate the presented test case. Overburden and underburden rocks are modeled in geomechanics simulator but not in the reservoir simulator.

Comparing these three simulations show the advantage of distinct grid system. As the geomechanics grid is independent of reservoir grid, different grids can be used for each simulator. Information obtained from one simulator grid is mapped to the other simulator grid. Using the distinct gridding system we could save up to 85 % of CPU time, which is really interesting especially in the case of a real field SAGD coupled simulation.

When a large reservoir field is simulated, it is recommended that a coarse (low-resolution) geomechanics grid be used to obtain approximate results before applying a fine (high-resolution) geomechanics grid to get the desired accuracy.

Acknowledgements

The authors wish to thank Michel Tijani (ENSMP) who initiated this work, for his help and useful discussions.

References

[1] Chakrabarty, C., Renard, G., Fossey, J.-P., and Gadelle, C. 1998. SAGD Process in the East Senlac Field: From Reservoir Characterization to Field Application. Paper 132 presented at the 1998 UNITAR Conference, Beijing, China, 27-31 October.

[2] Collins, P.M., Carlson, M.R., Walters, D.A., and Settari, A. 2002. Geomechanical and Thermal Reservoir Simulation Demonstrates SAGD Enhancement Due to Shear Dilation. Paper SPE 78237 presented at the SPE/ISRM Rock Mechanics Conference, Irving, Texas, 20-23 October.

[3] Ito, Y. and Suzuki, S. 1996. Numerical Simulation of the SAGD Process in the Hangingstone Oil Sands Reservoir. *Proc.*, 47th ATM of the Petroleum Society of CIM, Calgary, Alberta, June 10-12.

[4] Jeannin, L., Mainguy, M., and Masson, R. 2005. Comparison of Coupling Algorithms for Geomechanical-Reservoirs Simulations. *Proc.*, U.S. Rock mechanics symposium, Alaska ROCKS 2005, Anchorage, USA, 25-29 june. Paper ARMA/USRMS 05-677.

[5] Lerat, O., Adjemian, F., Auvinet, A., Baroni, A., Bemer, E., Eschard, R., Etienne, G. et al. 2009. Modelling of 4D Seismic Data for the Monitoring of the Steam Chamber Growth during SAGD Process. *Proc.*, Canadian International Petroleum Conference 2009, Calgary, Alberta, Canada, 16-18 June, Paper 2009-095.

[6] Lerat, O., Adjemian, F., Auvinet, A., Baroni, A., Bemer, E., Eschard, R., Etienne, G. et al. 2009. 4D Seismic Modelling Applied to SAGD Process Monitoring. *Proc.*, 15th European Symposium on Improved Oil Recovery, Paris, France, 27-29 April, Paper B14.

[7] Longuemare, P., Mainguy, M., Lemonnier, P., Onaisi, A., Gérard, Ch., and Koutsabeloulis, N. 2002. Geomechanics in Reservoir Simulation: Overview of Coupling Methods and Field Case Study. *Oil & Gas Science and Technology* 57(5): 471-483 .

[8] Nayroles, B., Touzot, G., and Villon, P., The diffuse approximation, *C. R. Acad. Sci. Paris, Serie II*, 313, 293-296 (1991)

[9] Savignat, JM. 2000. Approximation Diffuse Hermite et ses Applications, PhD Dissertation, Mines Paris Tech, Paris.

[10] Settari, A. and Mourits, F.M. 1998. A Coupled Reservoir and Geomechanical Simulation System. *SPE J***3**(3): 219-226. SPE-50939-PA.

[11] Shi, JQ. and Durucan, S. 2009. A coupled reservoir-geomechanical simulation study of CO2 storage in a nearly depleted natural gas reservoir, Energy Procedia 1(2009) 3039-3046.

[12] Touhidi-Baghini, A. 1998. Absolute Permeability of McMurray Formation Oil Sands at Low Confining Stresses. PhD dissertation, Departement of Civil Engineering, University of Alberta, Alberta.

[13] Tran, D., Buchanan, L. and Nghiem, L. 2008. Improved Gridding Technique for Coupling Geomechanics to Reservoir Flow. Paper SPE 115514 presented at the Annual Technical Conference and Exhibition in Denver, Colorado, USA, 21-24 September.

[14] Vidal-Gilbert, S., Nauroy, J.-F., and Brosse, E. 2009. 3D Geomechanical Modelling for CO2 Geologic Storage in the Dogger Carbonates of the ParisBasin. *Int J of Greenhouse Gas Control* 3: 288–299.

[15] Vidal-Gilbert, S. and Tisseau, E. 2006. Sensitivity Analysis of Geomechanical Behaviour on Time-lapse Seismic Velocity Modelling. Paper SPE 100142 presented at the SPE Europec/EAGE Annual Conference and Exhibition, Vienna, Austria, 12–15 June.

[16] Zandi, S., Renard, G., Nauroy, J.-F., Guy, N., and Tijani, M. 2010. Numerical Modelling of Geomechanical Effects during Steam Injection in SAGD Heavy Oil Recovery. Paper SPE 129250 presented at the EOR Conference at Oil & Gas West Asia, Muscat, Oman, 11-13 April.

[17] Zandi, S., Renard, G., Nauroy, J.-F., Guy, N., and Tijani, M. 2010. Numerical Coupling of Geomechanics and Fluid Flow during Steam Injection in SAGD. Paper SPE 129739 presented at the Improved Oil Recovery Symposium, Tulsa, USA, 24-28 April.

Modélisation des effets géomécaniques de l'injection de vapeur dans les réservoirs de bruts lourds

RESUME : Le SAGD (Steam Assisted Gravity Drainage) est un procédé de récupération des huiles lourdes qui remporte énormément de succès, en particulier pour le bitume. Le SAGD génère des interactions complexes entre la géomécanique et les écoulements polyphasiques en milieux poreux. Dans ce procédé, l'injection de vapeur modifie la pression et de la température dans le réservoir, ce qui peut augmenter ou diminuer les contraintes effectives dans le réservoir. La quantification de l'état de contrainte et déformation dans le réservoir est essentielle pour effectuer un bon pronostic de la productivité du réservoir, pour vérifier l'intégrité de la couverture et les risques de fracturation hydraulique, et également pour interpréter correctement la sismique 4D en termes d'évolution de la chambre de vapeur. Dans le procédé SAGD, les effets géomécaniques de l'injection de vapeur dans le réservoir sont liés aux écoulements de fluide.. Le couplage réservoir-géomécanique est un sujet de recherche important. Pour effectuer ce type de simulation, une solution consiste à utiliser un simulateur en éléments finis pour décrire la géomécanique et un simulateur en volumes finis pour décrire les écoulements.

Dans cette thèse, une simulation couplée thermo-hydro-mécanique du SAGD a été effectuée à l'aide du simulateur de réservoir PumaFlow et du simulateur de géomécanique Abaqus. Les principaux thèmes étudiés dans cette étude ont été (1) la stratégie de couplage, (2) la géométrie du système et (3) le type de maillage utilisé. Ce travail a été effectué sur des cas synthétiques.

Mots clés : Huiles lourdes, Sables bitumineux, SAGD, Couplage Réservoir-Géomécanique, Simulation numérique

Numerical modeling of geomechanical effects of steam injection in SAGD heavy oil recovery

ABSTRACT : The Steam Assisted Gravity Drainage (SAGD) process is a thermal enhanced oil recovery (EOR) method that appears tremendously successful, especially for bitumen. SAGD process results in a complex interaction of geomechanics and multiphase flow in cohesionless porous media. In this process, continuous steam injection changes reservoir pore pressure and temperature, which can increase or decrease the effective stresses in the reservoir. Quantification of the state of deformation and stress in the reservoir is essential for the correct prediction of reservoir productivity, seal integrity, hydro fracturing, well failure and also for the interpretation of 4D seismic used to follow the development of the steam chamber. In SAGD process, the analysis of reservoir-geomechanics is concerned with the simultaneous study of fluid flow and mechanical response of the reservoir. Reservoir-geomechanics coupled simulation is still an important research topic. To perform this kind of simulation, a solution is to use a finite element based simulator to describe geomechanics and a finite volume based simulator to describe fluid flow.

In this thesis, the SAGD coupled thermo-hydro-mechanical modelling is conducted using PumaFlow reservoir simulator and Abaqus as the geomechanical simulator. The main issues being investigated in this study were (1) the coupling strategy, (2) the geometry and (3) type of gridding system. This work was performed on synthetic cases.

Keywords : Heavy oil, oil sand, SAGD, Reservoir-Geomechanics Coupling, Numerical simulation

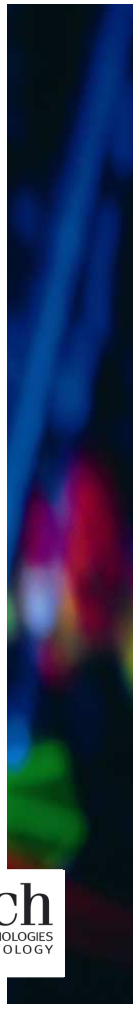

MINES ParisTech

ParisTech
INSTITUT DES SCIENCES ET TECHNOLOGIES
PARIS INSTITUTE OF TECHNOLOGY